NISTIR 6379

Evaluation of Active Suppression in Simulated Post-Collision Vehicle Fires

Anthony Hamins

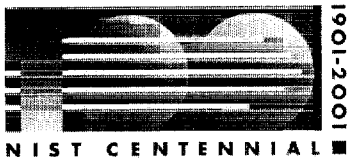

National Institute of Standards and Technology
Technology Administration, U.S. Department of Commerce

Evaluation of Active Suppression in Simulated Post-Collision Vehicle Fires

Anthony Hamins
Building and Fire Research Laboratory
National Institute of Standards and Technology
Gaithersburg, MD 20899

ABSTRACT

An investigation of the effectiveness of fire suppressants in simulated post-collision vehicle fires is presented. Two distinct fire scenarios were considered. The first configuration was a simulated engine compartment fire. The second configuration was a simulated underbody fire. The configurations were defined based on geometric and fire-related parameters. Experiments were performed using both laboratory test devices and a mid-size passenger vehicle.

A set of criteria was constructed for selection of suppressants for use in the suppression tests. The criteria were based on information from the fire literature and engineering judgement. Commercially available fire suppressants and several emerging suppressants were evaluated in terms of the criteria and a number of representative suppressants were selected for testing.

Both traditional and emerging active fire suppressants were tested. These included dry powders, inert suppressants, compressed liquefied halogenated compounds, and a number of unique devices. The suppressants tested in the engine compartment suppression experiments were HFC-125 (C_2HF_5), HFC-227ea (C_3HF_7), ABC powder ($NH_4H_2PO_4$, mono-ammonium phosphate), BC powder ($NaHCO_3$, sodium bicarbonate), a tubular suppression system, solid propellant generators, and aerosol generators. The suppressants tested in the underbody fire suppression experiments were HFC-125, ABC powder, BC powder, solid propellant generators, and aerosol generators.

A number of experimental protocols were developed to appraise the feasibility of fire suppression using the representative suppressants. The apparatus in each of the experimental configurations included a fire zone and a suppressant delivery system. The experimental procedure in each of the four configurations was essentially the same. A fire was established and after a specified duration, a controlled mass of suppressant was delivered to the fire zone. Suppressant distribution was optimized through careful nozzle selection, placement, and discharge duration. After suppressant delivery, observation determined whether the fire was suppressed or not suppressed. A number of experiments were conducted to test the importance of operating conditions on suppressant effectiveness in the simulated vehicle fires. These included geometrical factors and suppressant delivery parameters. Long fuel trails extending beyond the confines of the vehicle and environmental factors such as wind were considered.

The results showed that it is highly improbable that an on-board fire suppression system will be able to extinguish all engine compartment and underbody fires. Many suppressant types were found to be impractical for post-collision engine compartment applications. The experiments have shown, however, that under certain conditions, fire suppression is feasible. A unique pyrotechnic device, the solid propellant generator, was the most effective suppressant tested in the full-scale engine compartment scenario. These devices rapidly deliver a gas/particulate effluent. Full-scale suppression experiments in the engine compartment of an uncrashed stationary vehicle in the absence of forced ventilation (radiator fan off) showed that suppression of a 200 mL/min gasoline fire was achievable with less than 500 g of the solid propellant generator. Full-scale underbody experiments showed that suppression of a (333 mL volume) gasoline pool fire was achieved with less than 300 g of ABC and BC powder suppressants when the fuel was located under the vehicle footprint for low wind conditions. If a fuel puddle in an underbody fire extended beyond the vehicle footprint and if moderate to high winds were present, then the powder suppression system failed to reliably extinguish the fire.

This report was financed by General Motors pursuant to an agreement between General Motors and the United States Department of Transportation. The National Institute of Standards and Technology (NIST) is applying its expertise in fire science to this program because of the potentially high impact of this program on vehicle fire safety in the United States. As a matter of policy, NIST does not test commercial products, especially without the consent of the manufacturers of those products. The National Highway Traffic Safety Administration and General Motors have selected the vehicles to be crash tested and the procedures for those tests. These exploratory tests are only meant to produce a variety of types of vehicle damage that might occur. Not all collision conditions were studied, and the repeatability of the tests cannot be determined since in most cases replicate tests were not conducted due to budgetary constraints. Thus, the results of the tests may facilitate identification of opportunities for improvements in vehicle fire safety, but cannot by themselves be extrapolated to the full fleet of vehicles and all crash conditions. In analyzing the data from these tests, certain vehicles, equipment, instruments or materials are identified in this paper in order to specify the experimental procedure adequately. In no case does such identification imply recommendation or endorsement by the National Institute of Standards and Technology, nor does it imply that the fire safety of a particular vehicle is superior or inferior to any other. In addition, certain trade names and company products are mentioned in the text to specify adequately the experimental procedure and equipment used or to identify types of currently available commercial products. In no case does such identification imply recommendation or endorsement by the National Institute of Standards and Technology, nor does it imply that the products are necessarily the best available for the purpose.

TABLE OF CONTENTS

1. Overview

This is the second report of results from Project B.4, "Evaluation of Potential Fire Intervention Materials and Technologies," which was conducted as part of a Cooperative Research and Development Agreement between General Motors and NIST. It comprises one aspect of research resulting from an agreement between General Motors and the United States Department of Transportation (GM/DOT agreement).

In an earlier study, which was part of Project B.4 of the GM/DOT agreement, the effectiveness of intumescent coatings, a passive fire protection strategy, was tested in simulated post-collision body panels [Hamins, 1998]. In this study, the effectiveness of fire suppressants as an intervention strategy in vehicle fires was investigated. In particular, the fire scenarios were designed to represent certain aspects of post-collision vehicle fires. To accomplish this, a number of experimental protocols were developed to appraise the feasibility of extinguishing fires using common and emerging types of suppressants. Several experimental configurations were investigated including both full-scale and reduced-scale engine compartment and underbody fires. Several fire suppressants were selected for testing. These included dry powders, clean suppressants, and a number of prototype devices. This report describes the experimental results with an emphasis on the relative performance of the suppressants and the influence of various parameters associated with the vehicle itself (e.g., geometry) or the suppressant (e.g., delivery rate).

Vehicle fires represent approximately one-quarter of the total number of fires responded to by local fire services [U.S. Fire Administration, 1997]. Although fires represent only a small percentage of vehicle related injuries, they account for a significant percentage of U.S. fire injuries. In 1994, of the 15000 fire injuries in the U.S., approximately 10 % were vehicle related [U.S Fire Administration, 1997]. According to the National Fire Protection Association (NFPA), for the years from 1989 to 1993, there was an annual average of 425000 fires in vehicles per year and 320000 fires in passenger road transport vehicles [Stewart, 1996].

Post-accident vehicle fires are not frequent. Of the approximately 20000 automobile collisions (average per year) that led to fatalities during the period from 1979 to 1992, fire occurred in approximately 2.4 % of these cases [Tessmer, 1994]. For the period from 1990 to 1992, NHSTA estimated that the annual average number of deaths due to fire ranged from 261 to 490, depending on the measure used [Tessmer, 1994]. In addition to the fatalities, a large number of non-fatal burn injuries also occurred [Tessmer, 1994]. A breakdown of the Fatal Accident Reporting System (FARS) data for cars, vans and trucks according to location of collision impact showed that there was a factor of greater than four times more front end collisions in which fire was judged to be the most harmful event in the collision as compared to rear-end collisions [Tessmer, 1994]. A large proportion of fires also occur after rear-end collisions and are likely related to fuel system leaks and underbody fuel-fed fires [Tessmer, 1994]. The probability of a fire given a rear impact was about twice that of frontal impacts and the probability of fire being the most harmful event for rear impacts was approximately three times greater than for frontal

impacts [Tessmer, 1994]. Depending on the fire scenario, conditions in the passenger compartment can become untenable after several minutes [Mangs and Keski-Rahkonen, 1994; Santrock et al., 1999a]. In the event of a post-collision fire with passengers either trapped or incapacitated inside the vehicle, a rapid and adequate response to the fire may reduce fire-related injuries and fatalities. In this manner, an automatic fire suppression system resistant to collision and capable of suppressing vehicle fires might be beneficial. The main objectives of such a system would be extinguishment of the fire and the prevention of re-ignition. Incomplete extinguishment of the gas phase flames will probably lead to little delay of fire growth and spread. Extinguishment of the gas phase flames only (partial extinguishment), may be successful in gaining time for passenger rescue depending on the details of the scenario. In the case of partial extinguishment, smoldering combustion or hot surface ignition of a leaking flammable fluid could lead to re-flaming. The time gained for escape by partial extinguishment depends on the details of the collision/fire scenario. In this sense, the ultimate goal of a fire suppression system is complete extinguishment and prevention of re-ignition.

Active fire suppression systems are currently used in a wide range of applications. Commercial suppression systems are available for fire protection in trains, boats, mining equipment, military equipment, and aircraft. The U. S. Army, for example, uses automatic fire suppression systems in the engine compartments of armored vehicles [Bolt *et al.*, 1997]. Some types of road vehicles have been fitted with commercially available active suppression systems. These include buses, trucks, and specialized vehicles such as racecars. In racing applications, both the passenger and the engine compartments may be protected using manual and/or automatic suppressant delivery systems. Suppression systems are also being developed for civilian automobile applications. A German automobile manufacturer has developed an automatic fire suppression system for the engine compartment of its passenger cars [Lim et al., 1997]. A fire suppression company in the U.K., has developed an automatic fire suppression system for the engine compartment of passenger automobiles using Halon alternatives [Lim et al., 1997].

This report is divided into three main sections. The remainder of Section 1 addresses a variety of topics including an overview of the character of post-collision vehicle fires and a framework for analysis of compartment fires including the effect of ventilation (induced by vehicle geometry) on suppressant mass requirements. A summary of fire suppression fundamentals and a description of fire suppressants then follows. The last part of Section 1 discusses the criteria that were used to select suppressants for testing. Candidate suppressants are reviewed and evaluated based on these guidelines. A brief discussion of fire detection is also included. Section 2 describes experiments designed to measure the distribution of a suppressant discharged through various nozzle types. These experiments were isothermal and did not involve any type of fire. The nozzles were subsequently used in the fire suppression experiments described in Section 3 to investigate the feasibility of active suppression in simulated vehicle fires. In Section 3, the fire suppression experiments are discussed.

In this study, four experimental configurations were developed to investigate the feasibility of active suppression in post-collision vehicle fires. Two classes of vehicle fires were considered,

based on the spatial origin of the fire [Tessmer, 1994]. The first involved fires occurring in the engine compartment and the second involved fires occurring under the vehicle. Fires involving overturned vehicles were not considered. Each of the four sub-sections in Section 3 describes a different experimental configuration. The four experimental configurations are listed in Table 1.

No standard laboratory apparatus exists for evaluating the effectiveness of a suppressant in extinguishing post-collision vehicle fires. The fire suppression experiments shown in Table 1 included a reduced-scale simulated engine compartment, a full-scale engine compartment in a mid-size passenger vehicle, a full-scale simulated underbody fire, and an underbody fire in a mid-size passenger vehicle. The objective of the experiments was to determine the critical mass of suppressant required to extinguish the test fires. A definition of critical suppressant mass is presented in Section 3.0.1. Sections 1.2.2 and 3.0.2 outline elements of the post-collision vehicle fires that were simulated in the experiments. Sections 3.1-3.4 describe the experimental apparatus, procedures and results for each of the experimental configurations. The apparatus in each of the experimental configurations included a fire zone and a suppressant delivery system. The experimental procedure in each of the four configurations was essentially the same. A fire was established and after a specified duration, a controlled mass of suppressant was delivered to the fire zone. After suppressant delivery, observation determined whether the fire was suppressed or not suppressed. The results of the experiments were recorded. A number of experiments investigated the effect of operating conditions on the critical suppressant mass. Key findings of the suppression experiments are summarized at the end of each sub-section of Section 3. References are cited in Section 4.

Table 1. Overview of Experimental Configurations.

Configuration No.	Scale	Fire Type	Vehicle Type
1	Reduced	Engine Compartment	Simulated
2	Full	Engine Compartment	Actual
3	Full	Underbody	Simulated
4	Full	Underbody	Actual

1.1 Character of Post-Collision Fire Scenarios

An engine compartment contains flammable and combustible substances including gasoline, hydraulic fluids, windshield washer fluid, anti-freeze, engine and brake oils, rubber, thermoplastics, and possibly magnesium. For example, a post-collision vehicle fire could be associated with a collision-damaged gasoline fuel rail or a spraying combustible fluid. A fire could begin immediately after a collision or several minutes later as was observed in a front-end barrier crash that was conducted as part of Project B.3 of the DOT/GM Agreement [Jensen et al., 1999]. In that event, a collision damaged thermoplastic battery case was observed to be the initial fuel source.

At least three ignition sources may be present in a post-collision vehicle including friction sparks generated during the collision, hot surfaces (e.g., exhaust manifold or catalytic converter) to which flammable fluids (e.g., gasoline, windshield washer fluid) or combustible fluids (e.g., motor oil, transmission fluid) might be exposed, or shorted wires that could generate electrical sparks [Jung et al., 1997]. Understanding the early moments of a post-collision vehicle fire, that is, the initial interaction of ignition sources and combustible materials, would be helpful in developing appropriate fire suppression test protocols. A clear understanding of the identity of the initial fuel sources, ignition sources, and early fire time-lines would provide a realistic basis for formulating appropriate fire intervention strategies.

Unfortunately, detailed quantitative information is not available. Although anecdotal evidence exists regarding post-collision vehicle fires, there is little information available associated with early fire time lines, particularly ignition source and initial fuel type. For example, reliable quantitative information is not available regarding leak rates of flammable fluids (e.g., gasoline or windshield washer fluid) that occur in collisions. Nor is information available regarding the location of leaks relative to a vehicle, for example, the average length and orientation of a gasoline trail with respect to the vehicle. Because so little information is available on post-collision fire scenarios, the test protocols developed in this study were designed with the intent of creating plausible fire scenarios.

A post-crash vehicle fire, unlike many other fire scenarios, is characterized by several problems that combine to create a complex and challenging situation for active fire protection. Each of these challenges associated with suppression of a post-collision vehicle fire limits the range of possible fire protection solutions. A number of them are listed below:

- The post-collision vehicle fire problem is not well documented. In particular, early fire time lines have not been adequately researched, so that there is little information regarding the initial fuel, its relative location, spatial distribution, and amount.
- The geometry of every vehicle make and model differs, which influences fire spread and growth.
- Post-crash vehicle fires differ from fires in intact vehicles, as the geometric configuration may be modified by the collision in ways that cannot be precisely defined beforehand.
- Suppression system placement is restricted by limitations associated with vehicle function and the crash survivability.
- Practical considerations limit the mass and volume of an on-board suppression system.
- Ambient factors such as temperature and wind may impact suppression system performance.
- Vehicle fires occur in unconfined compartment that is partially open to the environment, which leads to suppressant losses.

The particular crash scenario will govern the rate and relative location of fuel leakage, and these details will influence the severity of the fire and the probability of successful fire suppression. Vehicle fuel system integrity in moderate speed collisions is governed by Federal Motor Vehicle Safety Standard 301, which became effective in 1978. Paragraph S5.6 of this standard mandates that fuel spillage will not exceed 5 ounces ($\approx$500 mL) for the first 5 minutes during a vehicle

rollover test. The purpose of this standard is to reduce deaths and injuries occurring from fires that result from fuel spillage during and after motor vehicle crashes. NHTSA research with high speed rear-end collisions led to a rough estimate of an average fuel leak rate of approximately 1 L/min [Ref. 9 in Ohlemiller and Cleary, 1998]. Such a leak rate could sustain a steadily burning pool fire with a diameter of nearly 0.5 m and flames nearly 1 m in height [Ohlemiller and Cleary, 1998]. Once a vehicle is stationary after a collision, leaking fuel will lead to a fire that is located under the vehicle underbody. It is also possible that a trail of fuel could extend beyond the vehicle footprint, due to fuel leakage during vehicle movement or due to the incline of the road surface. Depending on the collision scenario, it is also possible that a pool fire could be situated around the footprint of a vehicle tire. A tire would create a large flow obstacle for a stream of suppressant, making suppression more challenging. If the internal pressure of the fuel tank becomes super-atmospheric due to heating by a fire, a pressurized leak could occur, which may be challenging in terms of suppression [Demers, 1995].

1.2 Analytical Framework

An estimate of the critical mass required to suppress a fire in a compartment must consider the volume of the protected space. Other factors may also play a role in fire protection design. The geometry associated with an engine compartment or a vehicle underbody is complex and every vehicle make and model is characterized by a specific geometry. Every engine compartment and vehicle underbody is distinct in terms of size, dimensions, and arrangement or configuration. Every vehicle type contains unique components made from different materials, formed into unique shapes, and positioned in particular locations. Vehicle options, such as air conditioning or engine size, available on an individual make and model cause further differentiation. A collision can further differentiate vehicle geometry, depending on the collision scenario. For simplicity, this study considers vehicle geometry based on elements from the same four representative vehicle types that were selected for testing as part of Project B.3 of the Fire Safety Research Program established by the DOT/GM agreement [Jensen et al., 1999]. The first four entries in Table 2 are these representative vehicles, whereas the other entries refer to the experimental apparatus utilized in this study. Table 2 lists several relevant geometrical features of the representative vehicles and experimental apparatus, which are defined and described in detail in Section 1.2.2.

1.2.1 Review of Fundamental Aspects of Fire Suppression

The key parameters that affect flame stability and thereby control flame extinction and the prevention of reignition are suppressant concentration and flow field dynamics. Flow field dynamics govern the rate of suppressant entrainment and the concentration of suppressant in a fire zone. Engineering parameters involving the suppressant distribution system must be also considered because these impact suppressant dispersion, transport, and mixing. These include nozzle type, number, placement, orientation, reservoir size, and pressurization. Parameters

Table 2. Geometrical Features of Representative Uncrashed Vehicles and Test Apparatus.

Vehicle	$W \times L \times D'$ [A] (m^3)	V [B] (m^3)	$\%VF$ [C]	$\%SO$ [D]	$\%AF$ [E]	F [F] (m)
1997 sport coupe	1.5 x 0.8 x 0.8	1.0	40	12	84	0.18
1996 sport utility	1.4 x 0.8 x 1.1	1.4	20	19	83	0.33
1996 mini-van	1.5 x 0.7 x 1.0	1.0	50	11	86	0.16
1996 mid-size sedan	1.3 x 0.8 x 0.8	0.8	40	13	90	0.18
1984 mid-size sedan test vehicle	1.5 x 0.7 x 1.0	1.0	24	10	85	0.18
Engine compartment Simulator	0.7 x 0.9 x D' 0.51<D'<0.57	Variable 0.32 to 0.36	Variable 10 to 40	Variable 0.2 to 20	Variable 8 to 93	Variable 0.01 to 0.13
Underbody Simulator	na*	na	na	na	na	0.30

*: not applicable.

A: extended compartment dimensions, see Eq. 1 in Section 1.2.2.

B: extended compartment volume, see Eq. 1.

C: percentage of the compartment volume filled with components.

D: percentage of the compartment surface open to the environment.

E: percentage of the area of the top plane of the compartment that is occupied by components.

F: height of the vehicle side panels above the ground.

characteristic of the configuration should also be considered. These include ambient effects (wind), geometric effects (flow field obstacles; the percentage of an enclosure that is enclosed or open to the environment), and fuel effects (fuel type, its location, and its flow rate). Other factors may also influence fire suppression including heat transfer from nearby hot components or the flow field velocity, which is influenced by vehicle movement or operation of the engine fan. Bearing this in mind, it is valuable to consider simple analytic suppression models, thereby creating a framework by which the experimental results can be analyzed. Such a model is outlined in Section 1.3.1.

Pitts *et al.*, [1990] outlined current understanding of fire suppression, incorporating a comprehensive review of the relevant literature, in addition to a discussion of suppressant effectiveness, test methods, and the role of different suppression mechanisms. A large number of studies have been conducted on fire suppression and a great deal is known about the relative efficiencies of various suppressants in laminar flames [Grosshandler *et al.*, 1994]. Mechanisms of flame inhibition are discussed in Pitts *et al.* [1990] and Grosshandler *et al.* [1994]. Global mea-

sures of the chemical effectiveness of a suppressant can be quantified through flame enthalpy considerations [Tucker *et al.*, 1981; Sheinson *et al.*, 1989]. Fundamental theories have been developed that describe the interaction of chemical and transport processes that cause flame extinction in simple laminar systems [Williams, 1974]. In vehicles, combustible fluid fires may occur either in the form of a spray, a dripping leak, or a capillary type leak. A search of the fire and combustion literature indicates that no studies have focussed on the suppression of fires burning leaking fluids. In simple combustion configurations (i.e., cup burner and counterflow flame experiments), flame extinction studies have shown that, in general, gaseous fuels require higher agent concentrations to extinguish than liquid fuels, which require higher agent concentrations than solid combustibles [Hamins et al., 1994; Seshadri, 1977]. The fundamental studies of fire suppression in simple clean systems are directly relevant to an understanding of the suppression of turbulent fires burning in dirty, smoky, obstacle-laden flow fields, because the physics of flame extinction is configuration independent [Linan, 1974].

In turbulent flames, such as a pool fire or a spray flame situated behind an obstruction, the required suppressant concentration corresponds absolutely to the results from suppression experiments in the cup burner test or the opposed flow diffusion flame test [Hamins et al., 1994]. The critical concentration of a suppressant depends on the chemical and physical behavior of the suppressant, which is related to its transport, thermodynamic and chemical properties. The effect of fuel type on suppression requirements is secondary. For example, laminar flame studies show that heptane is somewhat more difficult (requiring 5 % to 15 % more suppressant) to extinguish than hydraulic fluids or other hydrocarbon fuels such as gasoline and toluene [Hamins and Seshadri, 1986; Hamins et al., 1994]. The central challenge for the fire suppression system designer is to insure a critically high concentration of suppressant simultaneously, throughout the flow field, insuring flame suppression wherever the fire may be. A reasonable target concentration for turbulent flames in an unventilated enclosure is the concentration that extinguishes cup burner flames [Grosshandler et al., 2000; Hamins et al., 1995]. Estimates of suppressant requirements of full-scale turbulent flames are adequately represented by cup burner flames because the same fundamental processes occurr in full-scale and reduced scale. The use of this notion is used in Section 1.2.3 to construct simple formulas for suppressant mass requirements within an enclosure. It should be noted that increased turbulence, which may be self-induced or associated with external forces, leads to "strained" flames that are actually easier to extinguish than flames that are not strained [Hamins and Seshadri, 1986].

The critical suppressant mass required to suppress a fire is directly proportional to the ventilation rate for a suppressant that is uniformly injected throughout the volume of interest (see Eq. 22 in Section 1.2.3). This implies that the effectiveness of an active fire suppression system would be compromised if the vehicle is moving or if the radiator fan is operating when the system is deployed. Immediately following a collision, a vehicle may continue to move for several seconds. As the vehicle is moving, the ventilation rate or the mass flow of air into the protected volume is related to the wind and vehicle velocities. In such a case, it might be advantageous to deliver a suppressant after the vehicle has stopped moving. In the event of an engine compartment fire, if the fan is off and the vehicle is not moving, then the ventilation rate into the compartment is

controlled by the air entrained by the fire and ambient winds. The ventilation rate with the fan on can be significantly higher than the ventilation due to the air entrained by the fire. Accordingly, it may be advantageous to deliver a suppressant when the fan is off. In this case, suppressant transport cannot rely on forced ventilation to carry the suppressant through an obstructed flow field to the fire zone. Instead, the suppressant must be actively propelled to the fire zone.

1.2.2 Effect of Vehicle Geometry and Ventilation on Suppressant Requirements

The size of openings in a compartment or enclosure and the position of those openings affect the burning behavior of a fire. The ventilation or compartment openings influence local mixing and temperatures [Drysdale, 1999], which has an impact on suppressant effectiveness. The size of openings on the surfaces bounding the perimeter of the compartment relative to the suppressant delivery location can affect the amount of suppressant required to achieve suppression. In a sealed compartment where there are no suppressant losses to the exterior, extinguishment is much easier to accomplish than in a partially open compartment. In a closed system, it is rather simple to estimate suppressant requirements. For an infinitesimally small fire in a sealed compartment, a good estimate of the required suppressant concentration is the critical suppressant concentration measured in small scale suppression experiments, such as the cup burner test [Hamins et al., 1994]. In an unventilated closed system, the suppressant discharge rate and location would be of lesser importance. In a typical passenger vehicle engine compartment, a bottom surface is not present, although a portion of that surface may be covered by air dams or close-out panels situated along the front bottom portion of the engine compartment. In addition, some vents may exist around the compartment perimeter.

The post-crash engine compartment environment was documented as part of Project B.3 of the DOT/GM agreement [Jensen, 1997]. Those experiments showed that a front-end crash can transform the engine compartment of a vehicle depending on the scenario. The hood may buckle, creating a gap or space between portions of the hood edges and the body panels. The size of these gaps, if they occur, depends on the details of the collision scenario as well as the hood design, which typically has a prescribed buckle line or crush initiator laterally traversing the hood. By design, the hood is tied to the vehicle body at several points, at the central front portion of the hood and at two locations towards the rear. The average gap distance (H) that the hood is lifted above the vehicle body is a function of the details of the crash scenario and vehicle design. The size of the gap can affect the amount of suppressant required to extinguish a fire. If the hood were completely removed, for example, it is likely that fire suppression would be very difficult to achieve. The effect of the hood opening on suppression requirements was investigated in the reduced-scale compartment fires (Section 3.1).

In this report, an "extended" compartment is considered, which is defined as the compartment volume plus the volume directly below the compartment that extends to the ground. Using this definition, a fire on the ground below the compartment is considered an engine compartment fire. This situation could occur, for example, due to the dripping of a melting/burning thermoplastic

component, or a burning puddle of combustible fluid. If not extinguished, a fire on the ground could re-light a dripping fluid in the compartment proper, posing a reignition hazard. For an idealized rectangular engine compartment, with the hood having the same length and width as the compartment, the extended compartment volume (V) is equal to the product of the compartment length, width, and depth, defined as:

$$V = L \cdot W \cdot (D + F + H) = L \cdot W \cdot D' \quad (1)$$

where H, F, D, W and D' are illustrated in Fig. 1. H is the average hood gap distance, F is the height of the frame above the ground, D is the compartment depth, W is the compartment width, and D' is the sum of F, D, and H, i.e., the average distance between the hood and the ground ($D'=F+D+H$). L is the compartment length. The values of H, F, D, W and D' are here taken to represent the idealized post-collision vehicle geometry. It is useful to consider the sum of the volume of the components within the compartment (VF). The difference between V and VF is equal to the unfilled volume or free space within the compartment. From a fire suppression perspective, this is the volume that must be protected. Table 2 lists the dimensions of the extended engine compartment ($WxLxD'$), the extended volume (V) of the compartment (defined in Eq. 1), the percentage of the extended volume filled with components ($\%VF$), the percentage of the perimeter surface of the compartment that is open to the environment ($\%SO$), the percentage of the area of the top plane of the compartment that is occupied by components ($\%AF$), and the nominal height of the vehicle side panels above the ground (F) for a number of representative vehicles and for the experimental devices used in this project. All of the parameters listed in Table 2 refer to the vehicle engine compartment or the simulated engine compartment used in the experiments described here. The parameter F is also useful in characterizing the underbody configuration.

Table 2 shows that the extended volume, V, (see Eq. 1) is typically about 1 m^3, with the percentage volume filled ($\%VF=100 \cdot VF/V$) varying from 20 % to 50 % for the extended uncrashed compartment volume. The percentage of the extended volume filled with components was estimated as 50 % for a minivan (with a 3 L engine). Placement of a larger engine into the same volume would significantly decrease the free volume and increase the volume displaced by components. Table 2 also lists the percentage of the surface bounding the engine compartment volume that is open (SO) to the environment. Table 2 shows that SO typically varies from 10 % to 13 %, with the exception of the uncrashed sport utility vehicle, for which SO=19 %. For the simple rectangular compartment shown in Fig. 1, the percentage of the perimeter surface that is open to the environment is defined as:

$$SO = 100 \cdot 2 \cdot (W + L)(H + F) / [2 \cdot (W + L)(F + D + H) + 2 \cdot (W \cdot L)] \quad (2)$$

and SO can be broken into two parts:

$$SO = SO_{frame} + SO_{hood} \quad (3)$$

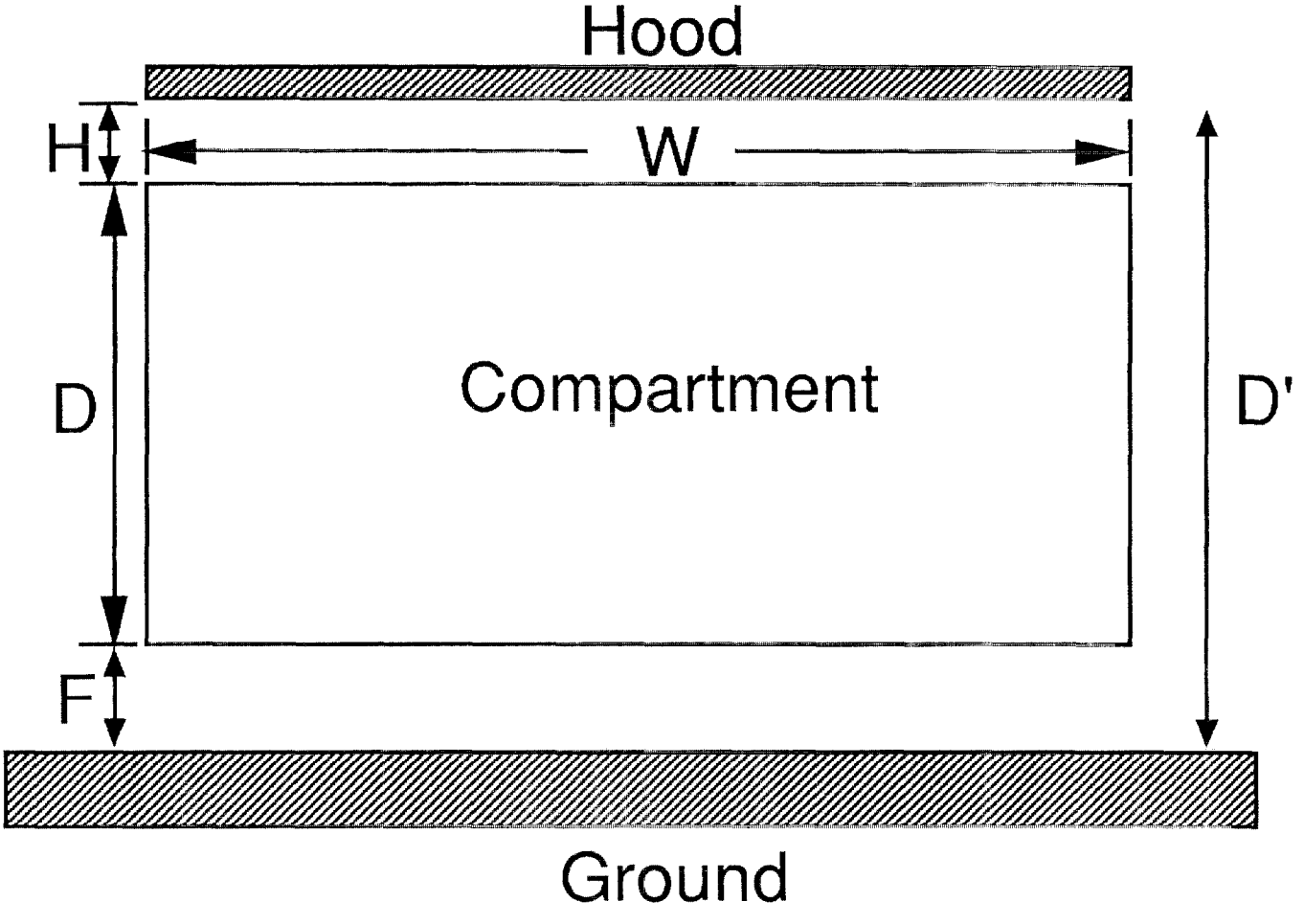

1. Schematic drawing of the frame of an idealized engine compartment.

The first term on the right hand side of Eq. 3 is due to the side panels or frame being lifted above the ground. Referring to Fig. 1,

$$SO_{frame} = 100 \cdot 2 \cdot (W + L)\, F / [2 \cdot (W + L)\, (H+F+D) + 2 \cdot (W \cdot L)] \quad (4)$$

And the second term is associated with the gap between the hood and the side panels:

$$SO_{hood} = 100 \cdot 2 \cdot (W + L)\, H / [2 \cdot (W + L)\, (H+F+D) + 2 \cdot (W \cdot L)] \quad (5)$$

In Eqs. 4 and 5, the first term in the denominator represents the sum of the lateral surfaces extending between the hood and the ground. The second term in the denominator represents the sum of the hood area and the ground area subtended by the compartment. The value of SO should be corrected for the surface enclosed by the tires, which in an actual vehicle typically reduces SO by a factor of approximately 0.1. The average gap distance (H) impacts the value of SO. Because no statistical information is available on the average value of H in post collision vehicles, this parameter was estimated based on engineering judgement and a small, informal survey of vehicles with crumpled hoods. The survey results showed that crumpled hoods had gaps or spaces between the hood and the body panels that typically were on the order of 2 to 10 cm high and 10 cm to 30 cm long, and approximately triangular in shape. Gaps usually occurred on both sides of the hood (laterally) and were also often observed at the rear of the hood. The total gap area was estimated as 0.003 m^2 to 0.05 m^2, which represented approximately ¼ % to ½ % of the compartment surface area (SO). The change in the value of SO associated with a bent hood was estimated as ≈5 %. The survey results may be biased towards small values of SO_{hood}, because the survey included only (presumably) functioning vehicles.

Table 2 shows that the percentage of the area of the top plane of the compartment that is occupied by components ($\%AF$) typically varies from 80 % to 90 %, depending on the make, model, and options. The top plane of the compartment is the plane defined by the uppermost components in the compartment. The depth of the voids or spaces between the components typically extends to the ground or to a layer of components just above the ground. If $\%AF$=100, then the top plane of the compartment would be completely filled with components, assuring that suppressant delivered above this plane would not be able to penetrate to the lower reaches of the compartment. For a suppressant delivered into the zone between the top layer of components and the top panel, it is expected that AF may impact suppressant effectiveness.

Since there are a multitude of crash scenarios and vehicle types, this study considers idealized geometric characteristics. For example, the engine compartment is idealized here as rectangular, which simplifies the analysis. Consideration of a complex geometric configuration would yield the same estimates of suppressant requirements, since the details of the geometry do not play a role in the simple analysis of suppression requirements outlined in this Section. After a front-end crash, the distribution of clutter will change as items move and are compressed by the impact. In general, length scales representing distance between objects will shorten in high crush zones. Depending on the crash scenario and vehicle, as the hood changes shape and as the front panel

separating the passenger and engine compartments is pushed backwards, the extended compartment volume will change. Observation of the vehicles crashed in Project B.3 suggest that the magnitude of the changes in the parameters listed in Table 2 (*%VF, %SO,* etc.) depend on the crash scenario as well as the make and model of the vehicle [Cleary, 2000]. Detailed measurements were not made on changes in the parameters listed in Table 2 (*V, %VF, %SO,* etc.) between crashed and uncrashed vehicles, but estimates of the change in the value of the parameters were considered. For example, changes in V due to collision ranged from approximately +10% to -30% [Cleary, 2000]. Changes in *%VF* due to a collision are proportional to changes in V. Changes in the average value of F are assumed to be negligible. It is presumed that collision induced changes in AF led to increased values on the order of several percent as compared to the values listed in Table 2, depending on the crash scenario and the vehicle type. Changes in *%SO* due to collision was estimated as ~5% (see discussion above, in this Section). For these reasons, changes in the values of the parameters listed in Table 2 due to a collision were taken as similar to the variation in these parameters associated with vehicle make, model, year, and options. The effect of these parameters on suppression requirements was investigated over a range of values in the reduced-scale engine compartment experiments and is discussed in detail in Section 3.1.4.2. Other assumptions used in this study are described in Section 3.0.2, which focuses on specifics of the design of the fire suppression experiments.

1.2.3 Estimate of Suppressant Requirements in a Compartment

From a design perspective it would be useful to have a simple analytical model that predicts suppressant requirements for a fire within a generic engine compartment for a given geometry and fire size. Conceptually, there are several possible approaches to modeling the interaction of a suppressant with a fire. In systems with well-defined ventilation, simple analytic models that idealize mixing have been successfully used to predict suppressant requirements. These models are less accurate in a situation without perfect mixing of the suppressant in the compartment or target volume, or when a significant percentage of the boundary is open to the environment. This is discussed in Section 3.1.4.2 in terms of experimental results in the reduced-scale compartment. Despite these obvious limitations, it is of value to consider these models because they highlight a number of the parameters that play a role in the suppression process.

Comparison of flame suppression measurements in different combustion configurations is facilitated by a discussion of the average suppressant concentration within a volume of interest. The suppressant mass required to extinguish an infinitesimally small flame in a sealed enclosure or compartment can be estimated from small scale suppression experiments. If the suppressant is uniformly delivered throughout the enclosure, the critical suppressant mass required to achieve suppression (W_i) is equal to:

$$W_i = \rho \cdot V \cdot Y_c \tag{6}$$

Where Y_c is the critical suppressant mass fraction in the (combined) air and suppressant streams.

The value of Y_c can be taken from the results of cup burner or other small-scale laboratory non-premixed flame suppression experiments and ρ is the average gas phase density within the compartment of volume V. If a portion of the volume is partially filled with components, then the required suppressant mass is reduced:

$$W_i = \rho (V - V_f) \cdot Y_c \tag{7}$$

where V_f is the volume filled by the components. Rearranging Eq. 7, the suppressant critical specific density ($\rho \cdot Y_c$) is equal to the mass requirement per unit volume:

$$\rho \cdot Y_c = W_i / (V - V_f) \tag{8}$$

Equation 7 suggests that the critical suppressant mass (W_i) scales with the free volume (V-V_f) in a closed compartment. If a suppressant is not uniformly delivered throughout a cluttered volume or, equivalently, if the gases in the compartment are not perfectly mixed, then the critical suppressant mass requirement (W) will differ from W_i. If the suppressant is delivered directly onto a small fire within a large volume and the gases are not perfectly mixed, then it is reasonable to expect that $W < W_i$. If the suppressant is delivered far from the fire and the gases are not perfectly mixed, then it is reasonable to expect that $W > W_i$.

For a fire within an enclosure that is not perfectly sealed, air is entrained into the fire and the enclosure at a rate approximately equal to [Delichatsios, 1995]:

$$\dot{M}_{air} = 10 \cdot (S + 1) \cdot \dot{M}_f \tag{9}$$

where S is the stoichiometric air to fuel mass ratio, $\dot{M}_i$ refers to the mass rate of air entrained into the fire, and $\dot{M}_f$ is the mass burning rate of fuel. Considering heptane (C_7H_{16}), for example, S is determined from the stoichiometric relation:

$$C_7H_{16} + 11\,(O_2 + 3.76\,N_2) \rightarrow 7\,CO_2 + 8\,H_2O + 11 \cdot 3.76\,N_2 \tag{10}$$

where 100 g (=1 mol) of heptane reacts with 1516 g (=52.36 mol) of air. For heptane, S = 15.16 and Eq. 9 yields: $\dot{M}_{air} = 161.6\dot{M}_f$.

Considering simplified flow conditions is often useful when describing fluid mixing and is imperative if simple analytical solutions for suppressant mixing in an enclosure are to be obtained. One such situation is to treat fluid flow within the enclosure as perfectly mixed. This may be appropriate for a high momentum discharge, such as the rapid discharge of a Solid Propellant Generator (SPG) fire suppression device in a partially open compartment. Application of other types of simple mixing models are possible, but are unlikely to represent the complex mixing and interaction with components. If mixing within the enclosure is considered perfectly stirred, such that the entrained air and injected suppressant are uniformly distributed instantaneously, then the

time dependent suppressant concentration (initially zero) in the compartment, X(t), is given by:

$$X(t) = (1/\tau)\, e^{-t/\tau} \int e^{t/\tau}\, X_i(t)\, dt \tag{11}$$

which is the solution to the non-homogeneous linear first order differential equation describing suppressant mixing:

$$X_i(t) = \tau\, [dX(t)/dt] + X(t) \tag{12}$$

where τ is the appropriate mixing time and $X_i(t)$ is defined as the ratio of the volumetric rate of suppressant injected into the compartment to the sum of the volumetric rates of entrained air and injected suppressant:

$$X_i(t) = \dot{Q}_i / (\dot{Q}_i + \dot{Q}_{air}) \tag{13}$$

For a perfectly stirred reactor, the characteristic time (τ) can be described in terms of the compartment volume, the volumetric rate of air entrainment ($\dot{Q}_{air}$) and the volumetric rate of suppressant discharge ($\dot{Q}_i$):

$$\tau = (V - V_f)/(\dot{Q}_{air} + \dot{Q}_i) \tag{14}$$

where $\dot{Q}_{air}$ is related to the mass of air entrained due to the fire:

$$\dot{Q}_{air} = \dot{M}_{air} / \rho_{air} \tag{15}$$

To assess whether the rate of suppressant delivery is sufficient to extinguish the fire, the integral in Eq. 11 must be evaluated. This can be accomplished either numerically or analytically. For a system with a square-wave type suppressant discharge, defined as:

$$X_i(t) = 0 \text{ for } t < 0 \tag{16}$$
$$= a \text{ for } 0 \le t \le \Delta t \tag{17}$$
$$= 0 \text{ for } t > \Delta t \tag{18}$$

where a is a constant, the solution to Eq. 11 for the concentration $X(t)$ in the compartment is:

$$X(t) = a\,(1 - e^{-t/\tau}) \tag{19}$$

When the suppressant discharge duration is Δt, then $t = \Delta t$, and the solution for the critical rate of suppressant discharge is similar to the form of Eq. 19 [Hamins et al., 1995]:

$$\dot{Q}_i / \dot{Q}_t = a/(1 - e^{-\Delta t/\tau}) \tag{20}$$

where $\dot{Q}_t$ is the total rate of volumetric addition to the compartment, which includes suppressant discharge and air entrainment:

$$\dot{Q}_t = \dot{Q}_i + \dot{Q}_{air} \tag{21}$$

To achieve suppression, the value of α in Eqs. 19 and 20 must be greater than or equal to a critical value, X_c. A reliable prediction of critical mass requirements in the suppression of baffle stabilized flames has been achieved using Eqs. 19 and 20, with the value of α (defined in Eq. 17) based on the results of suppression experiments using a cup burner [Takahashi et al., 1999; Grosshandler et al., 1999]. Solving for $\dot{Q}_i$ in Eqs. 20 and 21 leads to:

$$\dot{Q}_i = X_c \dot{Q}_{air} / (1 - X_c - e^{-\Delta t/\tau}) \tag{22}$$

For a long duration suppressant discharge (i.e., $\Delta t >> \tau$), Eq. 22 yields: $\dot{Q}_i = X_c \dot{Q}_{air} / (1 - X_c)$.

Using Eqs. 9, 15, and 19, Eq. 22 can be rewritten in terms of the critical rate of mass discharge of the suppressant ($\dot{M}_i$) as:

$$\dot{M}_i = 10 X_c (S+1) \dot{M}_f (\rho_i / \rho_{air}) / (1 - X_c - e^{-\Delta t/\tau}) \tag{23}$$

where $\dot{M}_i$ is related to $\dot{Q}_i$ as:

$$\dot{Q}_i = \dot{M}_i / \rho_i \tag{24}$$

Equation 23 relates the critical suppressant mass discharge rate to the fuel burning rate ($\dot{M}_f$) through Eq. 9. It should be noted that because τ is a function of $\dot{Q}_i$ and $\dot{M}_i$ through Eq. 14, Eq. 23 must be solved iteratively. For extinction of a heptane fire by gaseous N_2, $X_c = 0.32$ [Hamins et al., 1995], S=15.16, and (ρ_i / ρ_{air})=0.967. Then, for $\Delta t >> \tau$, Eq. (23) becomes:
$\dot{M}_i = 74\ \dot{M}_f$.

The required suppressant mass (W_i) is the product of the average suppressant discharge rate ($\dot{M}_i$) and the suppressant discharge duration (Δt):

$$W_i = 10\ \Delta t\ X_c (S+1)\ \dot{M}_f (\rho_i / \rho_{air})\ /\ (1 - X_c - e^{-\Delta t/\tau}) \tag{25}$$

Equation 25 shows that the value of W_i is linearly proportional to the fuel mass burning rate, $\dot{M}_f$. Equation 25 also suggests that it is advantageous to inject a suppressant over as short a duration as possible. To achieve flame suppression (*i.e.*, $X = X_c$), then the discharge duration is limited to periods such that the denominator is greater than zero or:

$$\Delta t > -\tau \ln(1 - X_c) \tag{26}$$

Equation 26 is consistent with the physical limits imposed by Eq. 20 for an infinitesimally small

fire and $\dot{Q}_t = \dot{Q}_i$. If wind is present, then $\dot{Q}_{air}$ must be modified to represent its effect.

In summary, many assumptions must be stipulated to develop a simple analytical model for fire suppression in a closed compartment. To achieve extinction assuming a perfectly stirred reactor model, the local suppressant volume based concentration (X) must be greater than the critical concentration (X_c) in the fire zone. Matters are further complicated because entrainment of a suppressant into a fire zone is influenced by the geometric configuration, such as the placement of components that obstruct suppressant transport to the fire zone. In an obstacle laden configuration, these difficulties can be overcome with deliveries of large suppressant mass. In an open compartment, with suppressant flow dependent on the clutter field and suppressant able to escape through the partially open compartment surface, the assumptions leading to Eqs. 23 and 25 become tenuous, and the equations will underestimate suppressant mass requirements. The utility of this model is tested in Section 3.1.4.3 using the results from the reduced-scale compartment suppression experiments.

An entirely different approach to analyzing suppression requirements within an enclosure is computational fluid dynamic (CFD) modeling. Comprehensive models of suppression in a cluttered flow field require a detailed understanding of the transient transport of suppressant and air, as well as the thermodynamics and chemical processes and their interaction. Such calculations are in their infancy and are certainly beyond the scope of this report [Tiezen, 1999]. A simplified CFD approach, however, is possible. The main value of this type of model is that it provides a picture of suppressant transport through flow field obstacles such as engine components and accounts for ventilation effects.

The NIST Large Eddy Simulation (LES) fire model has been described previously in detail [McGrattan et al., 1994; 1998a; 1998b]. The NIST models have been validated through detailed fire structure measurements as well as flame suppression measurements [McGrattan 1998a; Grosshandler et al., 1999; 2000]. The calculation determines a solution to the three-dimensional Navier-Stokes equations. The model was developed for low Mach number, buoyancy-driven flows. The model provides spatial resolution over length scales spanning two orders of magnitude. Any phenomena occurring at length scales smaller than the size of a grid cell need to be modeled, including sub-grid scale turbulence and combustion [McGrattan et al., 1994; 1998a; 1998b]. The intent of the LES model is to calculate the transport of suppressant in regions of the flow field where the Mach number is less than $\approx$0.3, because the model formulation includes a filtering of acoustic waves. Where the Mach number is greater than 0.3, i.e. at a suppressant nozzle, an approximation to the boundary condition is used. A fully compressible flow solver would increase the computing time by an order of magnitude, and the only benefit would be in the vicinity of the nozzle. In this study, the suppressant discharge was approximated by reducing the suppressant velocity and increasing the diameter of the nozzle, such that the mass flux was invariant. Using this approach, the general features of the mixing and transport away from the inlet have been shown to be accurate [McGrattan et al., 1996]. In this study, combustion was modeled using Lagrangian particles to represent the fuel, and their burning characteristics (McGrattan et al., 1998a; 1998b). The effect of an extinguishing suppressant such as N_2, on the

combustion process is modeled by turning off the combustion and heat release when the oxygen concentration falls below 14 % (based on cup burner suppression experiments). This model was used to interpret some of the experimental results described in Section 3.1.4.3.3.

1.3 Suppressants

Fire protection engineers classify suppressants according to their suitability for application on various fire types. Fire types are generally classified according to the fuel involved. Class A fires generally involve ordinary combustibles such as wood, fabrics, paper, rubber, and some types of thermoplastic. Class B fires generally involve flammable or combustible liquids, gases, and flammable liquid derived solids, such as paraffin or heavy lubricants. Class C fires involve energized electrical components, where safety to the operator requires an electrically nonconductive suppressant. Class D fires involve certain combustible metals. Specific suppressants may be appropriate for more than one type of fire.

Class A combustibles are found within the engine compartment of vehicles, but represent a small percentage of the total mass of flammable fluids and materials on a vehicle [Abu-Isa, 1997; Ohlemiller and Shields, 1998]. These include materials made of rubber and charring thermoplastics such as ABS or phenolic. The transition from smoldering combustion to flaming combustion can occur with these materials under certain conditions. Class B combustibles are also commonly found within the engine compartment. These substances include gasoline, hydraulic fluids, and other oils. Electrical shorting may lead to the creation of hot surfaces, which warrant a Class C fire designation. Under certain conditions, the vehicle battery and electrical system could pose such a hazard. Some recent measurements have shown that Class C fires can be controlled by suppressants at concentrations appropriate for Class A fires [McKenna et al., 1998]; others have presented results leading to the opposite conclusion [Smith et al., 1999]. The electrically energized fire is not simply a suppression problem. It is also an ignition problem that may be addressed through passive fire prevention strategies.

Although magnesium and other combustible metals are presently used in some vehicle components and are becoming more prevalent in vehicle applications, significant heating is required before ignition occurs. To be successful, it is beneficial that an active fire suppression system be activated early in the history of a fire, before the fire spreads and grows, and before a Class D material ignites. For this reason, Class D fires are not considered in this study. For use in engine compartment applications, a suppressant must, therefore, be effective primarily on fires involving combustible vehicle fluids and thermoplastics. It would also be beneficial if the suppressant is effective on smoldering materials and is able to cool hot surfaces.

Direct impingement of a suppressant onto a fire is the most mass efficient method of fire suppression. In an engine compartment, such a situation, regardless of suppression system design, is unlikely to occur due to flow field obstacles presented by components. This is also the case after a collision. Understanding key geometric parameters that affect suppressant dispersion is

important for estimation of minimum mass requirements.

Parameters potentially affecting suppressant delivery through clutter include the suppression system design and the clutter geometry. The relevance of these parameters remains largely unknown as little research has been conducted on this aspect of the engine compartment fire suppression problem. The effectiveness of a suppressant in an obstacle laden environment with an unpredictable layout is an important element in the development of a post-crash fire suppression system for vehicles. In this total flooding type approach, the suppressant must be transported throughout the zone to be protected.

Active fire suppression systems are currently used in a wide range of applications including trains, boats, mining equipment, military equipment, military and commercial aircraft, and motor vehicles such as buses, trucks, and racing cars. Table 3 lists a number of examples of applications of common and emerging fire suppression technologies [Bennett, 1997]. For each of the applications, fire protection system manufacturers and suppliers recommend specific suppressant types. Specifications for the suppressant systems are based on proprietary research programs and years of experience in the business. Unfortunately, little or none of that information is available publicly. The suppressants are typically dry powder or liquefied compressed halogenated gases. Some of these commercially available active suppression systems may prove to be appropriate for post-collision vehicle applications. A number of emerging technologies may also prove to be appropriate for post-collision applications including solid propellant generators (SPG) and their hybrids, SPG driven foam systems, fire activated tubular suppressants as well as others.

Table 3 indicates some of the options available in selecting fire suppressants for vehicle fire protection. A variety of suppressant types and delivery mechanisms are available. Suppressant types include inert and halogenated compounds, liquid mists, chemically generated agents and dry chemical powders. The next section describes a set of criteria used to guide suppressant selection for testing in the experiments conducted on fires in simulated vehicles (see Section 3).

1.3.1 Selection of Suppressants for Testing

In this section, a set of criteria is constructed for screening suppressants for the suppression experiments conducted in this study. Table 4 lists some of the major issues that were considered. Table 4 presents a list of representative and promising suppressant types, based on information from manufacturers and on Table 3. The suppressants were partitioned into four categories including the clean agents, which are the inert gases and halocarbons, water-based suppressants, dry-chemical powders, and prototype suppressants. The suppressants were evaluated in terms of certain selection criteria and a number of potentially promising suppressant types were selected for testing.

The first category in Table 4 is the clean suppressants. As their name implies, these chemicals leave no residue upon discharge. The clean suppressants include carbon dioxide (CO_2), as well as

the compressed liquefied halogenated compounds including HFC-125 (C_2HF_5) and HFC-227ea (C_3HF_7), which are common Halon 1301 (CF_3Br) replacement compounds. The clean suppressants act through a combination of physical and chemical mechanisms [Pitts et al., 1994]. All of the other suppressants listed in the Table leave some sort of residue.

Table 3. Examples of Commercially Available Suppressants and the Applications.

Application	Suppressant Type
Off-road vehicle engine compartment	ABC powder[A]
Enclosed marine engine compartment Bus engine compartment	Halon 1301[B] HFC-125[C] FE-241[D] ABC powder
Unventilated V-22 aircraft engine nacelles	SPG
Engine and passenger compartments in racing vehicles	Halon 1301 HFC-125
Ventilated and unventilated aircraft engine nacelles	Halon 1301 HFC-125 Halon 1202[E]
Limousine underbody protection	Aerosol Generator (under development) SPG (under development)
Tank Crew Compartment	Hybrid SPG[F]
Machinery Spaces	Water mist

A. mono-ammonium phosphate $(NH_4)H_2PO_4$, in the form of a powder.
B. Halon 1301 is a liquefied compressed gas (CF_3Br).
C. HFC-125 is a liquefied compressed gas (C_2HF_5).
D. FE-241 is a liquefied compressed gas (C_2HClF_4).
E. Halon 1202 is a liquefied compressed gas (CF_2Br_2).
F. Hybrid solid propellant generators rapidly discharge vaporized HFC-125 or water and some amount of CO_2, H_2O and N_2; (see discussion in the next section).

Table 4. Characteristics of Candidate Suppressants.

Type	Suppressant		Crash Vulnerable	False discharge Concern	Environmental concern	System mass	Hot[B] surface	$\rho \cdot Y_c$[C] (kg/m^3)
Clean	CO_2			X		**X**		0.41
	Halon 1301				**X**			0.19
	CF_3I			x[A]				0.20
	HFC-227ea							0.46
	HFC-125							0.43
Powder	Sodium Bicarbonate			Corrosion			p	0.12
	Mono-Ammonium Phosphate			Corrosion			**P**	0.13
Water-based	Water Mist/ Anti-Freeze		**X**	Electrically conductive		x	**P**	0.27
	Foam / Anti-freeze		x	conductive			**P**	16[D]
Prototype	Aerosol Generator			hot gas		x	p	≈0.1[E]
	Solid Propellant Generator	SPG1		hot gas				0.35[F]
		SPG2		hot gas			p	0.10
		SPG3		hot gas			p	0.18
	Hybrid SPG					**X**	p	0.3-0.5[G]
	Tubular						p	≈0.2

x indicates a minor concern; **X** indicates a serious concern (see text).

p indicates that some protection is provided; **P** indicates that significant hot surface/smoldering protection is likely provided.

A: NOAEL (no observed adverse effects level) value poses risks under certain circumstances [Tapscott, 1998].

B: suppresses smoldering and prevents hot surface ignition when applied indirectly to surface (total flooding).

C: values based on suppression measurements in cup burner [Hamins et al., 1995], pool fire [Ewing et al., 1988], and aircraft engine nacelles [Hamins et al., 1995]. The parameter ρ is the suppressant density (at STP); Y_c is the suppressant mass fraction in the oxidizer required for suppression. For reference, $\rho \cdot Y_c = 0.37$ for N_2.

D: based on an expansion ratio of 62 (Lim et al., 1997).

E: assuming that the effluent is 50 % K_2CO_3 and 50 % N_2 (mass basis) and that the particles are small (<15 μm).

F: estimate depends on effluent composition; see data in Table 5 and a description of this estimate in [Hamins et al., 1997], for example.

G: assuming that the secondary agent is water vapor or HFC-227ea [Mitchell, 1999].

The second category encompasses the powder suppressants. The powders are composed of solid particulates, typically 10 μm to 100 μm in diameter [Ewing, 1988]. In commercial powders, a small percentage of silica (SiO_2) is added to prevent agglomeration and insure suitable flow properties. The ABC powder is unique among the powders. When in contact with a hot surface it reacts to form cross-linked polyphosphoric acid [Camino et al., 1994], a glassy impenetrable substance that can smother a smoldering fire and create a layer of insulation over a hot surface, which prevents possible ignition of a combustible fluid on that surface. Other powders can also be expected to affect smoldering fires and prevent hot surface ignition, but mainly through physical processes rather than through a combination of chemical and physical processes.

The third category in Table 4 is the water-based suppressants. These include water mist and foam suppressants. Water-based suppressants cool surfaces and effectively address smoldering or Class A fires. Some of the water-mist suppression systems rely on a pressurized cylinder to force water through an array of small orifice nozzles that create a spray of micro-droplets. A concentrated chemical solution containing animal byproducts is the basis of Aqueous Film-Forming Foam (AFFF). Other types of foams are also available [Scheffey, 1997]. Foam is created when a pressurized gas (stored in a reservoir) forces a mixture of the concentrated solution (1 % to 10 % by volume) mixed with water through an aspirating nozzle. When foam is dispersed on a burning material, it smothers the fire by preventing fuel vapor from physically contacting the air. Foam breaks down as it ages and as it comes in contact with surfaces. The final form of the foam is characterized by the volume expansion associated with this process. Foam concentrate/water solutions (with anti-freeze) are limited to volume expansions of ≈3 to 30 [Madrzykowski, 1998]. The expansion ratio is important because in a simplified sense, the larger the expansion, the larger the volume that can be filled for a given mass of foam. The suppression effectiveness of foam, however, diminishes beyond a certain amount of expansion. For engine compartment applications, the entire compartment must be filled with foam to insure suppression. Expansion ratios larger than 30 may be possible using compressed gases and simple aeration techniques. Lim et al. [1997] were able to achieve a volume expansion of 62 using AFFF. Both water mist and foam systems, however, have problems related to freezing. For general use, freeze protection is desirable down to temperatures as low as -40°C. Selection of an appropriate anti-freeze is not trivial. Some anti-freezes alter the effectiveness of the suppressant, others are hazardous, and some are flammable. All of these issues must be considered for water-based suppressants.

The last category of suppressants in Table 4 is labeled prototypes and refers to emerging technologies. Most of these technologies are still being developed and are typically available in prototype form only. Not all of these systems were available for testing. Each of the prototype systems listed in Table 4, except the hybrid SPG, deliver some amount of the suppressant in the form of a particulate. The tubular device contains ammonium poly-phosphate, a solid powder (approximately 40 % by mass), HFC-134a ($C_3H_2F_6$), a compressed halogenated liquid (approximately 59 % by mass), and a small amount of a proprietary gelling agent (1 % by mass). The tubular system is a fire-activated device. In this manner, it is unique among the systems listed in Table 4, as it does not require active detection. The system is deployed when the tubing (approximately 2 mm thick) ruptures. This is designed to occur when a fire heats the tube,

weakening the thermoplastic and causing the pressure to build within the tube as the vapor pressure of the halogenated liquid increases. Eventually, the tubing ruptures, which causes the halogen/powder mixture to be expelled, driven by the vapor from the heated compressed liquid. The disadvantages of the tubular device are that it must be placed relatively close to the fire source to activate, and that there is no active control of suppressant dispersal. The direction of suppressant delivery depends on the placement and orientation of the system relative to the fire source.

Several types of pyrotechnic suppressant systems were considered. The solid propellant generators (SPG) and aerosol generators (AG) deliver combustion generated inert gases, principally carbon dioxide, water vapor, and nitrogen, as well as particulates composed of inorganic salts. Each component individually behaves as a fire suppressant. Table 5 shows estimates of the effluent compositions of these devices. The SPG propellants were identical to those tested recently in F-22 aircraft engine nacelles [Hamins et al., 1997]. The propellants undergo rapid solid-phase reactions producing an effluent that behaves as a fire suppressant. The SPG1 had the particulate filtered during deployment and only trace amounts of particulate are present in the effluent. The SPG2 and SPG3, on the other hand, used no filtering. The amounts of

Table 5. Mole Based Fractional Effluent Composition of Pyrotechnic Suppressants.[A]

Species	SPG1	SPG2	SPG3	AG1	AG2
CO_2	0.31	0.26	0.092	0.004	0.015
H_2O	0.22	0.18	0.56	*	*
N_2	0.47	0.40	0.32	*	*
O_2	0	0	0.0083	*	*
CO	0	0	0	0.001	0.001
NH_3	0	0	0	0.000150	*
NO_2	0	0	0	0.000002	*
HCN	0	0	0	*	*
K_2CO_3(s)	Trace	≈0.16	≈0.024	**	**
Inorganic salts including K_2CO_3(s)	*	*	*	≈0.5	*

A based on information supplied by the manufacturers.

* not specified by manufacturer.

** major constituent, but concentration not specified; also composed of other inorganic salts.

particulate listed in Table 5 are based on data supplied by the manufacturer, which are estimated from equilibrium chemistry. The Table 5 entry for the K_2CO_3 content of the SPG is an upper estimate, as some heavy particulate globules or slag is formed during SPG delivery, which does not assist in fire suppression because it is not effectively transported to the fire. Figure 2 is a photograph of a prototype SPG3 distribution nozzle after suppressant release. The nozzle was oriented vertically with the distribution nozzle near the ground for application to underbody fires. Less information is available on the effluent composition of the AGs (see Table 5), but they were also composed of inorganic salts.

The rapid release of suppressant has been found to be advantageous in some types of applications by filling a volume with suppressant faster than air is entrained into that volume. The SPG rapidly delivers its effluent ($\approx$1 to 10 kg/s) at a fairly high temperature ($\approx$2000 K near the exit), whereas the delivery rate associated with the AG is approximately two orders of magnitude slower ($\approx$0.02 kg/s). The AG effluent is cooler ($\approx$1000 K) than the SPG effluent and its composition differs as seen in Table 5. The hybrid generator uses the hot inert SPG exhaust to vaporize and expel a secondary suppressant, typically a liquid, such as water or a low boiling point halocarbon through a nozzle [Wierenga and Holland, 1999]. A 6:1 mass ratio of secondary suppressant to SPG propellant is typical [Mitchell, 1999]. The device is particularly attractive for some special situations such as inhabited spaces or cold temperature applications [Mitchell, 1999].

A number of other suppressants are commercially available, but they appear to offer no distinct advantage over those selected in Table 4 for evaluation. This is true of the compressed liquefied halocarbon gases. Although many suppressants other than HFC-125 or HFC-227ea are commercially available, these two compounds are common halon 1301 replacements, which are characterized by a number of positive attributes. In general, the compressed liquefied halocarbon replacements are highly similar in effectiveness on a mass basis in small scale laboratory tests [Grosshandler et al., 1994]. In terms of the powders, some other common powdered suppressants also exist, but the BC and ABC powders are both effective. A survey of suppliers showed that these powders are relatively inexpensive. Here, they are taken as representative of powders in general [Ewing, 1988].

Table 4 also lists the criteria that were considered to be most important for suppressant effectiveness. These criteria were used as a basis for suppressant selection. Other issues may certainly play a part in the selection process, but they were considered secondary. Some of the secondary criteria are listed in Table 6 (discussed below). The primary criteria listed in Table 4 include crash vulnerability potential, false discharge concerns, environmental concerns, system hardware mass, issues associated with hot surface and suppression of smoldering materials, and the critical suppressant specific density ($\rho \cdot Y_c$) as defined in Eq. 8. In the screening process conducted here, evaluation of the suppressants is based primarily on engineering judgement and any available data or measurements. In some cases, no data was available. For example, the evaluation of crash vulnerability was based entirely on engineering judgement, because no data exists.

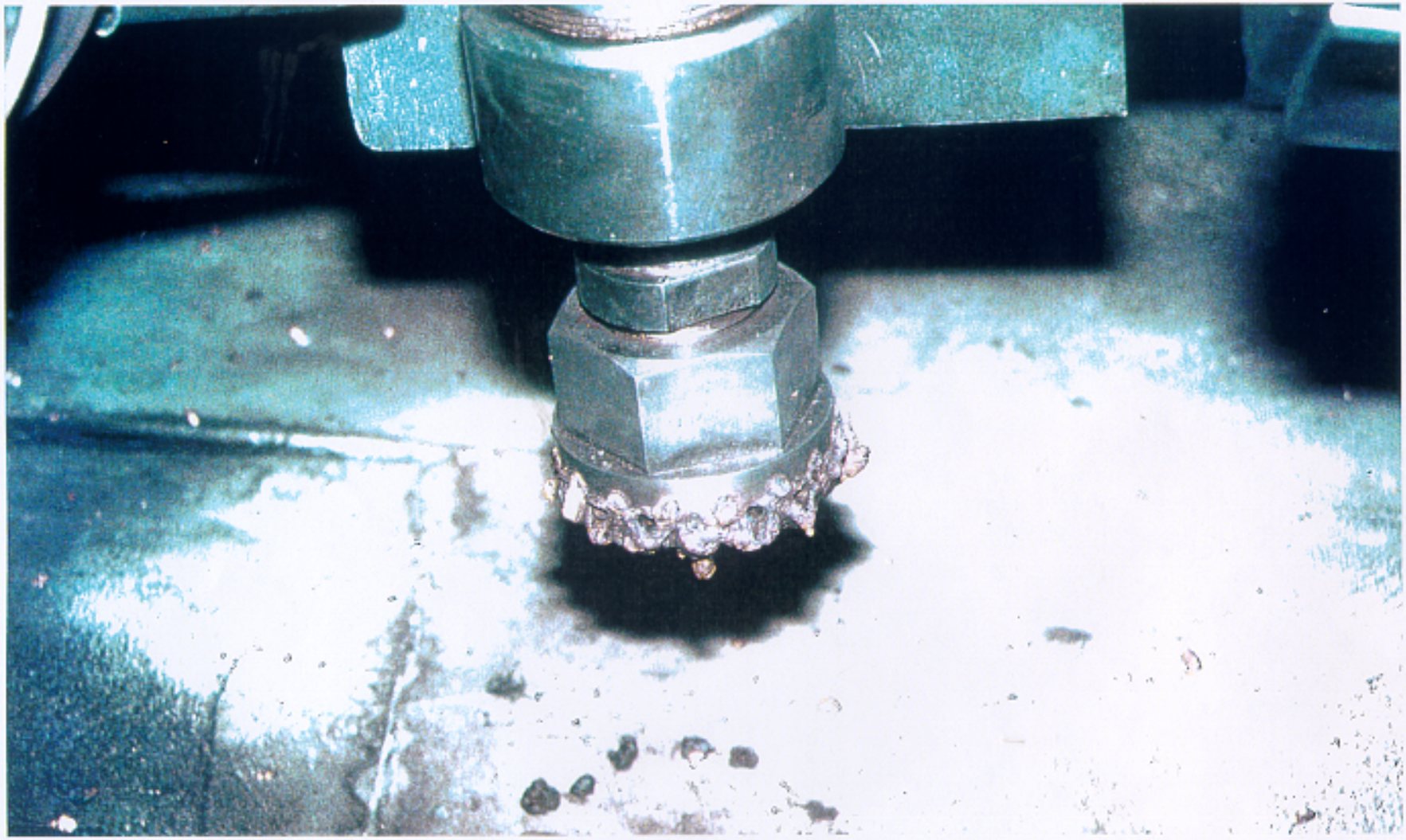

2. Photograph of a prototype SPG3 distribution nozzle after suppressant release.

The first criterion listed in Table 4 is vulnerability to collision damage. Any system that fails to survive a collision will be rendered useless. Collision vulnerability is a function of placement in the compartment, but certain suppression systems will be especially vulnerable to collisions due to system specific considerations. For example, water mist nozzles are particularly vulnerable to collision damage. Experiments on droplet dispersion conducted as part of this project showed that blockage of a mist discharge by a nearby solid surface (within approximately 5 cm from the nozzle) prevents adequate droplet dispersion, leading to zones that are not protected by a suppressant. It is concluded that water mist nozzles in the engine compartment will be particularly vulnerable to component movement due to a collision. Other suppressant types are also vulnerable to collision damage in engine compartment applications, but the water mist system seems to be particularly vulnerable, based on engineering judgement. For the underbody application, nozzle reorientation is a concern for all suppression systems unless a nozzle is circumferentially symmetric. For all systems, crash survivability poses limitations on system placement, which may impact system effectiveness and reliability. Some of these issues have been addressed as part of Projects B.3 and B.14 of the GM/DOT Agreement, where the survivability of a small number of detectors and suppression systems were tested in collisions.

The second criterion listed in Table 4 is false discharge. This refers to the discharge of suppressant due to a false or nuisance alarm. In some cases, this could lead to bodily injury or damage of vehicle components depending on the suppressant system, its placement and the location of the vehicle. Although the rate of detector false alarms is likely to be small [Goedeke and Gross, 1992], possible suppressant damage should be considered during system design. When this work was undertaken, the toxicology of CF_3I was not well characterized. Since then, CF_3I has been shown to be 25 times more toxic than Halon 1301 and more than 40 times more toxic than HFC-125 or HFC-227ea [Tapscott, 1998]. False discharge of CF_3I in an enclosed space such as a small closed garage could be detrimental. This is also true of CO_2 [EPA, 2000]. The toxicity issue is one of the main reasons that CF_3I has not been selected as a replacement for Halon 1301 (whose manufacture has been halted). For this reason, CF_3I was ruled out as a candidate suppressant in this test program. For the AG and SPG systems, false discharge could certainly be harmful. The effluent is rapid and hot ($\approx$1000 K to 2000 K, respectively, at the device exit). A false discharge into a person's face could result in serious injury. If pyrotechnic generators are ever used in vehicles, failsafe design will be needed to avoid damage associated with false discharge. In terms of component damage, certain types of dust are known to cause current tracking or shorting in electrical circuits, especially in the presence of moisture (Adler, 1993). This is a concern for false discharge of SPG or dry powder.

The third criterion listed in Table 4 is environmental concern. All fire protection extinguishing systems can affect the environment [Lataille, 1995]. Some halogenated suppressants, for example, contribute significantly to the destruction of the ozone layer. The evaluation of the environmental impact of suppressants is a new trend in fire protection. This is a significant concern from a practical perspective because legislation can impact material availability in both the short term and the long term. For example, although it still may be purchased, the manufacture of Halon 1301 has been halted since 1994 due to its high ozone depletion potential [Montreal

Protocol, 1987]. Although it is a highly effective suppressant and may still be available commercially, it is prohibitively expensive and cannot be considered a long-term solution to the vehicle fire suppression problem.

The fourth criterion listed in Table 4 is system mass. A high system mass is an unsatisfactory characteristic, particularly if a lighter equally effective alternative is available. In fact, excessive system size, weight, or pressure may preclude it from being used in passenger cars [Santrock, 1999b]. Carbon dioxide has a very high storage pressure at ambient temperature (≈6 MPa or 900 psig), much higher than the liquefied compressed halogenated compounds tested here, which have vapor pressures of between 0.7 MPa to 1.5 MPa (100 psig to 200 psig) at ambient temperature. A higher vapor pressure requires a thicker reservoir container. The mass of a reservoir is approximately proportional to its thickness, so CO_2 has an intrinsic disadvantage in relation to some of the other suppressants. The SPGs do not require a pressurized reservoir or piping. Also, due to the solid propellant density and system design, the device is lighter and less bulky than pressurized reservoir systems. A prototype production unit is shown in Fig. 3. The SPG manufacturers participating in this program independently stated that a production unit will ultimately have a propellant mass to device mass ratio of nearly 1 to 3, not including detector and electronics [Wierenga, 1999; Black, 1999].

The fifth criterion listed in Table 4 is related to hot surface ignition of a flammable fluid and suppression of a smoldering material. Smoldering may occur in some materials after flaming combustion has been suppressed. This may be a concern in engine compartments applications, but is not likely to be an issue in underbody applications where components composed of smoldering materials (rubber and charring thermoplastics such as ABS or phenolic) may be less prevalent. Section 1.4 describes some of the materials that may smolder. If a flammable mixture is present, then under the right circumstances, flaming ignition may occur. Table 4 denotes those suppressants that are effective against smoldering fires. These do not include the clean suppressants. Table 4 also denotes those suppressants that are known to be effective against smoldering, provided that they are delivered in sufficient quantities. These include suppressants that contain particulate, such as the SPG2, SPG3, the AGs, the tubular burner, and sodium bicarbonate powder. Most suppressants are effective in extinguishing smoldering fires when applied in a stream directly onto the smoldering material. The most effective suppressants against Class A smoldering fires are those that act to cool the burning/smoldering fuel surface and therefore extinguish not only the flaming combustion, but also the smoldering combustion. These include the water-based suppressants such as water mist and foam, as well as mono-ammonium phosphate (ABC powder), which endothermically decomposes upon heating to form phosphoric acid, a material that coats the surface, preventing contact with air. Sodium bicarbonate also endothermically decomposes (to sodium carbonate, water, and carbon dioxide at 150°C [Windholz et al., 1983]), but it does not form an impenetrable seal, as does ABC powder. In a total flooding application, such as that considered for use in an engine compartment, some suppressants will have little impact on smoldering combustion. For example, if a clean agent is applied near a smoldering material, it will impact the smoldering process through oxygen depletion. In an engine compartment, partially open to the environment, this time is not likely to

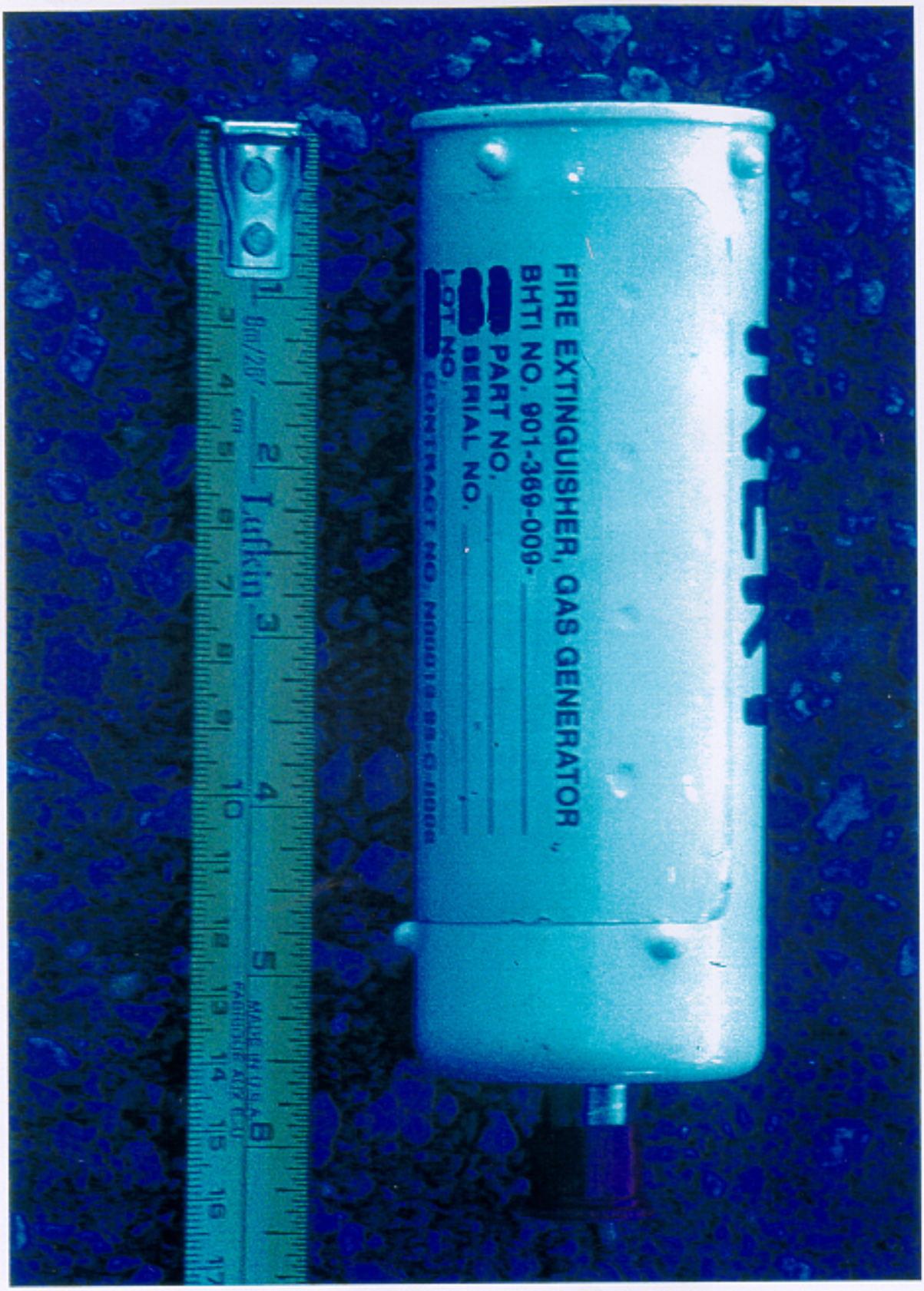

3. Photograph of a prototype SPG production unit.

be of sufficient duration to extinguish a smoldering fire. On the other hand, if a two-phase stream of clean agent (e.g., a liquefied compressed halogenated compound) happens to directly contact a smoldering surface, it will cool that surface through convective heat transfer associated with phase change (latent heat of vaporization) and heat capacity. This is also a possibility in an engine compartment, depending on the fire scenario and the geometric configuration.

Hot surface ignition is a concern in engine compartment and possibly underbody applications. Under the proper conditions, combustible and flammable fluids will autoignite. Autoignition is governed by the time/temperature history of a reactive mixture [Glassman, 1998]. This process is influenced by the surface temperature and the thermophysical properties of the fluid. Under certain conditions, hot surface reignition of a flammable fluid is possible after flame suppression has been successful. The same suppressants that are effective on smoldering materials are effective in cooling hot surfaces (see Table 4).

The final criterion in Table 4 is an estimate of suppression effectiveness, $\rho \cdot Y_c$, which was based on reported values of Y_c from cup burner or other laboratory-scale fire suppression experiments [Hamins et al., 1994; 1995; 1997; Ewing et al., 1988]. Although molecular transport plays a role in the cup burner extinguishment results, thermodynamic, transport, and other effects that are important in actual fire suppression applications do not play a role in the values shown in Table 4. Therefore, the $\rho \cdot Y_c$ values listed in Table 4 should not be considered predictions of suppressant requirements. Instead, these values should be thought of as rough estimates of minimum required suppressant density. For fires in enclosures partially open to the environment, such as vehicle applications, suppressant densities larger than those in Table 4 can be expected. From cup burner experiments, the critical mass fraction (Y_c) of N_2 in the oxidizer stream was measured as 0.31. The value of $\rho \cdot Y_c$ (see Table 4) is then equal to 0.37 [Hamins et al., 1994]. ABC powder has not been tested in the cup burner, but results are available for ABC and BC powders from small scale pool fire suppression experiments [Ewing, 1988]. For foams, it was assumed that the entire free volume would have to be filled to insure suppression. Table 4 shows that there are large differences in the effectiveness of the various suppressants. Assuming an expansion ratio of 62, to fill a 1 m^3 compartment with expanded foam would require: $\rho \cdot Y_c = 1000\ (kg/m^3)\ /62 = 16$ kg. Compared to the other types of suppressants listed in Table 4, foam is relatively ineffective on a mass basis.

Table 6 lists some criteria of secondary importance. The first criterion listed in Table 6 is maintenance. Periodic inspection and maintenance of an extinguisher is necessary and is generally recommended that it occur at least once a year. Maintenance means a complete and thorough examination of the extinguisher and involves examining all of its parts, and when appropriate replacing defective parts, and recharging or reassembling the extinguisher [Conroy, 1997]. Some suppressant types require periodic replacement due to possible degradation. The replacement of water-based suppressants is recommended annually by some fire protection engineers [Demers, 1995], whereas conversations with some manufacturers indicate that replacement of premixed foams is satisfactory every five years. NFPA 10 [1996] contains specific details related to maintenance. Hydrostatic testing of extinguishers that are subject to high internal pressure must

Table 6. Secondary Suppressant Characteristics

Type	Suppressant	Maintenance	Post-fire Toxicity	Cost/Mass[A] ($/kg)	Cost/Volume[B] ($/m^3)
Clean	CO_2	x	C	0.6	0.2
	Halon 1301	x	Acid Gas	Not avail.[D]	Not avail.[D]
	CF_3I	x	Acid gas	≈60	12
	HFC-227ea	x	Acid Gas	9	4
	HFC-125	x	Acid Gas	9	4
Powder	Sodium Bicarbonate	x	Basic Gas	0.23	0.03
	Mono-Ammonium Phosphate	x	Acid Gas	0.27	0.04
Water-Based	Water Mist/ Anti-Freeze	x		≈0.01	0.03
	Foam / Anti-Freeze	X		≈0.1	2
Prototype	Aerosol Generator	M		na	na
	SPG	M		na	na
	Tubular	M		na	na

A: estimated suppressant cost only. Total cost will depend on cost of hardware.
B: estimated suppressant cost only. Total cost will depend on cost of hardware.
C: false discharge concern (See Table 4), but no post-fire toxicity.
D: no longer manufactured.
na: information not available.
M: presumably very low maintenance (similar to vehicle air bags).
x: minor maintenance required (see text).
X: considerable maintenance required (see text).

be performed to protect against unexpected failure. The period between testing varies with extinguisher type as outlined by NFPA 10. For example, hydrostatic testing of extinguisher reservoirs is recommended every five years for most systems (CO_2, water-based suppressants, and steel shelled powder reservoirs), and every 12 years for halogenated compounds [NFPA 10, 1996]. It is recommended that cylinder pressurization should be verified on a regular basis, at least every few months. The shelf life of the SPGs and AGs is related to ambient conditions such as temperature, which will vary depending on engine operating conditions and placement within the compartment.

The second criterion in Table 6 is post-fire toxicity. Certain suppressants pose a potential toxicity hazard after exposure to flame. Halogenated compounds, ABC powder, and BC powders form toxic gases through flame reactions. Potentially, this could present a problem under certain conditions such as fires in enclosed spaces, for example, in a tunnel or a garage. Although this is not likely to be a significant issue in the vast majority of cases, post-fire toxicity issues should be considered.

The third criterion in Table 6 is suppressant cost and cost per unit of protection. Cost is a tangible attribute that at a minimum differentiates between equally effective systems and can be used to eliminate other systems. The prices listed in Table 6 do not include hardware and are based on current estimates of small lot sizes. Prices should decrease with larger lot sizes. The materials listed are commercially produced in large amounts. Precise cost information on the prototype systems is not available, although the cost of the SPG will likely be similar to the cost of an air bag inflator [Wierenga, 1999], which is similar in design [Wierenga, 1999]. Manufacturers sell production line airbag inflators for approximately $25 each [Wierenga, 1999]. The SPG system, as well as all of the other suppression systems except the tubular system, require a detector (discussed below). The cost of a detector will ultimately depend on its specifications. A variety of optical detectors are commercially available. Of those that may be suitable for vehicle applications, some cost as little as $30 per unit [Neidert, 1999].

1.3.2 System Hardware

In this report, the values reported for suppressant mass do not include associated hardware. The ultimate weight of a system will depend on design details. Components that add mass to a system include the detector (if needed) and associated electronics, the suppressant itself, and plumbing, which includes the suppressant reservoir, tubing, nozzles and mounting hardware. Nozzles vary in weight from a few grams to hundreds of grams. The piping that carries a suppressant is typically a metal tube, usually 1 cm to 2 cm in diameter. For post-collision engine compartment applications, a heavy stainless steel woven or braided tubing may be appropriate to prevent possible rupture during a collision, although this type of tubing can crimp when compressed or be cut through during a collision. In addition, the mass of this type of tubing may be large, depending on its length. For some suppressant systems, metal tubes, nozzles, and detectors are not necessary. This is true, for example, for the tubular suppressant system.

Conventional fire extinguishing systems (clean agents, powders, and foams) consist of a pressurized suppressant reservoir, a discharge valve, and some means to initiate the valve. The diameter of the tube carrying the suppressant is a means to control the rate of suppressant discharge. For the halogenated compounds listed in Table 4, the suppressant exits the delivery system as a two-phase flow. Once released into a fire environment, these materials flash vaporize. Suppressant is typically introduced through a single tube from the suppressant cylinder. Often a tee is used, to enhance protection of multiple targeted zones and to generally improve suppressant dispersion. Nozzles are typically used for dry powders, liquefied compressed gases, and SPG.

Commercial suppliers attempt to optimize suppressant distribution for each particular application through nozzle design.

The hardware associated with SPG is a derivative of that used to inflate automotive airbags. A prototype production unit is shown in Fig. 3. The hardware associated with the AGs appears to be similar. They are cylindrical in shape, contained in a metal outer case. The AGs used in this study had ratios of propellant mass to device mass similar to that envisioned for the SPGs, i.e., nearly 1 to 3.

1.3.2.1 Detection

All of the suppressant types listed in Table 4 requires detector control of the suppressant discharge with the exception of the tubular device, which is thermally activated. For post-collision vehicle fire applications suppressant deployment must be automatic, because a vehicle occupant may be unconscious or otherwise unable to activate the suppressant system. Many types of detectors are commercially available including spot, linear thermal, and optical detectors. These are described in some detail by Bennett [1997]. For post-collision vehicle applications, engineering judgement suggests that detectors should be fast (small response time), rugged (functional after a collision), have a very large view angle for engine compartment applications, moderate sensitivity, and sophisticated false alarm protection. Orientation and placement is critical to achieve early detection. An ideal detector would have complete coverage of the entire compartment (i.e., a hemispherical view). Ideal placement of such a detector might be at the center of the underside of the hood. Rapid response optical detectors with near-hemispherical view are being commercially developed [Sivathanu, 1999].

A few of the experiments (on the full-scale vehicle) used an optical detector for activation of the suppressant systems. The detector was manufactured for military applications and had many of the attributes necessary for vehicle applications. It was compact ($\approx$4 cm x $\approx$6 cm x $\approx$2 cm) and light weight ($\approx$300 g). The detector had a view angle of $\approx 90^{\circ}$, which is less than optimal for complete coverage of the engine compartment. Detectors were not used regularly during the suppression experiments because placement of the detector in the burning engine compartment put it at risk of thermal damage. Since suppressant effectiveness was the primary objective, the experimental procedure was streamlined to avoid inconsistencies associated with detector activation.

In general, early detection should increase the likelihood of successful suppression. Tens of seconds after fire initiation a fire may grow and spread such that many components are involved. This does not imply, however, that early detection should be accompanied by early suppressant activation.

2.0 Determination of Suppressant Distribution through a Nozzle

Regardless of the mass delivered by a suppression system, it is ineffective unless it reaches the fire zone. Nozzles are used to direct the suppressant discharge and assure effective suppressant distribution. Most common fire extinguishing suppressants are stored in pressurized reservoirs. The suppressant is delivered to a particular location through some sort of plumbing system. For effective suppressant delivery, system design may need to consider suppressant pressurization, piping length and diameter, as well as the nozzle number, type, placement, and orientation.

For the suppressants considered here (with the exception of the tubular device), a nozzle controls the distribution of suppressant and is therefore of critical importance in the effectiveness of a fire suppression system. In the engine compartment fire scenarios addressed here, total flooding of suppressant through the compartment and the zone between the ground and the engine compartment (i.e., the underbody region) is a practical fire suppression strategy. The primary selection criterion for a nozzle(s) for engine compartment applications was uniform distribution about the compartment. Testing with powder facilitated selection through observation of the post-discharge powder residue on top of engine components. For use in the underbody/fuel tank fire scenario addressed here, the suppressant target zone was throughout the rear portion of the underbody including coverage from tire to tire in the rear. Because of the possible presence of wind, a large suppressant mass delivery rate was thought to be advantageous in both cases. A high velocity delivery may be particularly important for an underbody fire where the suppressant momentum must overcome the wind.

A series of experiments was conducted using the nozzles listed in Table 7 to examine the effect of nozzle type on the distribution of a suppressant discharged from a pressurized reservoir (powders and halogenated suppressants). This information was valuable in designing suppressant delivery systems for suppression testing of the powder and halogenated suppressants. Some experiments investigated the effect of pressure on suppressant distribution (see Table 7). Nozzles were not tested for the other devices (SPG, tubular device, AG), but were used as provided by the suppliers. A large number of nozzle types and sizes are commercially available for fire suppression applications. A number of these are listed in Table 7. Both commercially available nozzles and a few customized nozzles were investigated in this study. The commercially manufactured nozzles are referred to by model number. Some nozzles were fabricated or modified at NIST for use in this study. The simplest nozzles tested were composed of a single round orifice, characterized by its diameter. Fan nozzles, as they are termed, provided a fan-like spread of suppressant. Spiral nozzles disburse suppressant axisymmetrically over a wide angle. A number of nozzles designed for specialized applications were tested. Some were composed of multiple small orifices such as Nozzles #11 in Table 7. Figures 4 and 5 show some of the spiral and fan type nozzles used here.

2.1 Experimental Procedure

The experiments were conducted using ABC powder, which facilitated visualization of the

suppressant flow and allowed determination of the angle of discharge and its velocity. The suppressant was discharged into uncluttered, empty space. The powder was weighed and then added to the reservoir using a funnel. The reservoir was sealed and then pressurized with gaseous

Table 7. Characteristics of ABC Powder Discharge from a 1 L Reservoir.

Nozzle	#	Mass (g)	P_o (MPa)	Discharge Angle (deg)	Velocity (m/s)	Axi-Symmetric	Discharge [G] Duration (s)
4.8 mm Orifice	1a	200±4	0.34 ±.07	8 ±2	17 ±3	Yes	1.7 ±0.1
4.8 mm Orifice	1b	200±4	0.68±0.07	8 ±2	19 ±4	Yes	1.5 ±0.1
4.8 mm Orifice	1c	200±4	1.4±0.08	11 ±2	20 ±4	Yes	1.0 ±0.1
4.8 mm Orifice	1d	200±4	2.7±0.07	12 ±2	22 ±4	Yes	1.0 ±0.1
3.2 mm Orifice	2a	200±4	0.34±0.07	7 ±2	14 ±2	Yes	4.3 ±0.1
3.2 mm Orifice	2b	200±4	0.68±0.07	8 ±2	11 ±2	Yes	3.3 ±0.1
3.2 mm Orifice	2c	200±4	1.4±0.07	11 ±2	16 ±3	Yes	2.6 ±0.1
3.2 mm Orifice	2d	200±4	2.0±0.07	10 ±2	21 ±4	Yes	2.3 ±0.1
L. F1	3	200±4	1.4±0.07	9 ±2	13 ±2	No	3.9 ±0.1
S. F1	4	200±4	1.4±0.07	10 ±2	13 ±2	No	11 ±0.1
17082 Spiral	5	200±4	1.4±0.07	140 ±10	5 ±1	Yes	0.7 ±0.1
17030 Spiral	6	200±4	1.4±0.07	150 ±10	4 ±1	Yes	1.1 ±0.1
K-40 Fan	7a	200±4	1.4±0.07	100 ±10	8 ±1	No	1.2 ±0.1
K-40 Fan	7b	250±5	4.1±0.07	100 ±10	7 ±1	No	0.7 ±0.1
K-40 Fan	7c	500±10	4.1±0.07	100 ±10	5±1	No	2.3±0.1
K-27 Fan	8	200±4	1.4±0.07	100 ±10	7 ±1	No	1.0 ±0.1
Custom 1[B]	9	200±4	1.4±0.07	240[E] ±10	3 ±0.5	Yes	1.7 ±0.1
5379 Cone	10	200±4	1.4±0.07	7 ±2	17 ±3	Yes	1.0 ±0.1
D1[C]	11	200±4	1.4±0.07	12 ±2	18 ±3	No	1.0 ±0.1
56748[D]	12	200±4	1.4±0.07	350 ±10	0.8 ±0.2	No	0.4 ±0.1
Slvr.5	13	200±4	1.4±0.07	10 ±1	16 ±3	Yes	0.90 ±0.1
2 x Fan(K-40)[D]	14	500±10	4.1±0.07	120 ±10	8 ±1	No	2 ±0.1
SPG 3 radial	15	450	na[F]	360	26 ±10	Yes	1 ±0.1
AG 1	16	190±4	na[F]	40 ±5	2.4 ±0.5	Yes	6 ±0.5

A. Internal screen removed
B. Modified sprinkler head: deflector inverted.
C. 8 x 3 mm Orifices
D. Oriented as shown in Fig. 14 with the fan nozzles oriented 10° to 20° off-axis.
E. Creates cloud.
F. na: not applicable
G. Duration of solid-phase discharge.

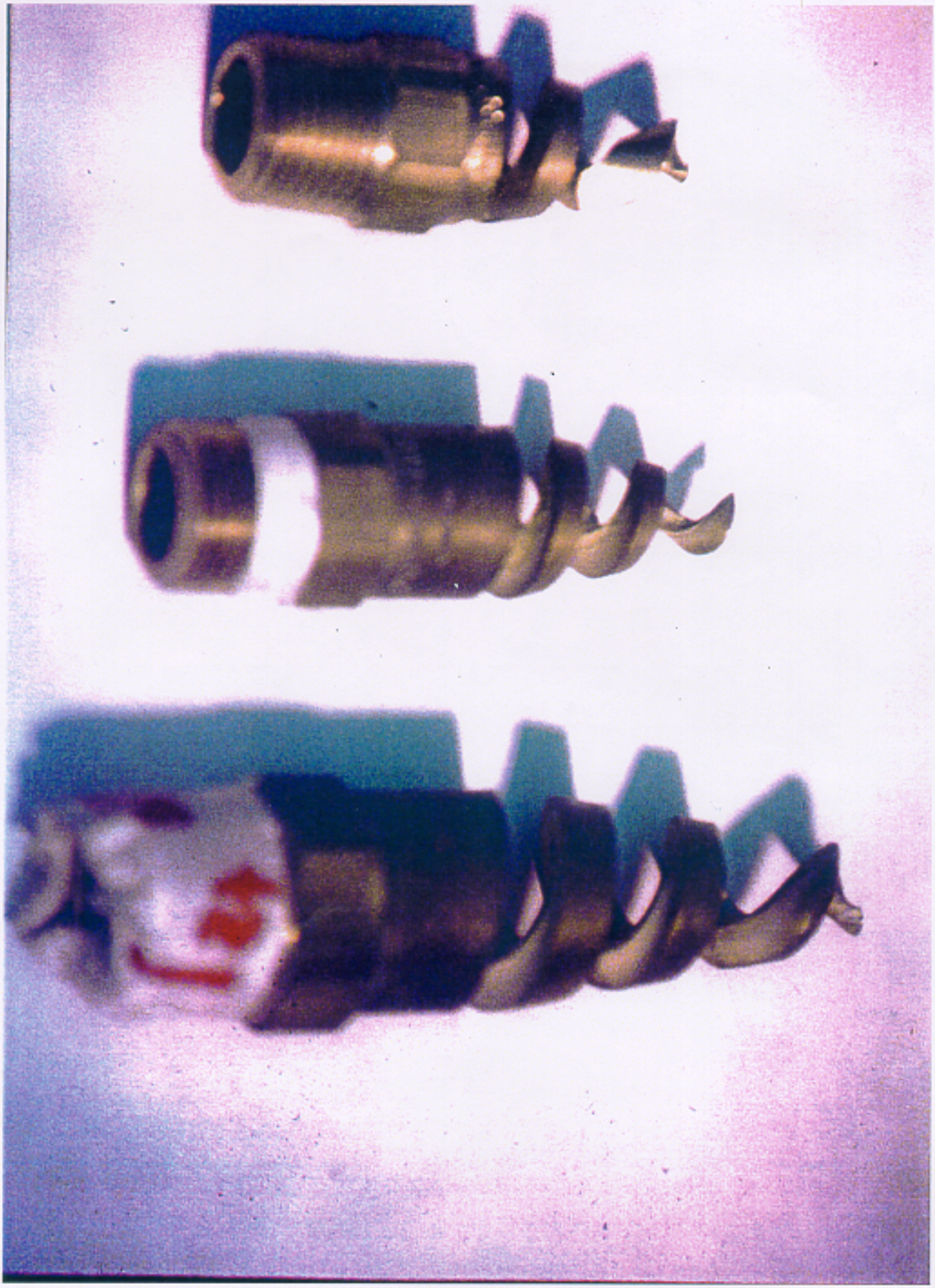

4. Photograph of some spiral nozzles.

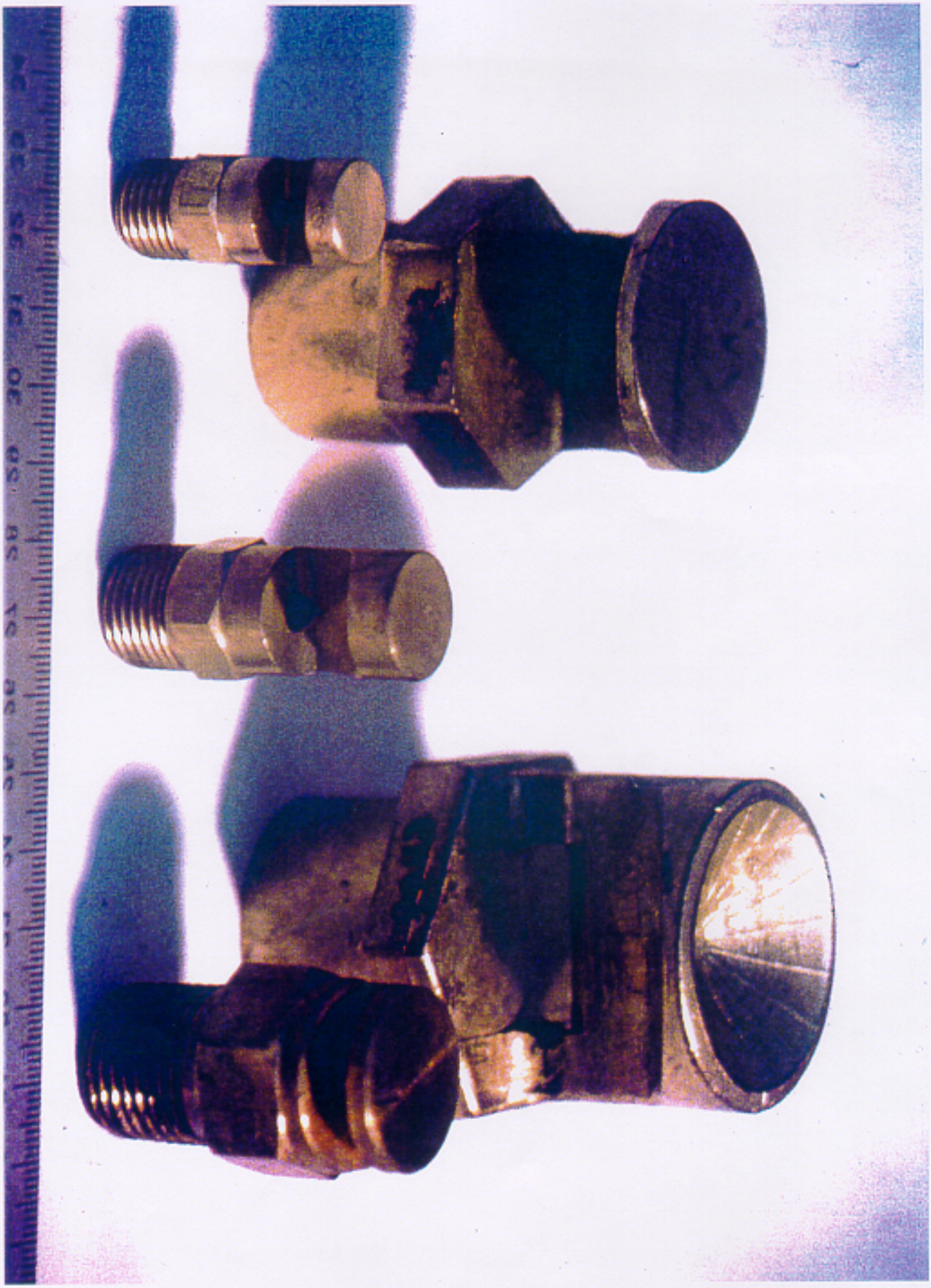

5. Photograph of some fan nozzles.

nitrogen, typically to 1.4 MPa (200 psig) as seen in Table 7. A fast-response pneumatic solenoid valve controlled the suppressant discharge from the reservoir. Figure 6 is a photograph of the experimental set-up.

Figure 7 is a close-up of a fan nozzle being tested. A calibrated pressure gauge (uncertainty of ± 30 kPa) monitored the suppressant storage reservoir. The suppressant flowed through the solenoid, turned through a 90° elbow, flowed horizontally into a ≈1 m tube (8 mm i.d.), and then through the nozzle.

A video record (30 Hz) of the suppressant discharge was acquired, which allowed determination of suppressant distribution. A side view camera orientation allowed visualization of the axial velocity of the discharge. A behind the nozzle camera orientation allowed visualization of the angular distribution of the suppressant. The suppressant delivery duration was also determined from a frame by frame analysis of the video record.

The ideal gas law was used to estimate the mass of gaseous nitrogen (M_{nit}) associated with reservoir pressurization:

$$M_{nit} = P \cdot (V - [M_i/\rho_i]) \cdot (MW_{nit})/(R \cdot T) \tag{27}$$

where the term $[M_i/\rho_i]$ represents the volume occupied by the condensed phase suppressant (powders and compressed liquid suppressants), ρ_i is the suppressant (true, not bulk) density (see Table 8), MW_{nit} is the molecular weight of nitrogen (=28 g/mol), V is the reservoir volume, R is the gas constant, P is the reservoir pressure, and T is the reservoir/ suppressant temperature. The expanded volume of the gas phase nitrogen in the suppressant reservoir referenced to standard conditions ($V_{nit,STP}$) is given by:

$$V_{nit,STP} = (V - [M_i/\rho_i])\ (P/1.0\ \text{atm})\ (298\ \text{K}/T) \tag{28}$$

Table 8. Suppressant Properties.

Suppressant	ρ_i (g/cm^3) (T=298 K)	P (T=298) MPa
HFC-125 (C_2HF_5)	1.19[A]	1.38[A]
HFC-227ea (C_3HF_7)	1.39[A]	0.46[A]
ABC powder ($NH_4H_2PO_4$)	≈ 2[B]	na
BC powder ($NaHCO_3$)	2.22[C]	na

na: not applicable.
A: Yang et al., 1995.
B: estimate.
C: Hamins et al., 1994.

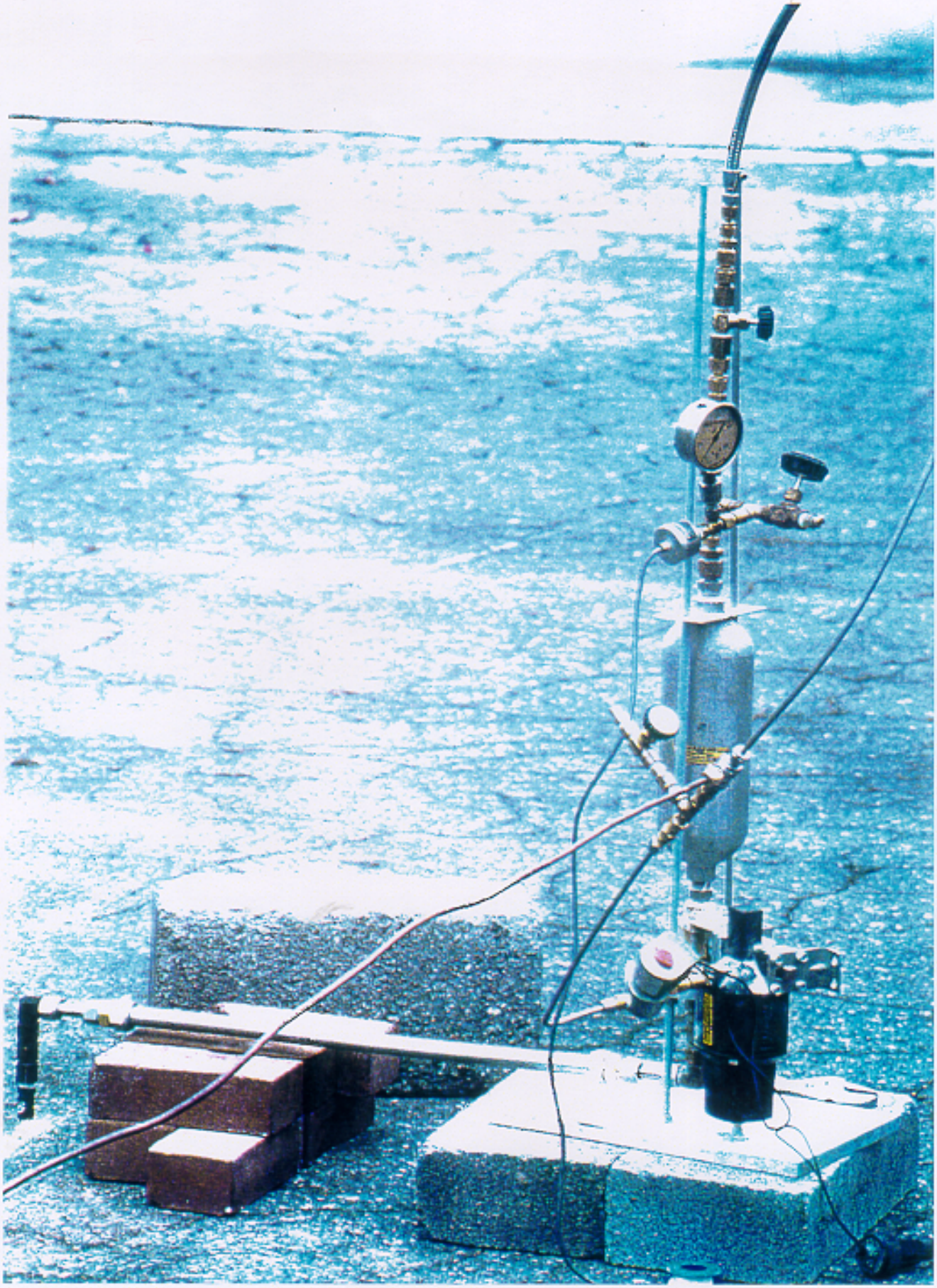

6. Photograph of the experimental set-up to test suppressant distribution.

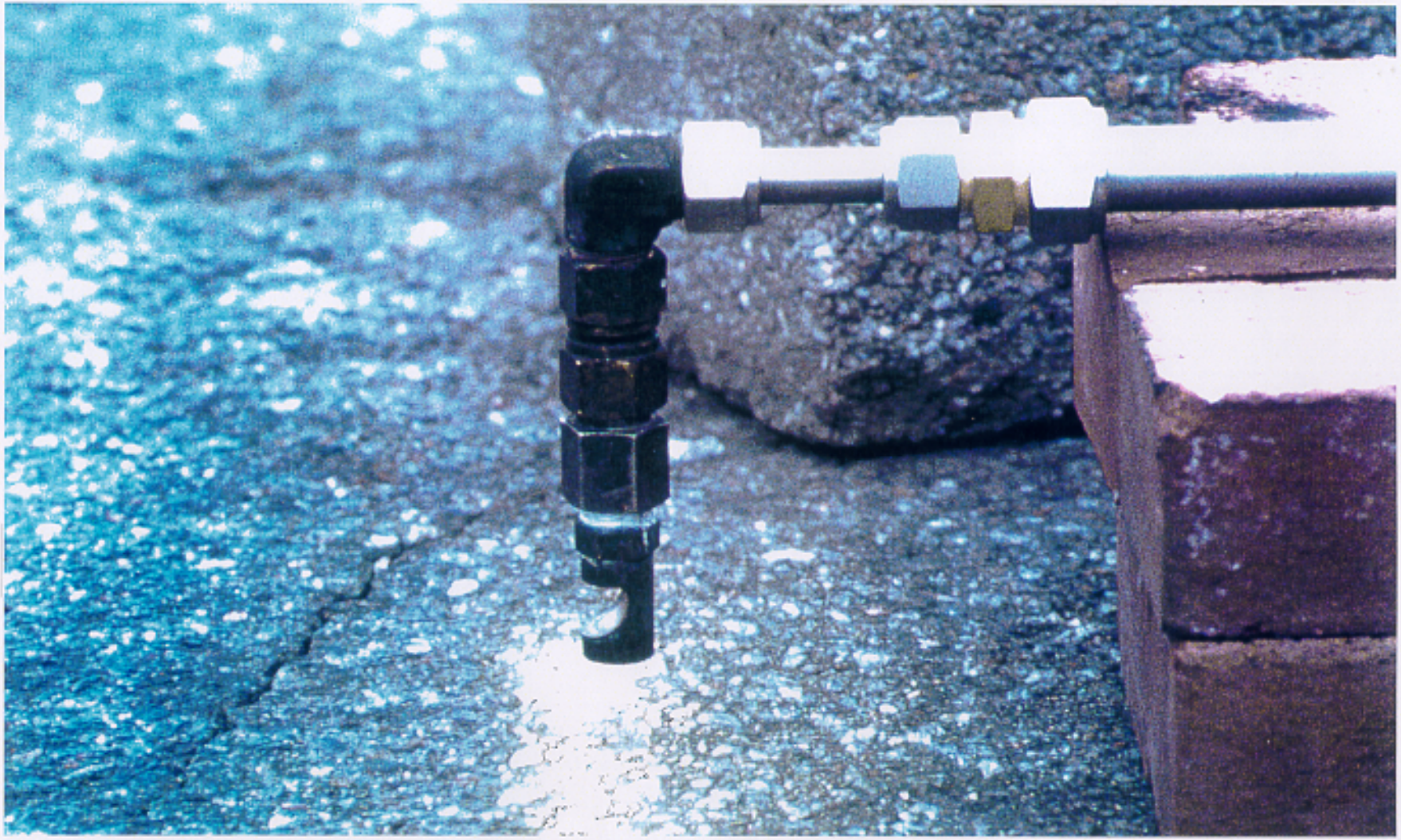

7. Close-up photograph of a fan nozzle.

The mass of nitrogen in the reservoir was typically much smaller (5 % to 10 % of the total suppressant mass) than the primary suppressant mass.

2.2 Experimental Results

The measured suppressant distribution for the nozzles studied here is listed in Table 7. Table 7 lists the experiment #, the nozzle type, the suppressant mass, reservoir pressurization, and the measured discharge angle, suppressant velocity, and the powder discharge duration. This data was determined through measurements rather than from information provided by the manufacturer. Table 7 characterizes the discharge as axisymmetric or non-axisymmetric, which was based on experimental observation. A range of nozzle types was tested and the video record provided quantitative information on the flow behavior of the suppressant as it exited the nozzles. Select frames from the video were used to estimate the velocity of the leading edge of the suppressant dispersion. The approach used image analysis to follow suppressant transport in a manner similar to that used by Pitts and coworkers (1994). Frame 1 of the image sequence was defined as the frame in which the suppressant was clearly exiting the nozzle. As a result, the uncertainty in the time of suppressant release was equal to the 33 ms framing period. The velocity listed in Table 7 was the average velocity measured 1 m downstream of the nozzle. This distance (1 m) was selected as representative of nozzle/target distances for the underbody application. The main contribution to the uncertainty in velocity was due to the framing rate, while the contribution of uncertainty in the location of the leading edge of the suppressant was negligible.

For the engine compartment application, the spread angle and the mass discharge rate may be more important than the velocity at a distance downstream. This is because components will block suppressant transport within a few tens of centimeters. Experimental observations showed that the value of the spread angle was invariant with downstream distance. Figure 8 is a frame from the video record of experiment 7b using nozzle 7 (see Table 7), which shows a side view 0.3 s after the release of 500 g of ABC powder through the fan nozzle shown in Fig.7. The velocity, spread angle, and height of the suppressant distribution varied with nozzle design. For all nozzles, the suppressant distribution was influenced by reservoir pressure. As expected, the discharge duration decreased with increased reservoir pressure and increased orifice size of the nozzle. Figure 9 shows the measured duration of the ABC powder discharge as a function of reservoir pressurization for the two simplest nozzles (#1 and #2 in Table 7). The filled and open symbols represent measurements for the 4.8 mm and 3.2 mm orifice nozzles, respectively, whereas the lines in the figure (and in all subsequent figures unless otherwise noted) represent a fit to the data. The total discharge duration (gas phase and solid phase) was typically a factor of 1.5 to 2 times longer than the duration of the solid phase discharge presented in Table 7. Depending on their attributes, a number of the nozzles listed in Table 7 were selected for use in the vehicle suppression experiments described in Section 3.

8. Image from the video record 0.3 s after the release of 500 g of ABC from a 1 L reservoir through the fan nozzle shown in Fig. 7.

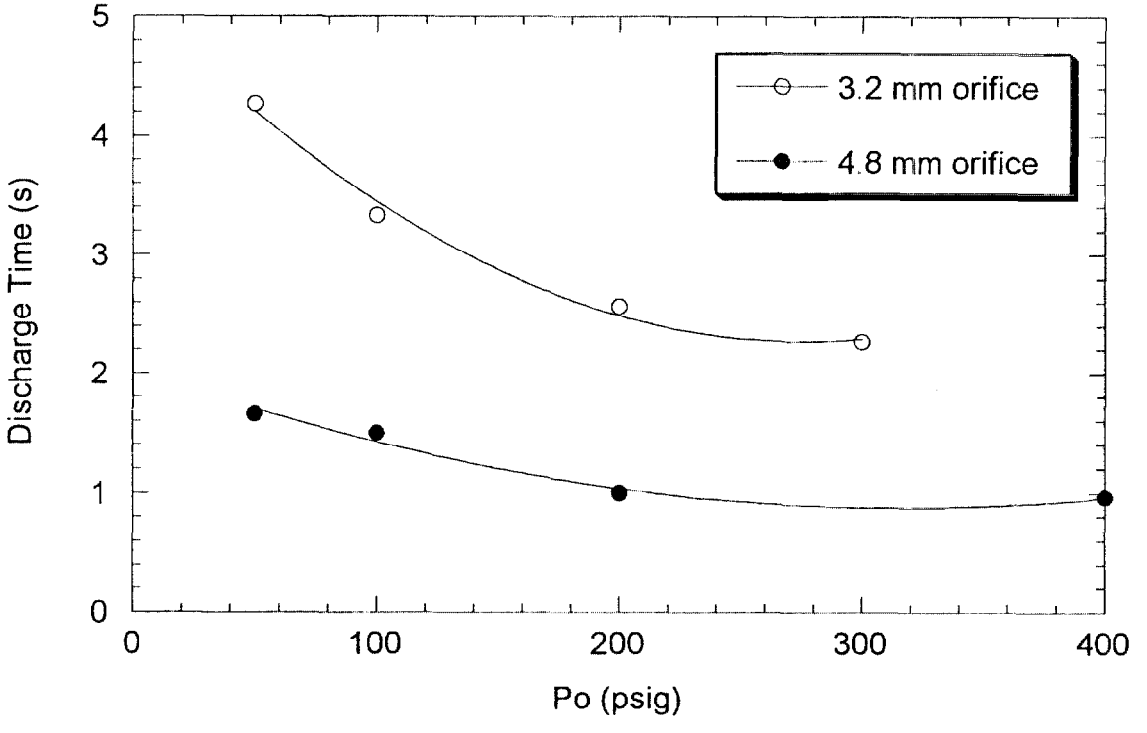

9. The measured discharge time as a function of reservoir pressure for two simple nozzles.

2.3 Nozzle Selection for Underbody Fires

The experiments described here considered the effect of wind on suppressant distribution for suppression of underbody fires. The wind speed is a function of distance above the ground. The local wind speed also depends on atmospheric conditions, local terrain, flow field obstacles, and surface roughness of the ground [Simiu and Scanlan, 1996]. Figure 10 shows measurements of the average wind speed and its variation (one standard deviation) as a function of distance above the ground, measured near the outdoor experimental site where our full-scale fire suppression experiments were conducted. The wind was flowing over terrain with a gentle downward slope, which was a field of grass. The data are adequately described by a logarithmic function, consistent with previous measurements [Simiu and Scanlan, 1996]. Figure 10 shows that the wind speed increased significantly with distance above the ground. Table 2 shows that vehicle underbodies are typically 20 cm above the ground. Wind will affect suppressant movement near the ground, but wind speeds near the ground are typically much less than wind speeds reported by meteorologists, which are measured by instruments positioned on buildings, often tens of meters above the ground.

Fan nozzle #7 and spiral nozzle #5 in Table 7 were selected for testing in the suppression experiments on underbody fires described in Sections 3.3 and 3.4. The experiments discussed in this Section focussed on the distribution of suppressant from nozzle #7. The effluent exiting nozzle #7 exhibited a wide angular dispersion ($\approx 100^{\circ}$). The velocity at the leading edge of the suppressant was constant (within a few percent) as a function of angle over the entire dispersion. Figure 11 shows the measured velocity of the leading edge of suppressant as a function of time for ABC powder discharged from nozzle #7 in experiment 7c (see Table 7). The same data are replotted in Fig. 12 as a function of downstream position.

To improve suppressant coverage of the area near the fuel tank (henceforth referred to as the suppressant target zone) in the presence of wind, two K-40 fan nozzles (nozzle #7 in Table 7) were combined, oriented as shown in Figs. 13 and 14 and denoted as nozzle #14 in Table 7. The nozzles were separated by 70 cm, placed 0.5 m upstream of the fuel tank and oriented 10° away from the central axis of the vehicle to insure adequate suppressant coverage over the target zone in the event of low-speed winds.

The effect of wind on suppressant coverage of the target zone by nozzle #14 was estimated by analysis of the video record of experiment 7c in Table 7. The front of the lateral edge of the suppressant dispersion was tracked as a function of downstream position. An estimate of the effect of wind on suppressant coverage was determined through vector addition by superimposing a velocity vector representing the wind on the measured suppressant velocity. Figure 15 shows the results of such a calculation, where the lateral position (X) of the leading edge of the suppressant front on the windward side is plotted as a function of downstream position (Y) for a range of imposed wind speeds from zero to 10 m/s. The off-axis nozzle orientation was set at 10° (see Fig. 14) and the fan nozzles were located at (X,Y)=($\pm$0.35 m, 0 m). The wind was taken as perpendicular to the effluent direction in all calculations. The target zone is also shown, which

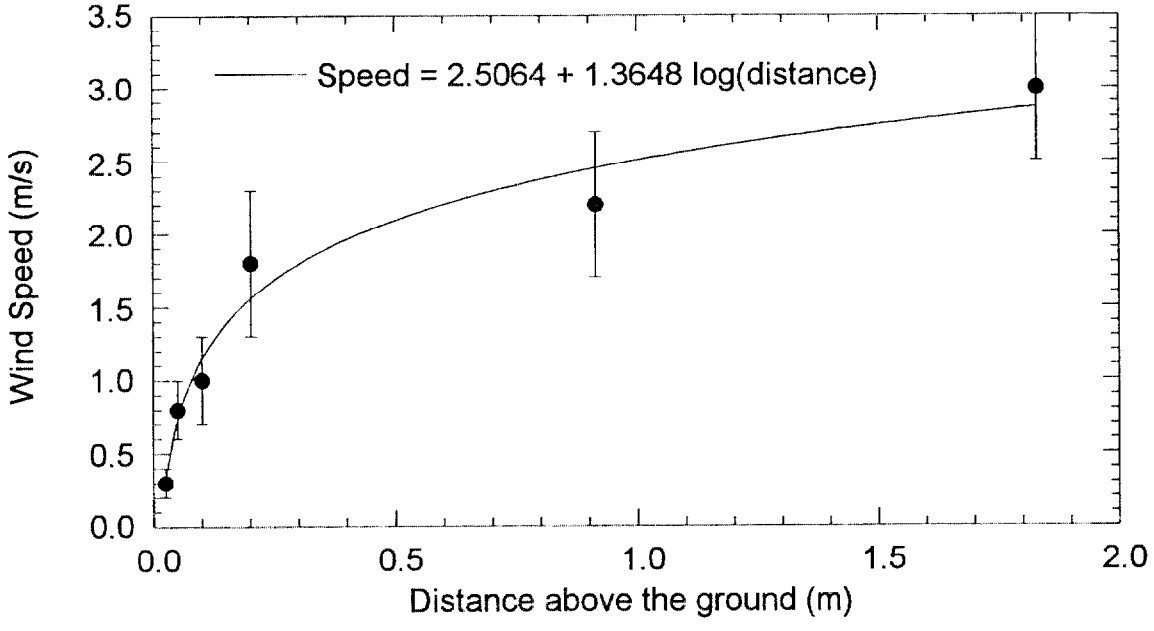

10. Measured value of the average wind speed and its variation as a function of distance above the ground.

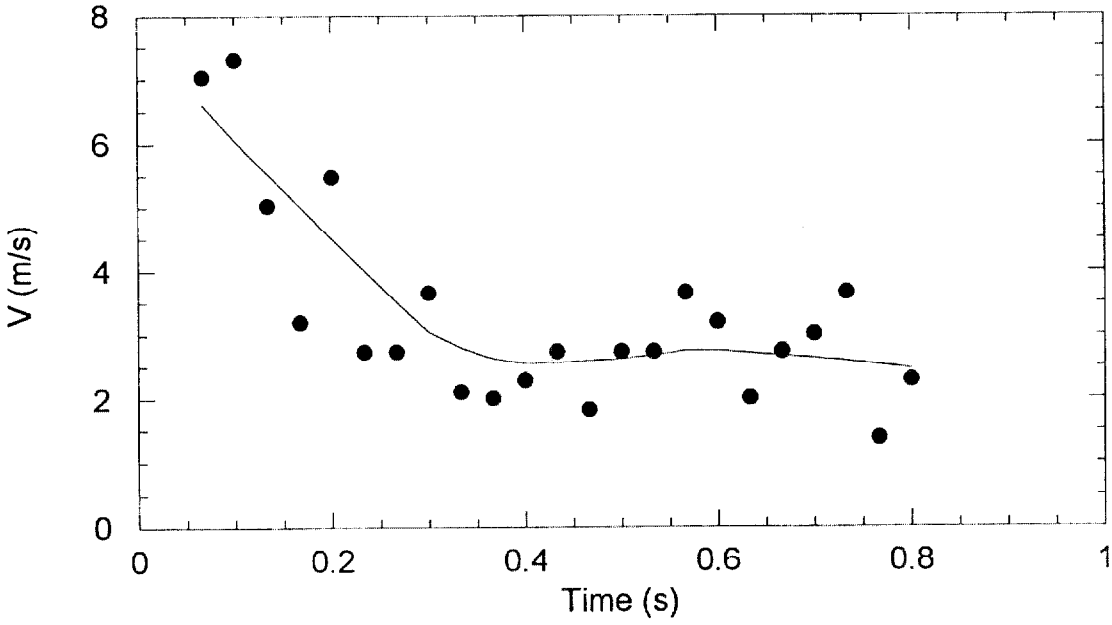

11. The measured velocity of the leading edge of suppressant as a function of time after discharge for Nozzle #7. The initial reservoir (1 L) pressure (P_o) was 4.2 MPa (600 psig).

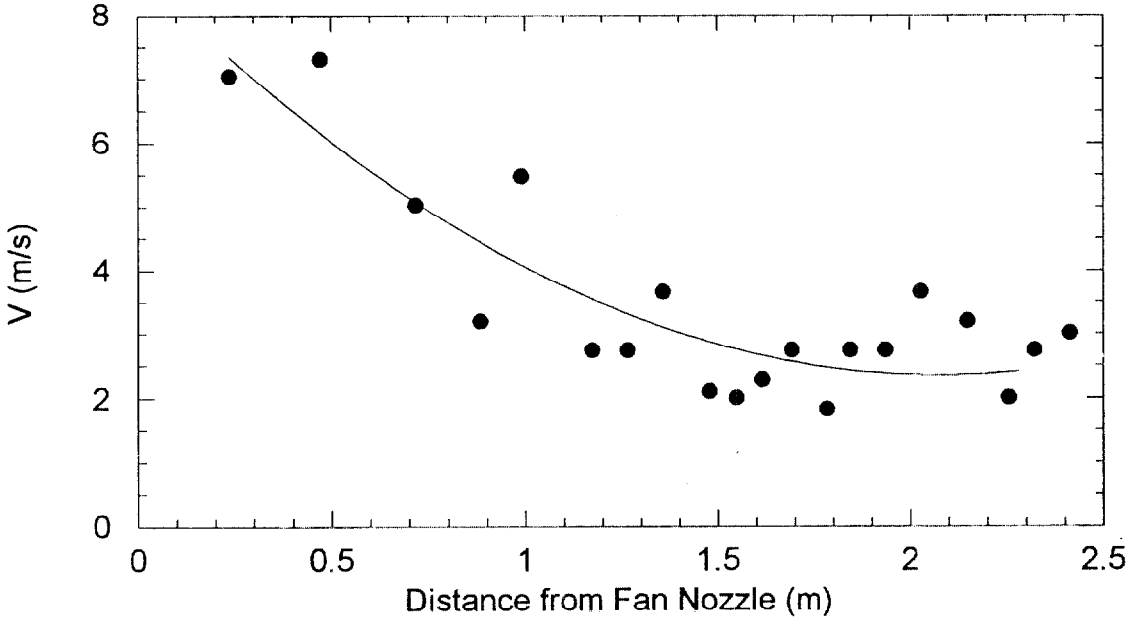

12. The measured velocity of the leading edge of suppressant as a function of downstream position for the same data as shown in Fig. 11.

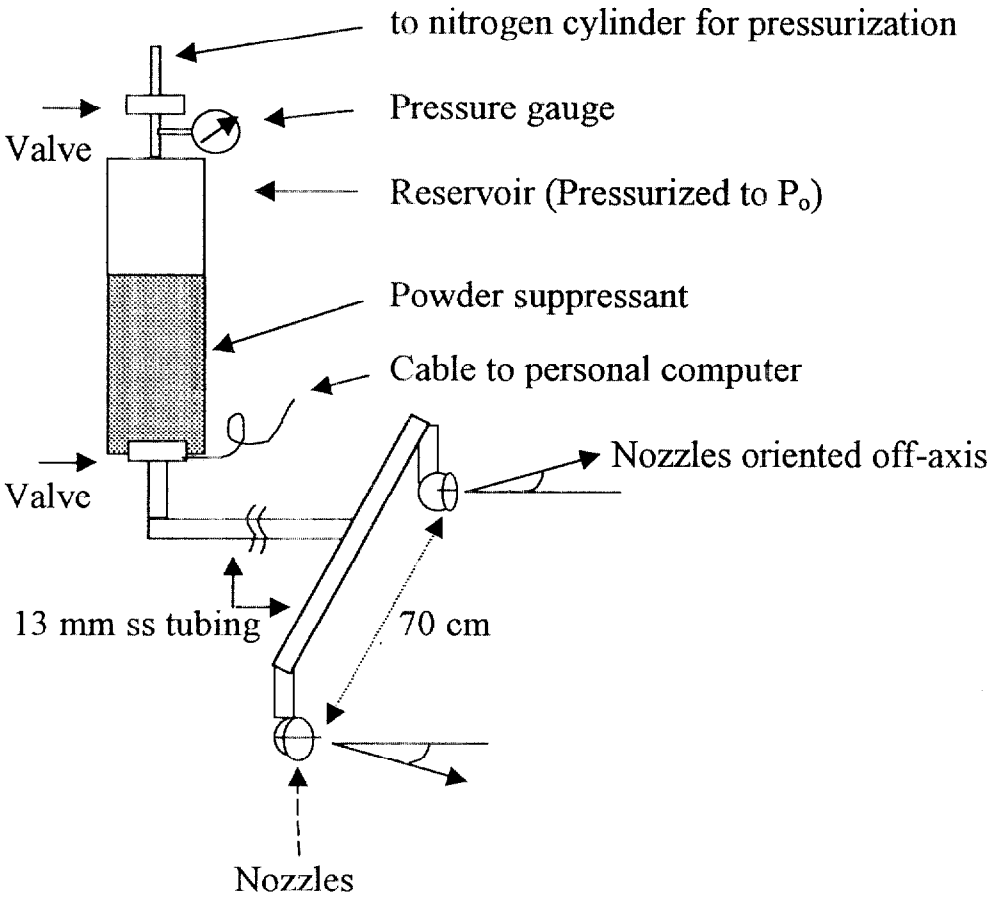

13. Perspective drawing of the suppression system used in the underbody suppression experiments.

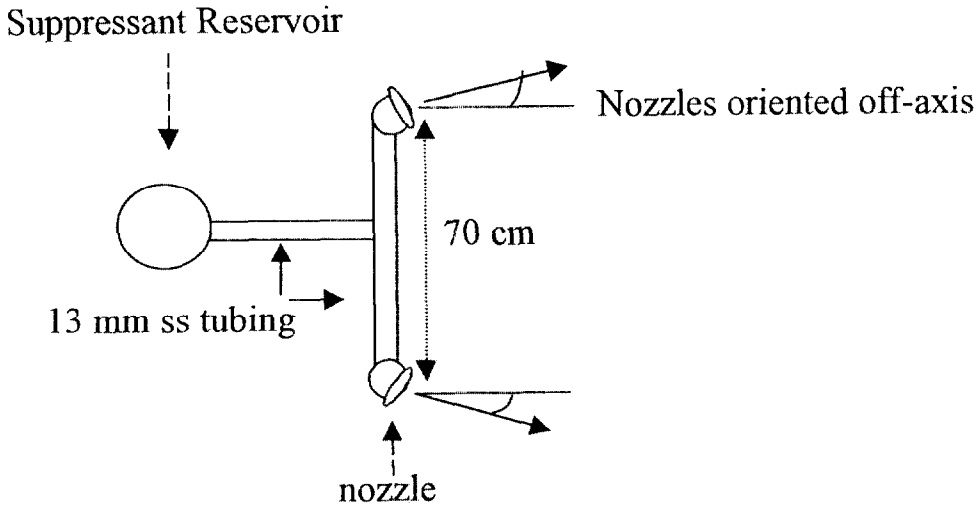

14. Top view drawing of the suppression system nozzle orientation used in the underbody suppression experiments.

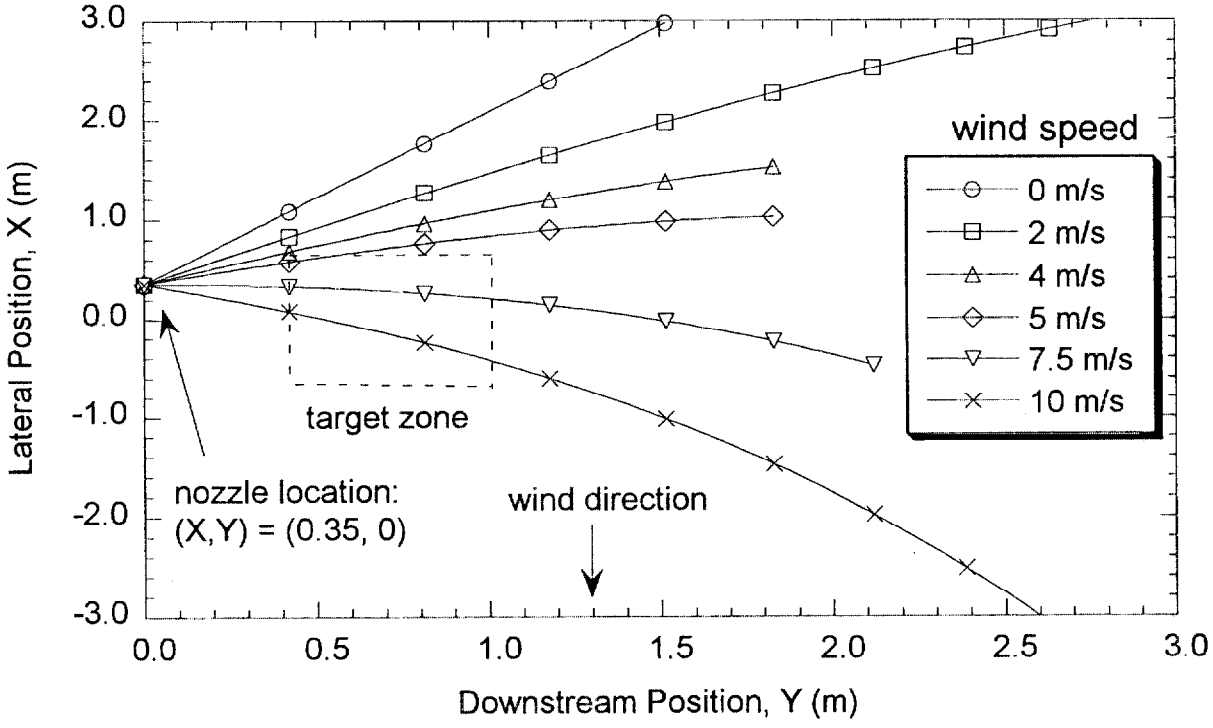

15. Calculation of the effect of wind on suppressant coverage for the velocity profile shown in Fig. 11 with the nozzles oriented 10° off-axis for the system shown in Figs. 13 and 14.

represents the area to be covered by the suppressant dispersion (e.g., the area under a fuel tank). At high wind speeds, the calculation results suggest that the wind will blow the suppressant past the edge of the target zone and even past the central axis (X=0). The calculations suggest that the target zone will be adequately covered for wind speeds up to 5 m/s (11 mph). Figure 16 shows the effect of wind on suppressant coverage when the off-axis nozzle orientation is changed from 10° to 20° in the calculation. The calculated suppressant coverage improves somewhat. Interpolating the results, coverage appears adequate for wind speeds approaching 6 m/s in this case.

An experiment was carried out to test the calculation results. A variable speed fan (43 cm diameter) was oriented perpendicular to the axis of effluent transport (X=0), 0.6 m downstream and at a lateral location of X= 3 m as seen in Fig. 17. The fan nozzles were oriented 20° ($\pm 3^{\circ}$) off-axis. The air velocity provided by the fan was measured by a Sierra Instruments air flow meter ($\pm$20 % uncertainty). Figure 17 shows that the fan provided a non-uniform "wind", ranging in value from 3 m/s to 5 m/s in a direction perpendicular to the fan system centerline, depending on the exact downstream and lateral location. Frame by frame analysis of the suppressant movement during the ABC suppressant discharge in experiment 15 of Table 7 showed that the lateral edge of the suppressant dispersion was not transported beyond X=1.2 m laterally. This result is consistent with the calculation shown in Fig. 16, where the 5 m/s wind speed prevented the suppressant edge from flowing beyond 1.2 m laterally. Nozzle #14 was ultimately selected for full-scale underbody suppression by powders and halogenated compounds under low wind conditions, as described in Section 3.4. The residence time of the suppressant over the target area is relatively unimportant and is not considered here since the characteristic time of chemical reaction, $O(10^{-6}$ s), is so much faster than the suppressant residence time, O(1 s). This nozzle arrangement was tested in Section 3.4 to suppress an underbody gasoline fire in a mid-sized sedan.

3.0 Fire Suppression Experiments

Four experimental configurations were developed to simulate post-collision vehicle fires. The configurations are listed in Table 1 and consist of full-scale and reduced-scale experiments addressing engine compartment and underbody fires in simulated vehicles and uncrashed passenger vehicles. The objective of the experiments was to determine the critical mass of suppressant required to extinguish the test fires in each of the four experimental configurations. An overview of the experiments described in this Section is given in Section 1.0.

3.0.1 Definition of Critical Mass and Its Uncertainty

The dependent experimental parameter in each of the fire suppression experiments (Configurations 1-4 in Table 1) was the critical suppressant mass. For consistency, the same definition of critical suppressant mass and its uncertainty is used throughout this report. Figure 18 shows the percentage of successful suppression experiments as a function of the mass of gaseous

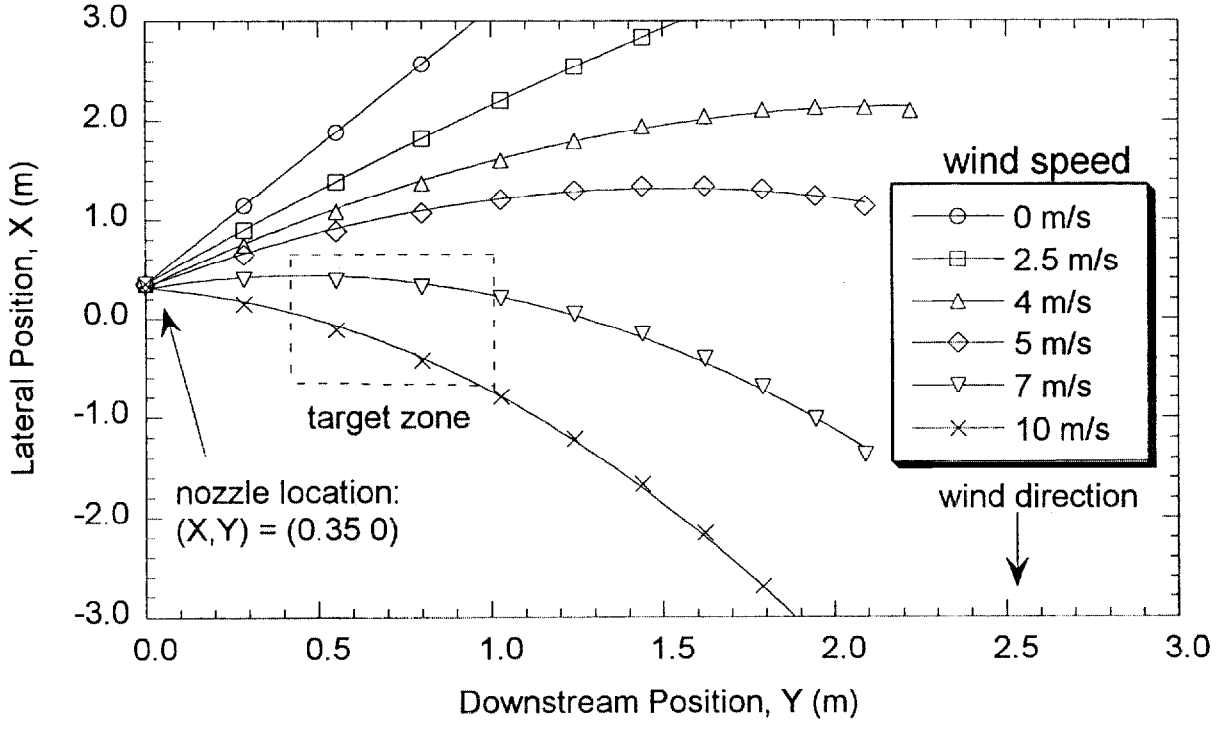

16. Calculation of the effect of wind on suppressant coverage for the velocity profile shown in Fig. 11 with the nozzles oriented 20° off-axis for the system shown in Figs. 13 and 14.

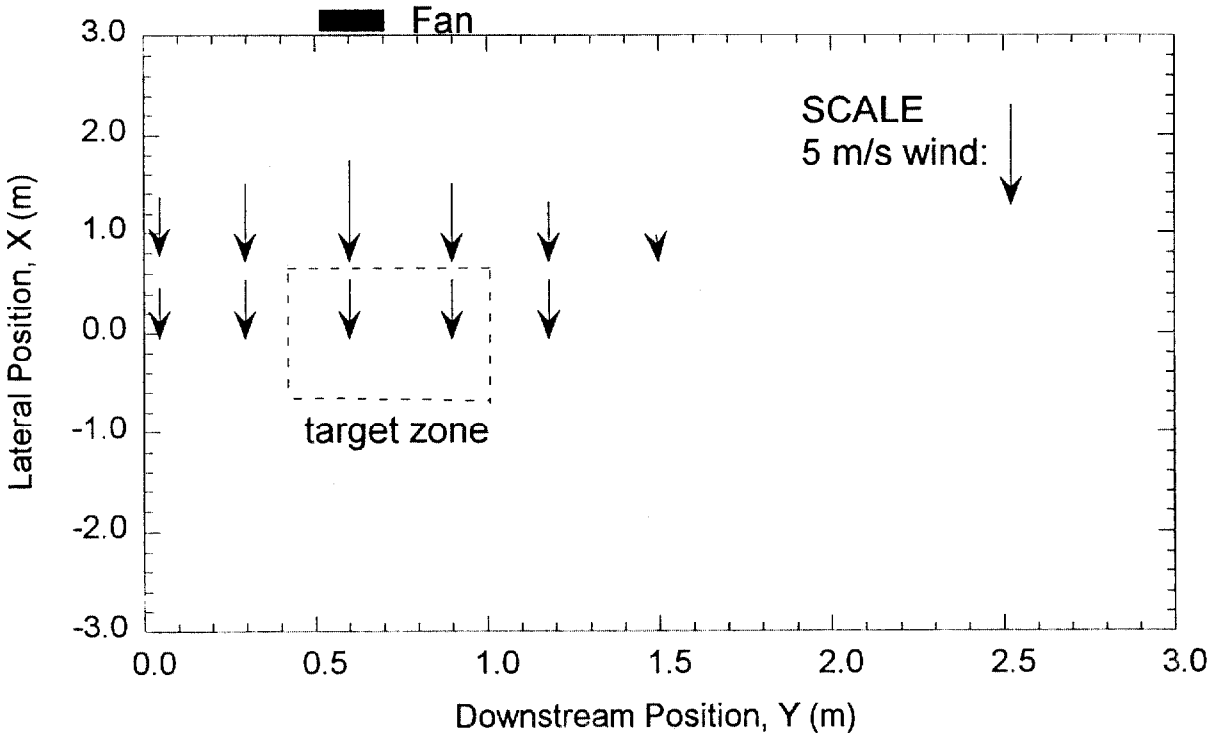

17. The measured velocity provided by the electric fan at several downstream locations.

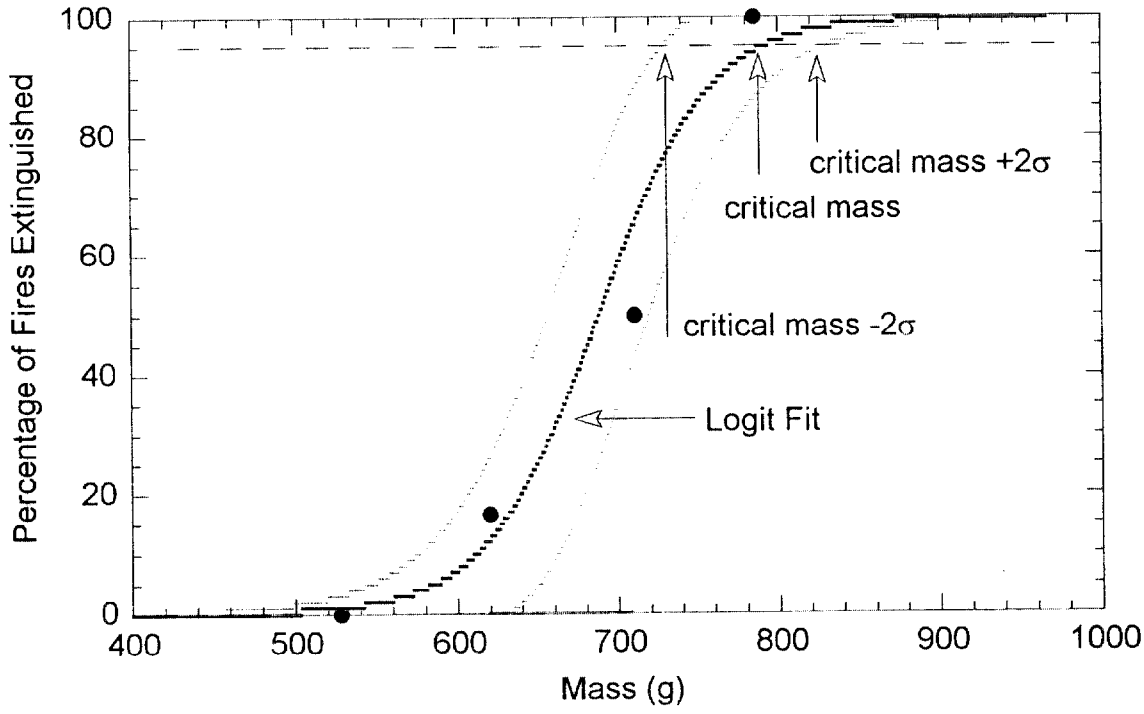

18. The percentage of fires extinguished as a function of the mass of gaseous suppressant (N_2) in the reduced-scale compartment. Also shown are the best fit to the data using the Linear Logit model as well as the curves representing the (2σ) uncertainty to the best fit.

N_2 suppressant delivered for a test fire in the reduced-scale compartment fire, referred to as Configuration 1 in Table 1. The Figure summarizes one data set that represents the results from 19 suppression experiments using one experimental configuration and conditions. In each of these experiments, varying amounts of suppressant mass was used and the fire was observed to be either suppressed or not suppressed. The experimental conditions in Figure 18 are not particularly relevant as the results are presented only to illustrate the definition of critical mass.

Figure 18 shows that the percentage of experiments in which the fires were extinguished increased as the suppressant mass increased. This was typical for all conditions in all experimental configurations. Suppression was assured for large suppressant mass (>780 g), whereas for small suppressant masses (<530 g) extinguishment never occurred. The large difference in the suppressant mass between completely successful suppression and completely unsuccessful suppression in Fig. 18 indicates the influence of random processes during the suppression event, including the turbulent nature of the flows of suppressant, air, and fuel, as well as their interaction. In this report, the experimentally determined apparent critical mass (M_c) is defined as the smallest suppressant amount that always resulted in successful fire suppression. In Fig. 18, for example, M_c was equal to 780 g.

To estimate the value of the uncertainty in M_c for each of the four experimental configurations, representative results from each of the four experimental configurations were analyzed using the Linear Logit model (McCullagh and Nelder, 1989). The number of experiments (N) analyzed was 7, 5, 6, and 4 for Configurations 1-4, respectively, as indicated in Table 9. The software program ***S*** (Chambers and Hastie, 1991) was used to fit the Linear Logit model. The predictor variable was taken as the mass normalized by the critical mass (a non-dimensional representation of the abscissa in Fig. 18) and the response variable was taken as the percent of the fires extinguished (ordinate in Fig. 18). The Logit model was implemented using one common slope for all of the experimental configurations. This approach was considered reasonable, because on a normalized scale the data yielded slopes that were very similar for the four configurations [Levenson, 2000]. At the same time, the intercept, which shifts the fits along the abscissa, was allowed to vary among the data sets for each configuration. A comparison of the fits to the input data suggests that the form of the Logit model as applied to the normalized masses was appropriate [Levenson, 2000].

Based on the results from the Linear Logit analysis, the inverse predictions of the normalized masses corresponding to a value of 95 % of the fires extinguished were calculated as well as the uncertainty in these values. The 95 % value was reasonable considering the form of the Logit model [Levenson, 2000]. A value of 100 % was not used, because the Logit fits obtain a value of 100 % only asymptotically. Figure 18 presents an example of the Logit fit and its use in determining an uncertainty estimate for M_c. The Figure shows the best fit through the dimensional data using the Logit model as well as the curves representing the (2σ) uncertainty to the fit. The Logit model prediction of the mass corresponding to 95 % of the fires extinguished (denoted here as M_L) was 811 g, which was 26 g (or 3 %) larger than M_c. The difference between M_L and M_c was taken as contributing to the uncertainty in M_c. This is expressed in

Table 9 as the ratio of the absolute value of the difference between M_L and M_c, $|M_L-M_c|$, to the value of M_c. For the data in Fig. 18, the expanded uncertainty in M_L (with a coverage factor of $2\cdot\sigma$ or a level of confidence of 95 % [Taylor and Kuyatt, 1993]) at a value of 95 % of the fires extinguished was 89 g or 11 % of the value of the predicted mass (M_L). The combined expanded uncertainty in M_c was estimated from the root sum of squares of the above two sources of uncertainty plus the instrument uncertainty (= 4 %, with a coverage factor of $2\cdot\sigma$), leading to a value equal to 23 % (with a coverage factor of $2\cdot\sigma$ or a level of confidence of 95 %).

A similar analysis using the representative data for Configurations 1-4 resulted in values of M_L such that the term ($|M_L-M_c|/M_c$) was 0.3 %, 11 %, 8 %, and 8 %, respectively, as indicated in Table 9. In these cases, M_c was typically within a $2\cdot\sigma$ relative uncertainty interval predicted by the Logit analysis for M_L. The expanded uncertainties (U) with a coverage factor of $1\cdot\sigma$ in the predicted masses (M_L) were 6 %, 7 %, 6 %, and 9 % for Configurations 1-4, respectively, as indicated in Table 9. The combined expanded uncertainty (U_c) in M_c for Configurations 1-4 was estimated from the root sum of squares of the above two sources of uncertainty and instrument uncertainty, which was relatively small (σ = 2 %). This procedure yielded U_c equal to12 %, 25 %, 20 %, and 24 % (with a coverage factor of $2\cdot\sigma$, which represents a 95% confidence level), respectively, as indicated in Table 9. For the remainder of this report, M_c is taken as representative of the critical mass defined by the Logit model.

Table 9. Uncertainty Analysis.

Configuration	N	M_L/M_c	$\lvert M_L-M_c\rvert/M_c$	U [a]	U_c [b]
1. Reduced-scale compartment	7	1.003	0.003	0.06	0.12
2. Full-scale compartment	5	1.11	0.11	0.07	0.25
3. Laboratory Underbody	6	1.08	0.08	0.06	0.20
4. Full-scale Underbody	4	0.92	0.08	0.09	0.24

a. The expanded uncertainty in M_L, with a coverage factor of $1\cdot\sigma$.
b. The combined expanded uncertainty in M_c, with a coverage factor of $2\cdot\sigma$.

3.0.2 Design of Suppression Experiments

Each of the suppression experiments described in this section were designed to represent aspects of post-collision vehicle fires. Several features were common among the four experiments including similarities in the experimental apparatus, the procedures, as well as a number of assumptions related to the post-collision aspects of the experiments and implicit in the experimental design:

(1) The geometry of the experimental apparatus and how it relates to a post-collision vehicle fire is described in Section 1.2.2.

The next two points involve the external air flow:

(2) The test vehicle was always stationary when the suppressant was discharged. In this sense,

the effect of vehicle movement on suppressant requirements was not addressed. Instead, it was assumed that a suppression system could be activated after vehicle movement had ceased. Operationally, this could be achieved by imposing a short time-delay (≈10 s to 20 s) on system activation after detection.

(3) The radiator fan was off during suppressant deployment. It was presumed that an on-board fire protection system could be designed such that a suppressant could be deployed after the engine fan is shut off. Assumptions (2) and (3) were imposed for a number of reasons, principally because suppression in a partially open compartment is challenging without an external air flow, which can drastically increase suppressant mass requirements. The effect of an external air flow on suppressant requirements was considered in the suppressant distribution experiments described in Section 2.

(4) The mid-sized sedan used for the suppression experiments in Configurations 2 and 4 (see Table 1 and Sections 3.2 and 3.4) was uncrashed. In a crash, vehicle components will move relative to the suppressant delivery system, possibly leading to obstruction of the suppressant system. The effect of this possibility was tested in the reduced-scale compartment (Section 3.1). In those experiments, the suppressant delivery nozzles were positioned in an obstructed location. Also, the suppressant delivery systems and the placement of these systems was not tested for crashworthiness. Instead, this study focussed on the feasibility of fire suppression. In that sense, this report does not specifically recommend suppressant system placement, which must be considered for each vehicle type. Further testing of suppressant placement and orientation should be considered.

(5) The full and reduced-scale engine compartment experiments (Sections 3.1 and 3.2) did not include a simulated engine that was powered. Thus, the metal and thermoplastic components were not preheated. Instead, the fire itself heated components. And in locations near the fire, measured temperatures were significantly higher than temperatures representative of typical steady-state operating temperatures in an engine compartment [Santrock, 1996]. The effect of preheating an engine component at the location where a fuel leak occurs was studied in Configuration 1 (see Table 1 and Section 3.1) as was the effect of varying the duration of the fire (or preheating) before suppressant discharge.

(6) It was assumed that detection could be satisfactorily accomplished if a fire is large enough and the experiments were typically performed without active detection. Judicious design needs to be applied to optimize detection placement and orientation in terms of crashworthiness and early detection (detection of a small fire). Several experiments were conducted using active detection for Configurations 2 and 4 (see Table 1 and Sections 3.2 and 3.4). These experiments demonstrated the efficacy of optical detection under the test conditions.

The protocol used for selection of suppressant mass was another key feature common among the suppression experiments. As mentioned in Section 3.01, the dependent experimental parameter in all of the fire suppression experiments (Configurations 1-4 in Table 1) was the critical suppressant mass, M_c. To experimentally determine the value of M_c, a series of suppression experiments were conducted. This involved selecting the value of the suppressant mass to be evaluated and was typically accomplished using the following protocol. The initial suppressant mass was selected based on engineering judgement. If suppression was successful, then the amount of suppressant

used in the subsequent test was reduced by ½. This protocol was used to select the suppressant mass until the experiments were not successful in obtaining suppression. Then, the mass selected for the next test was taken as an average of the largest mass that was not successful suppressing the test fire and the smallest mass that was successful. Testing stopped when the difference between the successful and unsuccessful tests was approximately less than ½ of the value of M_c. The critical mass was confirmed by repeating the experiment at least once. This protocol was developed to minimize the number of experiments necessary to determine M_c.

3.1 Reduced-Scale Engine Compartment Suppression Experiments

A reduced-scale apparatus was developed to conduct suppression experiments on simulated engine compartment fires. The main objective of the experiments was to determine the impact of changing experimental conditions on the critical suppressant mass requirements.

This section is organized into several parts. In Section 3.1.1, the geometry of the reduced-scale compartment and the gaseous and powdered suppressant delivery systems are described. An overview of the dependent and independent parameters that were investigated during the experiments is given in Section 3.1.2. Section 3.1.3 describes the experimental procedure including details of the test protocol. Section 3.1.4 describes the experimental results including measurements to characterize baseline conditions in the simulator. A detailed summary of the conditions during each experiment is presented. The impact of several independent experimental parameters on the critical mass suppressant requirements is described. The experimental results are summarized in Section 3.1.5.

3.1.1 Apparatus

Table 2 lists a number of geometrical features that characterize the reduced-scale engine compartment simulator. Figure 19 is a schematic drawing of the apparatus. The device incorporated a fuel delivery system, a suppressant delivery system, and a fire zone. The entire apparatus was placed under a variable flow exhaust hood. A screened wall surrounded the enclosure on all four sides. The reduced-scale compartment was rectangular, following the approach used in the analysis described in Sections 1.2 and 1.3 where an idealized rectangular compartment was taken as representative of the geometry of a post-collision engine compartment. The frame of the apparatus was rectangular with internal dimensions 70 cm wide, 90 cm long, and 40 cm deep. The bottom was open and raised above a cement slab a distance denoted as F in Fig. 1. The value of F was varied from 10 cm to 30 cm, yielding a volume varying from 0.3 m^3 to 0.4 m^3. This represents a 3:1 reduction in volume from the expanded (see Eq. 1) representative vehicle engine compartments listed in Table 2. The enclosure was partially filled with rectangular metal boxes, held in place by 1 cm rods or sheet metal strips. The boxes represented engine compartment components such as the air conditioning unit, the battery, pumps, and so on. A large central box simulated the engine block. The fixture was modular in structure, allowing changes in the

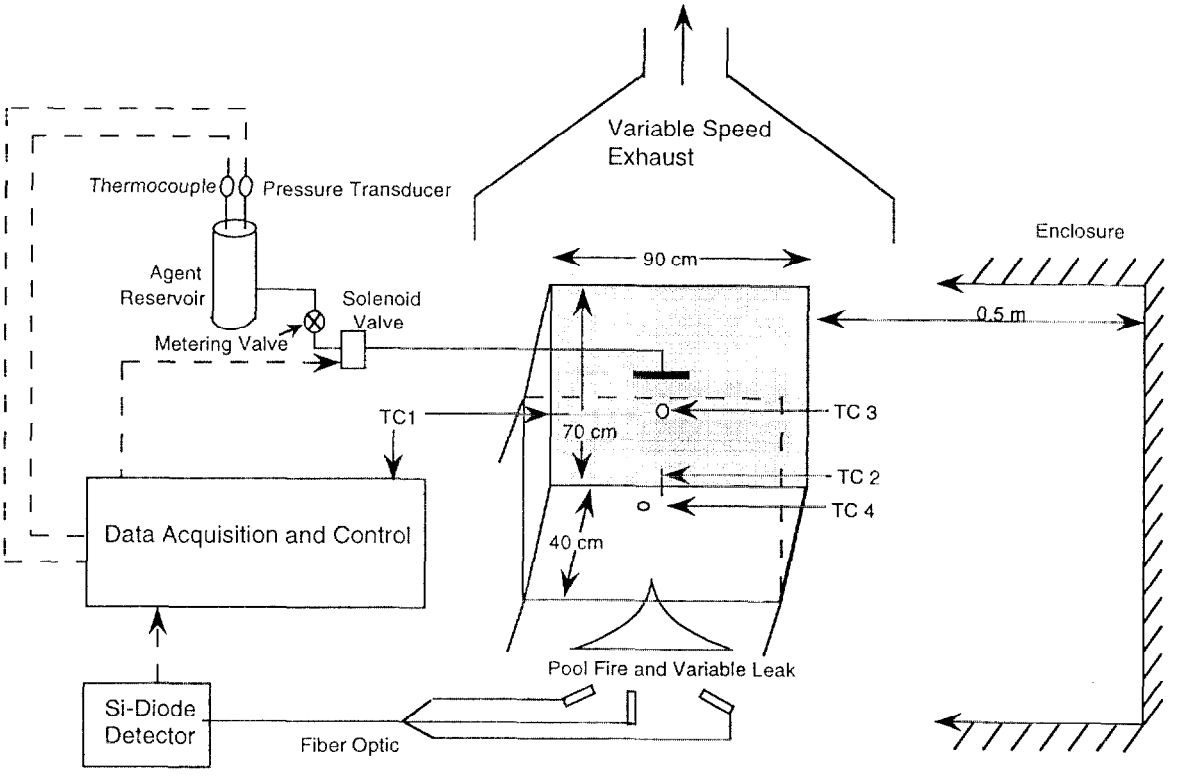

19. A schematic diagram of the reduced-scale engine compartment.

component configuration and thereby control of the volume filled percentage and the distance between components. From the perspective of mass transport, the boxes acted as flow obstacles, preventing direct suppressant impingement on the fire. Varying the compartment configuration

Table 10. Independent Experimental Parameters in the Reduced-Scale Engine Compartment.

Parameter Class	Parameter	Range of Values
Fuel	Type	Heptane, gasoline, transmission fluid, Motor oil, anti-freeze
	Fuel leak rate	0 to 50 mL/min
	Fuel puddle	0 to 100 mL
Fire	Preburn time	10 s to 90 s
Suppressant	Type	Clean suppressants, powders, SPG, AG, tubular
	Nozzle type	Spiral, straight tube, tee with straight tubes
	Δt	0.5 s to 4 s
	Supply line diameter	2 mm to 8 mm i.d.
	Nozzle location	top panel/front panel
	Reservoir Pressurization	0.2 MPa to 4.2 MPa (30 psig to 600 psig)
Geometry	*AF*	8 % to 93 %
	VF	10 % to 40 %
	SO	1 % to 20 %
	H	0 to 5 cm

(adding or eliminating the modular components) allowed simulation of geometric changes in the engine compartment configuration that accompanies the crush associated with a front-end collision.

The top panel was mounted above the frame using C-clamps and metal spacers. The frame was lifted above the ground using metal rods. Figure 20 is an image of the reduced-scale enclosure configured such that H=5 cm and F=12.5 cm. Figures 21 and 22 show cross-sectional and top views, respectively, of the reduced-scale engine compartment in a standard configuration with approximately 30 % of the extended volume (see Eq. 1) filled with components. Suppression experiments were also conducted using other geometric configurations and volume fill conditions as indicated in Table 10. The boxes in Figs. 21 and 22 are numbered for reference, with the shaded boxes (#16-19) situated in a lower layer of the enclosure.

A flammable liquid (see Table 10) was stored in a 1 L reservoir and delivered to the apparatus with a peristaltic pump. The fuel was pumped through a 6 mm (o.d.) copper tubing to the fuel discharge location. The fuel delivery rate was calibrated with a stopwatch and a graduated cylinder. Preheating of the fuel filled tube by flames was minimized by covering the tube with insulation and aluminum foil and by positioning the tube away from impinging flames. In addition, the fuel discharge was located remotely from the suppressant discharge location (see Fig. 19). In

20. Photograph of the exterior of the reduced-scale enclosure configured such that H=5 cm and F=12.5 cm.

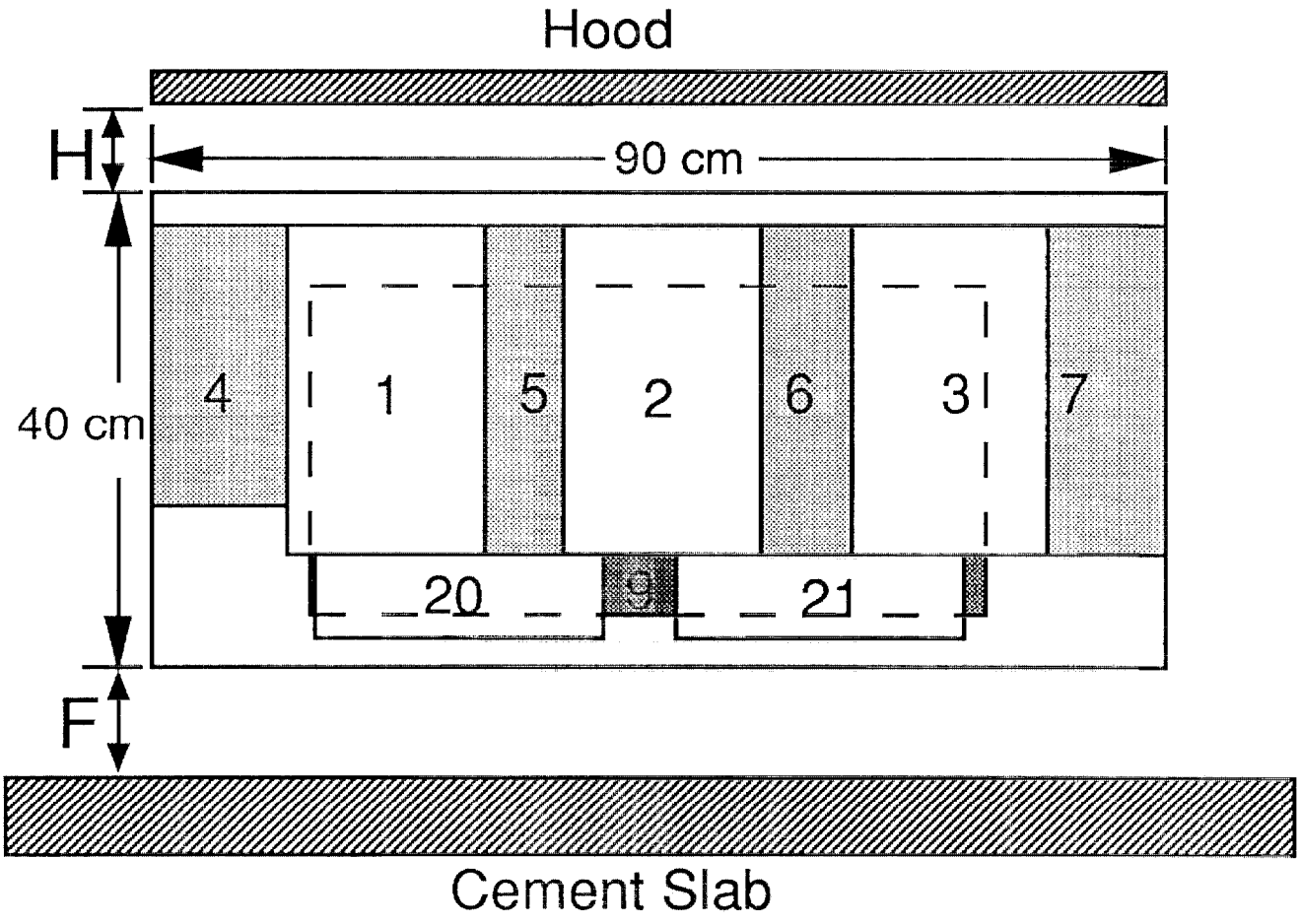

21. Cross-sectional diagram of the front three layers of the reduced-scale engine compartment configured with 30% of the volume filled with components.

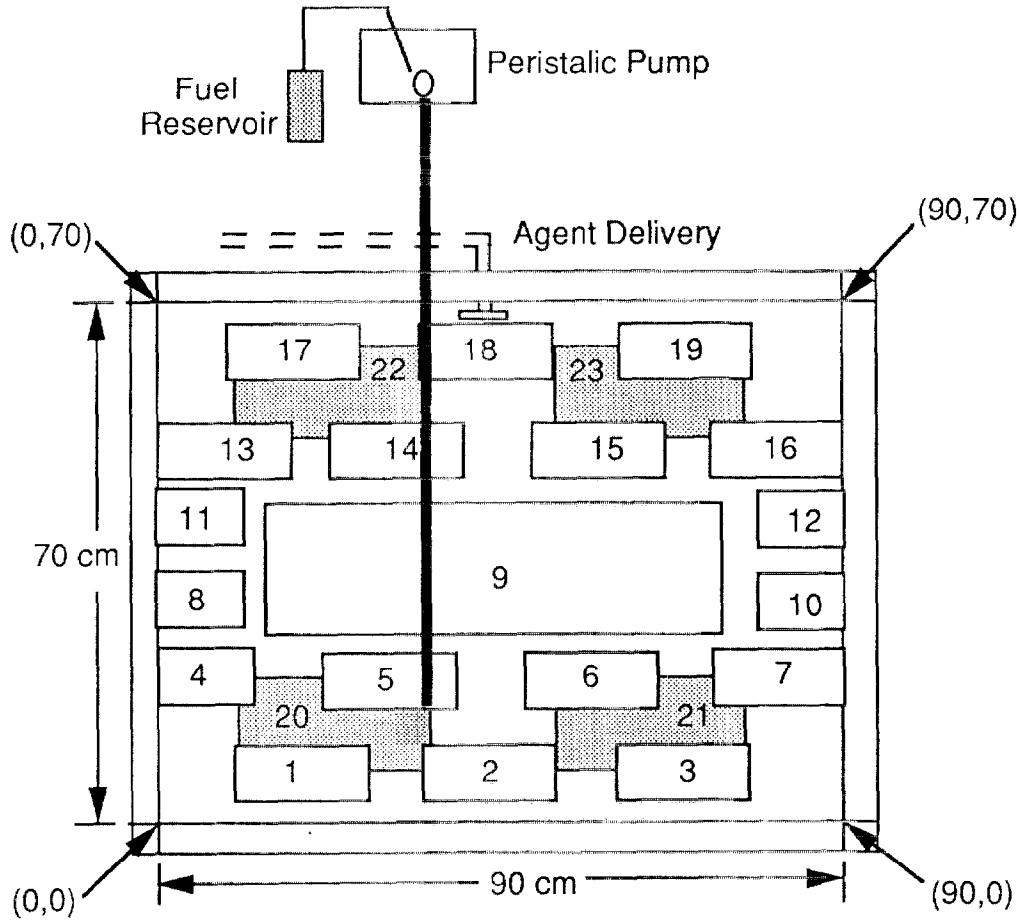

22. Top view drawing of the reduced-scale engine compartment configured with 30% of the volume filled with components.

some experiments a fuel puddle was positioned on the ground. In those cases, a measured volume of fuel was poured into a funnel, where it traveled through a rigidly positioned metal tube to the designated location on the cement slab.

In some experiments, temperatures were measured at several locations using type-K thermocouples. Figure 19 shows the position of some of the thermocouples, which were located approximately midway between the enclosure corners and below the center of the top panel; all in the plane of the top of the enclosure (at the plane defined by D = 40 cm in Fig. 1). The thermocouple locations (X,Y) referenced to the left front corner (see Fig. 22) were (2 cm, 35 cm), (45 cm, 2 cm), (88 cm, 35 cm), (45 cm, 68 cm) and below the top panel center at (45 cm, 35 cm). The time of flame extinction was indicated by cessation of flame emission in the enclosure as measured with a silicon-diode detector optically coupled to three fiber optic cables (see Fig. 19). The time response of the silicon-diode detector was approximately 5 ms.

3.1.1.1 Suppressant Delivery

For the clean and powdered suppressants, the delivery system consisted of the suppressant storage vessel, a computer controlled solenoid valve, and a delivery tube as shown in Fig. 19. For experiments using gaseous nitrogen, the storage volume was a 43.8 liter pressure vessel and associated plumbing, yielding a total suppressant storage volume of 44.0 L volume. For the experiments using powder or halogenated suppressants, the storage volumes were 1.02 L, 2.27 L, or 3.84 L. For the powdered suppressants and the halogenated compounds, the suppressant reservoir was typically pressurized to 1.4 MPa (200 psig) by gaseous nitrogen. A number of the experiments were conducted using larger or smaller pressures. The suppressant temperature and pressure in the storage vessels were measured with a type-K thermocouple and a fast response pressure transducer (1 kHz). An electronic or pneumatic solenoid valve was plumbed just downstream of the suppressant reservoir. Varying the opening duration of the solenoid valve and the reservoir pressure controlled the mass of suppressant discharged.

For the clean and powder suppressants, two discharge locations were used, through the center of the top panel and through the center of the simulated dash panel (referred to here as the front panel or forward bulkhead). The front panel location was selected to test suppressant effectiveness when suppressant discharge is directed into an obstruction, as may occur in a post-collision situation. The top panel center location was selected to test suppressant effectiveness from a different location that may be advantageous in terms of uniform suppressant delivery as compared to the front panel location.

The vehicle front (or dash) panel separates the passenger compartment from the engine compartment. The standard configuration of the discharge nozzle on the front panel consisted of a tee with 9 mm (i.d.) outlets oriented in a horizontal plane, located 1.5 cm from the inside wall of the enclosure. The outlets from the tee were straight tubes. The tee evenly split the incoming flow and directed it towards the side panels. In one series of experiments either a simple straight

tube (perpendicular to the front panel) replaced the tee or nozzles (#5 in Table 7) were attached to the tee outlets. The discharge nozzle on the top panel was a 9 mm (inner diameter) straight tube perpendicular to the plane defining the top panel. The top panel-mounted nozzle directed the suppressant towards the large central obstruction directly below (see Figs. 21 and 22). Both nozzles simulated suppressant delivery in a highly obstructed flow field. The top panel nozzle location was selected because preliminary experiments showed that suppressant dispersion about the top of the enclosure was rather uniform using this approach. An infinite number of other nozzle configurations could have been tested, but resource constraints limited the number of tests.

The prototype devices were mounted at locations suggested by manufacturer representatives, who were present during the testing. The devices could have been positioned remotely and the contents delivered into the compartment through piping in a manner similar to that of a conventional suppressant. Instead, the aerosol device was mounted in the rear corner of the compartment, near the simulated passenger/engine compartment bulkhead. In a second configuration, two units were simultaneously deployed. Each device was placed in a corner and tilted at 20° from the vertical, one directed up and the other down, both oriented towards the center of the compartment. When a single unit was used, it was positioned upwards, in a similar fashion. A photograph of two of the units is shown in Fig. 23. The gross weight of each unit was approximately 800 g. In the Figure, one of the units was unused and the other used, exposing its internal structure. Figure 24 shows one of the devices positioned in the rear corner of the configuration shown in Fig. 22 of the reduced scale enclosure.

The tubular device was mounted on the bottom of the top panel, with the center of the device near the center of the panel. Figure 25 is a photograph of the device. It was a 1 cm (outer) diameter nylon tube (0.16 cm wall) coiled in a planar, nearly circular shape of 0.3 m diameter. The tubes were filled with ≈300 g of ammonium poly-phosphate powder and pressurized to 1.4 MPa (200 psig) with HFC-134a (CH_2FCF_3). The gross weight of the mounting bracket and the suppressant filled tube was ≈800 g.

3.1.1.2 Experiments using Gaseous Nitrogen as Suppressant

A number of experiments used gaseous nitrogen as suppressant. The suppressant discharge system was designed to deliver a pulse of suppressant for a designated duration. A solenoid valve controlled the suppressant delivery duration. In order to avoid flow restrictions, a solenoid valve with a 1.3 cm inner diameter was used. The minimum achievable delivery time was approximately ¼ s. Control of the solenoid opening time was limited to approximately 50 ms, whereas measurement of the opening time was resolved to approximately 5 ms.

The mass of suppressant delivered to the enclosure (M_{nit}) was determined by calculating the mass released from the reservoir. This was accomplished by determining the initial and final reservoir mass, before opening and after closing the solenoid valve:

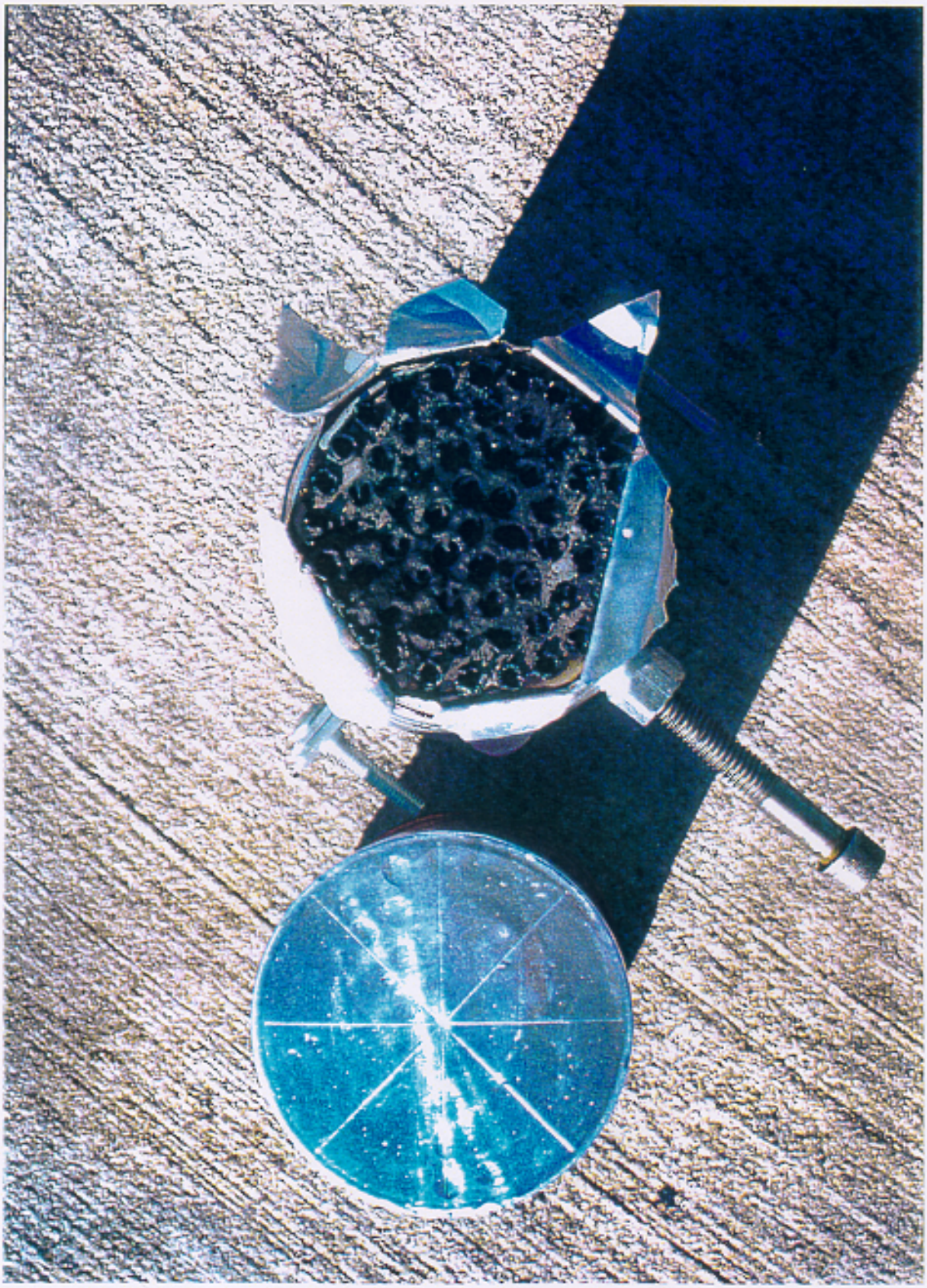

23. Photograph of two AG1 aerosol units.

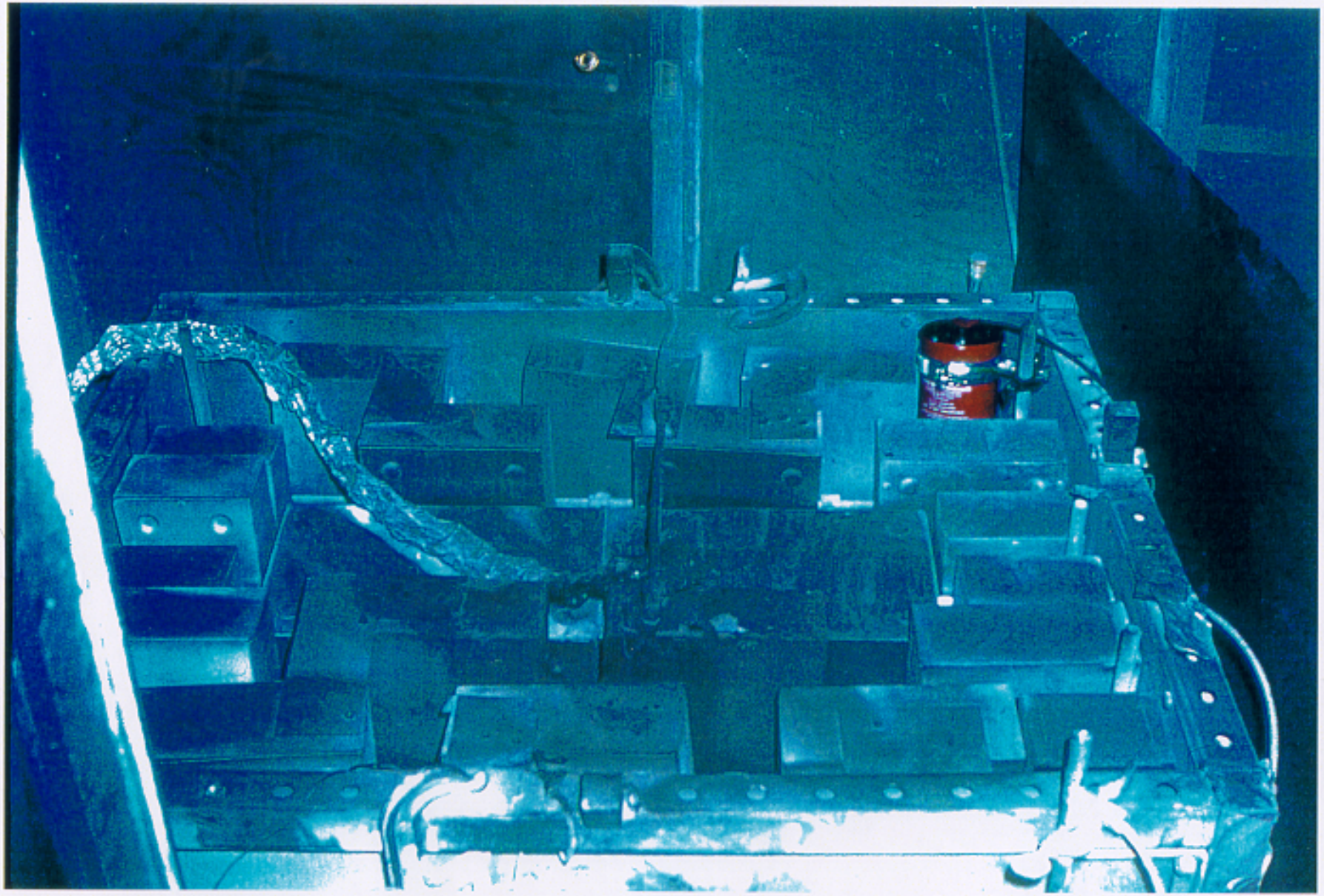

24. Photograph of one AG1 unit positioned in the rear corner of the reduced-scale enclosure for the configuration shown in Fig. 22.

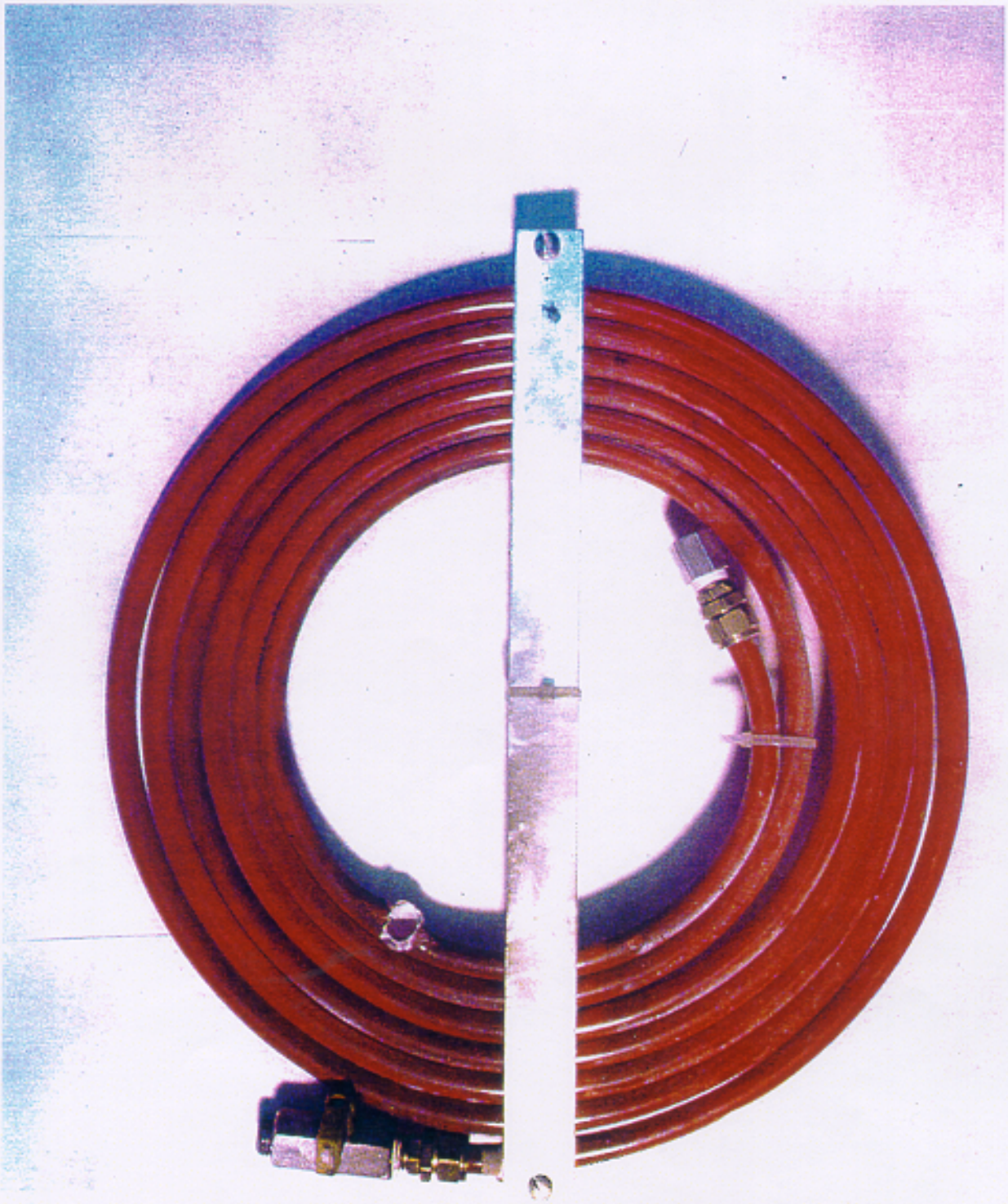

25. Photograph of the tubular suppression device used in the reduced-scale compartment experiments.

$$M_{nit} = V \cdot (MW_{nit}) \cdot [(P_o/T_o) - (P_f/T_f)] / R \quad (29)$$

where the terms in Eq. 29 are defined in Section 2.1 (see Eq. 27) and the subscripts o and f refer to the initial and final states, respectively. Equation 29 is an adequate description for an ideal gas like N_2 under the thermodynamic conditions considered here. The initial temperature in the reservoir was measured and the final temperature was determined by assuming that the expansion occurred isentropically:

$$T_f/T_o = (P_f/P_o)^{(\gamma-1/\gamma)} \quad (30)$$

where γ is the ratio of the specific heats of the gas (=1.4 for N_2). The mass leaving the reservoir and delivered to the compartment was determined by measuring T_o, P_f, and P_o and applying Eqs. 29 and 30. The pressure data were collected at a rate of ≈10 Hz, with the initial conditions determined from measurements made just prior to the release of the suppressant and the final conditions measured just after the solenoid valve closed. The duration of suppressant discharge was estimated from the change in slope of the reservoir pressure-time curve. The average rate of suppressant mass delivered was determined by considering the ratio of the mass delivered to the delivery duration.

Figure 26 shows a typical measurement of the transient reservoir pressure for a long solenoid opening time. The calculated mass of suppressant delivered and the rate of suppressant delivery are also shown. The reservoir was nearly empty at the end of the 25 s period. Many experiments used an initial pressure similar to that shown in the Fig. 26, but the solenoid valve was closed after less than 4 s. The calculated mass delivery rate rapidly increased from zero to a maximum value as the solenoid opened. At later times, the mass delivery rate slowly decreased with time.

3.1.1.3 Experiments using Powders and Compressed Halogenated Liquids

The procedure for loading the reservoir with a powder is described in Section 2.1. For the halogenated compounds, a somewhat different method was used. The large storage cylinder was connected to the suppressant reservoir, which was placed on a scale with 1 g reading accuracy. The tare weight was measured and recorded. The liquid-phase material was allowed to flow until the desired suppressant mass was in the reservoir. The reservoir was closed and the final weight was noted after the filling system was disconnected. The reservoir was then connected to the suppressant delivery system. The ideal gas law accounts for the nitrogen mass except for soluable nitrogen in the compressed halogenated liquid. The mass of nitrogen dissolved in the liquid depends on the temperature, final pressure, and suppressant type. The dissolved mass can be estimated from the PROFISSY computer program [Yang et al., 1995]. Experimentally, complete nitrogen saturation in the liquid suppressant was attained by shaking and repressurizing the reservoir. The masses reported below for the powder and compressed halogenated liquids do not include nitrogen, which typically was 5 % to 10 % of the suppressant mass. The suppressant density as a function of temperature is listed elsewhere (Yang et al., 1995). At room temperature,

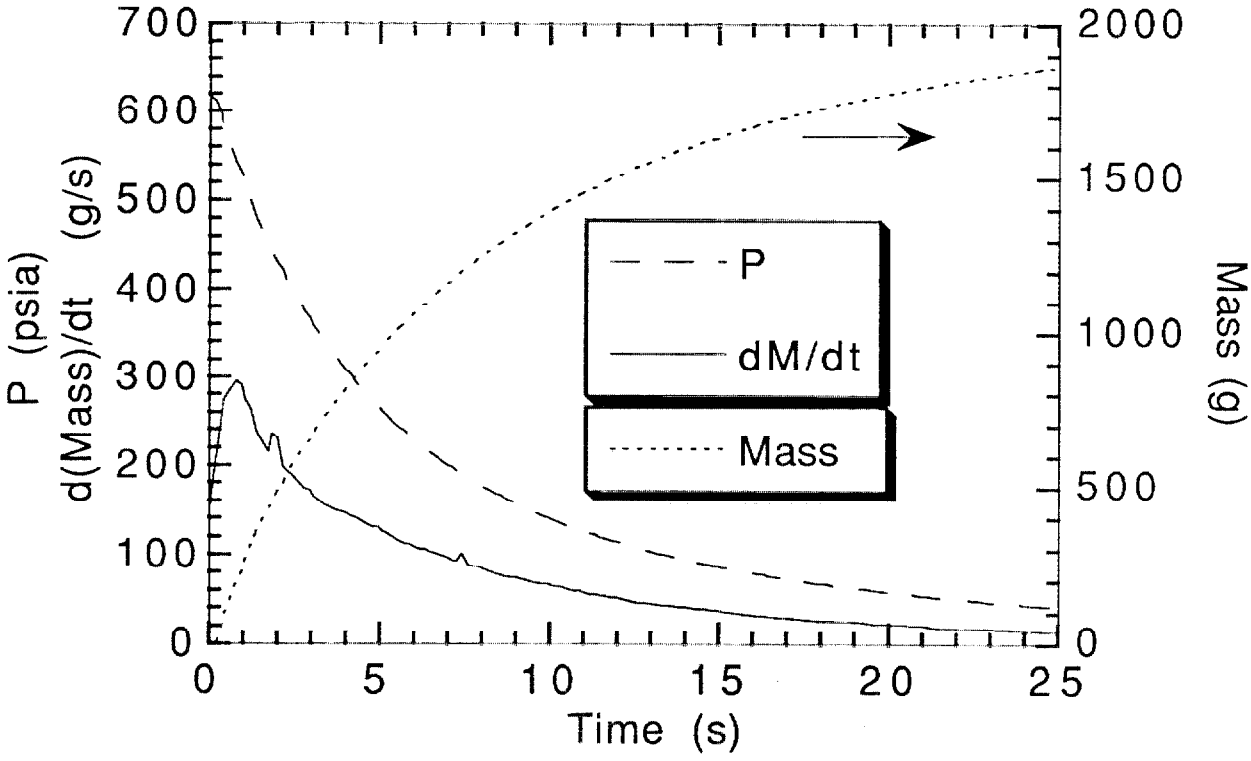

26. The gaseous N_2 reservoir pressure and the calculated mass and rate of mass discharge as a function of time.

Table 8 shows the density (ρ_i) and the vapor pressure (P) for some of the suppressants considered here.

3.1.2 Overview of Measurements

Experiments were conducted to determine the influence of several parameters on the requirements to achieve fire suppression. The dependent parameters that were considered in the experiments were the critical suppressant mass and delivery rate. The independent experimental parameters and their range of values are listed in Table 10. They were associated with the geometry of the simulated compartment, the fuel, the fire, and the suppressant. The independent experimental parameter associated with the fire was the preburn time, defined here as the period that the fire was allowed to burn before suppressant delivery was initiated. The independent experimental parameters associated with the suppressant were the suppressant type, reservoir pressurization, supply line diameter, and nozzle placement, type, orientation, number, delivery duration and rate.

The independent experimental parameters associated with the compartment geometry consisted of the values of F and H, as well as the configuration of the components within the compartment. In one series of experiments, the effect of AF (see Section 1) and the distribution of openings in the top layer of clutter were varied. Figures 27-31 are drawings that indicate the filled and open portions of the top layer of clutter, which was fabricated from thin sheet metal. The volume filled percentage in Figs. 27-31 was maintained at a constant value (10 %), represented by the large central box seen in the figures. Figure 32 is a photograph of Configuration 1 corresponding to the drawing shown in Fig. 27.

In another series of experiments, the effect of the volume percentage filled (VF) was varied (see Section 1.2 for a description of VF). This was accomplished by adding metal box "components" to the compartment. In another series of experiments, the percent of the enclosure surface that was open, SO, (see Eq. 2 for definition) was varied. This was accomplished by changing the depth (D) and frame height (F) of the compartment by either extending the body panels by increasing D and decreasing F or by lifting the frame legs by increasing F (see Fig. 1). The value of SO was also affected by the top panel distance (H in Fig. 1). Figure 33 shows the relation between SO and F for two different values of H and Fig. 34 shows the relation between SO and H for three different values of F using the definition in Eq. *2*. SO increases nearly linearly for larger values of F or H (see the definition of SO in Eq. 3).

The independent experimental parameters associated with the fuel involved the fuel type, its location, and its flow rate. These factors influenced the rate of air entrainment into the compartment and thereby the compartment ventilation rate (see Eq. 9). The configuration of the fuel included a spill on the concrete pad (situated below the compartment), a hydrocarbon leak flowing over the vertical surface of one of the compartment components (Box #5 in Figs. 21 and 22), and a combination leak and a spill.

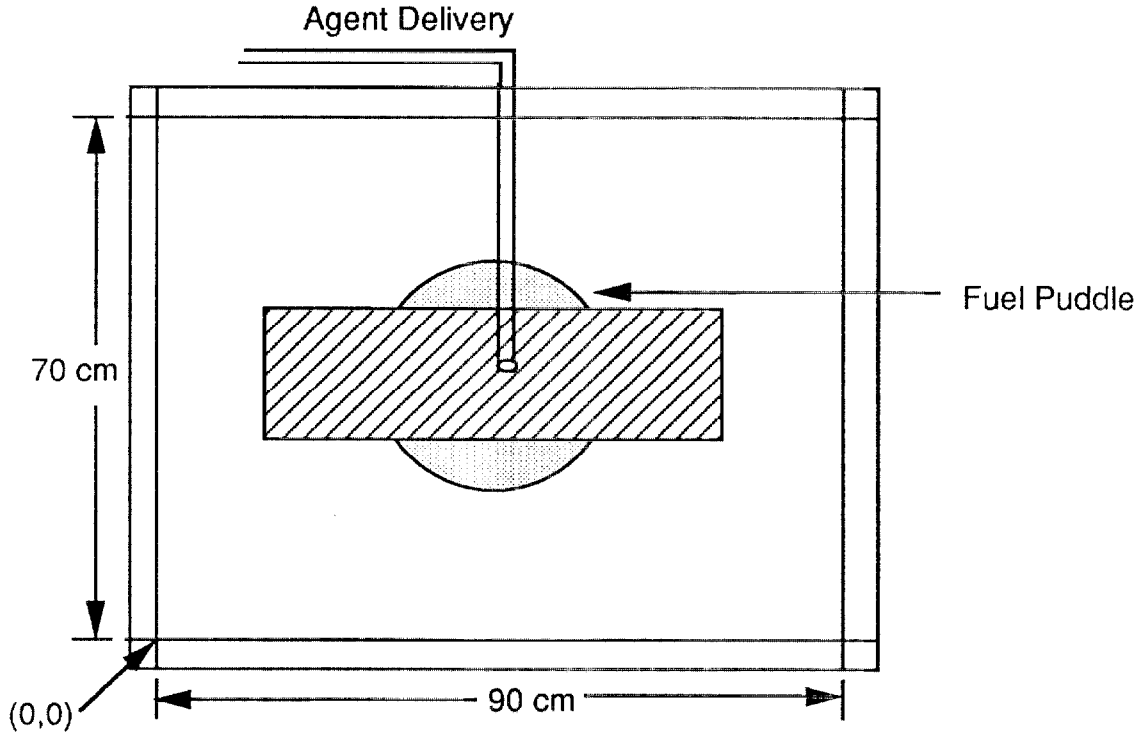

27. A top view of the arrangement of obstacles in the reduced-scale engine compartment for Configuration 1.

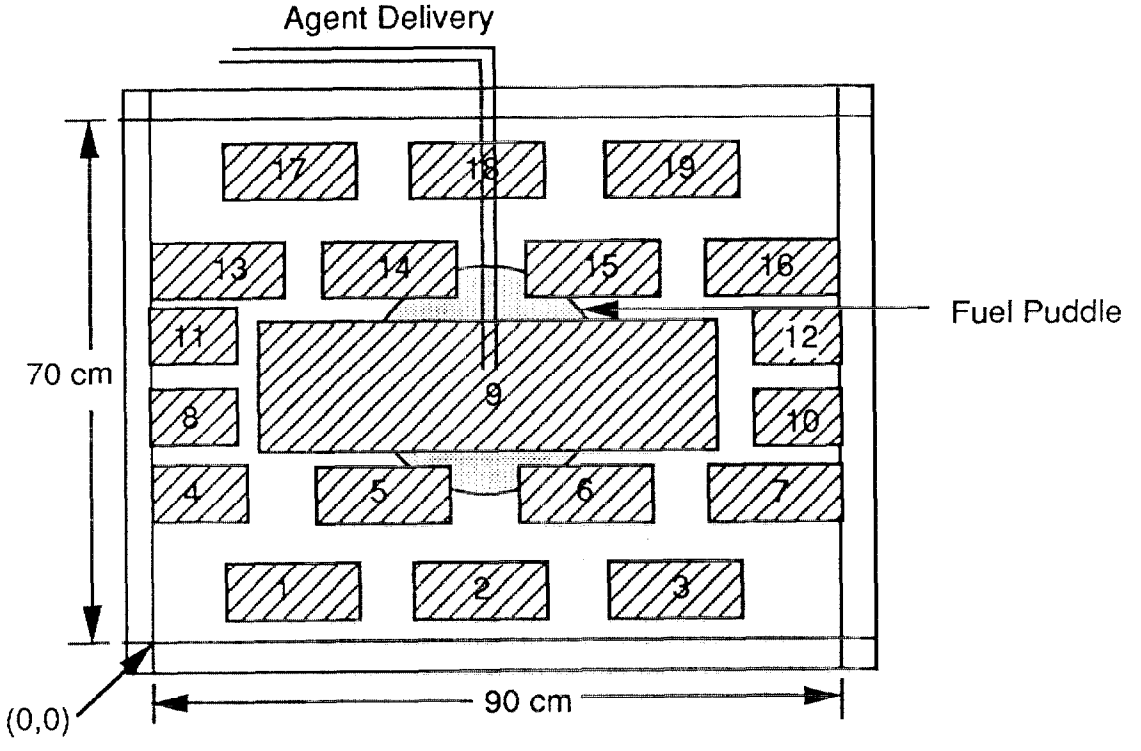

28. A top view of the arrangement of obstacles in the reduced-scale engine compartment for Configuration 2.

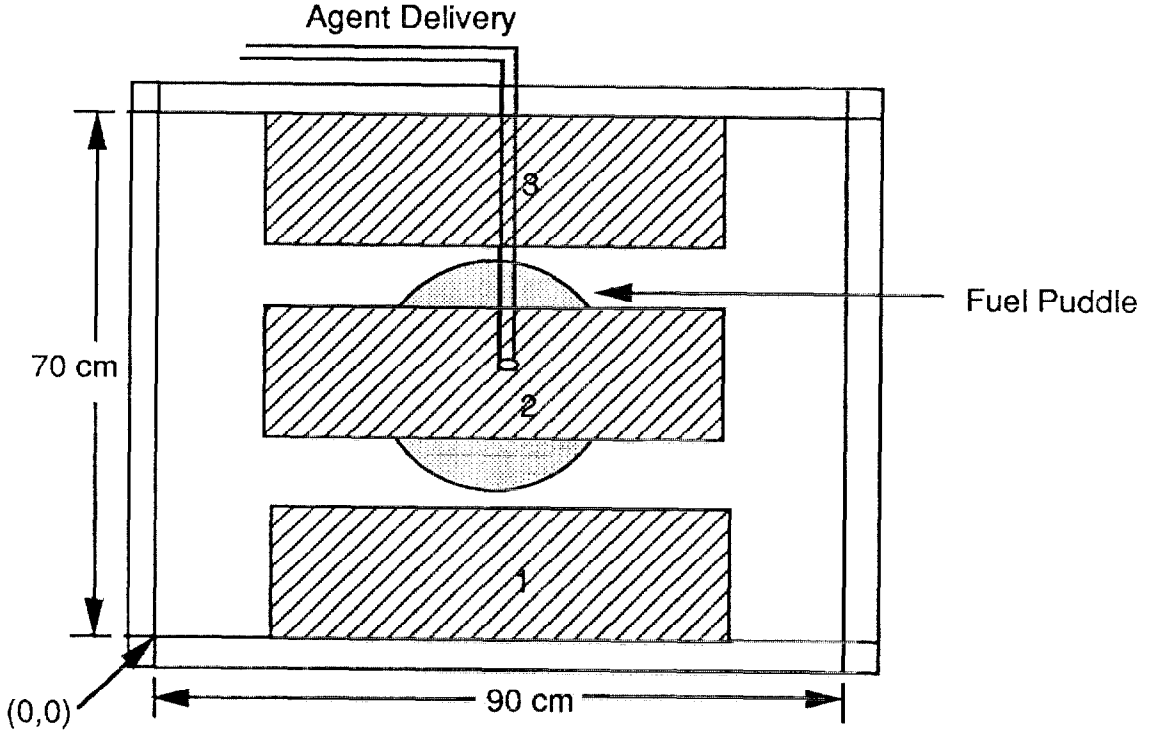

29. A top view of the arrangement of obstacles in the reduced-scale engine compartment for Configuration 3.

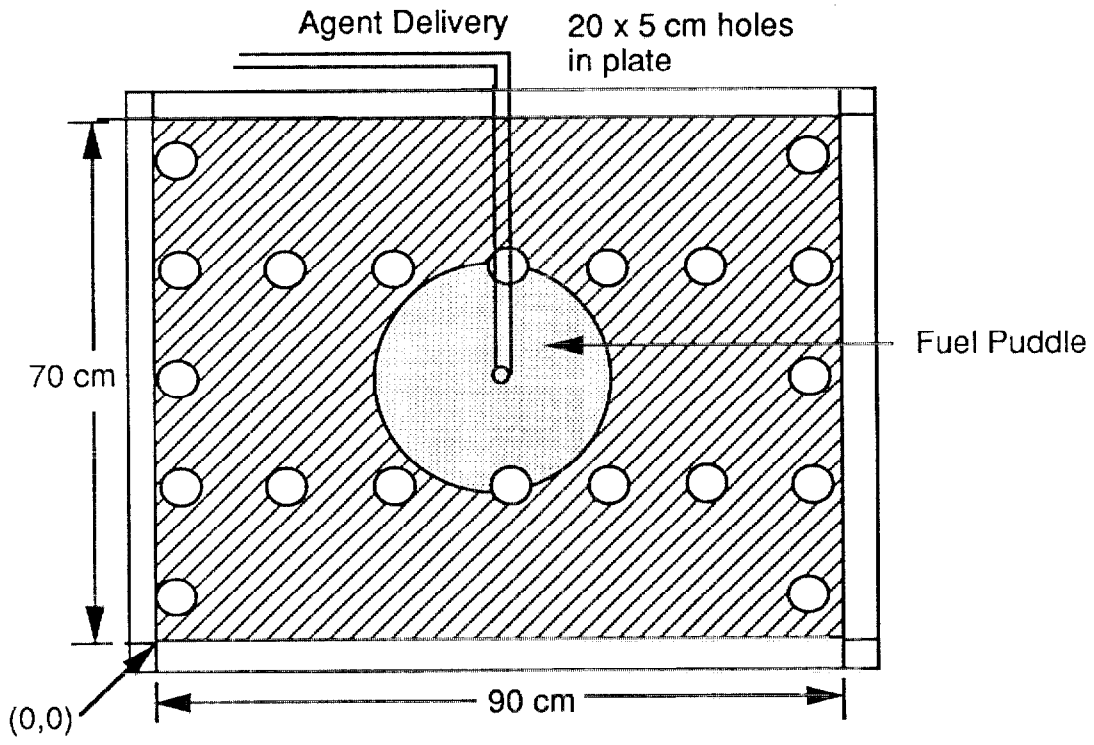

31. A top view of the arrangement of obstacles in the reduced-scale engine compartment for Configuration 5.

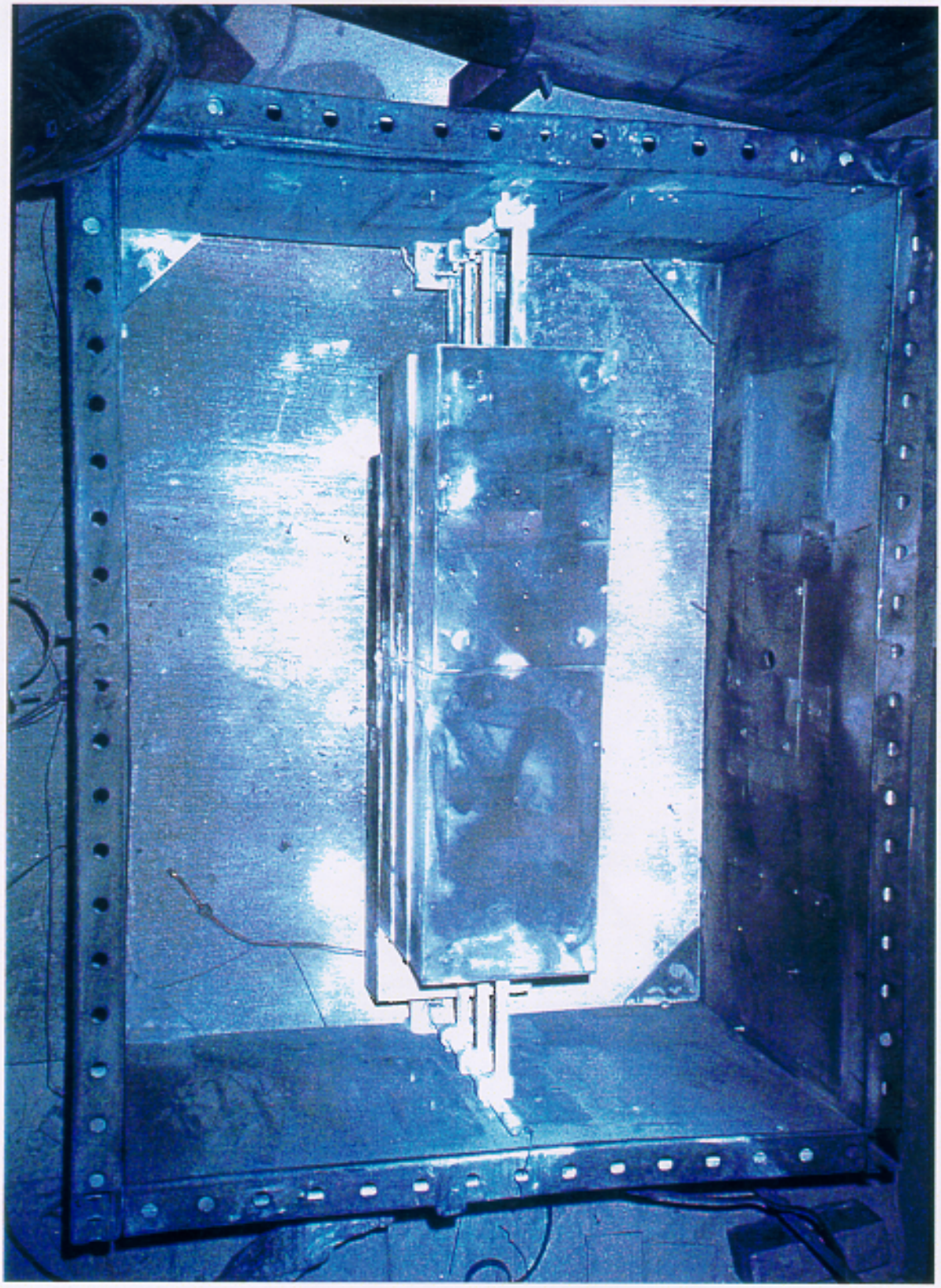

32. Photograph of the reduced-scale engine compartment for Configuration 1, corresponding to the drawing shown in Fig. 27.

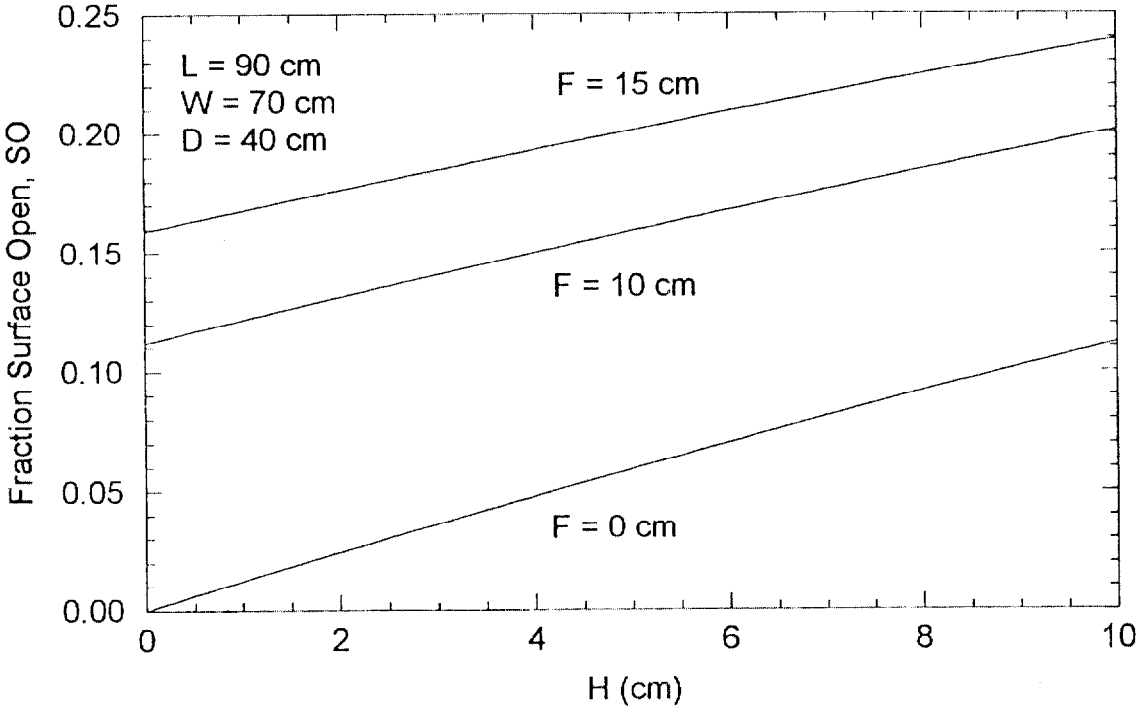

33. The value of SO as a function of H in the reduced-scale engine compartment.

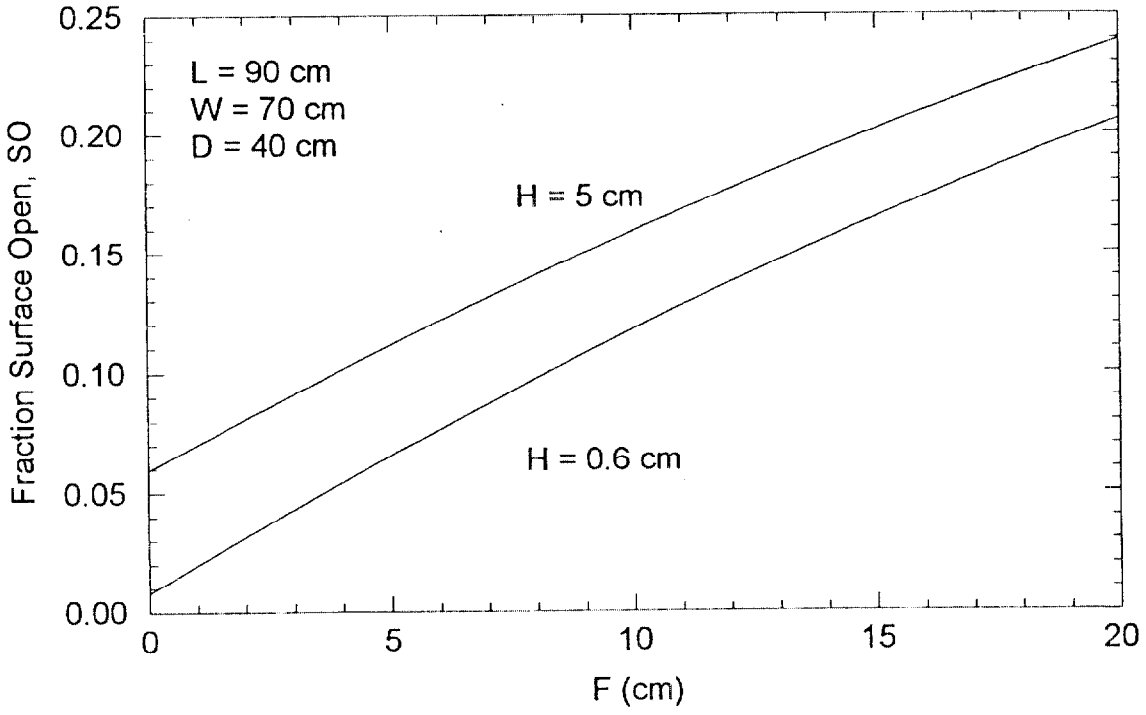

34. The value of SO as a function of F in the reduced-scale engine compartment.

Almost all of the fire suppression experiments in the reduced scale apparatus used heptane as the fuel. Heptane was considered a surrogate for flammable fluids found on a vehicle. Its selection was based on the results of suppression experiments conducted in the engine compartment simulator, which investigated the effect of fuel type on suppression requirements (see below) and showed that heptane was as difficult, or more difficult, to extinguish than many vehicle fluids. Although heptane is not a fluid used in vehicles, it is a single-component fluid, which facilitates experimental repeatability. Using a fuel of known stoichiometry yields an accurate estimate of air entrainment (Eq. 9), which is useful in analysis of some of the experimental results. In addition, heptane is a common fuel used in standardized tests, such as the cup burner suppression test, which provides a baseline for interpreting the experimental results. Previous suppression measurements in laminar laboratory flames have shown that heptane is slightly more difficult to extinguish than gasoline [Hamins and Seshadri, 1986] and other hydrocarbon-based fluids with higher boiling points [Hamins et al., 1994]. Pool and spray fire extinguishment experiments have shown that full-scale suppressant concentration requirements in a large compartment (56 m^3) are similar to or slightly greater than suppressant requirements measured in the cup burner [Baldwin et al., 1992]. In one series of experiments conducted here, the effect of vehicle fluids on suppression requirements was investigated. The fluids tested included gasoline, transmission fluid, motor oil, and undiluted anti-freeze. Undiluted anti-freeze rather than a water/anti-freeze mixture was used because it represents a worst-case situation. Undiluted anti-freeze is mainly composed of ethylene glycol. The fire and flash points for the fluids of interest are shown in Table 11 [Ohlemiller and Cleary, 1998; Babrauskas, 1997]. The boiling point is also listed for the pure fluids. The fire point is somewhat higher than the flash point. And the boiling point is typically higher than the fire point. Elevating the temperature of the surface of Box 5, where the leaking fluids were applied, facilitated ignition of the flammable (high flash point) fluids. This was accomplished by providing power to two inconel rod heating elements placed inside of Box #5. Figures 35 and 36 are front and side view schematic drawings, respectively, of the orientation of the heating elements inside of Box #5. The rods were separated by 2.5 cm and placed 1.5 cm from the inner wall of the front cover of the box, which was a thin (0.4 mm) steel plate coated with a spectrally absorbing black paint. The heating elements were connected in parallel and powered by a variable voltage control that provided as much as 15 amps of current. The box surface temperature was measured by pinning the bare bead of a type K (0.6 mm diameter) thermocouple to the surface of Box #5 by a screw. This insured continuous physical contact between the thermocouple and the surface. The thermocouple was located 4 cm from the top of the box and 3 cm from its edge.

In all tests, a small propane torch was used to ignite the fluid. Ignition of heptane and gasoline was easily achieved without preheating the box surface. Non-piloted ignition was observed to occur intermittently when the temperature of the box surface was sufficiently high (>450° C). Ignition under these conditions, however, was not repeatable, which precluded using the hot surface to test the effectiveness of the suppressants in suppressing re-ignition (after fire suppression).

A number of the suppressants listed in Table 4 were tested in the reduced-scale engine

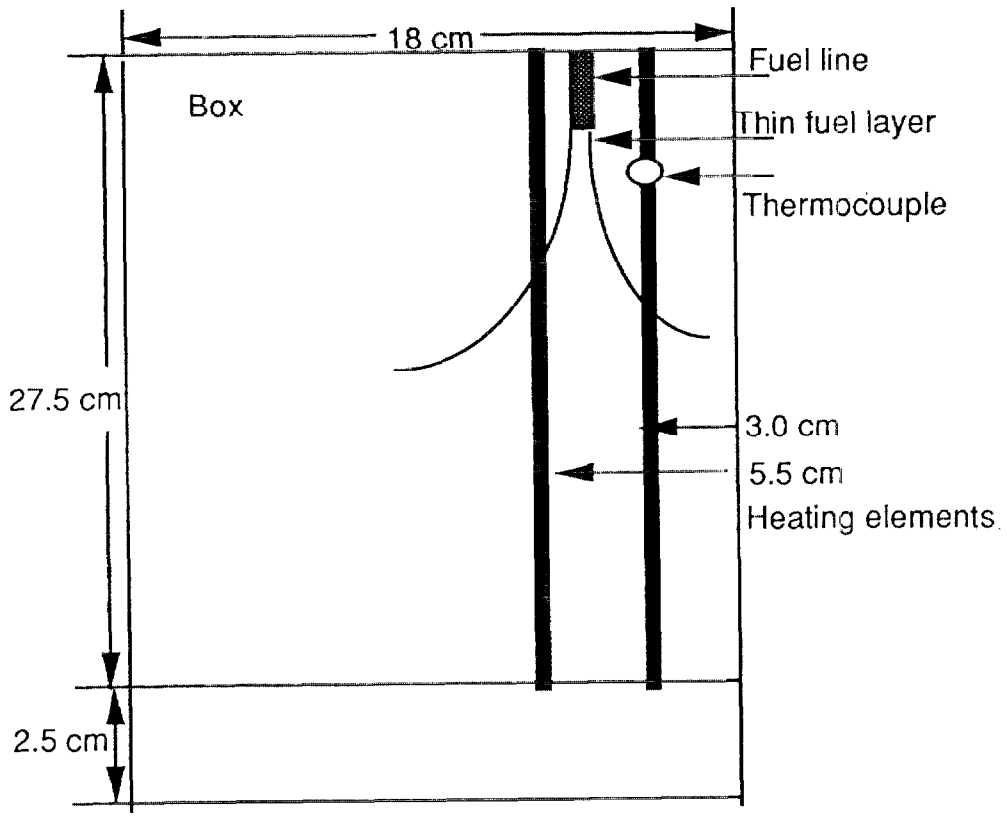

35. Front view of the inconel elements inside of Box 5 of Configuration 1 (see Figs. 19-22).

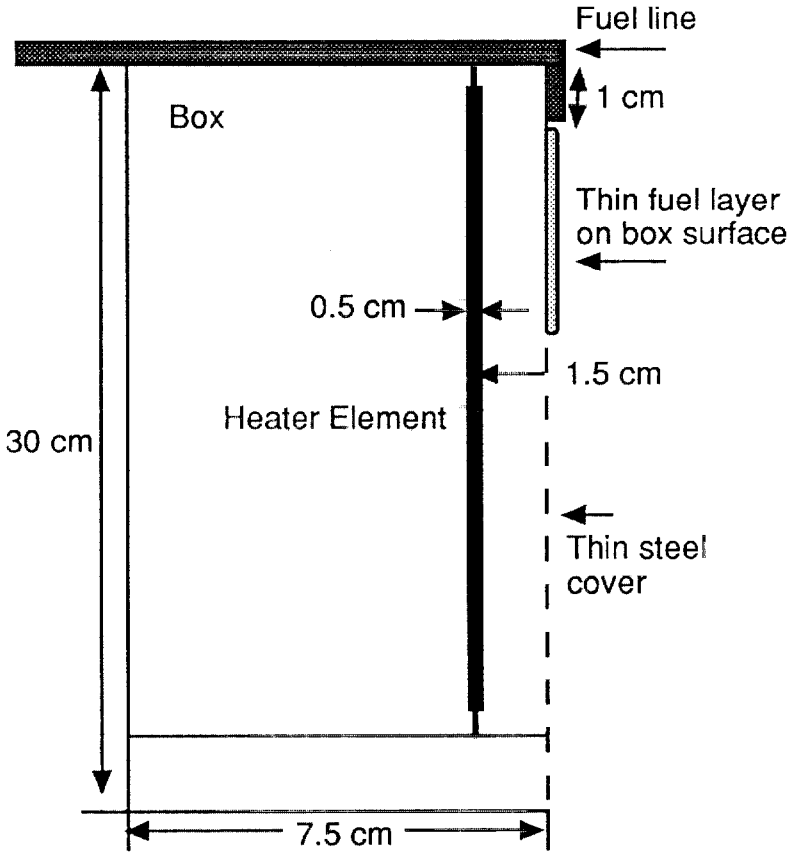

36. Side view of the inconel elements inside of Box 5 of Configuration 1 (see Figs. 19-22).

compartment, including some of the clean suppressants, powder suppressants, and prototype devices. Most of the experiments, however used gaseous nitrogen (N_2) or nitrogen driven ABC powder as the suppressant. These suppressants were selected because their dispersion was considered to be representative of clean agents, and powders, respectively. In addition, rapid discharge of N_2 was assumed to be representative of SPG discharge. In Section 3.2, it will be shown that on the order of 500 g of SPG was effective in rapidly suppressing a full-scale engine compartment fire when delivered at a mass discharge rate of $\approx$1 kg/m^3·s to 3 kg/m^3·s into the 1 m^3 enclosure. In the reduced-scale engine compartment discussed here, nitrogen extinguished fires at a similar mass discharge rate per unit volume when delivered at a rate of 0.2 kg/m^3·s to 2 kg/m^3·s into the 0.3 m^3 enclosure.

Table 11. Fluid Properties. [DiNenno et al., 1995; Ohlemiller and Cleary, 1998]

Fuel	Fire Point (°C)	Flash point (°C)	Boiling Point (°C)	H_c (kJ/g)	ρ (g/cm^3)
Heptane	-	14	99	44	0.69
Gasoline	-	-38	na	43	0.68
Ethylene glycol (100 %)	-	111	197	17	-
Motor oil	216	165-257	na	-	0.86
Transmission fluid	200	175-193	na	-	-

- data not available.
na: not applicable; a multi-component fluid.

3.1.3 Experimental Procedure

A range of fuel flows was tested (see Table 10). A fuel flow of 15 mL/min of heptane was selected as a standard operating condition because the flames were observed to be sufficiently visible such that an optical detector located between the top panel and the upper layer of components would readily detect the fire. The fire plume impinged on the bottom of the top panel and extended laterally to the edge of the compartment frame. The flame was turbulent and highly luminous. Assuming steady burning, this produced an 8 kW flame stabilized on the vertical surface of Box 5 (see Figs. 21 and 22).

The protocol used in the suppression experiments was: (1) prepare the ignition source (typically a propane torch); (2) spill a specified volume of fuel, typically centered about (X,Y) = (15 cm, 38 cm) as defined in Fig. 22; (3) initiate the data acquisition system; (4) initiate the fuel discharge approximately 10 s later; (5) ignite the fuel with a propane torch; (6) initiate the suppressant discharge 15 s later. Ignition of the fuel pool led to rapid flame spread to the fuel dripping from above and similarly, ignition at the fuel discharge high on Box 5 led to rapid flame spread to the fuel pool situated below. The fire was allowed to burn for 15 s before discharging the suppressant. Suppressant discharge was accomplished by opening the solenoid. Measurements showed that for a 50 mL spill of heptane, the fire continued to burn for approximately 60 s. Thus,

a few seconds after suppressant discharge, it was apparent whether suppression occurred. After a suppression experiment, the test apparatus was allowed to cool for a minimum of 10 min. This assured that the initial compartment temperature did not influence the suppression results.

Measurements from a typical experiment are shown in Fig. 37. The experimental conditions are denoted as Case 1 in Table 12. In this experiment, a (50 mL) pool and moderate leak (15 mL/min) of heptane were extinguished by a 3 s delivery of gaseous N_2. The conditions are described in more detail below. Figure 37 shows the temperature at three locations (thermocouples 1-3 in Fig. 19), the reservoir pressure, and the flame emission signal measured by the Silicon diode detector as a function of time. The fuel was ignited 10 s after initiation of the data acquisition system as indicated by the diode signal and thermocouple traces. The suppressant was released at 25 s as indicated by the reservoir pressure trace. The temperature just below the top

Table 12. Summary of Experimental Conditions in the Reduced-Scale Compartment Tests.

Case	Fig.	*H* (cm)	*F* (cm)	*SO%*	*VF* %	Spill[a] (mL)	Leak[a] (mL/min)	Suppressant[b]	Discharge Location
1	37	5	12.5	18	27	50	15	N_2[c]	Front panel
2	38	0.6	10	12	10	50	0	N_2 ABC	Top panel
3	39	0.6	10	12	10-40	50	0	N_2, ABC	Top panel
4	40	0.6	Vary	Vary	30	0	15	N_2	Front panel
5	41	5	Vary	Vary	26-30	0	15	N_2	Front panel
6	42	0.6;2.5	Vary	Vary	28-30	0	15	ABC	Top panel
7	43	Vary	12.5	Vary	26-30	0	15	N_2	Front panel
8	44	Vary	10	Vary	26-30	0	15	ABC	Top panel
9	45,46 53,54	0.6	10	12	30	0	15	N_2; ABC[d]	Top panel; Front panel
10	55	0.6	10	12	30	0	15[e]	N_2[f]	Front panel
11	56	0.6	10	12	30	0	15	N_2[f]	Front panel
12	57	0.6	10	12	30	Vary	Vary	N_2	Top panel
13	58	2.5	12.5	16	28	50	50	Various	Top panel; other[g]

a: heptane was used except for Case 10 (see note "e" below).
b: powders and clean suppressants used a 1 L reservoir pressurized to 1.4 MPa (200 psig); Unless otherwise noted the delivery duration of the gaseous N_2 suppressant was 4 s.
c: the delivery duration of the gaseous N_2 suppressant was 3 s.
d: the reservoir pressurization was varied from 0.2 MPa to 4.2 MPa in some experiments.
e: a number of fluids were tested including gasoline, motor oil, transmission fluid, and Anti-freeze.
f: the delivery duration of the gaseous N_2 suppressant was 1 s.
g: prototype devices were positioned according to manufacturer recommendations; see text.

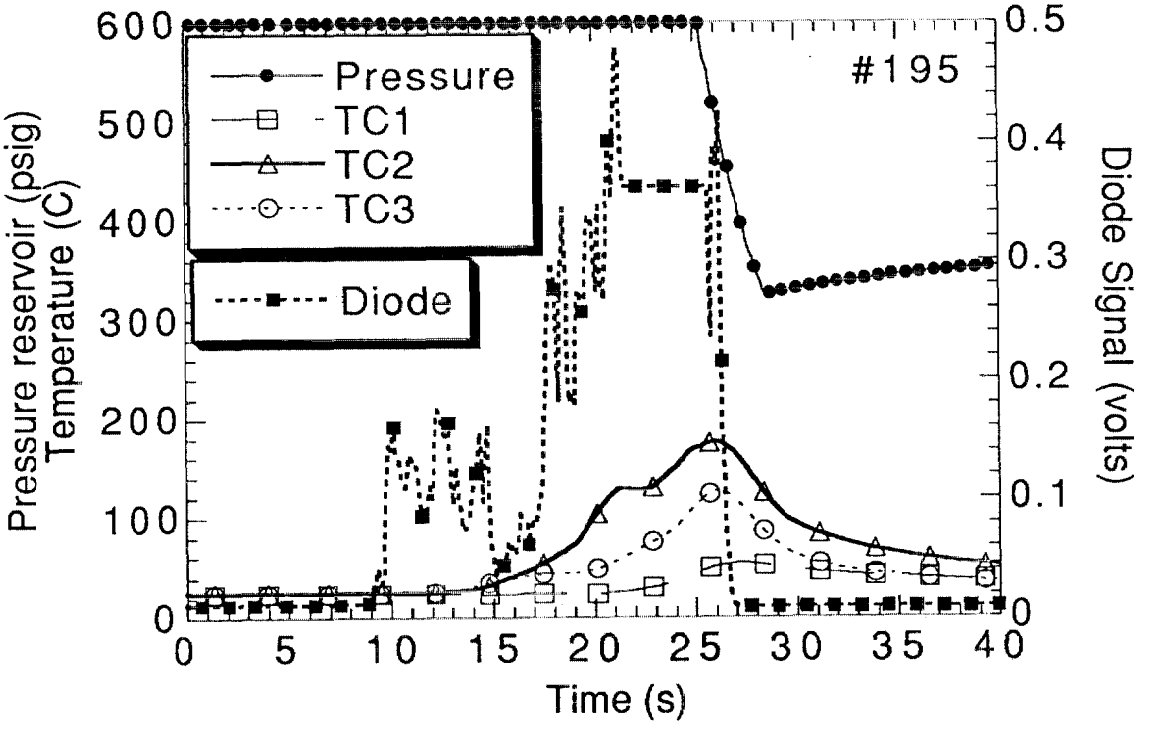

37. The measured reservoir pressure, fire emission signal measured by the diode, and compartment temperatures at three locations as a function of time for Case 1 in Table 12 where 780 g of gaseous nitrogen (N_2) was used in the reduced-scale compartment.

panel center (TC3) peaked at ≈120°C at the time of suppressant discharge. The other temperature traces also peaked at that time. The largest temperature was measured by TC2 (≈180°C), located at the top of the front frame of the compartment (see Fig. 19). During the N_2 discharge, the suppressant reservoir pressure decreased from nearly 4.24 MPa (617 psia) to 2.3 MPa (340 psia). The nitrogen was delivered by opening a solenoid valve for a pre-selected duration. Mass discharge was calculated using Eqs. 29 and 30, which required the values of the initial and final reservoir pressures and the initial reservoir temperature (nearly ambient in all cases). In this experiment 780 g ± 40 g of N_2 were delivered in 3 s, yielding an average delivery rate of ≈260 g/s ± 13 g/s. The delivery duration was confirmed by the transient reservoir pressure trace. The diode signal indicated that flame luminosity rapidly decreased approximately 2 s after initiation of the suppressant discharge. Immediately after discharge, the compartment temperatures also decreased. In cases where suppression was unsuccessful, the compartment temperatures continued to increase after discharge was terminated and the diode signal continued to be large.

3.1.4 Experimental Results

A summary of the experimental conditions utilized during the reduced-scale compartment suppression experiments is shown in Table 12, which specifies the values of *H*, *F*, *SO%*, *VF%*, the fuel spill volume and leak rate, and the suppressant type and discharge location. Table 12 also lists the figure in the text that corresponds to the particular experimental conditions.

3.1.4.1 Characterization of the Facility

A series of experiments was carried out to characterize the baseline conditions in the facility. These included measurements of the convection currents inside the enclosure. A Sierra Instruments air flow meter was used to measure the average velocity above the concrete slab (without a fire present), near the fuel spill location. The results are shown in Table 13. The X and Y directions are defined in Fig. 22 and the positive Z direction is upwards. Average velocities above the concrete slab with the exhaust hood operating were less than 1 m/s. The velocity field

Table 13. Velocities within the experimental facility without a fire present.

Location (x,y,z)	V_x (m/s)	V_y (m/s)
(35,0,7)	0.8 ± 0.1	0.8 ± 0.1
(35,15,0.5)	0.2 ± 0.1	0.1 ± 0.1
(35,15,7)	0.4 ± 0.1	0.2 ± 0.1
(0,20,7)	0.3 ± 0.1	0.2 ± 0.1

is influenced by the entrainment associated with the fire and with release of the suppressant. The flow associated with suppressant release is expected to dominate the flows associated with light wind or entrained air as the suppressant is delivered at high speeds. Exit velocities of the gaseous N_2 through each of the two (1 cm inner diameter) orifices were calculated to be as high as $\approx$1500 m/s based on Eqs. 29 and 30 and measurement of P_o (=800 psi), P_f, T_o, and the discharge duration. The measurements show that the flow field was not quiescent, but was similar to a light breeze.

3.1.4.2 The Effect of Vehicle Geometry

3.1.4.2.1 The Effect of a Component-Filled Flow Field

Figure 38 shows the critical mass of N_2 and ABC powder and its uncertainty (see Table 9) as a function of the percent surface area of the top layer of components that was filled (AF). The experimental conditions are denoted as Case 2 in Table 12. The values of the geometric parameters H and F were maintained constant in this series of experiments. The volume percent filled (VF) of the compartment was maintained at 10 %, represented by a central blockage in the middle of the enclosure (18 cm wide by 61 cm long and 30 cm deep). The layout of the top layer of clutter for each of the experiments (AF=17 %, 49 %, 52 %, 52 %, and 93 %, respectively) is shown in Figs. 27-31 and referred to as Configurations 1-5, respectively. The 1st, 2nd, and 5th configurations were similar, with the blockage distributed uniformly throughout the top layer (with the exception of the center of the enclosure). The value of AF was identical in the 3rd and 4th configurations, but the distribution of open and filled spaces was different (see Figs. 29 and 30). The fire scenario in this series of experiments consisted of a fuel puddle located on the ground, below the large central blockage that was common to all of the configurations. The suppressants were injected through a 13 mm tube, oriented perpendicularly to the top panel, and located at the top panel center. The powder suppressant was held in a 1 L reservoir, which was pressurized (P_o) to 1.4 MPa (200 psig). Unless otherwise noted, these conditions were used for all subsequent experiments.

The results in Fig. 38 show that as AF increased, there was little change (<20 %) in the critical mass of ABC powder. The change in the critical mass of N_2 was significant, increasing over a factor of three as AF increased from 20 % to 95 %. The results also showed that the ABC powder was more effective than N_2 for larger values of AF. This result was unexpected, considering that a horizontal surface can physically block and retain powder, whereas nitrogen can flow past any obstacle. The clutter layer was located approximately 8 cm below the top panel. This created a 50 L volume (=0.7 m x 0.9 m x 0.08 m) between the clutter layer and the bottom of the top panel. When expanded, nitrogen in the ABC suppressant reservoir yielded approximately 13 L (see Eq. 12), which is only a small fraction of the volume between the top layer and the top panel. The nitrogen exhaust velocity was sufficiently large to insure that the powder was transported through the blockage towards the fire zone. Figure 38 also shows the suppressant mass requirements (W_i) based on Eq. 7 and the Y_i listed in Table 4 (denoted as "cup

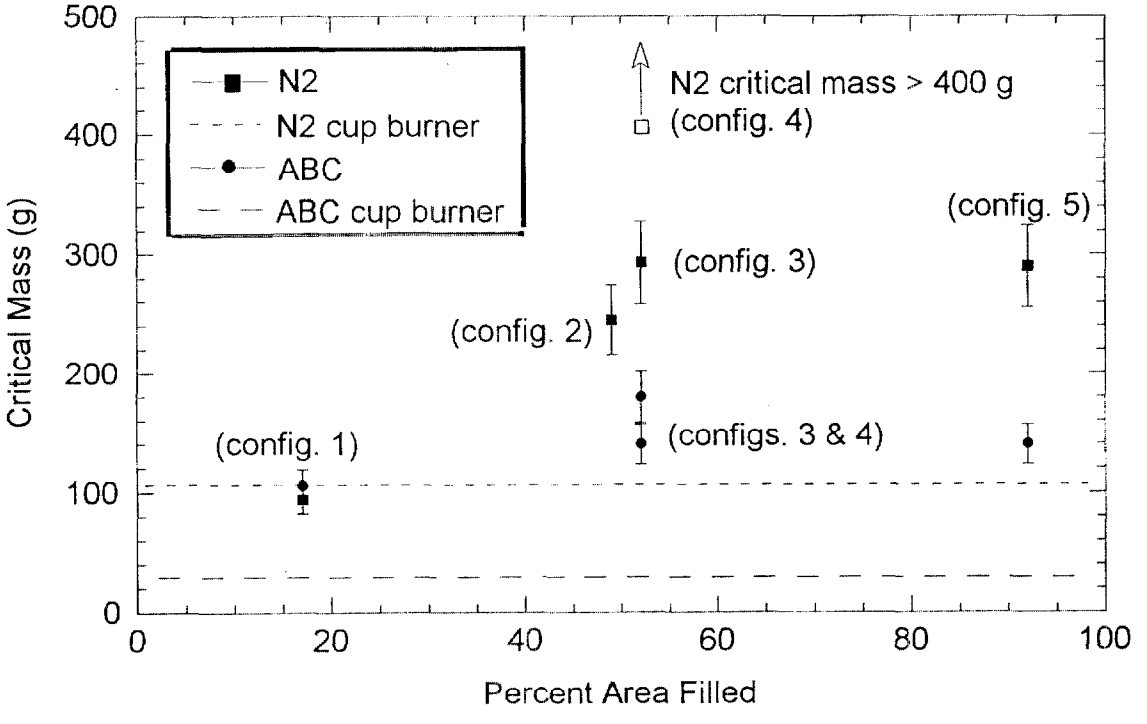

38. The measured critical mass of suppressant (gaseous N_2 and ABC powder) as a function of the percent surface area (of the top layer of components) that was filled (AF) in the reduced-scale compartment for Case 2 in Table 12.

burner"). As expected for an open ventilated system, the measured suppressant masses were larger than the cup burner values.

The critical N_2 mass was never determined for Configuration 4 as seen in Figure 38. As indicated by the open symbol and the arrow, 400 g of N_2 was insufficient to achieve suppression. These results differed quantitatively from the other results presented in Fig. 38. Although AF was nearly the same as in Configuration 2 ($AF \approx 50$ %), twice as much suppressant mass would not suppress these fires. This suggests that the distribution of holes and filled space (i.e., the flow field obstacles) are critical in determining the effectiveness of a high momentum suppressant discharge. Transport of the suppressant apparently depended on the details of the suppressant discharge and its relation to the flow field obstacles. Figure 38 shows that this was not the case for the powder, which was characterized by a lower velocity discharge. The results for the highest area filled percentage, AF=93 %, indicated that a single layer of blockage did not restrict suppressant dispersion. Of course, depending on the vehicle make, model, and options, an engine compartment contains three-dimensional components that may be arranged in multiple layers, which may be both horizontal and vertical. The next series of experiments addressed such a situation.

Figure 39 shows the critical mass of suppressant and its uncertainty (see Table 9) as a function of the volume percent of the compartment that was filled with obstacles (VF). The experimental conditions are denoted as Case 3 in Table 12. As in Case 2 (Fig. 38), the fire scenario was a 50 mL pool fire located below the center of the enclosure. Figure 39 shows the suppressant mass requirements (denoted as "cup burner") based on Eq. 7 and the Y_i data in Table 4, which predicted that the critical suppressant mass should decrease linearly with VF. The measurements did not exhibit this trend. Instead, Figure 39 shows that as VF increased, the critical mass increased and then leveled-off for both N_2 and the ABC powder. This was likely due to the effect of obstacles on suppressant transport. The measured critical suppressant masses are much larger than those estimated using Eq. 7. Of course, the enclosure was partially open (SO=12 %) and suppressant was lost through the lateral openings. As expected, the results showed that the ABC powder was somewhat more effective than N_2, but less than would be expected from Eq. 7 (labeled "cup burner" in the figure). Each data point in Fig. 39 corresponded to a distinct configuration. As VF increased, AF was not held constant, but increased as denoted in the figure. Figure 38 suggests that the critical suppressant mass should increase with AF. Of course, as VF increased, AF was not the only parameter that varied. Lateral blockage also increased and likely had a significant effect on the suppressant mass requirements. In this regard, the average distance between obstacles (d) increased as VF increased, from a value on the order of 30 cm when VF=10 % to approximately 1 cm when VF=40 %. The results presented in Figs. 38 and 39 highlight the importance of the geometric details of the experimental configuration on suppressant performance. As will be seen, suppressant delivery parameters, such as the nozzle location, orientation, and type, also contribute to suppressant effectiveness. The complexities of suppressant transport in an obstacle laden compartment hinder the creation of simple rules that describe suppressant requirements in the reduced-scale apparatus and which can be applied to actual vehicles. Configuration 1 ($d \approx 6$ cm, $AF \approx 50$ %), which was moderately cluttered relative to

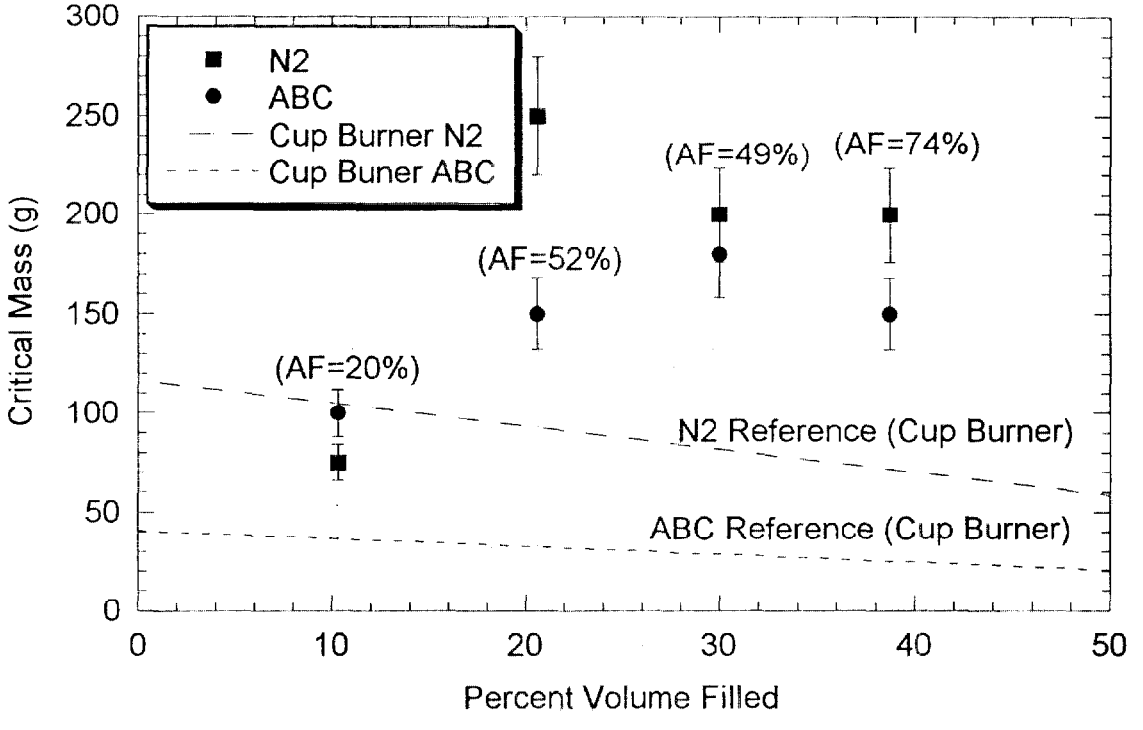

39. The measured critical mass of suppressant (gaseous N_2 and ABC powder) as a function of the volume percent of the reduced-scale compartment that was filled with obstacles (VF) for Case 3 in Table 12.

the other configurations considered was used in the subsequent experiments discussed in this Section.

3.1.4.2.2 The Effect of Compartment Surface Openings

Figures 40 and 41 show the measured critical N_2 mass and its uncertainty (see Table 9) required for suppression as a function of SO (defined in Eq. 2) for the experimental conditions denoted as Cases 4 and 5 in Table 12, respectively. The suppressant (N_2) was injected through a horizontally oriented tee attached to the middle of the front body panel (see Fig. 21). The value of *SO* was varied through changes in *F* and *D*, with *H* maintained at 0.6 cm and 5 cm in Figs. 40 and 41, respectively (see Eq. 2 and Figs. 21 and 22). Figures 40 and 41 show that as *SO* increased from 0 % to 10 %, the absolute value of the critical mass increased by more than a factor of 3. Further increases in *SO* led to smaller increases in the value of the critical mass. The value of H in cases 4 and 5 (corresponding to H=0.6 cm and 5 cm, respectively) did not have a strong influence on the observed trend that the measured N_2 mass required for suppression increased as *SO* increased.

Figure 42 shows the measured critical mass of ABC powder and its uncertainty (see Table 9) as a function of *SO*. The experimental conditions are denoted as Case 6 in Table 12. The suppressant (ABC powder) was injected through the middle of the hood (see Fig. 19). Unlike the results for N_2 (Figs. 40 and 41 corresponding to cases 4 and 5, respectively), Fig. 42 shows that the critical mass of ABC powder did not increase with *SO* (case 6 with H=0.6 cm and H=2.5 cm). The reason for this is likely related to the very different mixing behavior associated with these two suppressant types (powder versus gaseous agent). The dispersion of nitrogen was driven by a large volume discharge (on the order of the volume of the compartment), which partially inerted the compartment and diminished the concentration of oxygen. After discharge, the nitrogen rebounded off walls and became mixed within the compartment. Continued discharge pushed more suppressant to the furthest reaches of the compartment until it displaced air in the lower section of the compartment. When the suppressant concentration near the flame anchoring regions (i.e., locations of vaporizing liquid fuel) was sufficient, the fire was extinguished. Concurrently, a portion of the suppressant escaped through the open surfaces of the compartment. Detailed fluid flow modeling of this phenomenon using the methods outlined by McGrattan and coworkers [1994] substantiates this view of suppressant dispersion (see the detailed discussion in Section 3.1.4.3.3). The powder, on the other hand, was driven by a relatively tiny amount of driver gas. Once, the powder hits an object such as clutter, its momentum is diminished and it is less likely to be propelled out of the compartment.

Figures 40-42 also show the predicted suppressant requirements for *SO*=0, based on Eq. 7 and the value of ρY_c from Table 4. With the surface of the compartment partially open (SO>0), some amount of suppressant escaped from the compartment where it did not affect the fire. Assuming no suppressant losses, the cup burner predictions for the critical suppressant requirements in the partially filled compartment was $\approx$20 g and $\approx$80 g for the ABC powder and N_2 suppressants shown in Figs. 40-42, respectively. For nitrogen (Figs. 40 and 41), the measured critical

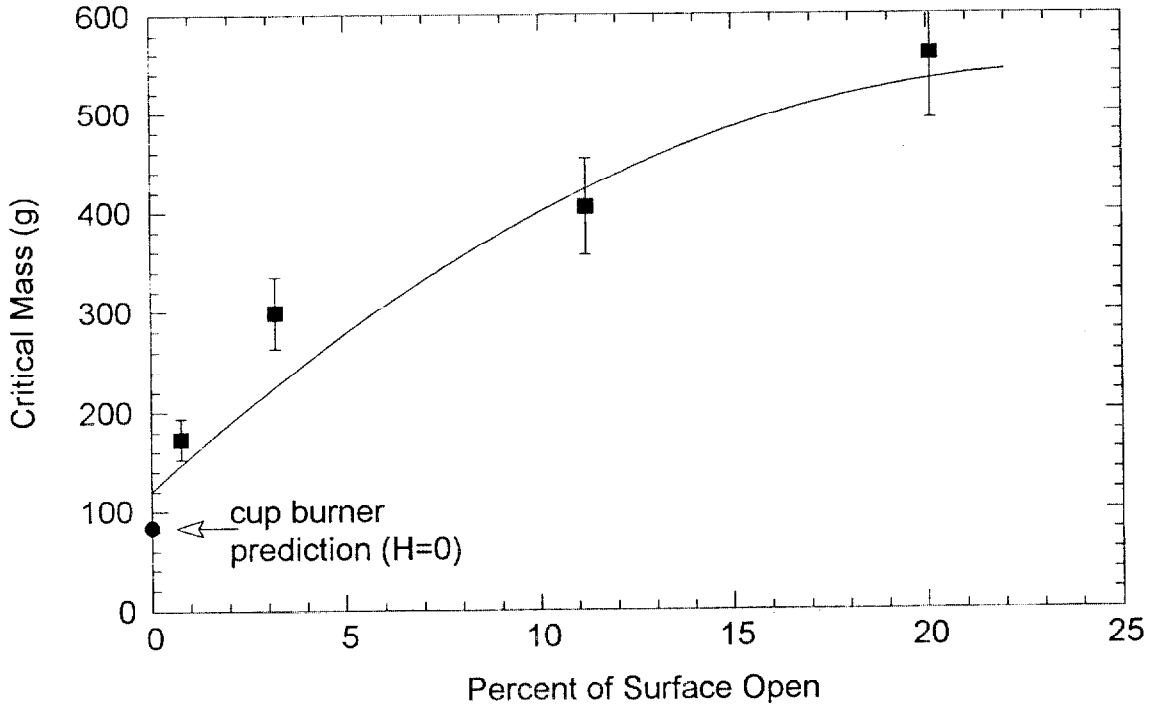

40. The measured critical mass of gaseous suppressant (N_2) as a function of the surface opening percentage (SO in Eq. 2) in the reduced-scale compartment for Case 4 in Table 12.

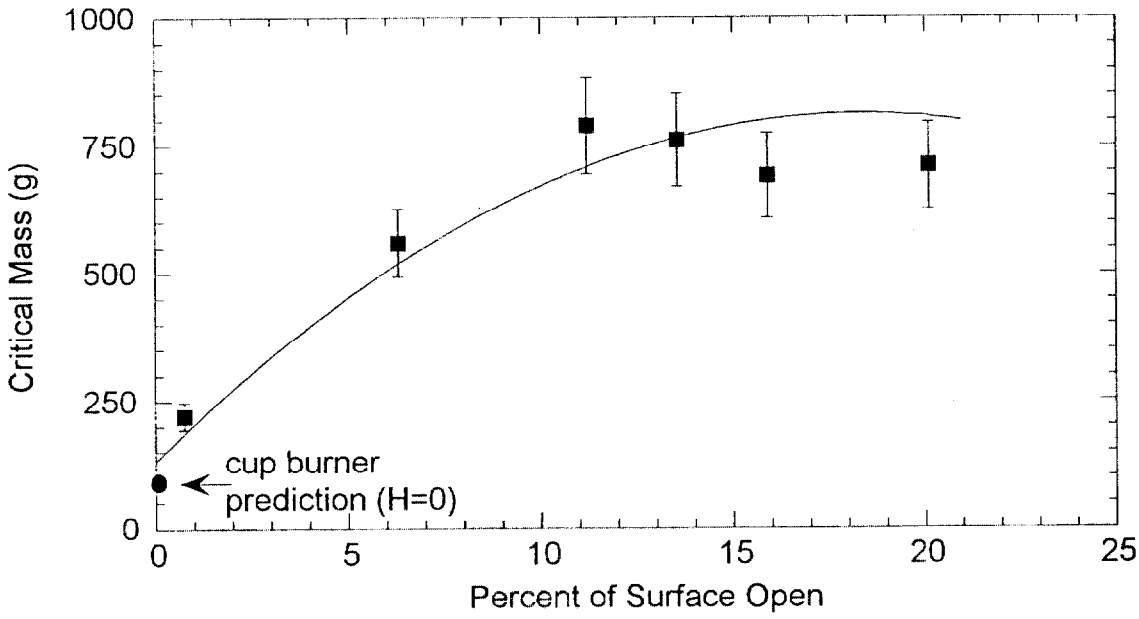

41. The measured critical mass of gaseous suppressant (N_2) as a function of the surface opening percentage (SO in Eq. 2) in the reduced-scale compartment for Case 5 in Table 12.

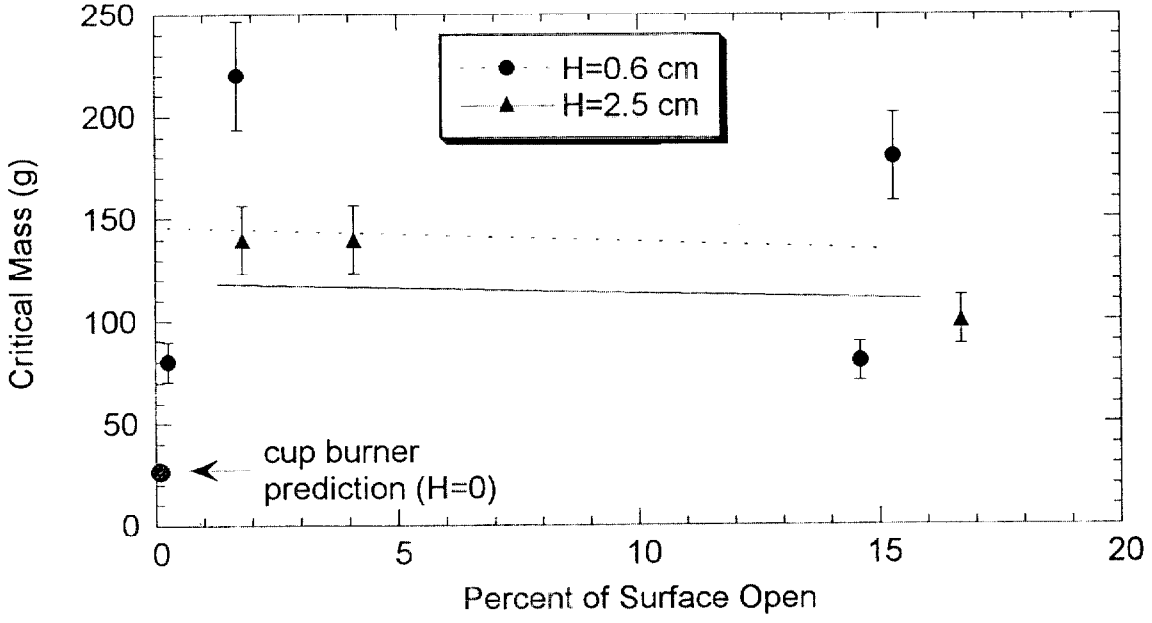

42. The measured critical mass of powder suppressant (ABC) as a function of the surface opening percentage (SO in Eq. 2) in the reduced-scale compartment for Case 6 in Table 12.

suppressant mass approached the cup burner predictions for small values of SO. This was not the case for the ABC powder. These results were interpreted as follows. In cup burner suppression experiments, the suppressant is perfectly mixed with the air flowing past a small (3 cm diameter) flame. In the suppression experiments conducted here, the suppressant was initially not uniformly mixed throughout the compartment. For a closed compartment (SO=0), the nitrogen rebounded off surfaces and eventually was distributed throughout the compartment, such that the critical suppressant mass approached the cup burner value. For the powder suppressant, the convective current associated with the nitrogen driving gas carried the individual particles. With only a small volume of carrier gas (relative to the compartment volume), the powder lost its momentum and was strongly influenced by buoyancy forces associated with the fire plume and by Stokes drag forces, which control particle settling time. Observations indicated that a portion of the powder remained levitated and slowly floated down, colliding with horizontal surfaces, either in the engine compartment or on the ground, and then came to a rest. In addition, a small portion of the powder was observed to adhere to vertical surfaces in the compartment and a portion of the powder was transported out of the engine compartment by the buoyant fire plume. The obstacles acted to block optimum powder distribution. For these reasons, the value of SO did not appear to have a strong influence on the ABC powder suppression results.

3.1.4.2.3 The Effect of Openings about the Top Panel

Figure 43 shows the critical mass of N_2 and its uncertainty (see Table 9) as a function of the distance of the top panel above the frame (H in Fig. 1). The experimental conditions are denoted as Case 7 in Table 12. The suppressant was injected through a horizontally oriented tee attached to the middle of the front body panel. The distance of the frame above the ground was maintained at 12.5 cm (F in Fig. 1). As the top panel was lifted above the frame, larger amounts of suppressant were required to achieve suppression.

Figure 44 shows the critical mass of ABC and its uncertainty (see Table 9) as a function of the distance of the top panel above the frame. The experimental conditions are denoted as Case 8 in Table 12. When $H \approx 0$, the top panel was placed on top of the frame, but not sealed, so some small gaps were present in a few locations due to bends or non-uniformities in the top panel. The ABC powder suppressant was pressurized with 1.4 MPa (200 psig) of N_2 in a 1 L reservoir and delivered down through the center of the top panel with a straight tube. A best-fit line through the data shows that as the top panel was lifted above the frame, larger amounts of suppressant were required to achieve suppression. This is consistent with the N_2 results and with the idea that a lifted top panel allows a portion of the suppressant to escape from the compartment, where it does not impact the fire. Values of $H = 5$ cm and 2.5 cm represent very large contributions to SO (for fixed values of F). Values of H, which may be more representative of post-collision vehicle geometries may be: ½ cm $< H <$ 1 cm and are not likely to be uniform about the compartment.

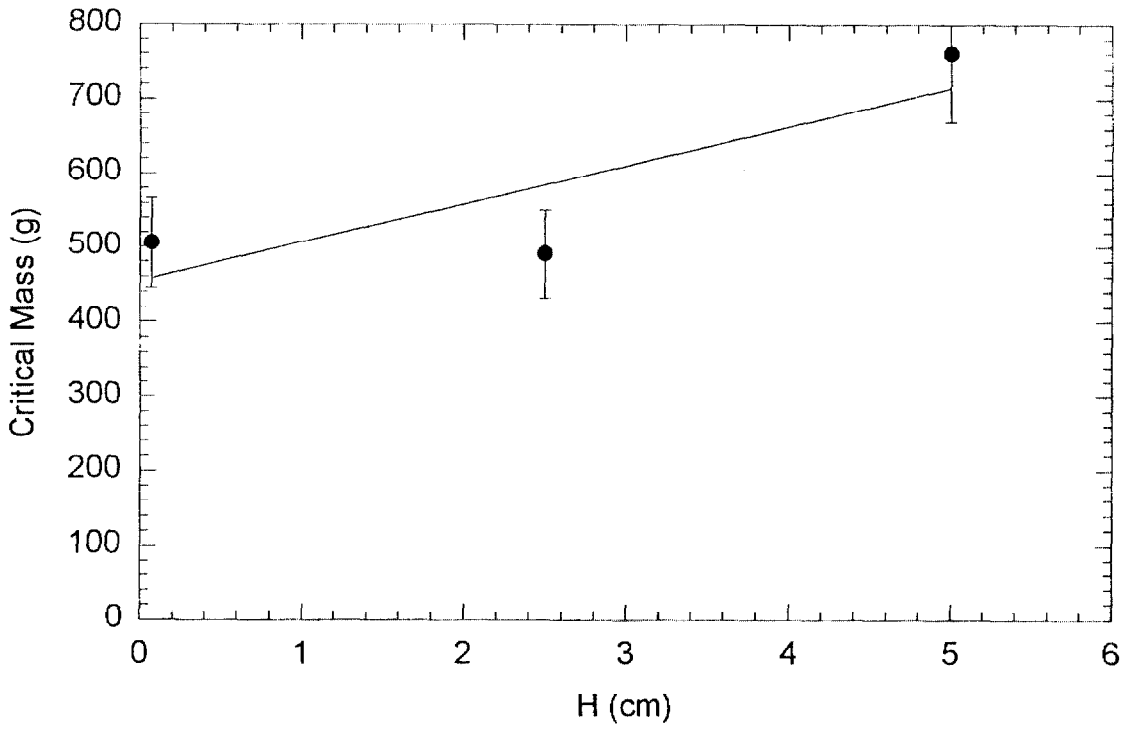

43. The measured critical mass of gaseous suppressant (N_2) as a function of the distance of the hood above the frame in the reduced-scale compartment for Case 7 (see Table 12).

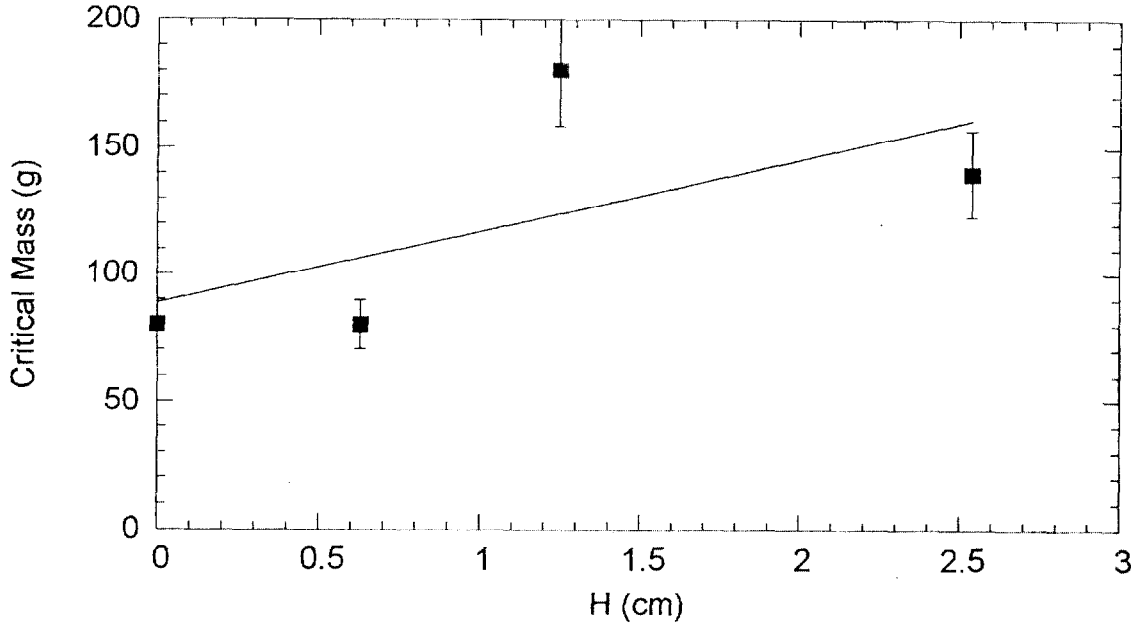

44. The measured critical mass of powder suppressant (ABC) as a function of the distance of the hood above the frame in the reduced-scale compartment for Case 8 (see Table 12).

3.1.4.3 Suppressant Effects

3.1.4.3.1 The Effect of Suppressant Delivery Location and Duration

Figure 45 shows the critical mass of gaseous suppressant (N_2) and its uncertainty (see Table 9) as a function of delivery duration for two suppressant nozzle locations. The suppressant delivery duration is defined as the length of time when the suppressant flowed into the compartment. Results are shown for the suppressant entering the compartment from a nozzle mounted on the middle of the front panel and for a nozzle mounted on the center of the top panel. Experimental conditions are denoted as Case 9 in Table 12.

Figure 45 shows that nozzle placement can impact the critical mass of suppressant. For a delivery duration greater than 1 s, the top panel was a more effective mounting location than the obstructed front panel. For the tee nozzle mounted on the front panel, the critical suppressant mass increased by nearly a factor of two as the delivery duration increased. This was not true for the top panel mounted nozzle, where the critical mass remained nearly constant as a function of delivery duration. Figure 45 indicates that for some nozzle locations, a short delivery duration was advantageous in terms of required suppressant mass. This result is consistent with experiments investigating suppression of baffle stabilized flames in wind tunnels [Hamins et al., 1995]. For a powder, the discharge duration was not expected to play an important role because buoyancy, rather than momentum, governs suppressant behavior. As mentioned in Section 3.1.4.2.2, powders are typically discharged with rather small amounts of driving gas. The amount of driving gas limits the relative effectiveness of powder suppressants due to obstacles impeding suppressant transport.

In a separate series of experiments using nitrogen as suppressant, the effectiveness of two different nozzle arrangements on the front panel was tested. A simple straight tube (perpendicular to the front panel) replaced the tee. A second arrangement tested the effectiveness of placing two spiral distribution nozzles (#10 in Table 7) on the outlets of the standard tee. Both nozzle arrangements proved to be less effective than the standard configuration. Significantly more (30 %) N_2 mass was required to achieve suppression in the second arrangement as compared to the standard configuration. For the first nozzle arrangement, 30 % more N_2 mass than the standard arrangement was still not sufficient to obtain suppression. Distribution is the key to suppressant effectiveness. These experiments showed that nozzle type, number, placement and orientation impact the effectiveness of a suppression delivery system.

3.1.4.3.2 The Effect of the Rate of Suppressant Delivery

Figure 46 shows the average rate of suppressant delivered as a function of delivery duration, for the same data that are shown in Figure 45. The average rate of suppressant delivered was defined as the suppressant mass divided by the delivery duration. Figure 46 shows that as the delivery duration decreased, a higher average delivery rate was required to suppress the fires for both the front panel and top panel mounted nozzles. The average delivery rate requirements for the two

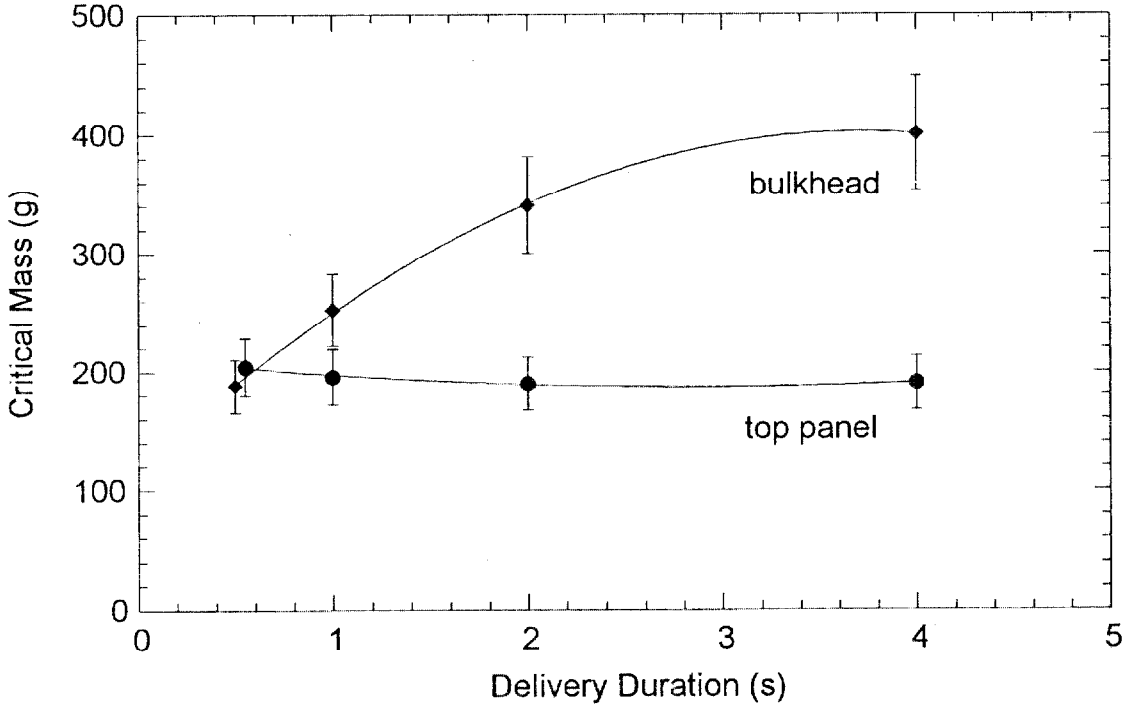

45. The measured critical mass of gaseous suppressant (N_2) as a function of delivery duration for two nozzle locations in the reduced-scale compartment for Case 10 (see Table 12).

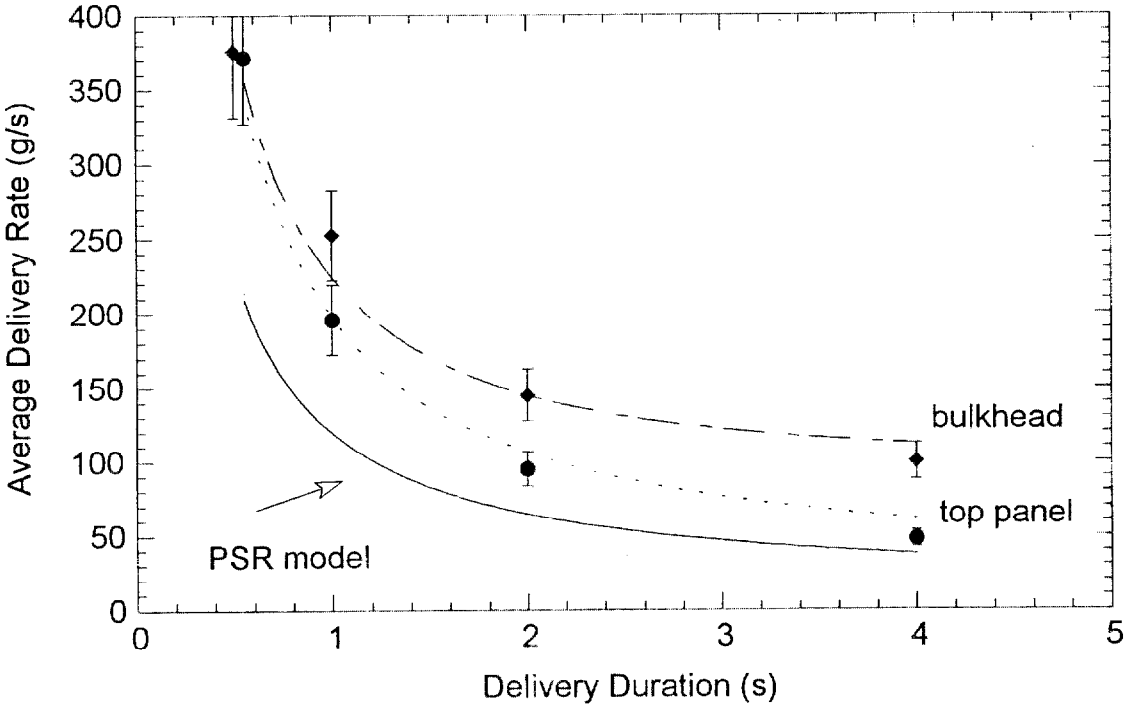

46. The measured critical mass delivery rate of gaseous suppressant (N_2) as a function of delivery duration for the same data presented in Fig. 45. Also shown is the predicted critical mass delivery rate based on Eq. 23.

nozzle locations were similar for small delivery durations, consistent with the results in Fig. 45.

Figures 45-46 indicate that for a gaseous suppressant it may be advantageous to deliver a suppressant as rapidly as possible. For small values of the delivery duration, a relatively large average delivery rate was required to obtain suppression. In the limit of small suppressant delivery rates in an open compartment, suppressant outflow may be higher than suppressant inflow and a critical suppressant concentration in the fire zone is never attained. The results in Figs. 45-46 are consistent with previous studies that used clean suppressants [Hamins et al., 1995; Klimenko et al., 1998], which is related to the small Δt associated with Eq. 25. In addition, the results show that some nozzle locations are more effective than other locations. This conclusion is consistent with the results presented in Section 3.1.4.3.1. The difference in critical mass requirements between the two nozzle mounting locations indicates that the top panel location was more effective than the front panel mounting location. This was not unexpected as the front panel location was designed to simulate suppressant discharge into a highly obstructed flow field. These results suggest that more suppressant may have been lost through the open sides when the suppressant was injected through the front panel as compared to the top panel. This is not an unreasonable interpretation considering the compartment geometry (see Figs. 21-22).

Figure 46 also shows the predicted critical suppressant mass delivery rate from Eq. 23 as a function of the discharge duration. Although the predicted curve has a curvature similar to that of the data, its absolute value differs by as much as a factor of three from the experimental results for the front panel location. The experimental results differ depending on the suppressant delivery location, although the model predicts identical results regardless of location. The difference between the model prediction and the data is attributed to the fact that the model assumes that the suppressant is instantaneously (perfectly) mixed throughout a closed compartment. Of course, perfect mixing did not occur and the compartment was not closed. In this case SO% was equal to 12% and the suppressant escaped through lateral openings in the compartment. Although the generic model cannot be used to accurately predict the absolute value of the required suppressant mass, the results indicate that the model can be used as a lower bound predictor for suppressant requirements. Modeling the difference between the predictions and the data points requires an understanding of the details of the suppressant flow for each configuration of interest. Modeling those details defeats the purpose of the generic predictive model given by Eq. 25. Because of the limitations of generic models, a detailed fluid dynamic approach may be useful in predicting suppressant effectiveness.

3.1.4.3.3 CFD Modeling of Suppressant Distribution

A computational study of the effect of N_2 delivery rate on suppression effectiveness was conducted. The calculation methodology considers solutions to the three-dimensional Navier-Stokes equations of fluid transport, described in Section 1.2.3. Modeling conditions are denoted as Case 9 in Table 12, with the suppressant discharge located at the top panel center and directed downwards. Based on observations, the heptane flow (15 mL/min) was approximated as

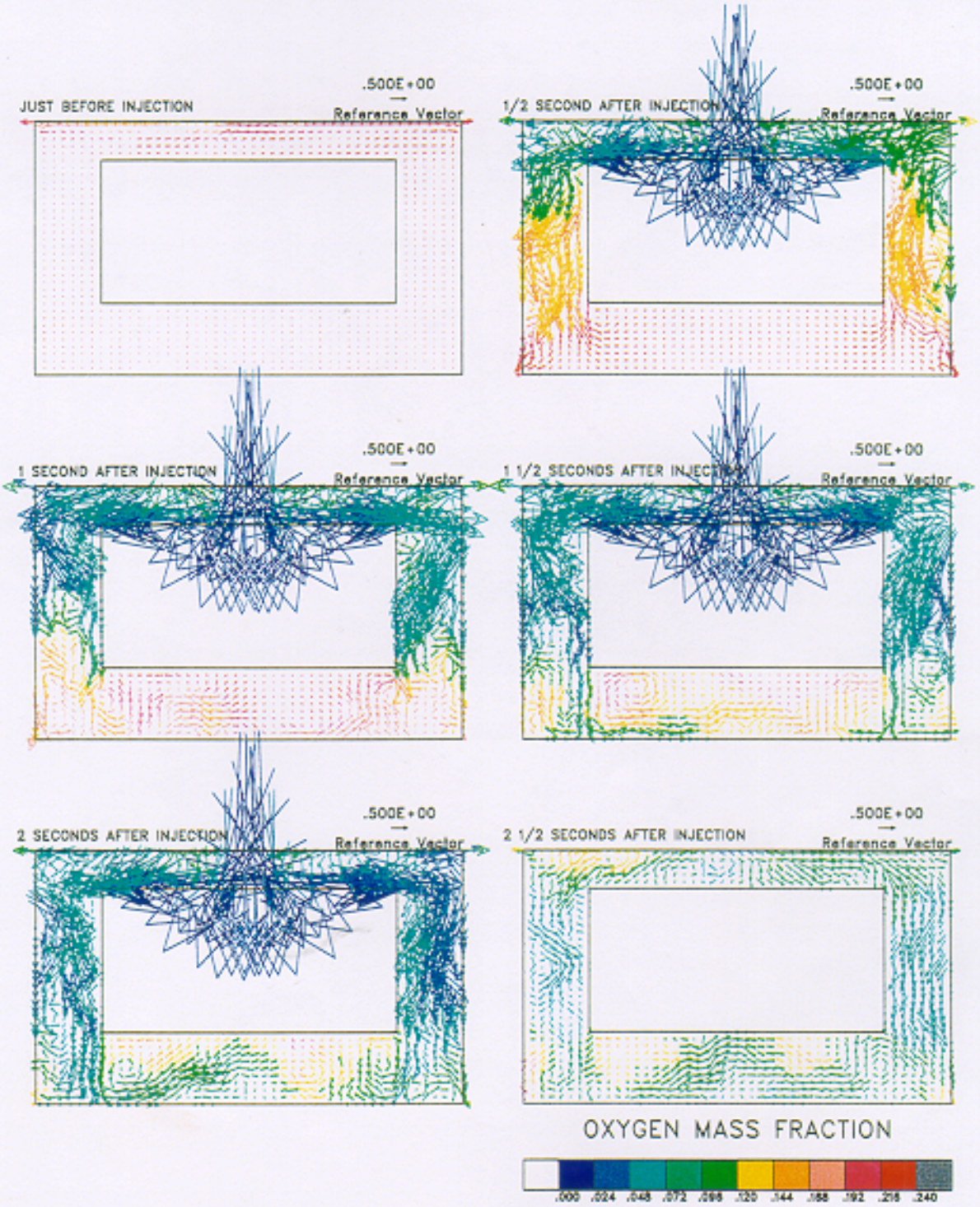

47. The calculated flow field at a cross-section parallel to the passenger/engine compartment bulkhead and through the middle of the reduced-scale engine compartment, just before and 0.5 s, 1 s, 1.5 s, 2 s, and 2.5 s after suppressant injection (200 g of N_2 in 2 s).

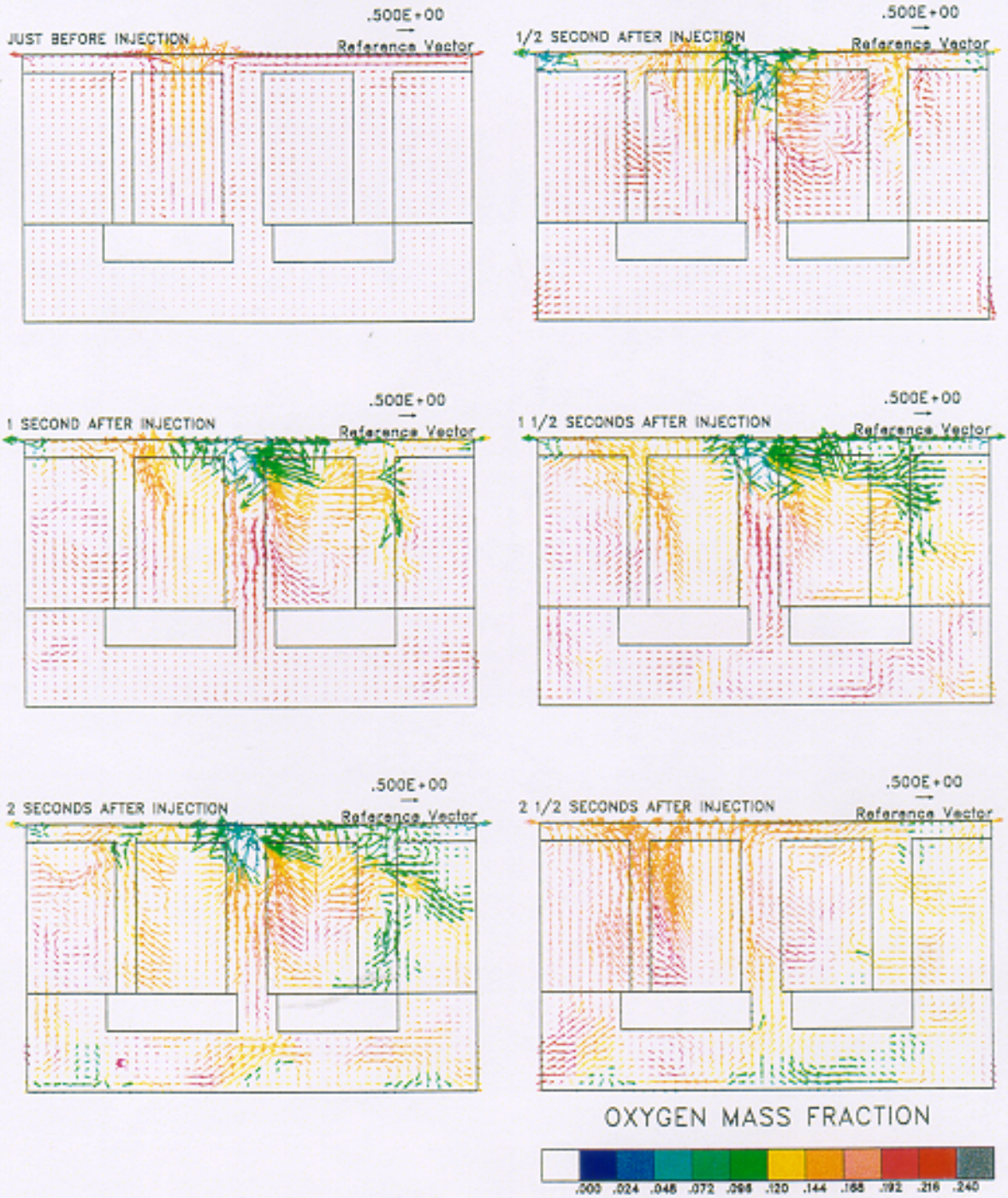

48. The calculated flow field at a cross-section parallel to the passenger/engine compartment bulkhead, 16 cm from the front of the reduced-scale engine compartment (in front of Box 5), just before and 0.5 s, 1 s, 1.5 s, 2 s, and 2.5 s after suppressant injection (200 g of N_2 in 2 s).

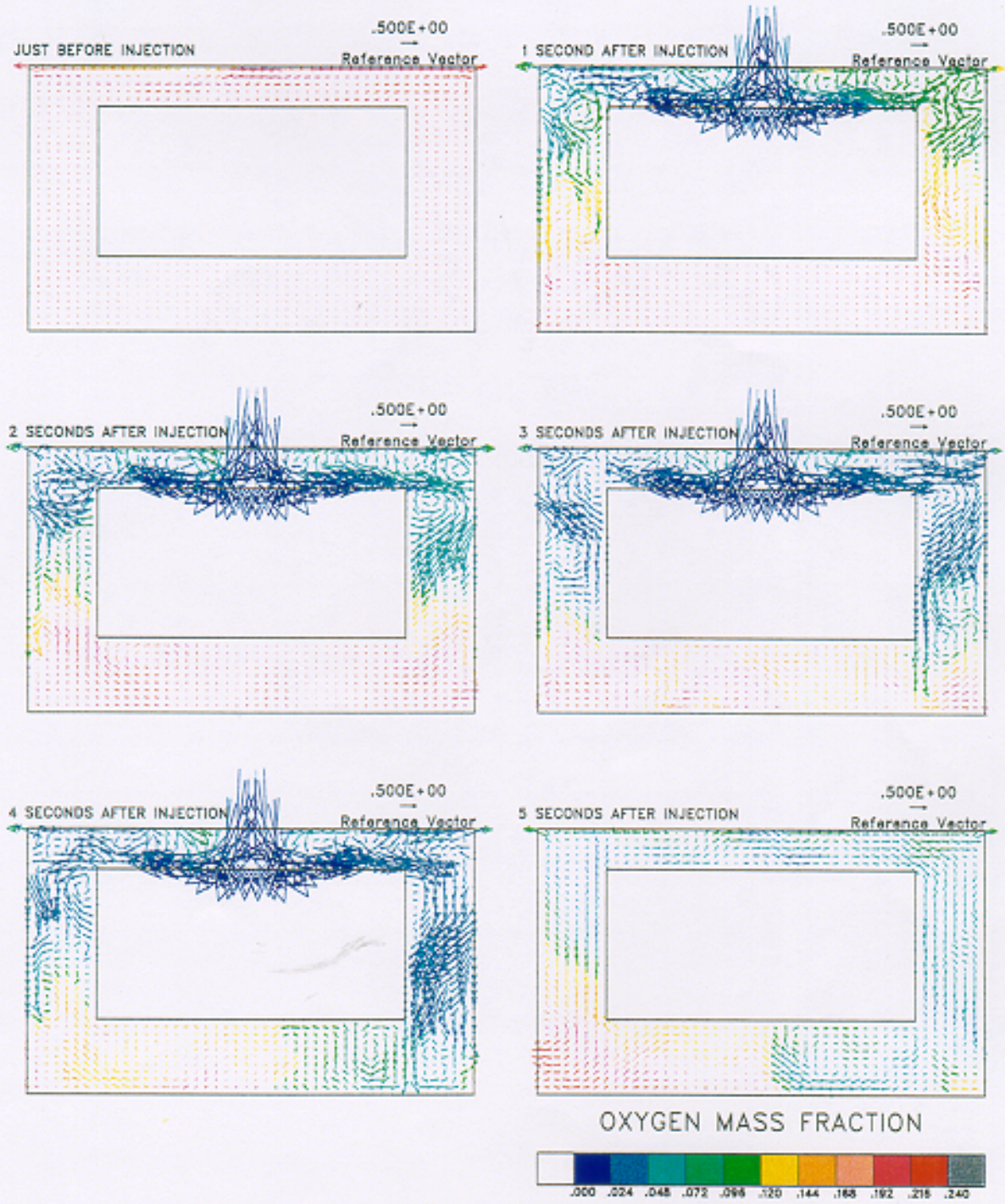

49. The calculated flow field at a cross-section parallel to the passenger/engine compartment bulkhead and through the middle of the reduced-scale engine compartment, just before and 1 s, 2 s, 3 s, 4 s and 5 s after suppressant injection (200 g of N_2 in 4 s).

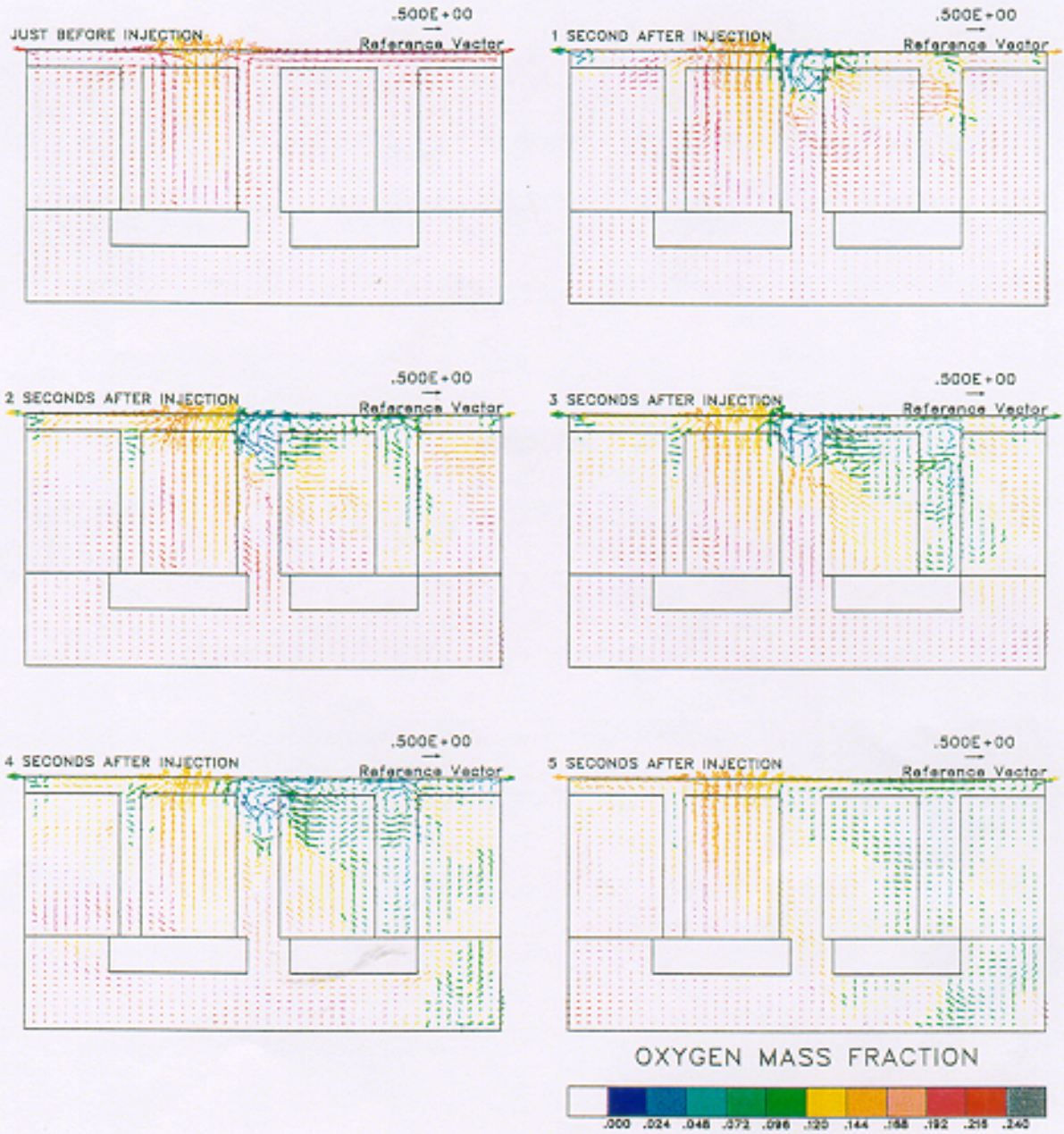

50. The calculated flow field at a cross-section parallel to the passenger/engine compartment bulkhead, 16 cm from the front of the reduced-scale engine compartment (in front of Box 5), just before and 1 s, 2 s, 3 s, 4 s and 5 s after suppressant injection (200 g of N_2 in 4 s).

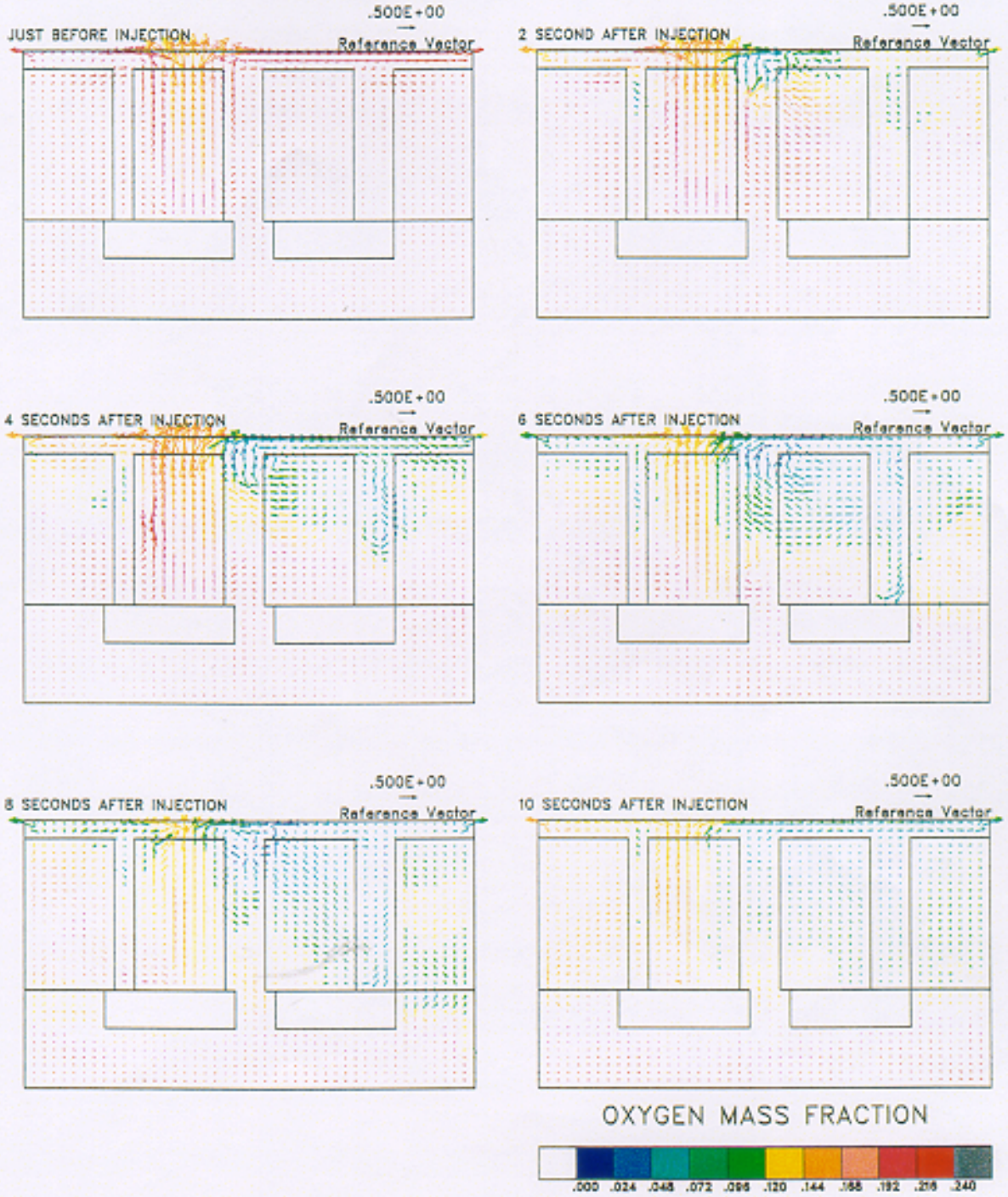

51. The calculated flow field at a cross-section parallel to the passenger/engine compartment bulkhead and through the middle of the reduced-scale engine compartment, just before and 2 s, 4 s, 6 s, 8 s and 10 s after suppressant injection (200 g of N_2 in 8 s).

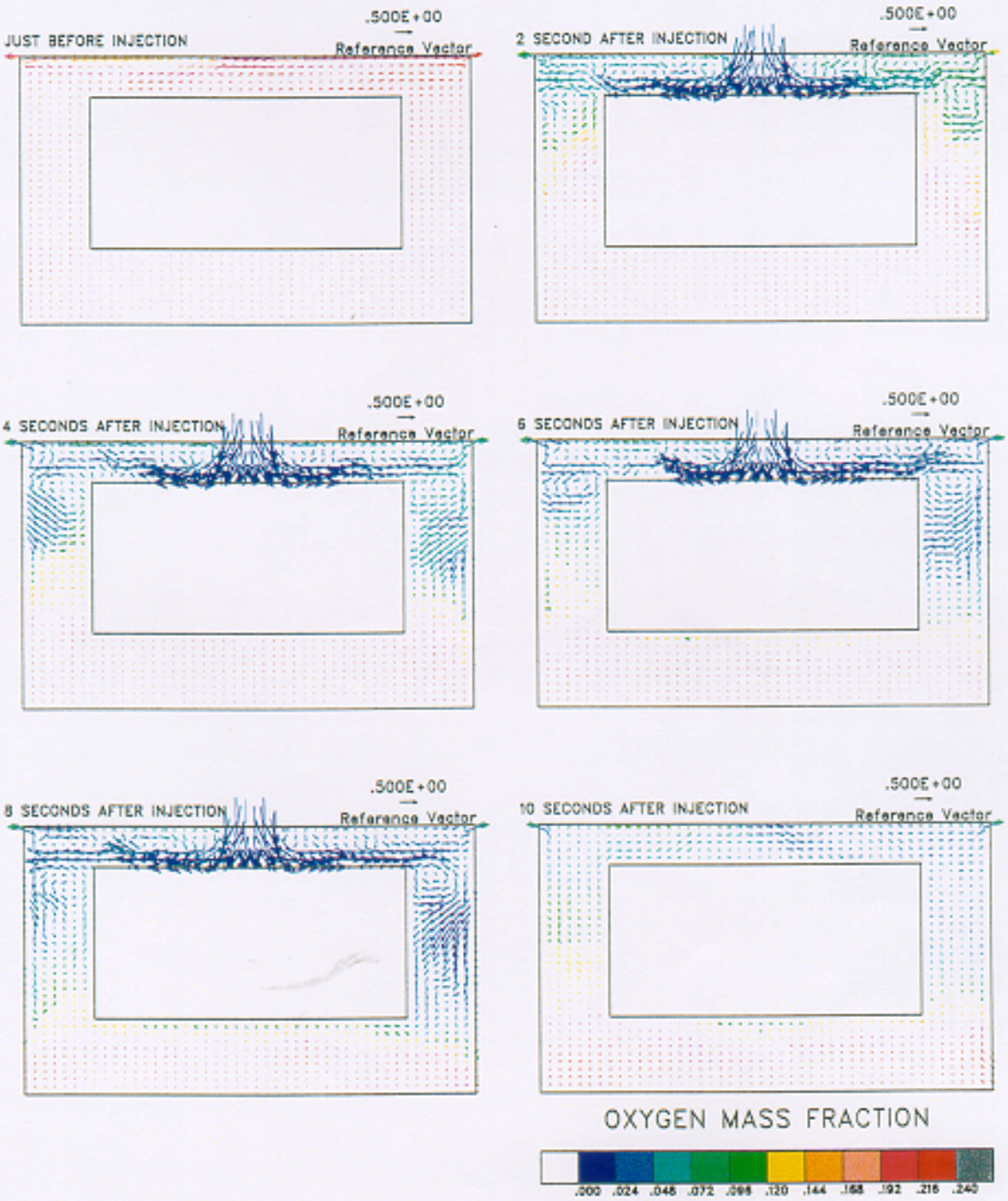

52. The calculated flow field at a cross-section parallel to the passenger/engine compartment bulkhead, 16 cm from the front of the reduced-scale engine compartment (in front of Box 5), just before and 2 s, 4 s, 6 s, 8 s and 10 s after suppressant injection (200 g of N_2 in 8 s).

uniformly covering the entire vertical surface of Box 5 (without a pool fire below). The calculated flow field is shown at two cross sections in the compartment in Figs. 47-52 for three steady suppressant delivery rates of 200 g of N_2 delivered in 2 s, 4 s, and 8 s. Figures 47, 49, and 51 show the cross-section parallel to the passenger/engine compartment front panel and through the middle of the reduced-scale apparatus (see Fig. 22). Figures 48, 50, and 52 show the cross-section parallel to the front panel and through the plane 16 cm from the front of the enclosure of the reduced-scale apparatus in the plane defined by the face of Box 5 in Fig. 22. Figures 47 and 48 show the flow field just before discharge and 0.5 s, 1 s, 1.5 s, 2 s, and 2.5 s after the 2 s suppressant delivery. Figures 49 and 50 show cross sections of the flow field just before discharge and 1 s, 2 s, 3 s, 4 s, and 5 s after the 4 s suppressant delivery. Figures 51 and 52 show cross sections of the flow field just before discharge and 2 s, 4 s, 6 s, 8 s, and 10 s after the 8 s suppressant delivery. The two shorter delivery times correspond to the results shown in Fig. 45.

The colored arrows in the figures represent the transient velocity and oxygen concentration distributions. The arrows represent the local fluid velocity direction and speed in the plane parallel to the front panel, whereas the colors represent the local oxygen mass fractions. A key to the oxygen concentration is shown at the bottom of each figure, while a reference velocity vector (=0.5 m/s) is shown in the right-hand corner of each figure. The middle of the arrows corresponds to the location that represents the position of the velocity vector. Therefore, sometimes the arrows extend past the confines of the boundaries (i.e., out of the enclosure or into the obstacles). These arrows typically represent high velocities, such as the location of suppressant discharge into the enclosure. As nitrogen was transported through the flow field, it mixed with ambient air and reduced the oxygen concentration. At the same time, oxygen was reduced through chemical reactions with the fuel, which led to combustion heating of the product gases. Cup burner suppression experiments show that a fire, with the air at ambient temperature, cannot be sustained for oxygen mass fractions below approximately 14 % [Hamins et al., 1994]. For the simple model used here, the calculation equates the fire heat release rate to zero at that concentration level. A more sophisticated model would consider the effect of elevated air temperatures and finite rate kinetics. The model is considered adequate for analysis of these experiments, because the lower compartment locations are the most difficult to adequately cover with suppressant and the air temperature there is unlikely to be preheated by hot surfaces.

Figures 47-52 show the flow field just before the suppressant was injected. At that time, a fire plume struck the top panel, turned, flowed along its bottom, and exited the compartment. The arrows at the compartment bottom indicate that a small amount of ambient air was entrained into the compartment through those openings. At the next snapshot, the suppressant was injected through the top panel. The largest suppressant velocity was for the 2 s discharge (Figs. 47 and 48), which was two times faster than the 4 s discharge (Figs. 49 and 50) and four times larger than the 8 s discharge (Figs. 51 and 52). As time proceeded, the suppressant was transported through the upper portion of the flow field and some amount of suppressant was forced down towards the ground. Figures 47-52 show that as the suppressant delivery ended, the calculated oxygen concentration began to increase. The velocity vectors and the oxygen concentration show that there was little outflow at the openings near the ground for slow suppressant discharge as seen 6 s

after discharge in Fig. 51. A comparison of Figs. 47 and 48 with Figs. 49 and 50, and Figs. 51 and 52, shows that in general, the faster the discharge, the greater the suppressant penetration through the flow field. For example, Figs. 50, and 52 show that near the ground, there were some locations where the O_2 concentration was greater than 14 % by volume, a concentration not sufficient to insure suppression at all locations. On the other hand, Fig. 48 shows that the suppressant concentration was adequate (as the O_2 concentration was less than 14 % by volume) in the zone of interest. A faster rate of discharge, however, did not guarantee low oxygen concentrations throughout the flow field. Figures 48, 50, and 52 show that there was little difference in the oxygen concentration near the fire anchoring zone on Box 5 (see Fig. 22) as the suppressant delivery rate varied. The calculation results were consistent with the suppression measurements shown in Fig. 45 for discharge through the top panel.

3.1.4.3.4 Parameters influencing Powder Delivery

A suppressant supply line may become crimped during a collision. Table 14 summarizes the results from experiments examining the effect of inserting a 1 cm long orifice in the middle of the suppressant delivery line on the critical mass requirements for ABC powder. Experimental conditions are denoted as Case 9 in Table 12. The transient N_2 pressure in the suppressant reservoir are shown in Fig. 53, from which the delivery duration was determined (see Table 14). A comparison of the critical mass requirements for the 2 mm and 9 mm diameter experiments show that although the measured critical mass delivery rate doubled from 0.11 kg/s to 0.23 kg/s and the delivery duration reduced from 1.0 s to 2.2 s, there was no significant change in the critical mass requirements. Collision induced crimping of a supply line may slow the suppressant mass delivery rate, but unless the supply line is significantly closed, the results shown in Table 14 suggest that suppressant performance is not significantly effected.

Figure 54 shows the results from experiments examining the effect of reservoir pressure on the critical mass requirements for ABC powder. Experimental conditions are denoted as Case 9 in Table 12. Figure 54 shows that reservoir pressurization had a negligible effect on suppressant mass requirements for pressures greater than the minimum required to expel the powder, 0.2 MPa (30 psig). Figure 54 also shows the effect of nozzle placement on the critical suppressant requirements for ABC powder. Similar to the results determined for relatively slow discharges of gaseous N_2 (see Fig. 45), the top panel was a more effective nozzle mount location than the obstructed front-panel (or bulkhead) location.

Table 14. Effect of Orifice diameter in the Supply Line on ABC powder Mass Requirements.

Orifice Diameter (mm)	Delivery Duration (s)	Critical Mass (g)
2 ± 0.2	2.2 ± 0.2	250 ± 30
6 ± 0.2	1.2 ± 0.2	180 ± 20
9 ± 0.2	1.0 ± 0.2	225 ± 30

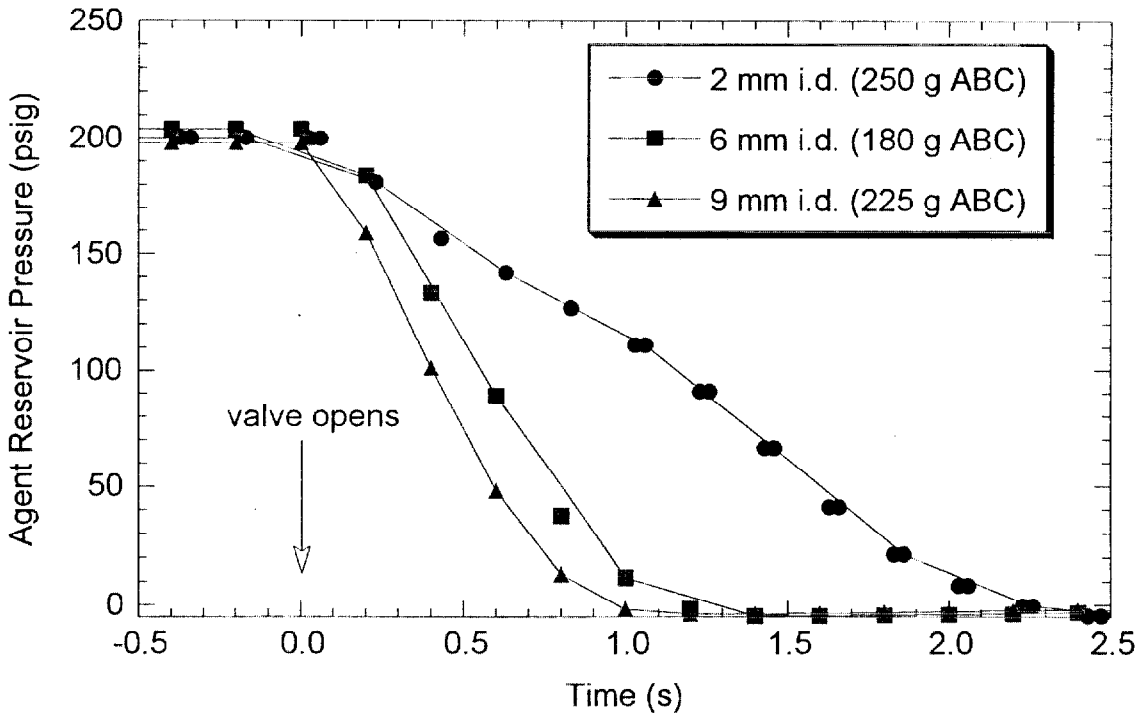

53. The transient reservoir pressures for different line diameters during suppression experiments in the reduced-scale compartment.

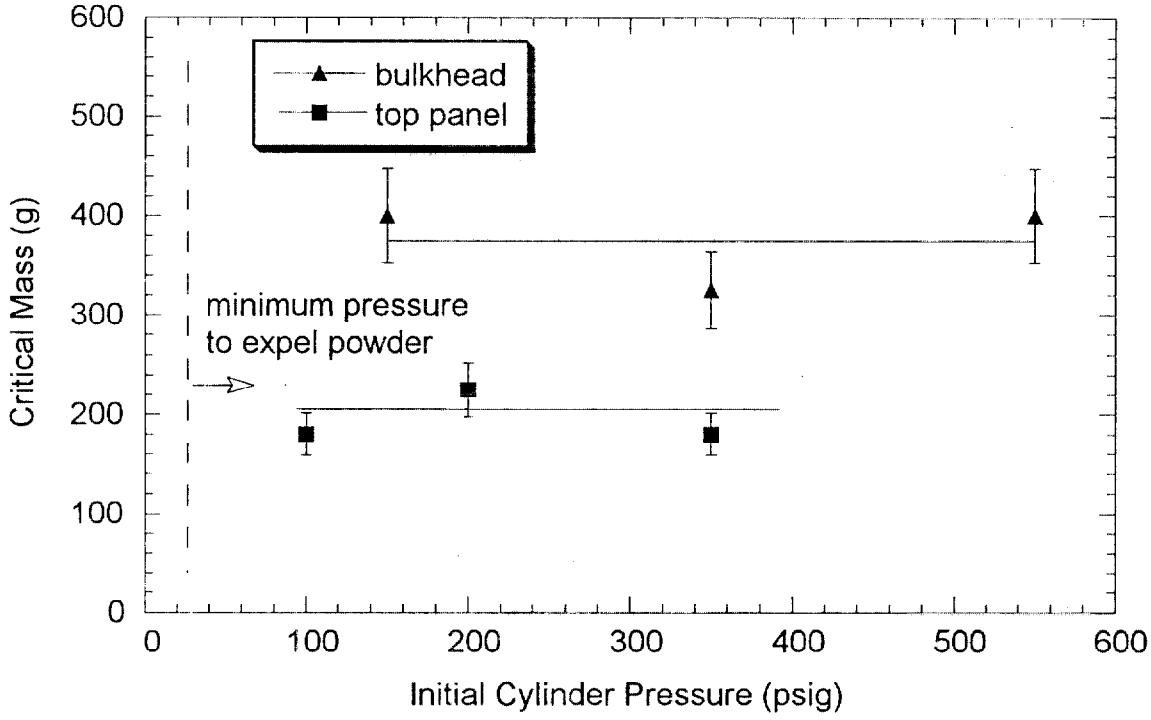

54. The critical mass requirements for ABC powder as a function of the initial cylinder pressure for two nozzle locations in the reduced-scale compartment for Case 9 in Table 12.

3.1.4.4 The Effect of Fuel Type

Figure 55 shows the critical mass of nitrogen and its uncertainty (see Table 9) for fires burning various fluids. The fluids tested were heptane, gasoline, undiluted anti-freeze, motor oil, and transmission fluid. Experimental conditions are denoted as Case 10 in Table 12. Ignition of the anti-freeze, motor oil, and transmission fluid was not possible unless these fluids were preheated. This was accomplished by continuously heating the surface of Box 5, where the leaking fluids were discharged. Ignition of these fluids was facilitated by initially raising the temperature of Box 5 such that the surface thermocouple measurement was 250 °C ± 20°C for the transmission fluid, 250 °C ± 20°C for the motor oil, and 220 °C ± 20°C for the undiluted anti-freeze. The propane torch was used to initiate ignition of the hot fluid vapor. After burning for several seconds, the Box surface temperature exceeded ≈300°C in all cases, due to heating by the fire. Ignition of heptane and gasoline was accomplished without preheating Box 5. Under these conditions, the results in Fig. 55 show that gasoline required somewhat more suppressant mass to extinguish than the other fluids. For the other fluids, the results suggest that once a fluid was burning, fluid type had only a small impact on the critical suppressant mass.

3.1.4.5 The Effect of Component Surface Temperature

Figure 56 shows the critical suppressant mass of gaseous nitrogen and its uncertainty (see Table 9) as a function of the initial temperature of the surface of Box 5 for fires burning heptane that was discharged over the Box 5 surface. Experimental conditions are denoted as Case 11 in Table 12. The results show that over the range of temperatures tested, as the initial surface temperature increased, the critical suppressant mass significantly decreased. These results are interpreted as follows. The metal surfaces coated by fuel were the source of flammable vapor that sustained the fire. They are denoted here as the flame anchoring locations. These surfaces were considered significant in terms of fire suppression, which was accomplished when a sufficient suppressant concentration was simultaneously present about all flame anchoring locations. Even if nearly all flames are extinguished, a fire will not fully extinguish unless all flames about the fuel source are extinguished. If not fully extinguished, a fire will rapidly relight. In the results presented in Fig. 56, preheating of the surface of Box 5 enhanced the rate of fuel vaporization. For a given fluid flow, increased surface temperature was observed to yield a decreased surface amount of surface area coated by liquid fuel. As the surface temperature was increased, the fuel was observed to vaporize more rapidly, leaving lower portions of the hot surface dry without liquid fuel present. Therefore, less surface area had to be protected by high suppressant concentrations, indicating that less mass was needed to achieve suppression. This interpretation is consistent with the results in Fig. 56 and if correct, is valid for surface temperatures below the autoignition temperature, which is on the order of 200°C to 600 °C for liquid hydrocarbon fuels (Glassman, 1997). For surface temperatures above the autoignition temperature, a clean suppressant like nitrogen will not be able to indefinitely prevent fuel reignition after fire

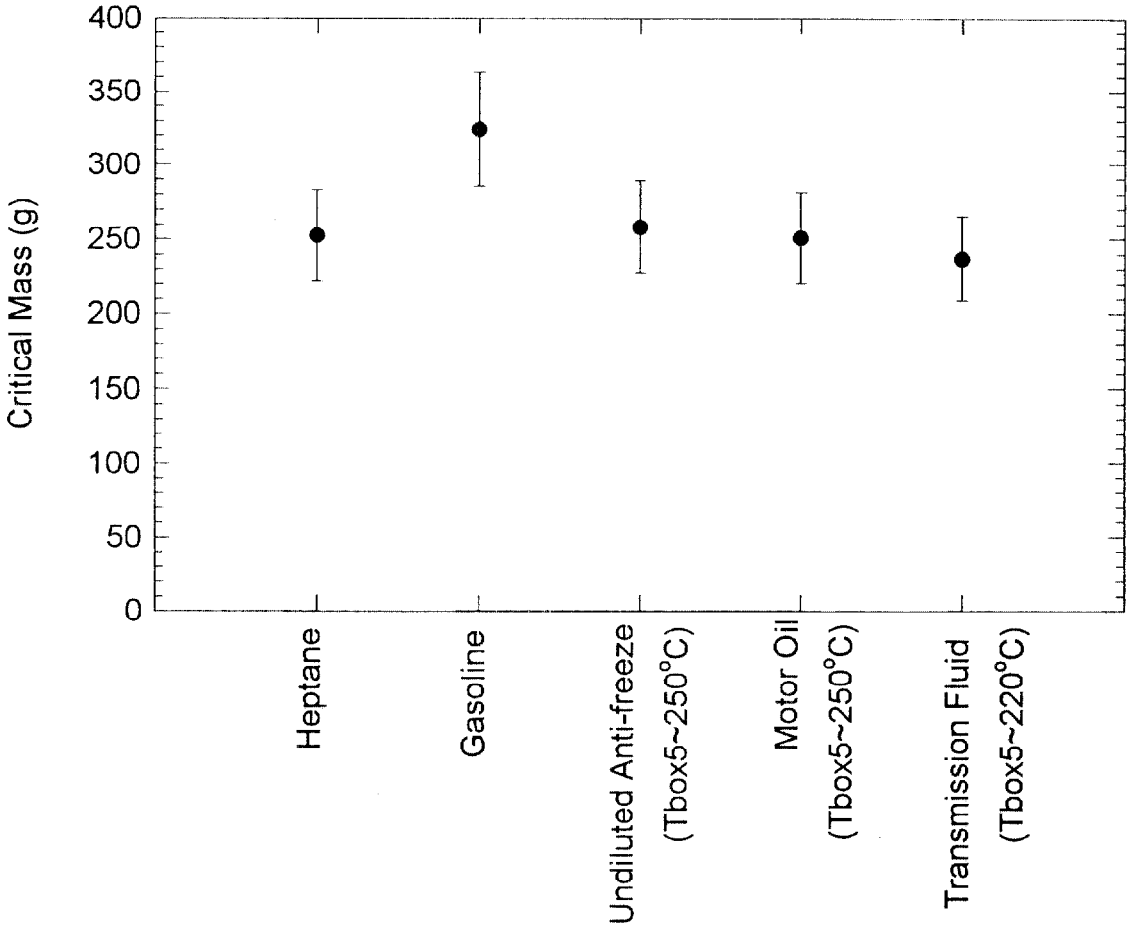

55. The measured critical mass of gaseous suppressant (N_2) for different types of fluids burning in the reduced-scale compartment for Case 10 in Table 12.

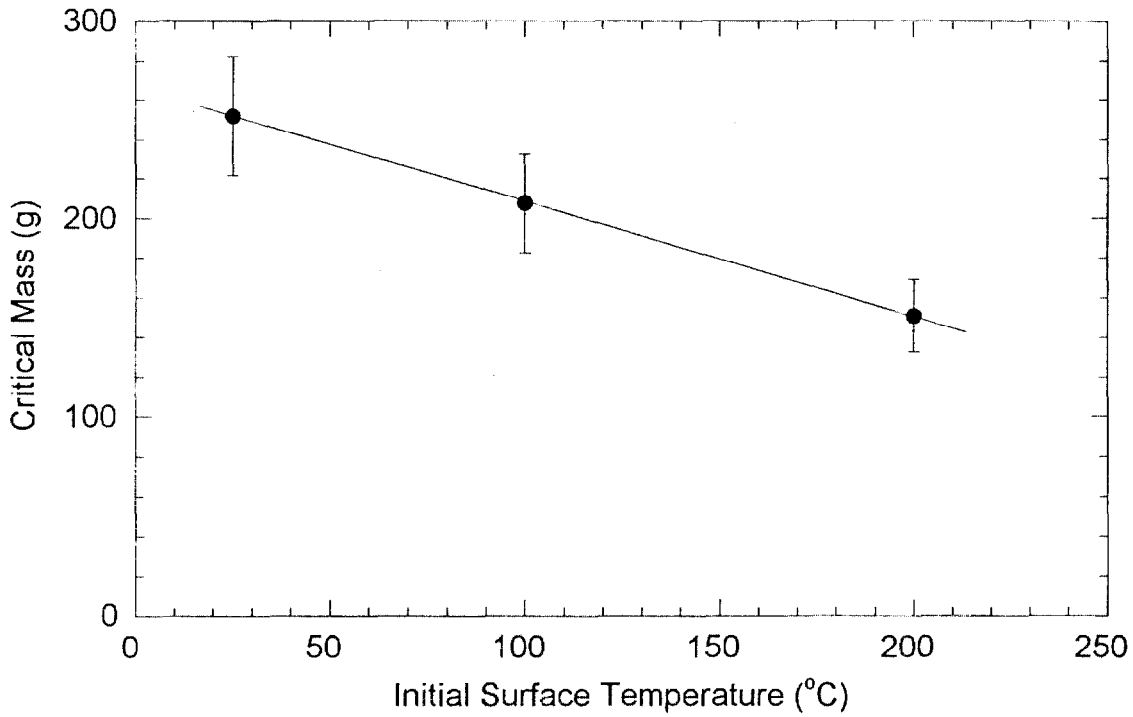

56. The measured critical mass of gaseous suppressant (N_2) as a function of the initial temperature of the surface of Box 5 in the reduced-scale compartment for Case 11 in Table 12.

suppression. In that case, after high suppressant concentrations have dissipated, fuel near the hot surface would vaporize, creating a hot reactant mixture that would autoignite.

Hot surfaces within the compartment also act to preheat fuel vapor and entrained air. This increases the critical suppressant requirements as indicated by calculations based on enthalpy considerations and a critical temperature criterion for flame extinction [Sheinson et al., 1989]. The calculations show that raising the temperature increases the required agent concentration by approximately 10 %, a much smaller value than observed in Fig. 56.

In another experiment, the burn period was increased to test the effect of increasing the Box 5 surface temperature through fire heating, rather than electrical preheating. The critical mass for a burn period of 90 s was measured as 210 g ± 25 g. This was not significantly different from the results of the critical mass for a burn period of 15 s (with Box 5 initially at ambient temperature), which was 252 g ± 30 g, as seen in Fig. 56. Although not statistically significant, the trends in these results are not inconsistent with the interpretation associated with fuel anchoring given above.

3.1.4.5.1 Reignition

At higher temperatures and long residence times, auto-ignition becomes important and post-suppression reignition must be considered [Glassman, 1989]. A series of experiments was conducted to investigate the effectiveness of a suppressant to prevent ignition. Autoignition of the heptane discharge (15 mL/min) on the heated surface of Box 5, however, was not a repeatable phenomenon.

Ignition was observed on occasion when the Box 5 surface thermocouple temperature was greater than approximately 360°C. Increasing the surface temperature did not improve repeatability. As the surface temperature was increased, the fuel was observed to vaporize on contact and presumably diffuse away. The fluid temperature in this case was higher than the flash and fire point temperatures (Table 11), but without a spark, very hot wire, or other ignition source, ignition did not repeatably occur. Similar experiments were conducted with gasoline and undiluted anti-freeze, yielding similar results.

Because of the repeatability problems using the Box 5 surface as an ignition source, experiments were instead performed using a surface that allowed higher temperatures. A 5 cm long piece of inconel wire was oriented horizontally and placed ≈ 5 cm below the top of Box 5, 2 cm in from the edge, just touching its surface. The wire was resistively heated. Ignition of the heptane fuel flow (15 mL/min) was repeatedly achieved if the wire was greater than or equal to ≈950 °C ±100°C, as measured by an optical pyrometer. The effectiveness of ABC powder in preventing ignition was tested. The powder was discharged for conditions consistent with Case 2 in Table 12. The suppression experiment was conducted delivering twice the mass necessary to achieve suppression in the compartment. The hot wire was initially not energized. The standard fire

suppression experiment was conducted. Suppression was observed to be successful. At this temperature, ignition (actually re-ignition) was observed to rapidly occur after energizing the hot wire to the minimum temperature required to achieve ignition (950 °C). The powder did not prevent the reignition event. The experiment was repeated with the same result.

A similar experiment was conducted using a spark igniter placed above a 10 cm diameter, 2 cm deep Pyrex dish, filled with 1 cm of gasoline at ambient temperature. The spark igniter was placed ≈1cm above the fuel surface. Ignition was repeatedly achieved by energizing the sparker. The spark igniter was placed beside the edge of the reduced-scale compartment, seen near the leg on the left side of the enclosure in Fig. 20. After suppression was successfully completed, the sparker was initiated. Flaming was observed to occur rapidly, within 1 to 3 seconds. Re-ignition was presumably prevented until high suppressant concentrations dissipated. Submerged powder was observed in the liquid fuel. The dish was cleaned and the experiment was repeated. Spark ignition of the gasoline did not appear to be affected by the mass of powder used.

These experiments suggest that strong ignition sources can defeat a powder suppression system. It is highly unlikely that a 950°C surface will exist in an engine compartment, but sparking, arcing and moderately hot surfaces (300°C to 400°C) may occur at some locations in a post-collision vehicle (e.g. the exhaust manifold, catalytic converter, exhaust pipes). Depending on the scenario, post suppression reignition may pose a challenge to successful suppression.

3.1.4.6 The Effect of Fire Scenario

Figure 57 shows the results of 7 series of experiments that investigated the effect of fuel location and amount on the critical suppressant mass. The experimental conditions are denoted as Case 12 in Table 12. The results are organized into fires that were fuel leaks only, those that were fuel spills only, and those that were a combination of spills and leaks. When the fuel leak rate was 50 mL/min (≈27 kW heat release rate), flames were evident along the side of Box 5 and along the top and sides of Box 20 (see Figs. 21 and 22), which was located just below Box 5. At this rate of flow, the discharged fuel created a pool on the cement slab. Flames were observed to occasionally extend beyond the top panel, past the compartment frame. As the fuel flow was increased, Figure 57 shows that the critical suppressant mass increased.

The amount of fuel spilled was varied in three suppression experiments. In the first experiment, 50 mL of fuel was spilled on the cement slab directly below the center of the compartment. In the other two experiments, 50 mL and 100 mL of fuel were spilled below Box 5, at a location (X,Y) equal to (15 cm, 38 cm) in Fig. 22. The puddles were not round, but were somewhat irregular as the fuel spread over the rough cement surface. The area of the puddles was determined through image analysis of video recordings as described by Ohlemiller and Cleary [1998]. The 100 mL spill had an equivalent radius of approximately 18 cm, as compared to 13 cm for the 50 mL puddle. Although every spill yielded a somewhat different puddle shape, the 100 mL spill centered at (15 cm, 38 cm) extended ≈3 cm past the inner edge of the compartment frame, whereas the

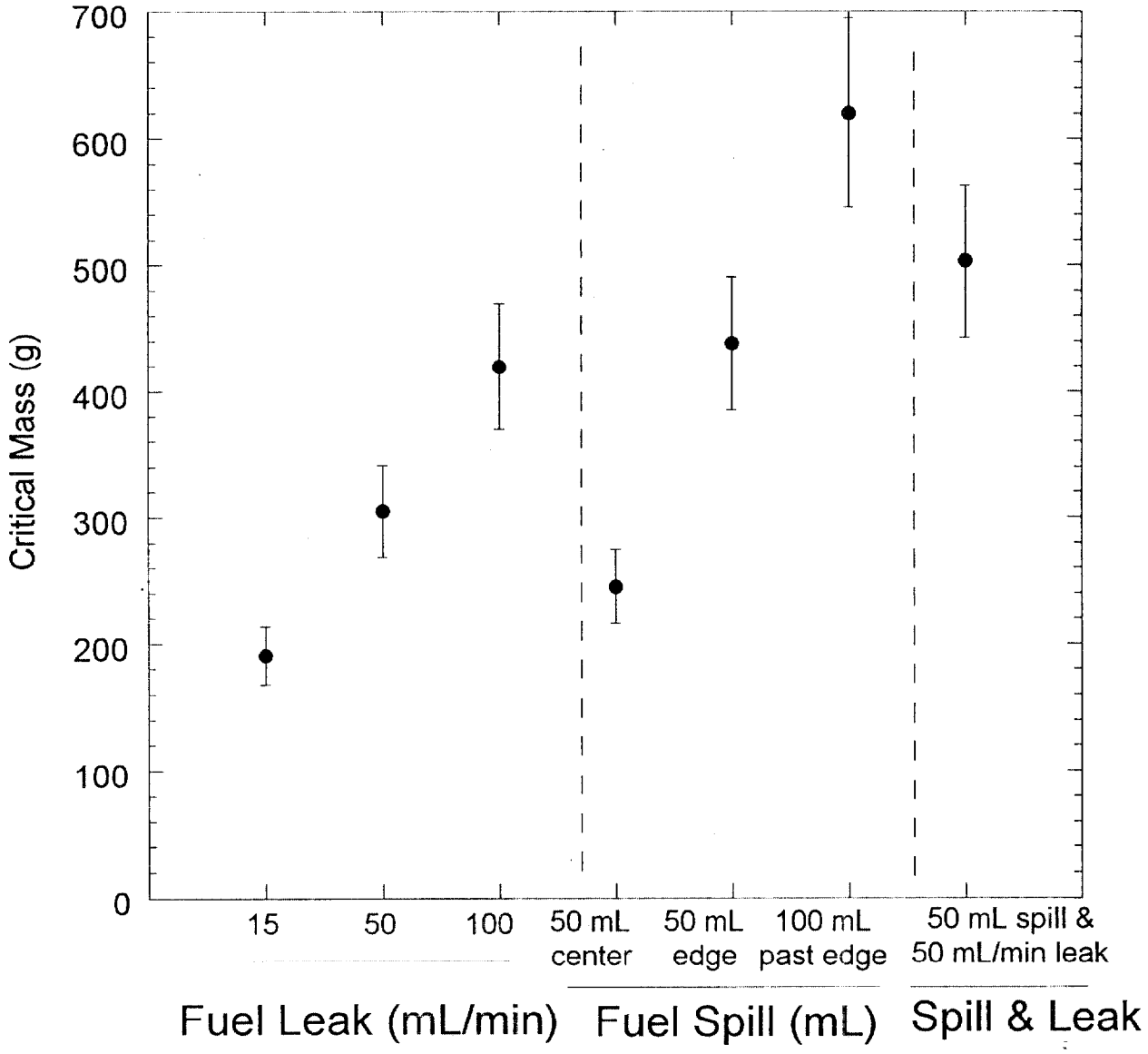

57. The measured critical mass of gaseous suppressant (N_2) as a function of fuel location and amount in the reduced-scale compartment for Case 12 (see Table 12).

50 mL spill centered at (15 cm, 38 cm) was within the frame. Figure 57 shows that a larger mass was required to suppress the 100 mL spill as compared to the 50 mL spill near the compartment edge. The 50 mL spill at the compartment center was easier to extinguish than the 50 mL spill near the compartment edge. These results indicate that both the size and location of the fuel spill influence suppressant requirements. The results for the experiment that combined a 50 mL/min leak and a 50 mL spill showed that although the leak/spill combination was somewhat more difficult to extinguish than the 50 mL/min leak, the difference was not significant when measurement uncertainty was considered.

3.1.4.7 The Effect of Suppressant Type

Figure 58 shows the results of experiments that investigated the effect of suppressant type on the critical suppressant mass requirements. Experimental conditions are denoted as Case 13 in Table 12. The suppressants that were tested included four clean agents, two powders, and two prototype devices (AG1 and the tubular device). The suppressants are described in detail in Section 1.3. Experiments were not performed using SPG due to safety concerns associated with use of pre-production line units. In these experiments, the powders and clean agents were delivered through the center of the top panel. The placement of the tubular device and AG1 are described in Section 3.1.1.1.

An example of the diode signal and temperatures at two locations in the compartment as a function of time are shown in Fig. 59 for Case 13 in Table 12. The suppressant was the tubular device mounted on the underside of the top panel. Approximately 11 s after ignition, the tubular device activated. At that time, the temperature 5 cm below the center of the top panel was 150°C (see TC3). Fire suppression occurred approximately 1.5 s later as indicated by the diode signal. Figure 25 is a photograph of the device after the experiment. The coil was approximately 30 cm in diameter. The rupture location on the tube is clearly seen on the inner-most portion of the coil, close to the mounting bracket. The difference in the mass of the tubular device before and after discharge indicated that approximately 95 % of the suppressant was ejected during the discharge.

The results shown in Figure 58 show that the suppressants for Case 13 in Table 12 can be broken into two groups distinguished by their mass-based performance. The first group consists of the powder suppressants, the tubular and the aerosol devices. The second group includes the halogenated agents. There was little difference between the suppressants within each of these two groups. The results are consistent with the values of ρY_c shown in Table 4, which predicts that the most effective suppressants should fall into the same two groups. The first group is characterized by $\rho Y_c<0.2$ and includes the AGs, powders, and tubular suppressant, and the second group is characterized by $\rho Y_c>0.4$, which includes HFC-125 and HFC-227ea. It is somewhat surprising that the results are consistent with ρY_c when transport was shown to effect suppression in the reduced-scale test apparatus and the term ρY_c does not account for transport effects.

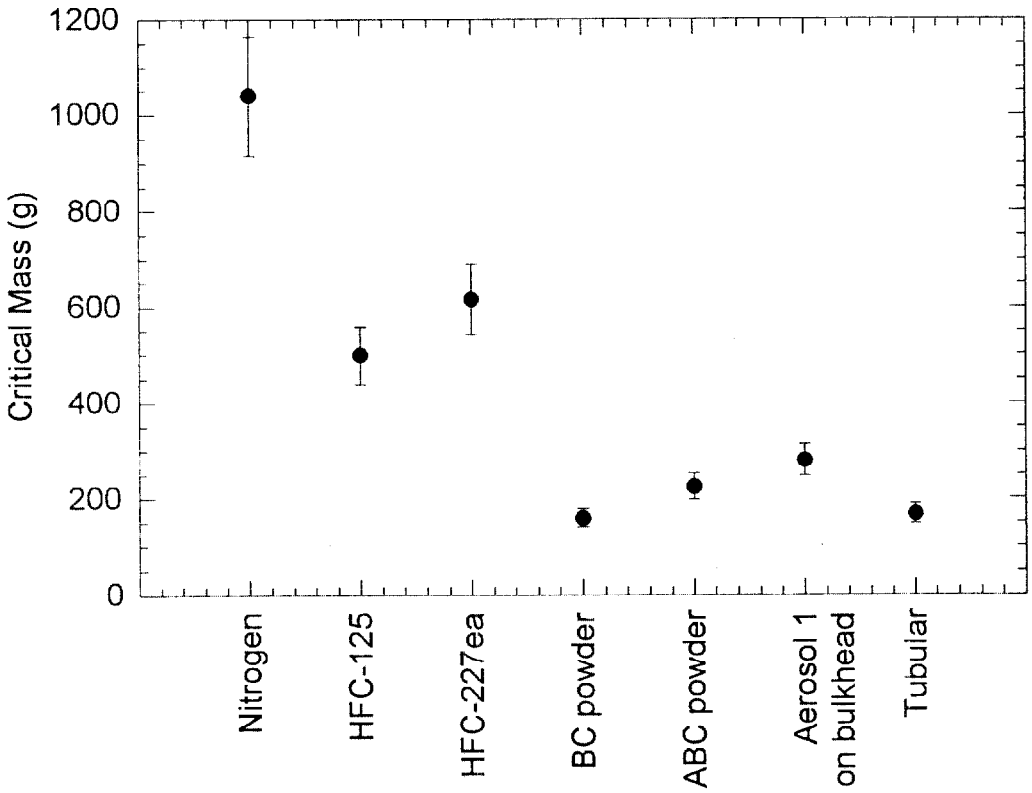

58. The measured critical mass for different suppressant types in the reduced-scale compartment for Case 13 (see Table 12).

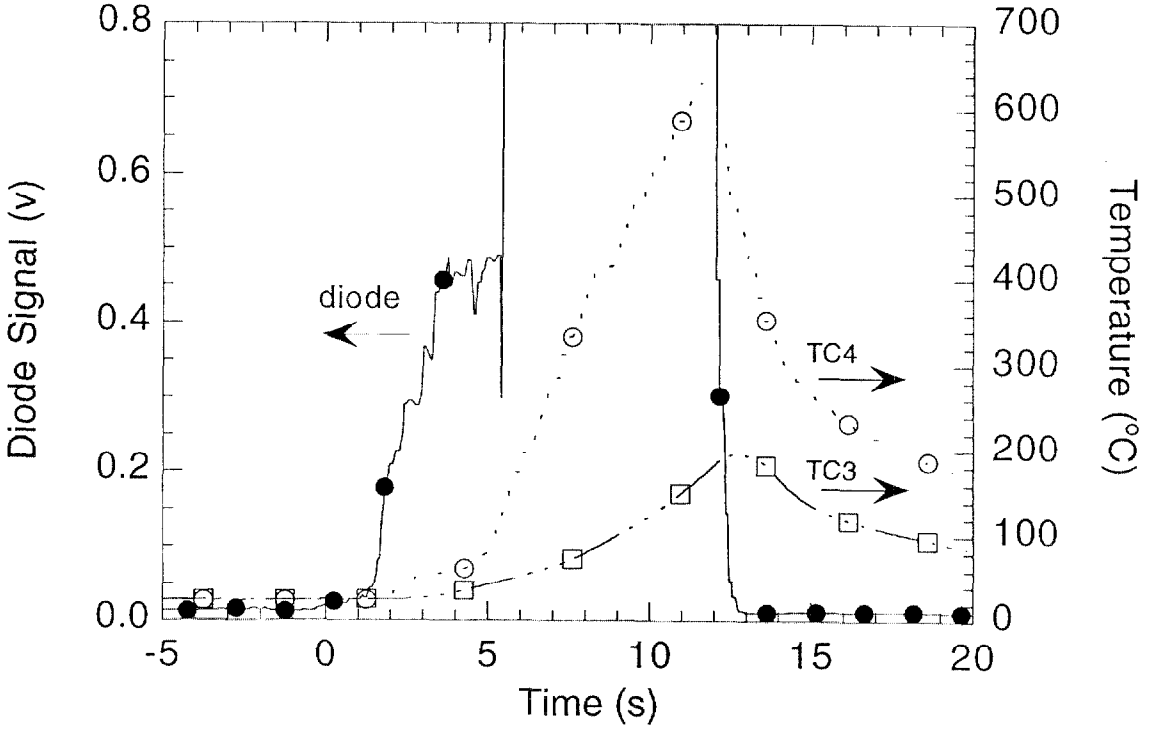

59. The flame emission signal and the temperature 5 cm below the top panel (TC#3; see Fig. 19) as a function of time after ignition using the tubular fire suppression device in the reduced-scale engine compartment.

3.1.5 Summary

The suppression effectiveness of a number of suppressants was tested in a reduced-scale compartment. These included a number of commonly used fire suppressants such as powders and clean agents, as well as some prototype devices. The suppression measurements showed that the critical suppressant mass varied with suppressant type.

It was not possible to construct a simple correlation that summarizes the critical suppressant mass requirements in the reduced-scale engine compartment as a function of compartment geometry, because of unsystematic variations in the data. This was evident in the measurements showing that the placement of obstacles and nozzle location had a strong influence on the critical mass requirements. In this regard, the details of suppressant transport around obstacles in the cluttered partially open compartment effected suppressant performance. Suppressant transport is dependent on the details of the geometry, the fire, and the suppressant delivery system. Thus, simple analytic mixing models and correlations do not adequately predict suppressant mass requirements. Experiments suggest that suppression system parameters and the fire location relative to the suppressant release have a significant bearing on the suppressant mass requirements. This conclusion is consistent with detailed CFD modeling of suppression transport. Transport issues take on a heightened importance because the compartment is not closed. Because the compartment has a relatively large portion of its surface open to the environment, large suppressant mass must be used to overcome suppressant losses from the compartment. The experiments and CFD modeling indicate that rapid suppressant discharge was an effective strategy in minimizing the critical suppressant mass in the reduced-scale apparatus.

Although it is not possible to construct a simple correlation that summarizes the critical suppressant mass requirements as a function of operating conditions, certain trends in the data presented in Section 3.1.4 are evident in terms of the independent experimental variables (i.e., geometrical features, fuel-associated parameters, and suppressant-related parameters). The data that forms the basis of Table 15 is contained in Section 3.1.4.2 –3.1.4.5 as noted in the column labeled "data" in the table.

To describe the experimental trends, a range factor (RF) and a mass penalty factor (PF) are defined as:

$$RF = f_{iref} / f_i \tag{31}$$

$$PF = W_{iref} / W_i \tag{32}$$

where f_{iref} is taken as a reference value of one of the experimental parameters (e.g., *VF%*, *SO%*, etc.) in the reduced-scale apparatus and f_i is an extreme value of the parameter within the range of experimental conditions tested. W_i is the critical suppressant mass associated with f_i and W_{iref} is the critical suppressant mass associated with f_{iref}. The RF and PF factors are valid only over the range of conditions investigated. Table 15 lists the experimental parameter, the location in this

report where the data is discussed, and the corresponding values of f_{iref}, RF, and PF. A penalty factor with a value equal to 1.0 indicates that there was negligible change in the measured critical mass over the range of conditions considered in the experiments. A penalty factor significantly greater than 1.0 or significantly less than 1.0, implies that there was significant change in the measured critical mass over the range of test conditions. Table 15 shows that the PF depended on suppressant type (gas versus powder), taking on values close to 1.0 and as large as 3. The largest penalty factor was associated with changes in *SO%* for the gaseous suppressant.

The next Section describes suppression experiments in a full-scale engine compartment fire. Many of the same suppressant types that were tested in the reduced-scale compartment fires were tested in full-scale experiments, within the range of experimental conditions tested in the reduced scale.

Table 15. Range and Mass Penalty Factors for the Reduced-Scale Compartment Tests.

Parameter	Data	Reference Value	Range Factor	Penalty Factor gas; powder
Percent Volume Filled	Sec. 3.1.4.2.1	20 %	2	≈1; 0.8
Percent Surface Open (body panels)	Sec. 3.1.4.2.2	12 %	1.7	3; 1
Percent Surface Open (top panel)	Sec. 3.1.4.2.3	½ %	6	1.3; 1.5
Fuel Leak/Burning rate	Sec. 3.1.4.5	15 mL/min	7	2; nm
Fuel Leak location	Sec. 3.1.4.5	Compartment center	Edge	2; nm
Fuel Type	Sec. 3.1.4.4	Heptane	other fluids	1.2; nm
Component Surface Temperature	Sec. 3.1.4.5	50 °C	4	0.5; nm
Delivery duration	Sec. 3.1.4.3.2	4 s	8	0.5; nm
nm: not measured.				

3.2 Full-scale Engine Compartment Suppression Experiments

3.2.1 Apparatus

A series of suppression tests was conducted using an uncrashed mid-sized sedan as the experimental apparatus. Some key geometric characteristics of the vehicle are described in Table 2. A photo of the engine compartment is shown in Figure 60 and a top-view schematic diagram is shown in Fig. 61. The central portion of the compartment was occupied by a six cylinder transverse mounted power train. The remainder of the compartment was filled with standard components with the exception of the battery, which was removed.

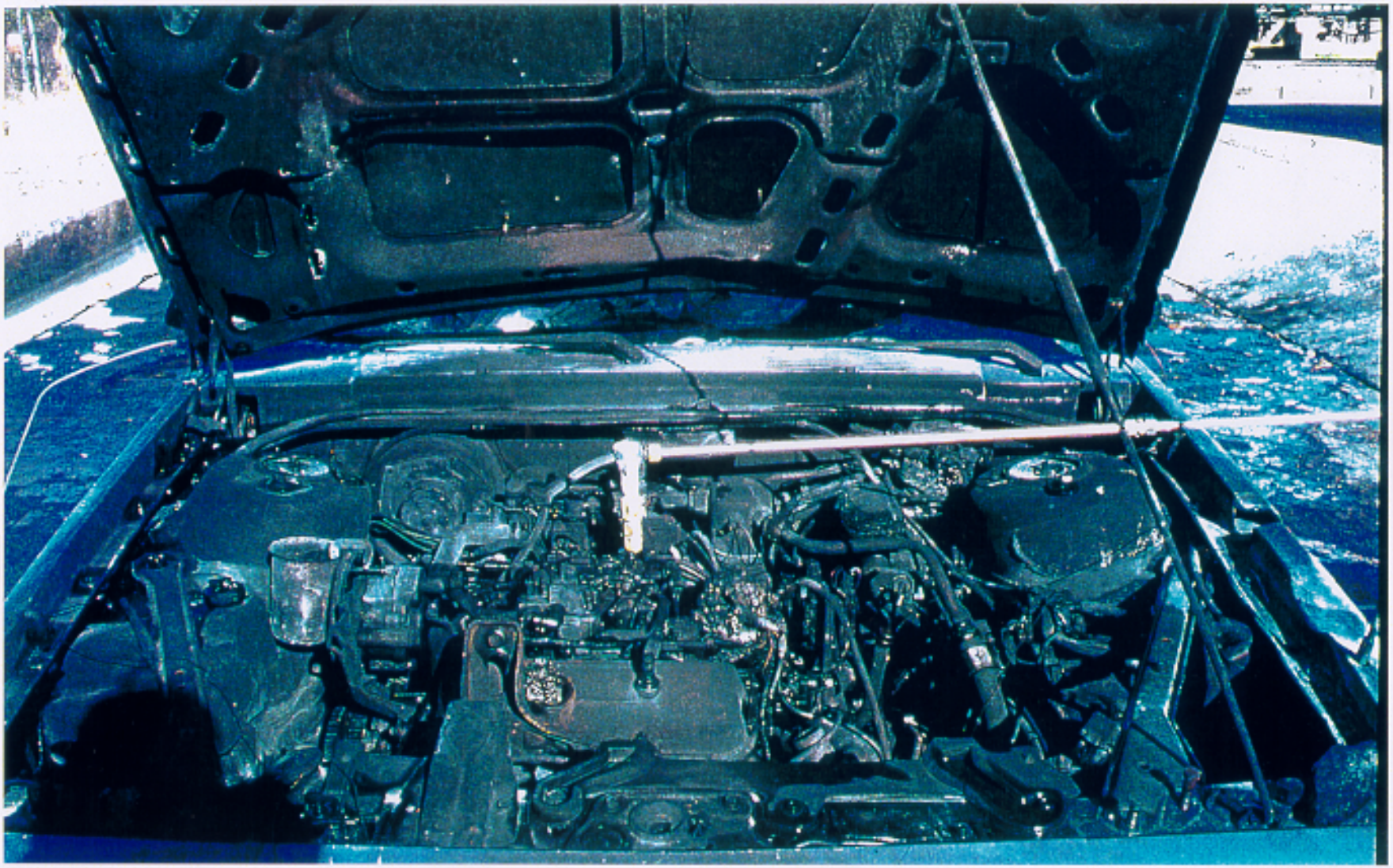

60. A photo of the vehicle engine compartment.

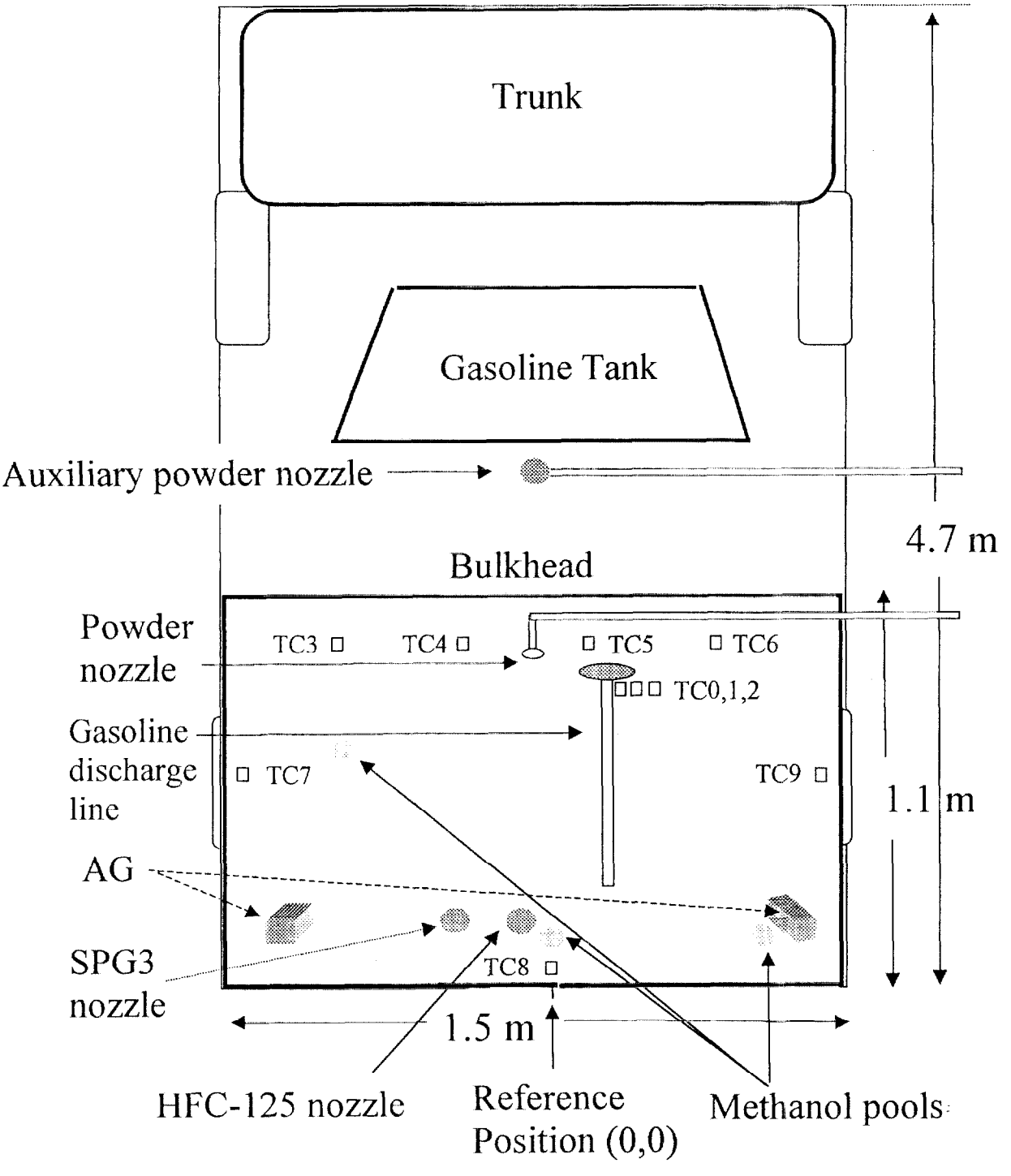

61. A top view diagram of the instrumented vehicle engine compartment (not to scale).

To simulate one possible post-collision scenario, the hood was bent along its two crush initiators and lifted above its normal configuration such that $SO_{hood} \approx ½$ % (see Eq. 5). This is evident in Figs. 62 and 63, which are perspective and side (close-up) views of the test vehicle. A pool fire is evident under the vehicle in Fig. 62. Figure 63 shows a side-view of the hood. The gap created by bending the hood, allowed observation of the flames and smoke within the compartment. At the top of the photograph, flames can be seen flowing from a gap at the rear of the hood onto the windshield.

Commercial unleaded gasoline (86 octane) was held in a 10 L container and was delivered at a controlled rate via 6 mm (o.d.) metal tubing to a location in the rear-central portion of the compartment as shown in Fig. 61, on the rear driver-side portion of the engine manifold, approximately 15 cm from the front panel and 20 cm below the hood. This was a relatively cluttered region of the engine compartment with typical distances between components on the order of 2 cm. The gasoline was forced through its delivery line by pressurizing the reservoir with gaseous nitrogen. The gasoline discharge (200 ± 10 mL/min) was controlled by a regulating valve located at the outlet of the reservoir. This flow was selected because it produced a fire that scaled with the fire heat release rate in the reduced-scale experiments when multiplied by the ratio of the free volume of the full-scale compartment to the free volume of the reduced-scale engine compartment (Section 3.1). Figure 64 shows the inside of the compartment with the fire burning as the fuel flowed at a rate of 200 mL/min. This represents a heat release rate (HRR) of approximately 100 kW as determined from the relation: $HRR = \dot{M}_f \cdot H_c$ and the data in Table 11. The fire extended approximately 20 cm above the engine components as seen in Fig. 64. With the hood closed, flames were observed to escape through the rear of the compartment, coming into contact with the lower portion of the windshield. A smaller fire would have been less challenging, as suggested by the experimental results in the reduced-scale compartment presented in Section 3.1.4.5. A properly designed detection system would be able to detect a fire of this size, which extended from the ground through the entire compartment and onto the hood. Therefore, testing of a larger fire was considered unnecessary.

A small propane flame (≈3 cm long) was typically used to ignite the gasoline. It consisted of a long (2 m) metal tube (6 mm o.d.) attached to a 1 L propane reservoir. Approximately 40 s after ignition of the gasoline flow, a small pool fire (≈20 cm diameter) was established below the vehicle. This indicated that a long vertical trail of burning fuel existed from the middle of the exhaust manifold continuously to the ground. The gasoline dripped from one component to another, cascading to the ground where a small burning puddle was created, approximately 30 cm in diameter.

Three small containers of burning methanol (8 cm diameter) were positioned about the top portion of the compartment. These small methanol flames acted as monitors of the local suppressant concentration, indicating whether the suppressant concentration was above the critical value near the containers. The containers were positioned away from the primary fuel source to avoid any interaction. One of the three small (8 cm diameter) methanol pool fire burners can be seen on the passenger (left) central side of Fig. 60. The position of all three methanol

62. A perspective view of the test vehicle showing the hood bent and raised.

63. A side (close-up) view of the test vehicle with a gap in the bent hood allowing observation of the fire in the compartment.

64. A photo of the engine compartment with a 200 ml/min gasoline discharge burning at the standard location.

burners is indicated in the schematic diagram of the engine compartment (Fig. 61). The methanol container (X,Y) positions were located at (-50 cm, 50 cm), (0 cm, 15 cm), and (50 cm, 15 cm) relative to the front-center top portion of the compartment. One of the methanol containers is visible in the middle-left portion of Fig. 64, located 40 cm from the passenger/engine compartment front panel, 44 cm from the centerline of the compartment, and ≈10 cm below the hood. The two other methanol containers were positioned towards the front of the compartment, one located adjacent to the radiator fan housing and the second located where the vehicle battery is normally stationed. For some experiments, it was necessary to reposition the methanol pools to avoid methanol splashing due to direct impingement by suppressant.

A number of bare bead (0.63 mm or 0.25 in diameter) type K thermocouples were mounted in the engine compartment to monitor the temperature. Their positions are indicated in Fig. 61. Thermocouples TC3-TC6 were hung 3 cm below the hood and TC7-TC9 were positioned just inside the compartment, ≈5 cm from the edge of the compartment in the plane of the hood/body panel interface as shown in Fig. 61. Thermocouples TC0 and TC1 were pinned (by a screw) at two locations onto a thin (≈2 mm) steel shield that was an intrinsic part of the vehicle that was attached to the exhaust manifold and located below the gasoline delivery line outlet. TC2 was hung 20 cm below the hood, directly above the gasoline discharge location.

The placement of a number of the suppressant nozzles are shown in Fig. 61. Except for the powders and the halogenated compound, the other suppressant systems were positioned according to manufacturer recommendations. The suppressant system positions (X,Y, Z) are listed in Table 16 and are indicated in Fig. 61. An attempt was made to optimize ABC powder delivery to extinguish the test fire by examining the effectiveness of a number of different nozzle configurations, which are summarized in Table 17. The suppression system supply line and nozzle for the powdered suppressants are evident in Figs. 60 and 61. In all configurations, the nozzle was positioned in the central rear portion of the compartment. The nozzles were located between the top layer of components and the hood, except in two cases (FS5 and FS6) where the suppressant was split into two portions (see Table 17). In that case, approximately one-half of the suppressant flow was delivered from the middle of the underbody by a spiral nozzle directed forward along the ground towards the pool fire and the second half was delivered about the top of the engine compartment.

Configuration FS1 is shown in Figs. 65 and 66. This configuration was used for both ABC powder and BC powder. In this configuration, Nozzle #9 (see Table 7) was oriented upwards and positioned towards the rear (20 cm from the bulkhead) of the compartment center, approximately 10 cm above the engine components. This nozzle distributed the suppressant in all directions, creating a cloud of suppressant above the nozzle as described in Section 2. Figure 65 shows the compartment and surrounding area after an experiment using 1500 g of ABC powder. A fairly uniform layer of whitish powder was observed on the uppermost engine components. The powder was also observed on the ground. Figure 66 is a close-up view of nozzle #9 (see Table 7), which was used to discharge powder (Configurations FS1 and FS5) and HFC-125.

65. A photograph of the ABC powder delivery system using Configuration FS1 in the full-scale engine compartment.

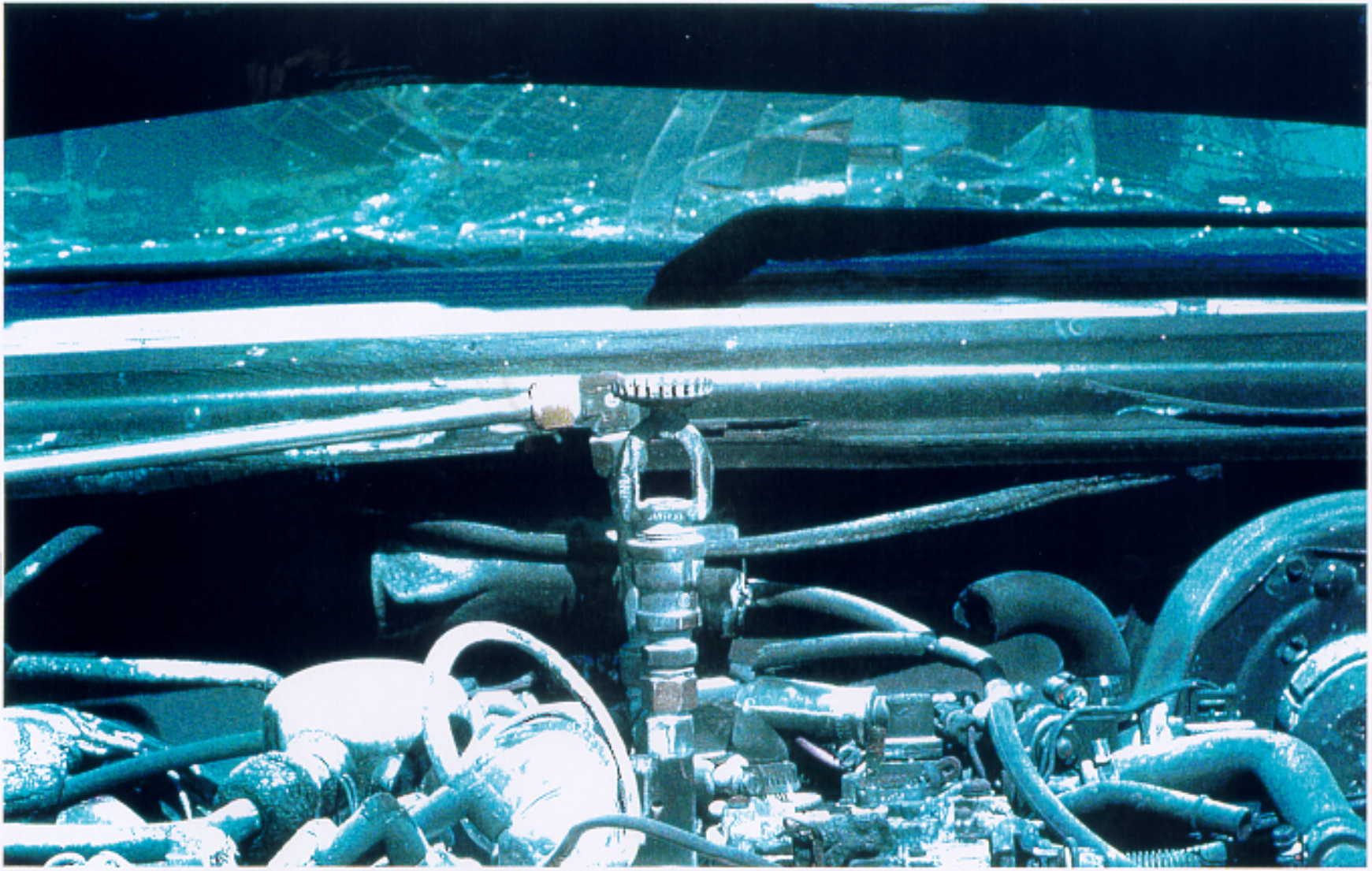

66. A close-up photograph of the nozzle seen in Fig. 65.

Configurations FS2 and FS3 (see Table 17) consisted of four spiral nozzles or four open tubes oriented downward about the center of the compartment separated by 30 cm. The flow was balanced by using a series of union tee tube fittings, such that each of the four nozzles received ¼ of the total suppressant flow. The plumbing system was rigidly held in place, with the nozzle ducts approximately 5 cm above the plane defining the tops of the engine components. Configuration FS4 consisted of two fan nozzles oriented in the horizontal plane, opposed in direction, and approximately 3 cm above the engine components.

Three HFC-125 systems were tested, all three used Nozzle #9 (see Table 7), placed as shown in Fig 61. The first system used 15 mm i.d. tubing connected to a 1.0 L reservoir, which was pressurized to 4.2 MPa (600 psig) with gaseous N_2. The second and third systems used a 2.3 L reservoir, which was pressurized to 2.1 MPa (300 psig) or 1.4 MPa (200 psig) respectively, with gaseous N_2. Reservoir pressurization governs the required burst pressure of the suppressant

Table 16. Suppressant Device Location.[a]

Suppressant	Location (lateral, axial)	X (cm)	Y (cm)	Z (cm)
Powders	Center; rear	0	90	10
HFC-125	Center, top front	0	20	0
SPG1 and 2	Center of hood bottom	0	30	15
SPG3	Passenger side; front	-20	20	10
Tubular	Rear of hood bottom	-60 to +60	50 to 100	15
Aerosols	Corners; front; directed to center	-80; +80	20	-10

a. Referenced to top front center of engine compartment, (X, Y, Z) = (0, 0, 0); see Fig. 61.

Table 17. Nozzles Tested in the Full-scale Engine Compartment Experiments with ABC Powder

Config.	Nozzle Number & Type	Nozzle Orientation/Location
FS1	1 x Nozzle (#9)	Compartment rear center; 10 cm above components
FS2	4 x spiral (#5)	Oriented down; about center of compartment; ≈10 cm above components
FS3	4 x tube (10 mm i.d.)	Oriented down; about center of compartment; ≈10 cm above components
FS4	2 x fan (#7)	Opposed; Compartment rear center; 3 cm above components
FS5	1 x Nozzle (#9) 1 x Spiral (#5)	Compartment center; 3 cm above components Mid-underbody
FS6	2 x fan (#7) 1 x spiral (#5)	Compartment center; 3 cm above components Mid-underbody directed forward

reservoir material and thereby has a bearing on the reservoir thickness and system mass. The reservoir volumes for the condensed phase (halogenated, powder) suppressants were selected such that the suppressant filled approximately ½ of the reservoir.

The tubular suppressant was positioned on the underside of the hood according to manufacturer recommendation (see Fig. 67). The tubes were configured in two sets of ≈40 cm diameter coils. Several tube lengths were tested, with the longest tube 7 m long, as seen in Fig. 67.

The AG units were positioned as shown in Fig. 61. Figure 68 is a photograph of an AG1 unit within the engine compartment. The units were placed in the front corners of the compartment and directed toward the center. These locations obviously were not collision resistant, but were used because of space limitations. In this sense the experiments were focussed on suppression feasibility rather than the details associated with suppressant placement.

In addition to the suppressant types that had been tested in the reduced-scale engine compartment, Solid propellant generators (SPGs) were also tested here. Three types of gas generators (SPG1, SPG2 and SPG 3) were considered (see Table 5). SPG1 and SPG2 were from the same supplier and were identical in every manner, except particulate filtering was utilized in SPG1, but not in SPG2. Figure 69 shows a prototype SPG1/SPG2 device mounted on the hood bottom. The device was cylindrical, 5 cm in diameter and 35 cm long. Three sets of small (2 mm to 5 mm) exhaust ports were positioned every 1 cm along the axis of the cylinder, 120° apart. The test device (see Figs. 69 and 70) is much heavier and bulkier than the production unit envisioned by the manufacturer (see Fig. 3). In one set of experiments, a unit was positioned in each of the front corners of the engine compartment at (X,Y) = (±80 cm, 20 cm) as seen in Fig. 61.

The SPG3 design was completely different than the SPG1/SPG2, based on a different chemical formulation (see Table 5) and using a different nozzle configuration. The hardware used in the experiments was in prototype form. Two nozzle designs were used for the SPG3 in the engine compartment application, referred to as "radial" and "mini-radial". In both devices, a series of radial holes around one end of the cylindrical device served as the nozzle. Figure 70 shows a close-up of the SPG3 device mounted next to the engine fan housing near the front of the compartment. The cylindrical cap/nozzle was approximately 7 cm (o.d.) and approximately 10 cm long. The propellant was held in a cylinder with a length that varied from 20 cm to 40 cm depending on the propellant mass. The nozzle was raised approximately 10 cm above the top layer of engine components. The manufacturer representatives of both SPG types stipulated that the devices could be significantly reduced in mass and volume through use of a standard production design.

3.2.2 Experimental Procedure

The experimental procedure consisted of insuring that the gasoline delivery line was charged with

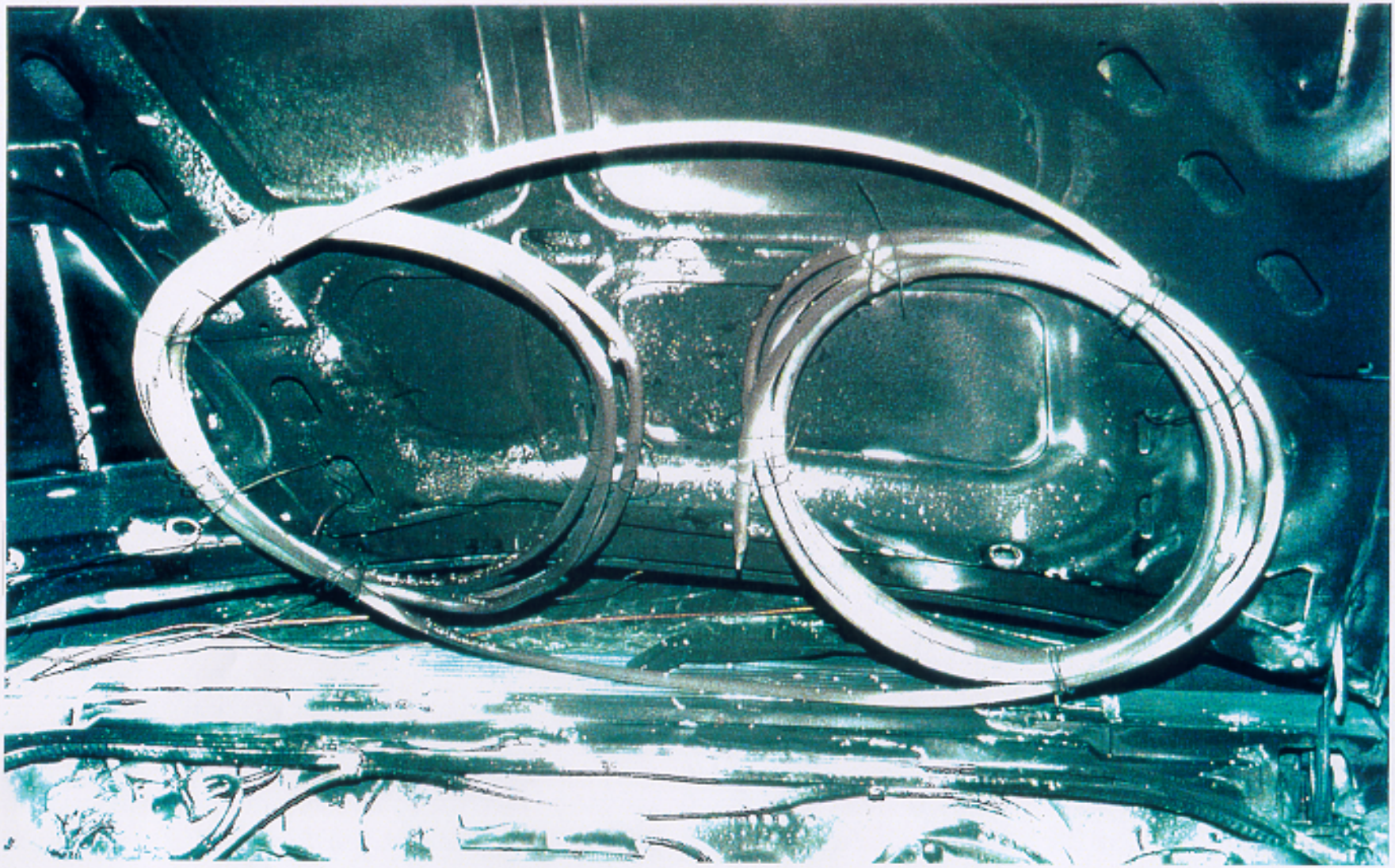

67. The prototype tubular suppression device positioned on the underside of the hood.

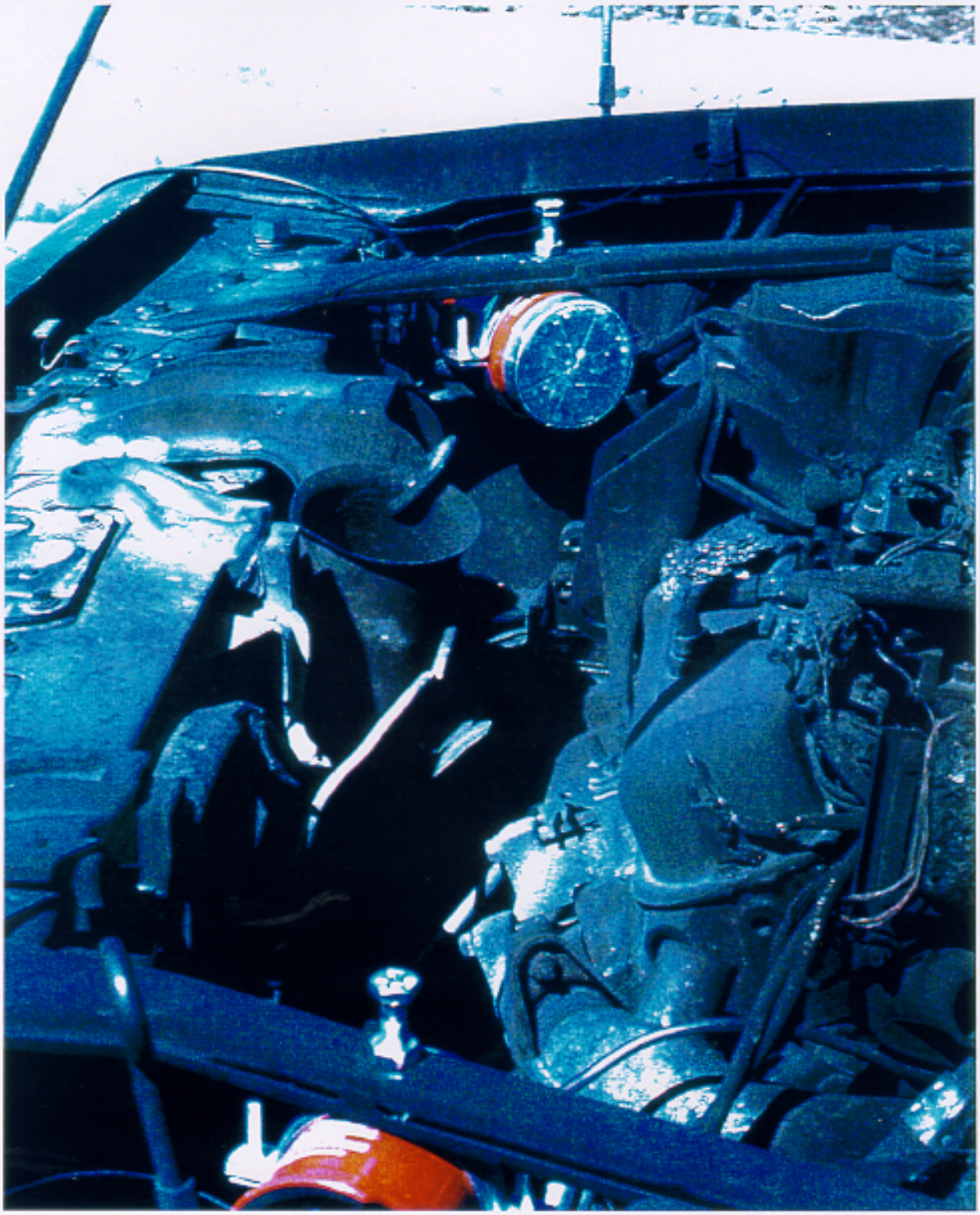

68. A photograph of two AG1 units within the engine compartment.

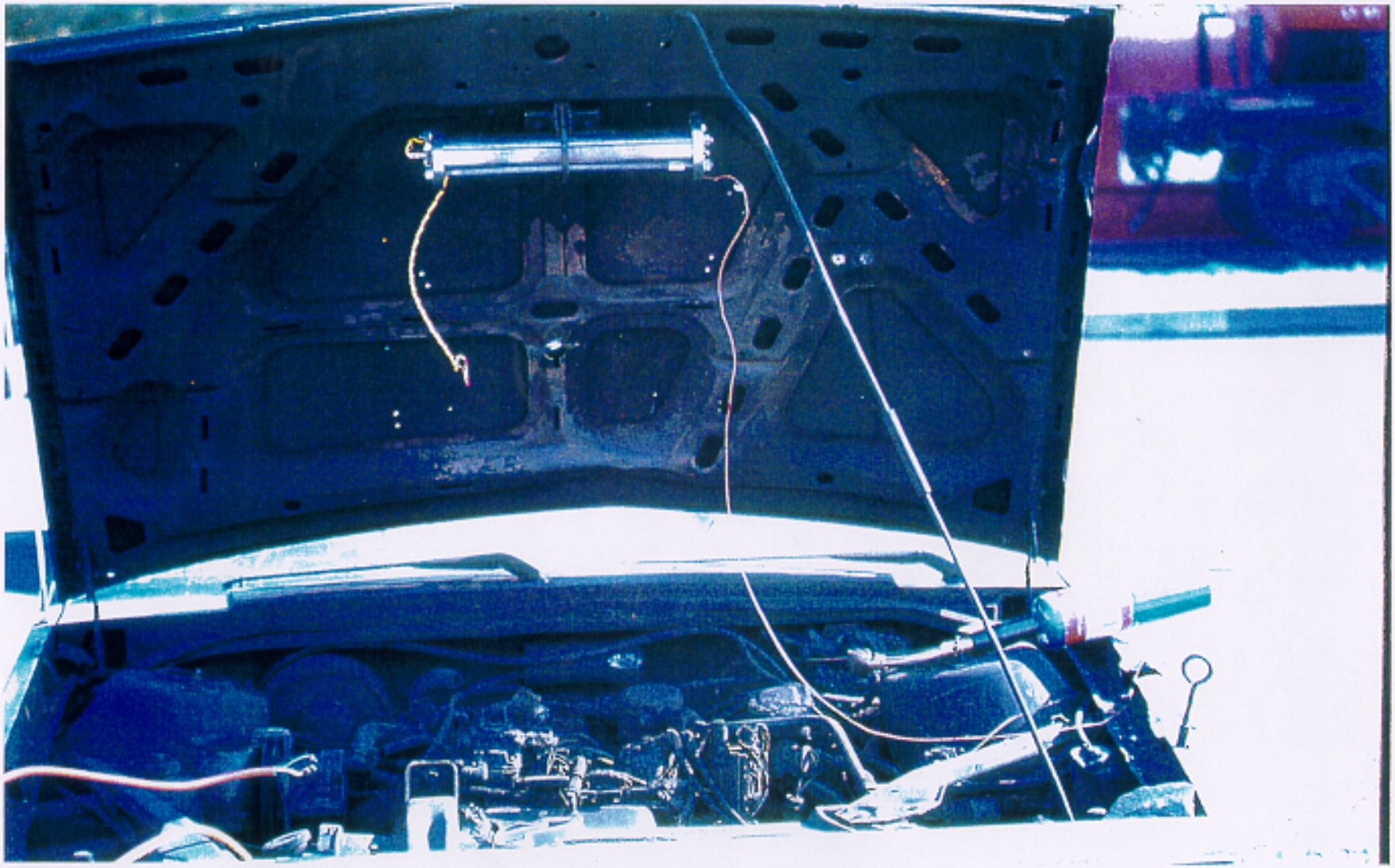

69. The prototype SPG1/SPG2 device positioned on the underside of the hood.

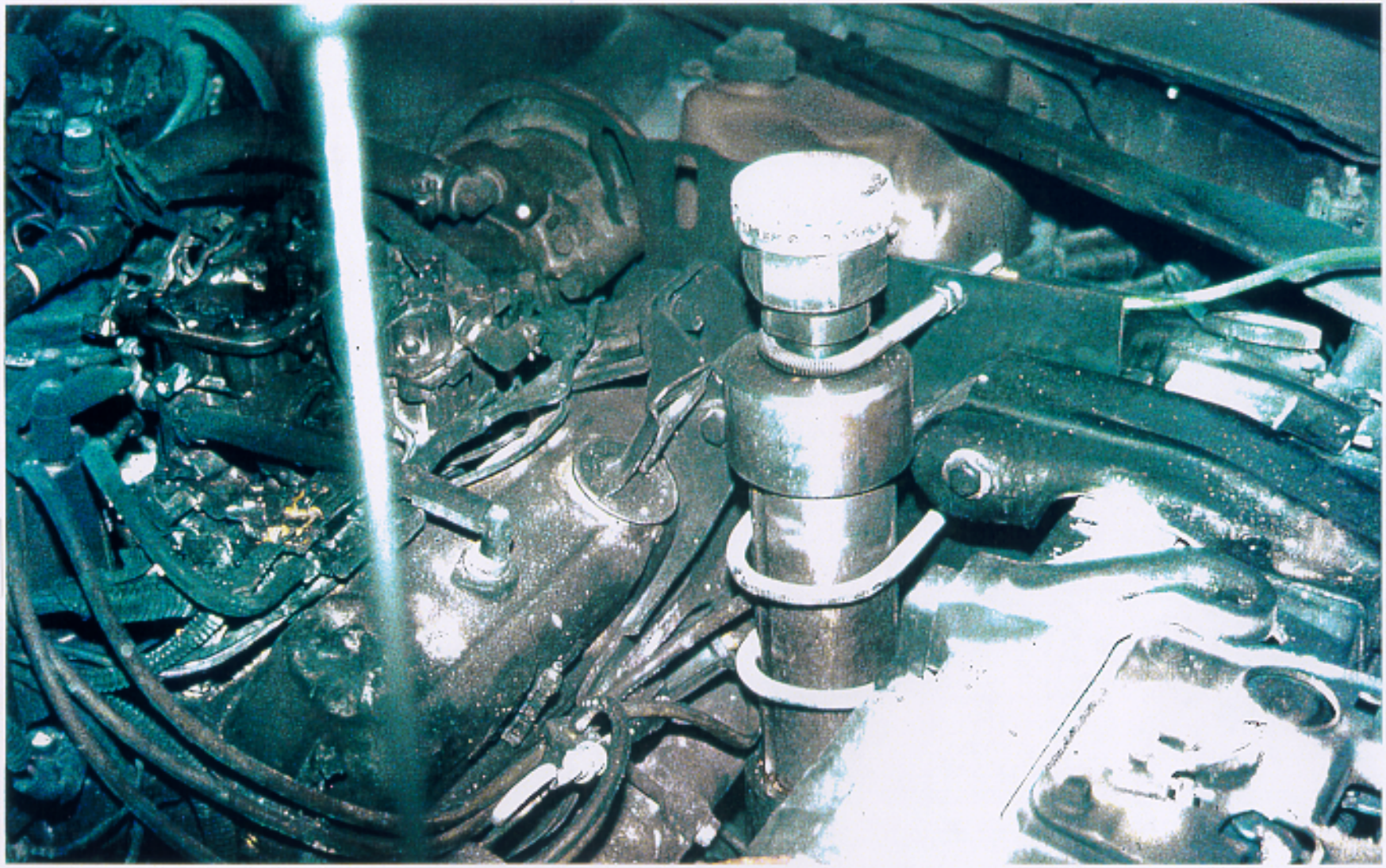

70. The prototype SPG3 device positioned in the engine compartment.

fuel. The small propane igniter flame was positioned just below and to the side of the outlet of the fuel discharge location. The data acquisition system and video cameras were started. The propane flow to the small igniter flame was initiated. Ignition was accomplished using a secondary propane torch. The methanol pools were also ignited using this torch. The vehicle hood was closed and the gasoline flow was initiated 20 s later. This provided time for personnel to clear the test area and allowed the methanol pool flames to heat the underhood to approximately 90 ($\pm$ 20) °C (depending on location), a temperature representative of a steady state engine compartment with the engine running from 30 mph to 40 mph [Santrock, 1996]. Upon initiation of the gasoline flow, the gasoline was repeatedly ignited within approximately 1 s to 2 s. The burning dripping gasoline led to a fire that was luminous and turbulent. The propane igniter flame was extinguished and the fire was allowed to burn for 90 s. The suppressant was then discharged.

A different procedure was used to test the tubular suppressant system and the SPG3/optical detector system. In this case, the suppressant discharge time was not pre-selected, but was governed by the system response. In the case of the tubular suppressant, this depended on the time to rupture the thermoplastic tubing. In the case of the SPG3/optical detector system, the SPG was activated by the detector, which had a response time of 50 ms according to the manufacturer. A fast system is potentially useful for engine compartment fires where components may block direct view of the fire as the fire pulsates, varies in length, and translates. Because the fire may be visible for only a fraction of a second, a fast detector response may be beneficial for early detection of engine compartment fires. This notion was confirmed by experiments investigating the effectiveness of an optical detector with a slow (6 s) response time.

The question of when to activate a suppressant system is distinct from the question of optimal detector response time. Delaying suppressant discharge several seconds after a fire has been detected may be beneficial, allowing time for the vehicle to come to a rest and to turn off the radiator fan. Otherwise, large rates of ventilation in the extended compartment (due to the radiator fan or vehicle movement) will diminish the probability of fire suppression. On the other hand, delayed suppressant discharge ($\approx$10 s) could lead to the presence of a fuel trail beyond the vehicle footprint due to fuel leakage during vehicle movement. A fire scenario involving a fuel trail could prove difficult to extinguish.

The second experimental procedure was identical to the first procedure except that the gasoline (200 mL/min) was allowed to flow 40 s before ignition. After 40 s, approximately 133 mL of gasoline was delivered to the compartment and a liquid pool formed on the ground below the vehicle. The fuel delivery location was identical to the first procedure. Ignition was initiated with an electronic spark or electric matches placed near the fuel puddle. Electric matches are a book of paper matches (2 cm by 2 cm) wrapped by high resistance (13 ohm/m) thin (0.3 mm) nichrome wire energized by a 10 V power supply. The electric matches created a small flame within 1 s to 3 s of energization. In this procedure, suppressant delivery depended on detector activation. The matches themselves did not trigger the optical detector, which was directed towards the center of the engine compartment at a vertical plane level with the hood.

In both procedures, the fuel was allowed to flow for an additional 10 s approximately after termination of suppressant discharge to provide enough time to observe whether the primary fire was suppressed. The fuel flow was then stopped, the vehicle hood was opened, and the status of the methanol pool fires was ascertained. If any of the methanol pool fires was not extinguished, then suppression was considered unsuccessful. All experiments were performed using this procedure unless otherwise noted. When powders were used as the suppressant, residual suppressant was washed away with water before the next experiment. Residual water on the ground was swept away and the subsequent experiment was initiated after approximately a 40 min period, which allowed residual water to evaporate.

3.2.3 Experimental Results and Discussion

Transient temperature profiles from a typical experiment are shown in Figure 71. Initially, the temperatures were low. During the first 20 s, when the hood was closed and the small methanol pools were burning, portions of the compartment achieved a temperature of ≈90 (±20) °C, depending on location. After 20 s, the gasoline discharge was initiated, which ignited rapidly (<2 s) and the compartment temperature began to increase. Thermocouples TC4 and TC5, which were closest to the fire, measured the highest temperatures, with values from 500 °C to 700 °C measured 90 s after ignition. Thermocouples TC0 and TC1 indicated that sections of the exhaust manifold steadily increased in temperature during the 90 s burn period and ultimately obtained temperatures close to 200 °C. These temperatures typically attained higher values, often as high as 300 °C (e.g., Fig. 72). After the 90 s burn period for the experiment shown in Fig. 71, the delivery of 800 g of HFC-125 suppressant was initiated. The suppressant was delivered within ≈1 s, and the thermocouples indicated that the temperatures throughout the compartment stopped increasing. Suppression was successful and the temperatures continued to decrease after suppressant discharge was complete. The measured temperatures were similar from experiment to experiment. Figure 72 shows the transient temperatures using the first experimental procedure with 347 g of SPG2 delivered at 110 s. Peak temperatures are somewhat higher than those seen in Fig. 71, but the trends are similar.

Results from the suppression experiments are summarized in Fig. 73, which shows the critical suppressant mass and its uncertainty (see Table 9) for the full-scale engine compartment suppression experiments. Results for both the first and second series of experiments are shown. The values of the critical suppressant mass do not include associated hardware, whose value is typically three times the suppressant mass. In Fig. 73, an open symbol with an upward pointing arrow indicates that suppression was not achieved using the indicated suppressant mass. This was the case for a number of suppressant types (e.g., the powders, the aerosol generators). The most effective suppressant type was SPG. All three SPGs were more effective than the other suppressant types tested. The difference between the three types of SPGs was small (≈ 100 g) and within experimental uncertainty. Pressure measurements of SPG delivery for identical propellant formulations as used here indicated that the delivery duration was approximately 150 ms for SPG1 and SPG2, and approximately 700 ms for SPG3 [Hamins et al., 1997]. The manufacturers

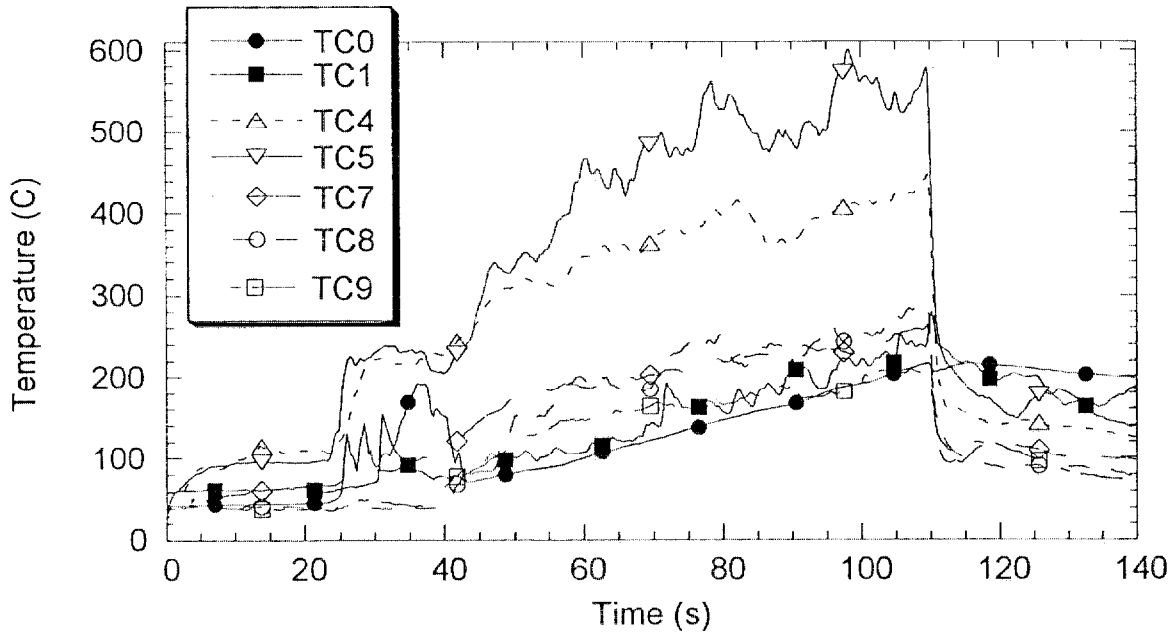

71. Measured temperature at select locations in the full-scale engine compartment as a function of time using 800 g of HFC-125 (delivered at 110 s).

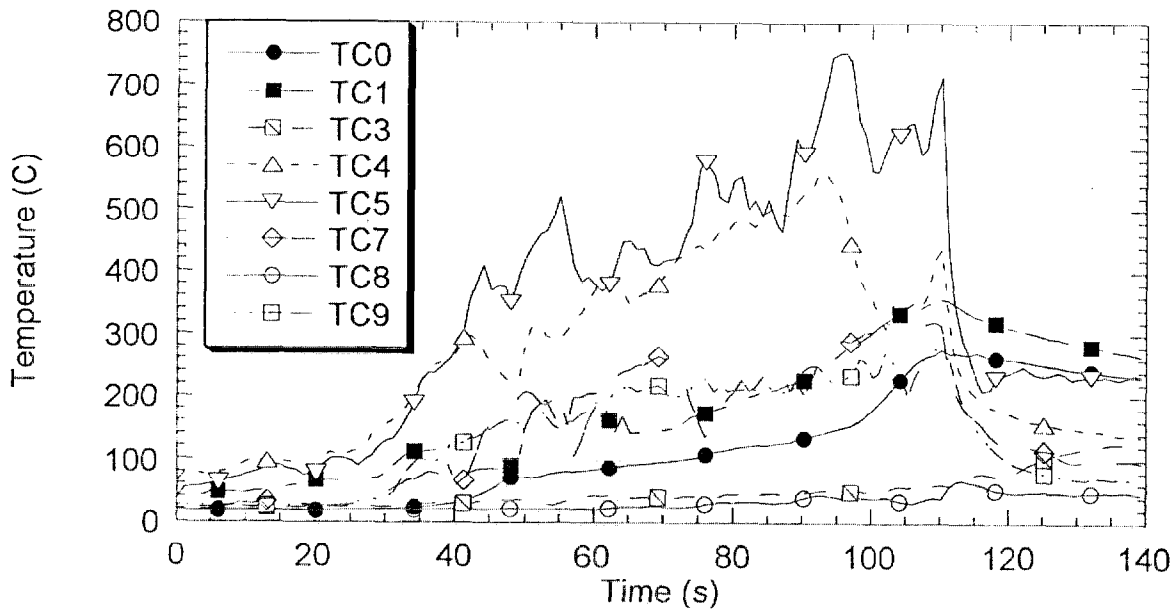

72. Measured temperature at select locations in the full-scale engine compartment as a function of time using 347 g of SPG2 (delivered at 110 s).

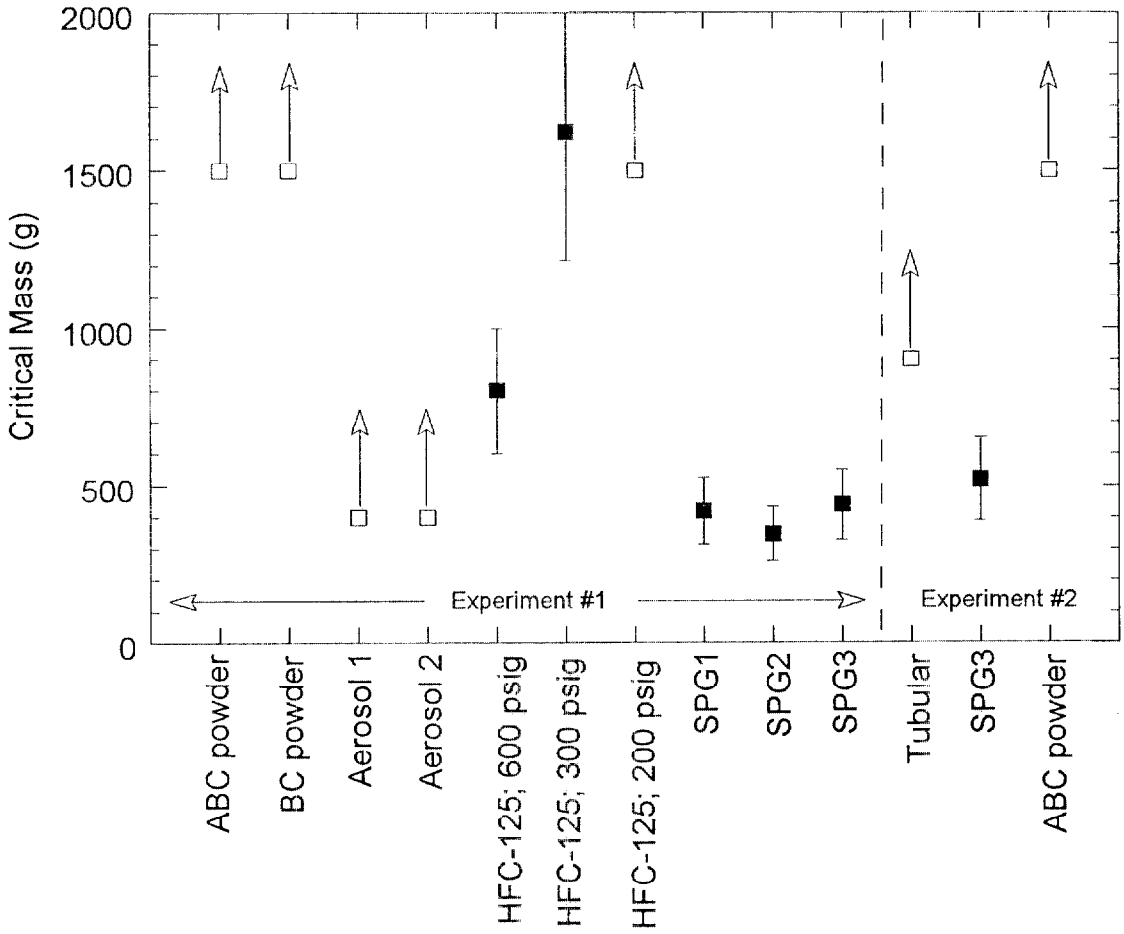

73. The measured critical mass for different suppressant types tested in the full-scale engine compartment.

confirmed these values [Wierenga, 1999; Black, 1999].

Figure 73 shows that HFC-125 was most effective when a high reservoir storage pressure (P_o) was used. This insured rapid suppressant delivery. This is seen in Fig. 74, which shows the transient reservoir pressure for three different initial reservoir pressures during HFC-125 discharge. The suppressant masses were different in each case, with values of 780 g, 1560 g, and 1620 g for the 4.2 MPa (600 psig), 2.2 MPa (300 psig), and the 1.4 MPa (200 psig) initial reservoir pressures (P_o), respectively. The suppressant was stored in the reservoir under nominally ½-fill conditions, such that the volume occupied by the suppressant was approximately 56 %, 52 %, and 50 % of the total reservoir volume for the 800 g, 1560 g, and 1620 g mass discharges, respectively. For safety and other reasons, the ½ fill condition is commonly used [Pitts et al., 1994; Yang et al.; 1995]. The pressure traces in Fig. 74 are characteristic for flow of a compressed liquid through a large orifice and the duration of the liquid phase delivery and the total (liquid phase and gas phase) delivery are evident from the pressure traces [Pitts et al., 1994; Yang et al.; 1995]. The duration of the liquid phase discharges was equal to approximately 0.9 s, 2.1 s, and 1.7 s, whereas the duration of the total (liquid phase plus gas phase) discharges were somewhat longer, approximately 1.5 s, 3.8 s, and 4.3 s, for the P_o= 4.2 MPa (600 psig), 2.2 MPa (300 psig), and 1.4 MPa (200 psig) pressurizations, respectively. As expected, the higher the reservoir pressurization, the smaller the discharge duration.

As noted in Fig. 73, 1500 g of ABC powder suppressant applied in Configuration FS1 (Table 17) was not effective, extinguishing the fire only once of five tests. An attempt was made to improve suppressant distribution through changes in the design of the powder delivery system. Suppression experiments conducted using Configurations FS2 through FS6 (see Table 17) with 1500 g of ABC powder in a 2.3 L reservoir pressurized to 2.4 MPa (350 psig) with gaseous N_2 failed to extinguish the fire at least once of one or two tests. These results demonstrated that the ABC powder was not an effective suppressant in this fire scenario.

Experiments using AGs proved that these suppressants were also not effective. Experiments using 400 g of AG1 were unable to extinguish the test fire and similar results were obtained for AG2. Observation of the transport of the AG particulate effluent indicated that the suppressant was not well-distributed within the extended engine compartment. Because the AG effluent is relatively hot, buoyancy transports the effluent in an upward direction, leading to low suppressant concentrations in lower extremities of the compartment. Suppressant that did make its way down was transported away by any wind present. Because of the transport behavior of the AG effluent, discharge of larger suppressant mass was not tested. The AGs have ρY_c values that are as effective as the SPGs (see Table 4), yet the relatively slow delivery rate hampered their effectiveness. The results for the AGs are consistent with the notion that rapid suppressant discharge in a partially open enclosure is critical to effectively transporting suppressant throughout a compartment. The results suggest that a suppressant was most effective when rapidly delivered, within approximately 1 s. This was observed for both the SPGs and HFC-125 (P_o= 4.2 MPa or 600 psig).

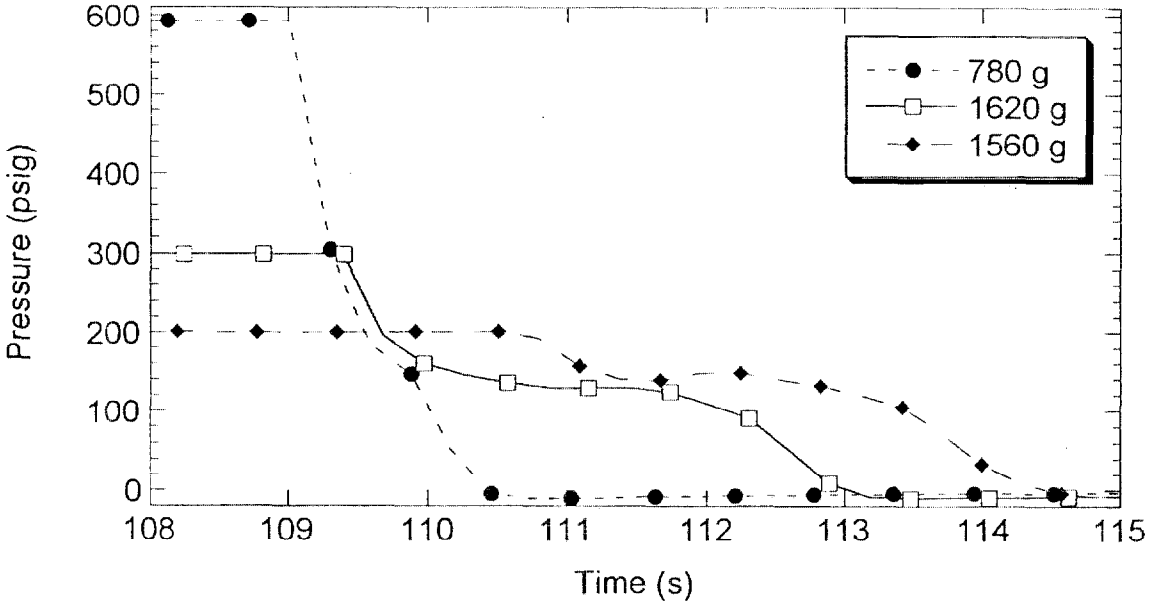

74. The transient reservoir pressure for three different initial reservoir pressurization's (with N_2) using HFC-125 in the full-scale engine compartment.

Figure 73 also shows the results when the second test procedure was used. Three suppressant types were tested including SPG3, the tubular suppressant device, and ABC powder (Configuration FS1). Suppressant deployment typically required ≈10 s after ignition of the gasoline for the tubular device and less than 1 s for the SPG3/optical detector. The SPG3 results showed that 520 g suppressed the fire three times out of three attempts, whereas 440 g of SPG 3 suppressed the fire once out of three tests. The results using the second procedure were consistent with those using the first procedure. Discharge of 1500 g of ABC powder was not effective in either test, whereas SPG was the most effective suppressant type using either test procedure. The value of the measured critical mass for SPG3 was similar in both test series, suggesting that the two tests offered a similar level of difficulty or challenge.

The tubular suppressant was tested using the second procedure only. The results showed that 900 g of suppressant did not suppress the second test fire. Although the primary gasoline fire was extinguished once out of two tests, the device failed to extinguish the small methanol pool fires in both tests. This indicated that suppressant distribution was poor within the compartment. The advantage of the tubular device is that active detection is not needed. The disadvantage of the system is that the suppressant is not distributed by a nozzle, which hampers uniform distribution of the suppressant and prevents suppression of a fire that is not spatially localized.

Whereas the SPG2 and SPG 3 effluent contained a finite amount of particulate, only trace amounts of particulate were emitted from SPG1 [see Table 5 and Hamins et al., 1997]. SPG2, which had the highest particulate output, had the lowest value of $\rho \cdot Y_c$ in Table 4. The suppression results showed that all three SPGs had similar mass requirements, far from the factor of four difference expected from consideration of the value of $\rho \cdot Y_c$ in Table 4. This indicates that the relatively low mass requirements of the SPG cannot be attributed to its constituents alone, but is likely related to supplementary effects such as fluid dynamic straining of the fire [Hamins et al., 1986] associated with its rapid discharge within the engine compartment. Nor is it possible, however, to differentiate SPG performance based on the rate of delivery. This is seen by considering the results in Fig. 73 for the three SPGs types. Although SPG1 and SPG2 were discharged almost five times faster than SPG3, they did not require significantly less mass than SPG3. This suggests that above some critical suppressant discharge rate, faster discharge rates did not lead to enhanced suppressant effectiveness.

Rapid discharge improved the HFC-125 suppressant performance. When rapidly discharged, the most effective suppressant after the SPGs was HFC-125. In that case, the rate of HFC-125 discharge was approximately 900 g/s, not significantly different from the 700 g/s for the SPG3. Transport effects associated with suppressant dispersion for the two suppressant types are likely similar when injected at such fast rates. Consistent with the value of $\rho \cdot Y_c$ in Table 4, HFC-125 required a factor of two more mass than the SPG3.

A comparison of the reduced and full-scale experimental results showed that the rank order of suppressant mass requirements was different. The suppressants in the reduced scale experiments fell into two groups in terms of mass-based performance: the powder suppressants, the tubular

device and the AGs, and secondly, the halogenated suppressants. In the full-scale experiments, the suppressants fell into three groups in terms of mass-based performance. The suppressant type requiring the smallest mass was the SPGs followed by HFC-125. The results showed that the powders, the tubular suppressant, and the AGs were not effective suppressants in the full-scale fire tests. The difference in ranking between the reduced-scale and full-scale experiments may be related to a number of factors. The relatively slow release suppressants performed well in extinguishing the smaller fires in the reduced-scale compartment experiments. This was not true in the larger full-scale compartment. In the full-scale experiments, the suppressants that created a rapid and large volume displacement required less mass. Such a strategy was also effective in the reduced-scale apparatus under some conditions (see Section 3.1.4.3.1). Suppressant transport through the large buoyant fire plume in the cluttered full-scale compartment may have been too large to overcome for the AG and powder suppressants, which provide limited volume displacement. In the full-scale experiments, rapid suppressant mass delivery was found to be advantageous. The rapid delivery of HFC-125 assured large volume displacement as the compressed liquid suppressant vaporized and also enhanced its transport throughout the compartment. Rapid delivery of the powders does not improve performance because large volume displacement does not occur due to the high powder density, which remains in the condensed phase unlike the compressed liquid HFC-125.

3.2.4 Summary

The mass required to extinguish a gasoline fire using various types of suppressants was investigated in a full-scale uncrashed vehicle. The SPGs, unique pyrotechnic devices that rapidly deliver a gas/particulate effluent, were the most effective suppressants, requiring approximately 300 g to 400 g to extinguish the test fire depending on the SPG type. After the SPGs, the most effective suppressant tested was HFC-125, which required a critical mass of 800 g when rapidly discharged (900 g/s).

Rapid suppressant discharge promotes air displacement in a compartment. A rapid discharge also carries high momentum, enabling suppressant transport throughout the compartment. For the tests conducted here, the results showed that the rapidly discharged suppressants were able to penetrate the clutter in the engine compartment and extinguish the pool fire on the ground. The performance advantages of rapid suppressant discharge are consistent with a simple analysis of fire suppression in an enclosure, as exemplified by Eq. 25. Rapid delivery, however, may be disadvantageous in terms of the reignition problem, because a rapid suppressant discharge implies a short residence time of the suppressant in the compartment. And a short suppressant residence time suggests that prevention of reignition will not be assured for long times by a gas-phase suppressant. For this reason, use of suppressants that offer reignition protection (such as SPG; see Hamins et al. [1997]) should be considered.

3.3 Laboratory Underbody Suppression Experiments

An underbody gasoline fire differs from the post-collision fire scenario associated with an engine compartment fire. Although a number of combustible materials are present on a vehicle (e.g. hydraulic fluid, thermoplastics, rubber), this study used gasoline as the initial fuel in the underbody test fires due to its relatively large volume on-board and its relatively low flash point (-38 °C) as compared to other vehicle fluids (see Table 11). It should be noted that a fuel leak does not automatically lead to a fire. There must be an ignition source present at the location where an ignitable vapor mixture exists. An ignition source for a post-collision fuel spill might be a friction spark or possibly an electric arc.

If a post-collision fuel system leak occurs, it may be associated with the fuel tank itself, may occur in the proximity of the tank (in a fuel line or a coupling between the tank and a fuel line), or away from the fuel tank such as in a ruptured fuel line. The spatial extent of the fuel spill may extend beyond the footprint of the vehicle, depending on the details of the collision scenario. The volume of the spill and the location relative to the vehicle is critical in developing a mediation strategy. As mentioned previously, NHTSA research with high speed rear-end collisions led to a rough estimate of an average fuel leak rate of approximately 1 L/min [Ref. 9 in Ohlemiller and Cleary, 1998].

The experiments described in this section consider fires associated with a dripping gasoline discharge in the proximity of a fuel tank. In a moving and possibly spinning vehicle, ventilation through the underbody would hamper suppression by affecting suppressant transport. It is assumed that suppressant discharge could be delayed until vehicle movement was terminated. The consequence of this strategy is that a gasoline trail ccould exist beyond the footprint of the vehicle. The existence and character (length, orientation, etc.) of such a trail would depend on the details of the scenario. The goal of this section is to test various suppressant types in addressing underbody fires in a simulated stationary vehicle. To achieve this, gasoline was supplied from an external reservoir to the location of the simulated fuel leak. Gasoline trails and wind effects in underbody applications are considered in Section 3.4.

The underbody simulator did not contain simulated exhaust system components, a simulated rear axle, suspension components or a simulated spare tire well. Instead, these experiments examined the feasibility of fire suppression in a simplified geometry. Once feasibility is established, suppressant distribution for specific vehicle makes and models can be optimized through engineering considerations such as nozzle design including consideration of the size, shape, placement, and orientation of vehicle components.

3.3.1 Apparatus

Figures 75 and 76 show a top and side view of the full-scale underbody fire simulator. The fuel

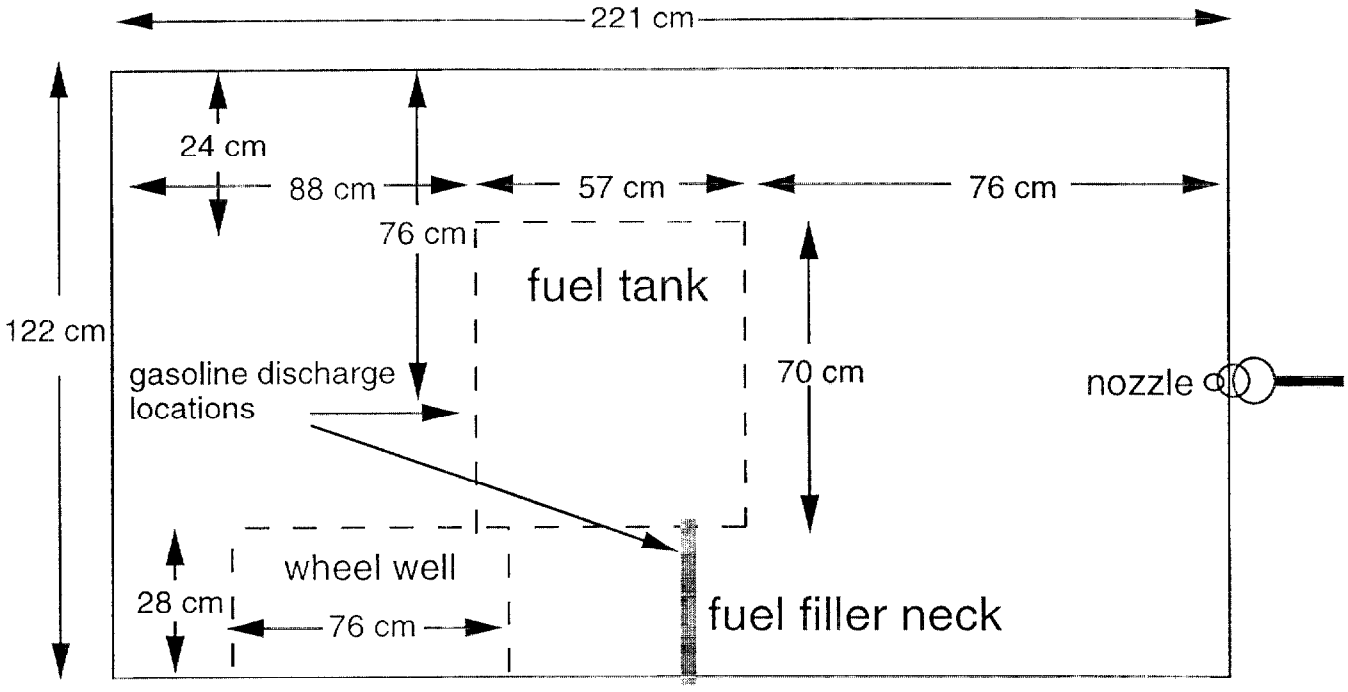

75. Top view drawing of the full-scale underbody fire simulator (not to scale).

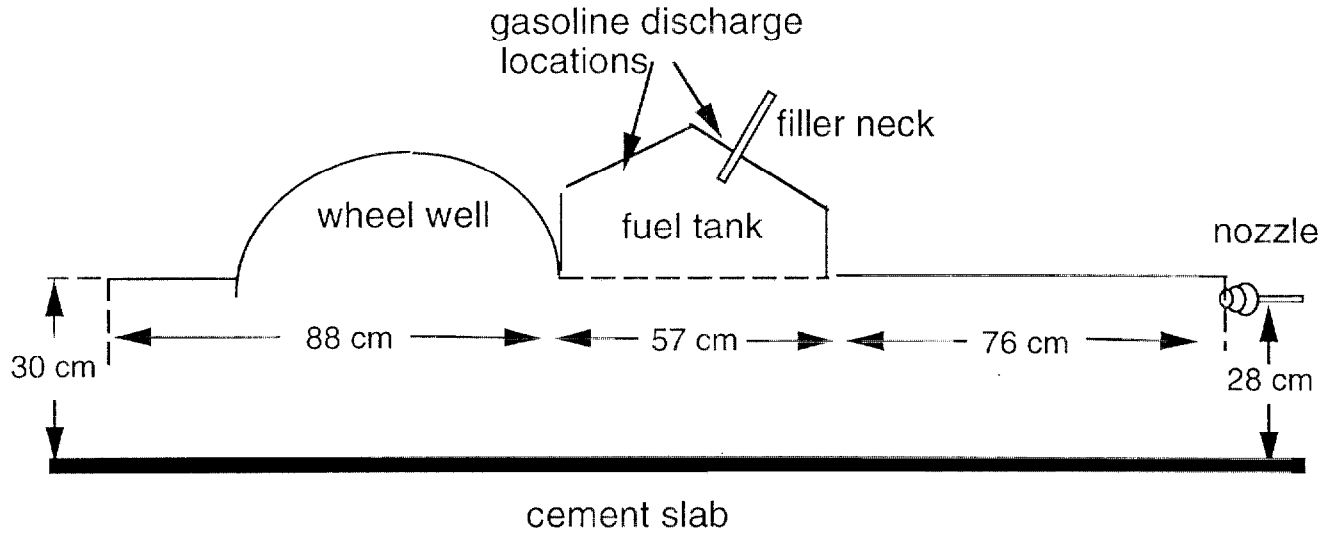

76. Side view drawing of the full-scale underbody fire simulator.

tank/filler neck from a 1994 mid-sized sedan was removed and mounted in a simulated uncrashed vehicle underbody, which was 1.22 m wide and 2.21 m long. The simulated underbody was composed of steel sheet metal. The fuel tank itself was positioned such that its height off the ground (0.30 m) and its distance to the edge of the simulated vehicle underbody were similar to the values in the original vehicle configuration. The underbody simulator included a single wheel well, 0.76 m in diameter and 0.28 m deep, in which a fully pressurized rubber tire (taken from a vehicle) was placed. The tire well was positioned 0.88 m from the rear of the simulated vehicle at a location similar to a typical sedan. The fuel tank was mounted 30 cm above sheets of a cement-filled fiberboard that simulated a road surface. The boundaries between the sheets were filled with a cement joint compound. The fuel tank was partially filled with water. The entire apparatus was located within a 3 m (wide) x 4 m (long) x 3 m (tall) enclosure, which was under an exhaust hood. Figure 77 is a photograph of the underbody simulator. The suppressant nozzle and tubing are seen next to a cinder block that was used to support the front end of the simulator. Behind the tire, cabinets in the laboratory are seen through a transparent plastic sheet attached to the compartment door. The fuel line running to the rear portion of the fuel tank is evident above the sheet-metal that defined the underbody.

Gasoline was held in a 10 L container and was delivered at a controlled rate to the discharge location via 6 mm (o.d.) steel tubing. The rate of gasoline flow was controlled by varying the nitrogen gas pressurization of the gasoline reservoir and the fuel line exit valve attached to the reservoir. The volumetric rate of fuel flow was determined using a graduated cylinder and a stopwatch. Pressure gauges monitored the reservoir pressure and the pressure just upstream of the discharge outlet.

Two gasoline discharge locations were considered. The first location (A) was on top of the filler neck, within 2 cm of its union with the fuel tank (see Figs. 75 and 76). The second gasoline discharge location (B) was just above the seam on the rear center of the fuel tank (see Figs. 75 and 76). The suppressant stream did not directly impinge on the fuel discharge. At location B, the fuel tank blocked direct suppressant impingement. At fuel discharge location A, the filler neck was located above the central plane defined by the sheet-metal underbody, which precluded direct suppressant impingement (see Figs. 75 and 76). In both scenarios, burning gasoline flowed onto the fuel tank or filler neck where it adhered and then dripped onto the cement surface below, creating a burning puddle of gasoline that yielded a luminous and turbulent fire. Gasoline flows of 500 mL/min and 10000 mL/min were tested. The spatial extent of the burning gasoline puddle was measured to be approximately 1000 cm^2 for the case when the gasoline flowed for 10 s at 500 mL/min before suppressant discharge.

The suppressant nozzle was located in the middle of the simulated underbody, positioned 75 cm forward of the front edge of the fuel tank (see Figs. 75 and 76). The nozzle was aligned parallel to the vehicle axis, and directed towards the fuel tank. These experiments were performed using a single spiral-shaped nozzle (#5 in Table 7). A dual nozzle system was tested in the next section where experiments were performed outdoors and a larger suppressant target area was needed to overcome wind effects. All experiments were conducted using ABC powder (mono-ammonium

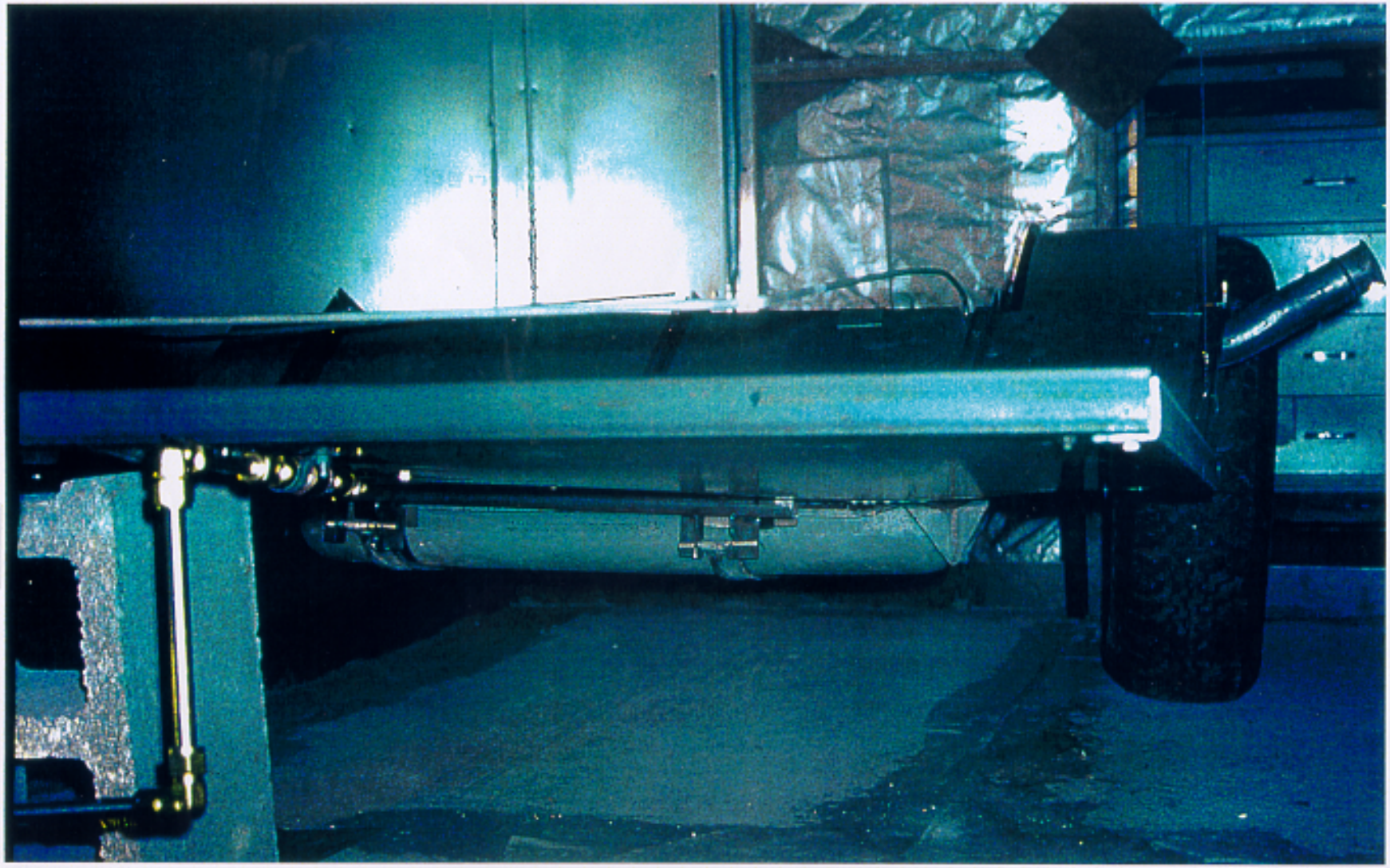

77. Photograph of the full-scale underbody fire simulator.

phosphate). The powder was discharged from a (1.0 L or 2.3 L) cylinder pressurized by N_2 to 2.4 kPa or 4.8 kPa. The powder traveled through 1 m of 13 mm (o.d.) stainless steel tubing to the nozzle. Other suppressant types were not tested in the laboratory due to safety concerns. SPG manufacturers were concerned about the integrity of their prototype units and NIST was concerned about acid gases associated with the use of halogenated compounds such as HFC-125.

3.3.2 Experimental Procedure

The ABC powder suppressant was loaded into the storage reservoir as described in Section 2. The suppressant reservoir was pressurized to 2.4 MPa (350 psig) with gaseous nitrogen unless otherwise stated. A few experiments used a pressurization of 5 MPa (700 psig).

The experimental procedure began by closing the hood exhaust fan to provide near quiescent conditions. Ignition was accomplished by positioning a small torch (6 mm o.d. tubing attached to a propane cylinder) under the gasoline discharge location. Ignition began as soon as the gasoline flow was initiated. After ignition, the propane flow was immediately closed and the torch removed from the enclosure. The gasoline flowed and burned for 10 s (unless otherwise stated) before suppressant discharge. The suppressant was discharged through manual control. The gasoline was allowed to flow for several seconds after suppressant discharge had terminated. This allowed observation of whether the fire had extinguished. The fuel flow was then halted. A fire, if present, was extinguished with portable CO_2 extinguishers.

In one series of experiments, the effect of the gasoline outlet pressure on suppression requirements was investigated. A constant gasoline flow was maintained by varying the size of the orifice outlet and the reservoir pressure, which was monitored with a pressure gauge. The pressure just upstream of the fuel outlet was also monitored. The pressure at the fuel outlet impacted the character of the flow. For the same fuel flow rate, a smaller orifice yielded a faster gasoline outlet velocity, which tended to splatter against solid objects and cover a wider area.

3.3.3 Experimental Results and Discussion

Table 18 summarizes the experimental conditions and the measured critical ABC powder mass and its uncertainty (see Table 9) for a number of the suppression experiments. Table 18 lists the fuel discharge location, the gasoline discharge rate, the burn time, the total gasoline volume delivered before suppressant discharge, the suppressant reservoir volume and pressure, and the apparent suppressant critical mass. The uncertainty bounds were determined using the Logit analysis described in Section 3.0.1. The values listed in Table 18 for the critical suppressant mass do not include associated hardware.

Table 18. Conditions and Critical Mass for Suppression of Simulated Underbody Fires using ABC Powder.

Location	Fuel flow (mL/min)	Burn time (s)	Fuel volume (mL)	Agent reservoir (L)	Pressure (kPa of N_2)	Mass (g)
A	500 ± 20	2 ± 0.5	17 ± 4	2.25 ± 0.02	4.8 ± 0.1	150 ± 30
A	500± 20	10 ± 0.5	83 ± 6	2.25 ± 0.02	4.8 ± 0.1	200 ± 40
A	500 ± 20	2 ± 0.5	17 ± 4	1.0 1± 0.02	4.8 ± 0.1	150 ± 30
A	500 ± 20	10 ± 0.5	83 ± 6	1.01 ± 0.02	4.8 ± 0.1	225 ± 45
A	1000 ± 20	10 ± 0.5	167 ± 12	1.01 ± 0.02	2.4 ± 0.1	250 ± 50
B	1000 ± 20	10 ± 0.5	167 ± 12	1.01 ± 0.02	2.4 ± 0.1	75 ± 15

Fire A: fuel was discharged on top of the fuel tank filler neck (see text).
Fire B: fuel was discharged at the weld seam on the central rear portion of the fuel tank.

In the experiments, the reservoir pressurization and volume were varied. Table 18 shows that the critical mass varied from 150 g to 250 g of ABC powder depending on the gasoline volume delivered at the time of discharge for the fire at location A. The suppressant reservoir size had no discernable effect on the measured ABC powder required for suppression. Table 18 also shows that the critical ABC mass required to extinguish a 1000 mL/min gasoline leak for the two fuel discharge locations differed by a factor of greater than 3. The critical suppressant mass was 75 g for the fires associated with Location B.

Figure 78 shows the critical ABC mass and its uncertainty (see Table 9) required to extinguish a fire burning 167 mL of gasoline delivered for 10 s at a rate of 1000 mL/min on the fuel tank filler neck as a function of the fuel outlet pressure. In these experiments, changing the size of the fuel outlet orifice from approximately 3 mm to 0.05 mm, allowed variation of the line pressure from ≈7 kPa to 35 kPa (1 psig to 5 psig). Correspondingly, the average fuel velocity exiting the outlet varied inversely with orifice area, as the total flow was maintained at a constant value. The powder suppressant reservoir was charged with 350 psig (2.4 kPa) of gaseous N_2. Figure 78 shows that the gasoline outlet pressure had little impact on the critical suppressant requirements over the range of conditions used in the tests.

3.3.4 Summary

A full-scale underbody fire simulator was developed for testing the feasibility of active fire suppression. A series of fire suppression experiments was conducted under quiescent ambient conditions. The results demonstrated that it is feasible to suppress a dripping gasoline fire with

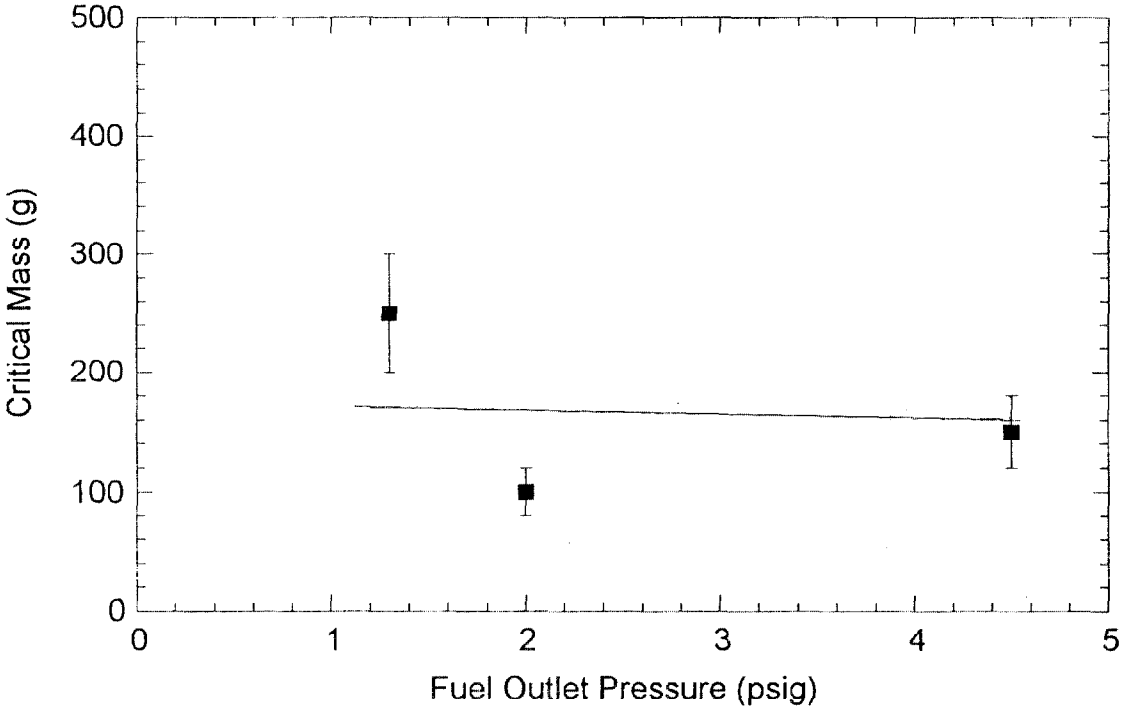

78. The critical ABC mass required to extinguish a 10 s leak of 1000 ml/min gasoline on the fuel tank filler neck as a function of the fuel outlet pressure.

total fuel volumes as large as 170 mL with a few hundred grams of suppressant. Experiments under more realistic conditions are considered in the next section, where experiments were performed using an uncrashed vehicle outdoors under ambient conditions.

3.4 Full-Scale Underbody Suppression Experiments

The objective of this series of experiments was to determine the suppressant mass required to suppress an underbody gasoline-fed pool fire. The fire scenario was limited to small gasoline pool fires (less than 350 mL) and small gasoline trails extending up to 2 m beyond the vehicle. Test scenarios did not include large gasoline volumes representative of catastrophic fuel tank failure.

3.4.1 Apparatus

Like the other suppression experiments, the vehicle was stationary during suppressant release. The vehicle used for the suppression experiments was an uncrashed mid-size sedan (see Table 2). Experiments were performed outdoors with the test vehicle placed on an asphalt surface. The suppressants tested were SPG3, ABC and BC powders, and HFC-125. A description of the procedure for filling the reservoir with the powder and compressed halogenated liquid suppressants is given in Sections 2.1 and 3.1.1.3, respectively. The powder and compressed liquid suppressants were stored in a stainless steel reservoir fitted with a thermocouple and a fast response analog output pressure gauge. The instruments were monitored by a personal computer at a $\approx$10 Hz sampling rate. A 1 L suppressant reservoir was pressurized with gaseous N_2 to a particular pressure, typically 4.2 MPa (600 psig). The compressed halogenated liquids were shaken as they were filled to ensure nitrogen saturation, which enhances the rate of agent flashing, vaporization, and dispersion [Yang et al., 1995]. The suppressant reservoir was connected to the nozzles through $\approx$2 m of 13 mm o.d. stainless steel tubing.

A single spiral nozzle (#5 in Table 7) was used in the underbody suppression experiments described in Section 3.3. The spiral nozzle has a wide angular dispersion (140°) and an effluent exit velocity that diminished rapidly with distance, permitting even low winds (<2 m/s) to influence suppressant distribution. In the outdoor experiments described here, low wind speeds (<2 m/s) were generally present and the experiments demonstrated that no single nozzle listed in Table 7 could provide adequate suppressant coverage for the target zone below the fuel tank. The implementation of a second nozzle enabled suppressant coverage throughout the target zone. In the series of experiments described here, suppression tests were performed using a pair of fan nozzles as described in Section 2 (nozzle system #14 in Table 7). The nozzles were configured as shown in Figs. 13 and 14 with the nozzles oriented 20° off-axis. Figure 16 is an example of suppressant distribution from the nozzles in the experimental configuration.

Figures 79 and 80 are top and side views of the placement of the nozzle distribution system in relation to the vehicle fuel tank. The nozzle configuration shown in Figs. 79 and 80 was used for

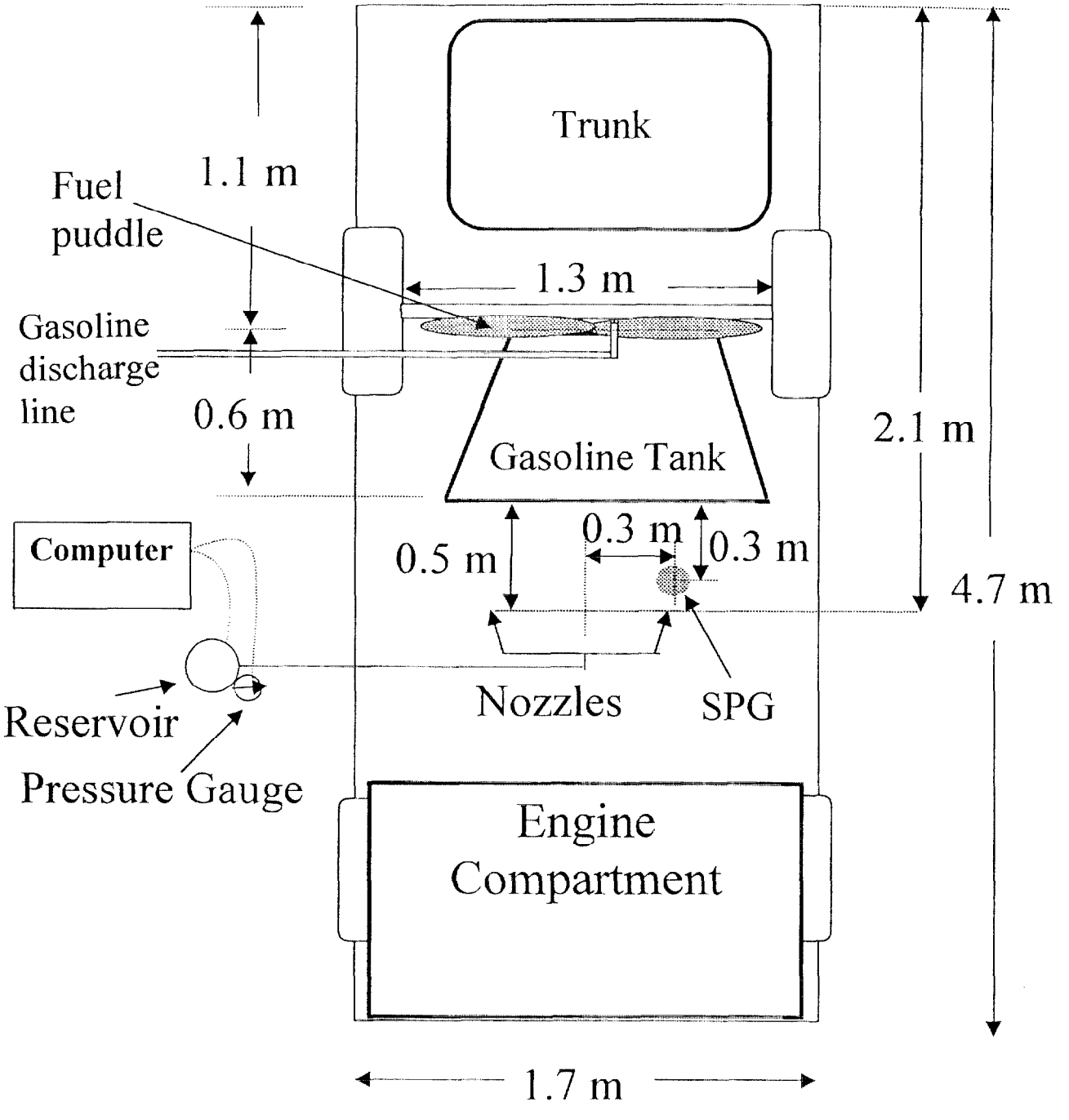

79. Top view drawing of the vehicle used for the underbody fire suppression experiments.

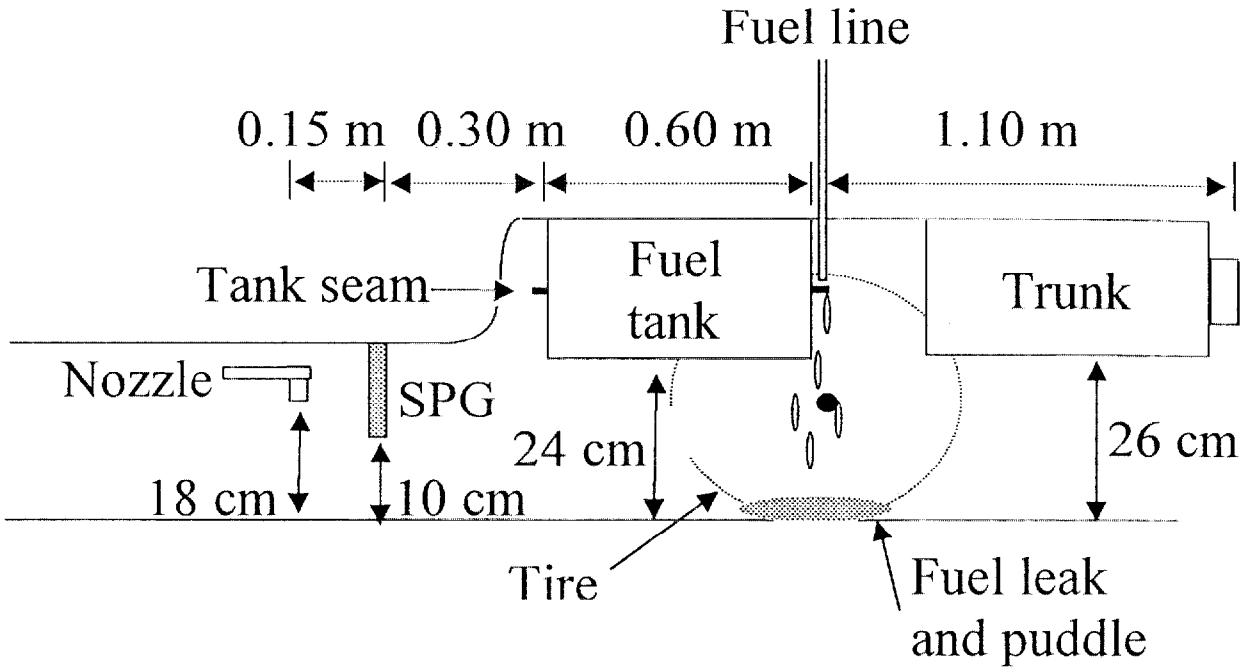

80. Side view drawing of the mid-sized sedan used in the underbody suppression experiments.

suppression tests with the powders and the halogenated compounds (HFC-125). The nozzles were positioned 0.45 m from the front edge of the fuel tank and 0.18 m off the ground (approximately 6 cm below the under-carriage). For comparison, the fuel tank was 0.24 m above the ground and the burning gasoline flowing over the rear seam of the fuel tank was approximately 0.34 m above the ground.

For suppression tests using the SPG3 device, the manufacturer provided a prototype that was held within a cylindrical stainless steel shield, approximately 20 cm long and 5 cm wide. The suppressant exited through a multiple-orifice semicircular distribution nozzle on one end of the cylinder. Some preliminary experiments were also conducted using SPG3 with a radial distribution nozzle. The device was mounted 10 cm above the ground, just below the underbody, through a hole in the floor pan in the rear portion of the passenger compartment. Figures 79 and 80 show the specific location of the device in relation to the vehicle. This configuration was used to investigate the feasibility of suppression in underbody vehicle applications and does not imply that a production line version of the device should be positioned in this precise manner.

3.4.2 Experimental Procedure

In the suppression experiments, 250 mL of gasoline flowed for 30 s at a rate of 500 mL/min just above the middle of the rear seam of the gasoline tank as shown in Figs. 79 and 80. The splashing, dripping gasoline created a puddle that extended across the rear portion of the vehicle underbody, typically covering a large fraction of the 1.3 m distance between the rear tires. The gasoline puddle was typically 0.3 m in width. A similarly sized fuel puddle could have been achieved by flowing the fuel at a rate of 1000 mL/min for 15 s, or 1500 mL/min for 10 s, within the range of fuel leak rates described by Ragland [Ohlemiller and Cleary, 1998]. After 30 s, the puddle was ignited, by a propane torch or remotely by a "book of electric matches," (see Section 3.2.2).

Ignition of the fuel puddle yielded a luminous turbulent fire that stretched along the ground below the rear axle of the vehicle as seen in Figs. 81 and 82. Ten seconds after ignition, suppressant discharge was initiated by opening a pneumatic valve downstream of the suppressant reservoir. The transient reservoir pressure was monitored during suppressant release. The pyrotechnic devices were activated by use of a 12 V vehicle battery or similar power source. After suppressant delivery, the fire was observed. If suppression was not achieved, then the fuel flow was stopped and the fire was suppressed manually with hand-held CO_2 extinguishers. If suppression appeared to be successful, the fuel flow was maintained for approximately 10 s after suppressant discharge was complete to insure that the fire was completely extinguished. Any residual suppressant and fuel were washed away with water before the next experiment. Water puddles on the ground were removed by a squeegee or broom. The subsequent experiment was initiated after a ½ hour period, allowing the residual water to evaporate.

81. Photograph of the luminous turbulent gasoline fire below the rear portion of the fuel tank.

82. Photograph of the luminous turbulent gasoline fire below the rear portion of the fuel tank.

3.4.3 Experimental Results and Discussion

The results of the suppression experiments are summarized in Table 19. The Table lists the experimental conditions, as well as critical suppressant masses and uncertainties. The column labeled "Fuel Volume" refers to the total amount of fuel that was delivered before suppressant deployment. The average wind speed measured 0.2 m above the ground was less than ≈2 m/s in all cases with momentary gusts as large as 5 m/s. The prevailing wind was perpendicular to the central axis of the vehicle, from the passenger side towards the driver side. Table 19 shows that the critical mass of ABC or BC powder required to suppress the 330 mL gasoline underbody fire using nozzle type 14 was 250 g ± 60 g. Nozzle types 5 and 6 required a significantly higher critical mass. For a discussion of the uncertainty estimate, see Section 3.0.1. The mass values reported here represent suppressant mass only and do not include associated system hardware.

The HFC-125 failed to extinguish the test fires with as much as 1500 g of suppressant using the two system designs tested as noted in Table 19. Figure 83 shows a sequence of frames from the video record for the delivery of 740 g of HFC-125 from a 2.25 L reservoir pressurized to 2.5 MPa (350 psig). The average wind speed near the ground was small (<1 m/s) during this experiment. The sequence of frames begins in the upper left, continues down the left column and through the right column. Frame (a) was just before suppressant discharge. Frames (b)-(h) represent 0.1 s, 0.3 s, 0.6 s, 0.8 s, 2.1 s, 2.9 s, and 3.2 s after suppressant release, respectively. The suppressant was delivered in approximately 1.5 s. During the first 1 s, flames were blown downstream past the rear bumper. Some smoke was observed in Frame (a) blowing towards the upper right portion of the image. In Frame (b) some amount of haze was also visible on the left side of the vehicle, probably due to the suppressant itself. Condensed phase HFC-125 was not observed, indicating that the suppressant rapidly vaporized in the hot environment. By Frame (e), the fire appeared to be nearly extinguished and few flames remained in the underbody portion of the vehicle. A kernel of flame, however, was not suppressed, as seen in Frame (f). Frame (h) shows that the flame kernel served to re-light the gasoline puddle located below the vehicle.

Figure 84 shows a sequence of frames from the video record for the delivery of 250 g of ABC powder from a 1 L reservoir pressurized to 4.2 MPa (600 psig). The wind was gusty, blowing from 1 m/s to 2 m/s from right to left in the Figure. Frame (a) was 0.03 s after the initiation of the suppressant discharge. Frames (b)-(d) were recorded 0.9 s, 1.3 s, and 1.6 s after discharge, respectively. In Frames (b) and (c), the powder was transported through the fire zone, inhibiting the fire as well as obscuring its visibility. By Frame (d), the fire was completely suppressed. With gasoline continuing to flow for approximately 10 s, flame reignition was not observed. The suppression system in Figure 84 rotated ≈ 45° from its original orientation upon suppressant discharge. An indication of this can be seen in the powder flow pattern in Fig. 84. System movement is attributed to improper clamping and the very large thrust associated with suppressant delivery. Although the fire was extinguished in this particular case, system restraint is a concern particularly for post-collision functionality.

The controlled experiments described in Section 3.3 showed that suppression could be obtained with low reservoir pressurization (≈1.4 MPa or 200 psig) in the absence of wind. Table 19 shows

A

E

B

F

C

G

D

H

83. A sequence of frames from the video record of an underbody suppression experiment using 740 g of HFC-125 (2.25 L reservoir).

a

c

b

d

84. A sequence of frames from the video record of an underbody suppression experiment using 250 g of ABC powder (1 L reservoir).

that increased reservoir pressurization facilitated suppressant transport to the fire zone in the presence of wind such that only 250 g of powder suppressant was required to suppress the underbody fires as seen in Table 19.

Table 19. Results from the Underbody Fire Suppression Experiments.

Suppressant	Nozzles; Type	Fuel Flow (mL/min)	Preburn & burn time (s)	Fuel Volume (mL)	Reservoir (L)	Pressure (MPa)	Critical Mass (g)
ABC	2; #14	500 ± 10	30 ± 2 10 ± 2	330 ± 30	1.02± 0.01	4.22 ±0.1	250 ±60
ABC	2; #6	500 ± 10	30 ± 2 10 ± 2	330 ± 30	1.02± 0.01	2.51 ±0.1	1000 ±250
ABC	2; #5	500 ± 10	30 ± 2 10 ± 2	330 ± 30	2.32± 0.01	2.51 ±0.1	>1000
BC	2; #14	500 ± 10	30 ± 2 10 ± 2	330 ± 30	1.02± 0.01	4.22 ±0.1	250 ± 60
HFC-125	1; #5	500 ± 10	30 ± 2 10 ± 2	330 ± 30	2.32± 0.01	1.48 ±0.1	>1520
HFC-125	2; #14	500 ± 10	30 ± 2 10 ± 2	330 ± 30	2.32± 0.01	4.22 ±0.1	>1480

3.4.3.1 Gasoline Trails

The effectiveness of the suppressants in addressing a gasoline trail, which is defined here as a gasoline puddle of any shape that extends beyond the vehicle footprint, was investigated. As in the case of the fire under the fuel tank, suppressant transport to the target zone is critical. In the absence of wind, the powder suppressants were transported past the vehicle underbody, in an unaltered direction. It was possible to extinguish gasoline trails extending up to 2 m beyond the rear portion of the fuel tank and directly behind the vehicle using the powder systems evaluated here.

The direction of the powder suppressant discharge was significantly affected by wind. Calculations were made on the effect of wind on the velocity profiles for the leading edge of the ABC suppressant as delivered by a fan nozzle. Beyond the vehicle confines, the wind dominates suppressant transport. This was confirmed by experiments that showed that even under low wind conditions, the powder systems tested here did not provide the momentum necessary to propel the powder past the vehicle footprint if the wind speed and direction were not favorable. For example, with the wind perpendicular to the vehicle length, a wind speed greater than 5 m/s turned the suppressant such that it missed its target (see Section 2.3 for further discussion). The powder systems were successful in the zone near the fuel tank because of its proximity. Close to

the nozzle outlets, the suppressant momentum overcame the effect of small wind speeds. Beyond the confines of the vehicle, however, the suppressant momentum was too small and adequate distribution of the suppressant beyond the vehicle footprint was not possible.

A rapidly discharged suppressant may be able to overcome the effects of moderate wind speeds. To investigate this possibility, three experiments were conducted using SPG3. A semicircular distribution nozzle was used under low wind conditions. Two of the three experiments were successful. In one experiment, a 2 m trail of gasoline (250 mL) was placed behind the driver-side rear tire, extending 45° off-axis away from the vehicle. It was not possible to extinguish such an obstructed gasoline trail using the "semicircular" nozzle provided by the manufacturer. The experiments did show that it was possible to extinguish a ≈1 m gasoline trail beyond the vehicle using the SPG3 and a semicircular distribution nozzle in an unobstructed configuration - away from the tire.

3.4.4 Summary

The effectiveness of a number of suppressants was tested in an uncrashed full-scale vehicle underbody. The suppressants included ABC and BC powders, HFC-125, and SPGs. The measurements showed that the critical mass varied with suppressant type. For the scenarios and conditions considered here including low-winds, underbody fire suppression was possible with a few hundred grams of ABC or BC powder. In the event of moderate or high winds, the powder suppression system tested here would not be adequate. Preliminary results using SPG suggest that the high momentum suppressant discharge can overcome the effects of moderate winds, but engineering the suppressant dispersion needs further development. Adequate suppressant coverage of the target zone may require multiple nozzles or use of a different delivery system entirely.

3.5 Conclusions

It is conceptually possible to successfully suppress any fire, if enough suppressant is utilized. In practice, however, penalties such as system mass, volume, and cost will limit the fire scenarios that can be addressed. The main goal of this study was to examine the feasibility of active fire suppression in some selected vehicle fire scenarios. A number of test devices and protocols were developed for testing the effectiveness of fire suppressants in full-scale underbody and engine compartment fire scenarios. Since little is known about post-collision fire conditions, the scenarios were developed based on available information, laboratory experiments, and engineering judgement. Several technologies were selected for underbody and engine compartment fire suppression including commercially available fire suppressants and a number of prototype devices. The following conclusions summarize the results of the study:

- Full-scale suppression experiments in the engine compartment of an uncrashed stationary vehicle in the absence of forced ventilation (radiator fan off) showed that:
  1. the most effective suppressant type tested was the solid propellant generator (SPG).

These unique pyrotechnic devices rapidly deliver a gas/particulate effluent. Suppression of a 200 mL/min flaming gasoline discharge was achievable with less than 500 g of solid propellant generator (SPG) suppressant. The total system mass of such a suppression system can be expected to be approximately three to four times larger.

2. penetration of suppressant through the flow field obstacles (i.e., engine components) in the engine compartment was best achieved by rapid suppressant discharge.

- Reduced-scale suppression experiments in a simulated engine compartment showed that:
  1. suppressant effectiveness is dependent on the details of the flow field geometry, the fire, and suppressant delivery. Certain trends in the data were evident among geometrical features, fuel-associated parameters, and suppressant-related parameters. The trends are enumerated as penalty factors on the suppressant mass requirements as detailed in Table 15.
  2. a major challenge to active suppression presented by engine compartment fires is suppressant dispersion around vehicle components, which act as flow field obstacles and prevent direct suppressant impingement on a fire.
  3. engineering correlations and simple analytic models of suppressant mixing do not adequately predict suppressant mass requirements due to complications associated with modeling transport in an enclosure with relatively large surface openings.

- Full and reduced-scale suppression experiments showed that several suppressant types were impractical for the engine compartment fires tested here. These included the powder, aerosol generator (AG), and tubular suppressant systems, which did not provide sufficient discharge momentum to assure adequate suppressant distribution within the compartment.

- Full-scale uncrashed underbody suppression experiments showed that:
  1. suppression of a (333 mL volume) gasoline fed pool fire was achieved with less than 300 g of ABC and BC powder suppressants when the fuel was located under the vehicle footprint under low wind conditions.
  2. if a fuel puddle in an underbody fire extended beyond the vehicle footprint and if moderate to high winds were present, then the powder suppression system failed to reliably extinguish the fire. Preliminary results indicated that solid propellant generators may be effective under conditions of low to moderate winds and for fires burning within approximately 1 m of the footprint of a vehicle, when the fuel puddle is not behind a tire.

- Full and reduced-scale uncrashed underbody and engine compartment suppression experiments showed that:
  1. nozzle type, orientation, and placement is critical in the design of an effective suppression system.
  2. maximizing the rate of mass delivery of a suppressant is an effective strategy for suppressing engine compartment fires and for overcoming wind effects in an underbody fire.

- Although computational fluid dynamic modeling of fire suppression is not a fully developed technology, it may be used to screen suppression system design options and interpret experimental measurements.

4. References

Abu-Isa, I.A., General Motors Corp., Notes on the quantity of Bulk Thermoplastics used in the Automotive Industry, personal communication, 1997.

Adler, U. (Ed.), Bosch Automotive Handbook, 3rd Ed., Society of Automotive Engineers, Warrendale, PA, 1993.

Babrauskas, V., "Tables and Charts" in *Fire Protection Handbook* (ed.: A.E. Cote) 18th ed., 1997.

Baldwin, S.P., Brown, R., Burchall, H., Eaton, H.G., Salmon, G., Aubin, J.St., Sheinson, R.S., and Smith, W.D., "Halon Replacements: Cup Burner and Intermediate Size Fire Evaluation," *Proceedings of the Int. CFC and Halon Alternatives Conference*, pp. 812-815, Washington, D.C., Sept. 29- Oct. 1, 1992.

Bennett, J.M., "Survey of Fire Intervention Technologies for Their Application in Motor Vehicles," Draft Report to General Motors as part of Project B.4 of the DOT/GM agreement, July 1997.

Black, R., personal communication, 1999, Atlantic Research Corp., Gainesville, VA.

Bolt, W., Herud, C., and Treanor, T., "Halon Replacement Program for Combat Vehicles, A Status Report", *Proceedings of the Halon Options Technical Working Conference*, Alberquerque, NM, May 1997.

Camino, G., Luda, M.P., and Costa, L., "Developments in Intumescent Fire-Retardant Systems," Chapter 6 in *Fire and Polymers II* (ed.: G.L. Nelson), ACS Symposium Series 599, American Chemical Society, Washington D.C., 1995.

Chambers, J.M., and Hastie, T.J. (Eds.), *Statistical Models in Science*, 1991, Wadsworth.

Cleary, T., personal communication, 2000, NIST, Gaithersburg, MD.

Conroy, M.T., "Fire Extinguisher Use and Maintenance", in *Fire Protection Handbook,* 18th ed., pp. 6-368 to 6-385, 1997.

Delichatsios, M.A., "Air Entrainment into Buoyant Jet Flames and Pool Fires", Section 2/Chapter

3, *The SFPE Handbook of Fire Protection Engineering*, 2nd Edition, 1995.

Demers, D.P., "Selection, Operation, Distribution, Inspection and Maintenance of Fire Extinguishers", 5-294 to 5-312, *The SFPE Handbook of Fire Protection Engineering*, 2nd Edition, 1995.

DiNenno, P.J., Beyler, C., Custer, R.L., Walton, W.D., Watts, J.M., Drysdale, D. Hall, J.R. (eds.), Appendices, *SFPE Handbook of Fire Protection Engineering*, 2nd ed., NFPA, Quincy, MA, 1995.

Drysdale, D., *An Introduction to Fire Dynamics*, 2nd ed., John Wiley and Sons, Chichester, England, 1999.

Environmental Protection Agency, *Carbon Dioxide as a Fire Suppressant: Examining the Risks,* Report # EPA 430-R-00-002 (http://www.epa.gov/ozone/title6/snap/co2report.html), February 2000.

Ewing, C.T., Faith,F.R., Hughes, J.T., Carhart, H.W., *Fire Tech.*, **25**, 134 (1988).

Glassman, I., *Combustion*, 2nd ed. Academic Press, San Diego, CA, 1987.

Goedeke and Gross, H.G., *Characteristics of Optical Fire Detector False Alarm Sources and Qualification test Procedures to Prove Immunity*, Tyndall AFB, FL, Report WL-TR-93-3522, NTIS # ADA 276878, 1992.

Grosshandler, W., Gann, R.G., and Pitts, W.M., eds., *Evaluation of Alternative In-Flight Fire Suppressants for Full-Scale Testing in Simulated Aircraft Engine Nacelles and Dry Bays*, NIST Special Publication Number SP-861, 1994.

Grosshandler, W., Selepak, M., Donnaly, M., Charagundla, R, and Presser, C., "Suppressant Performance Evaluation in a Baffle-Stabilized Pool Fire," *Proceedings of the Halon Options Technical Working Conference*, Alberquerque, NM, 105-116, Apirl 1999.

Grosshandler, W., Hamins, A., McGrattan, K., Presser, C., and Characgula, R., "Suppression of a Non-Premixed Flame Behind a Step," *Twenty-eighth Sym. (Int.) on Combustion*, The Combustion Institute, to appear (2000).

Hamins, A., *Evaluation of Intumescent Body Panel Coatings in Simulated Post-Accident Vehicle Fires*, NISTIR 6157, 1998.

Hamins, A., Cleary, T., and Yang, J., *An Analysis of the Wright Patterson Full-Scale Engine Nacelle Fire Suppression Experiments*, NISTIR 6193, 1997.

Hamins, A., Cleary, T., Borthwick, P., Gorchkov, N., McGrattan, Forney, G., and Grosshandler, W., "Suppression of Engine Nacelle Fires," Section 9 in (Gann, R.G., Ed.), *Fire Suppression System Performance of Alternative Suppressants in Aircraft Engine and Dry Bay Laboratory Simula-*

tions, NIST Special Publication Number SP-890, 1995.

Hamins, A., Gmurczyk, G., Grosshandler, W., Rehwoldt, R.G., Vasquez, I., Cleary, T., Presser, C., and Seshadri, K., "Flame Suppression Effectiveness," Chapter 4 in (Grosshandler, W., Gann, R.G., and Pitts, W.M., Eds.), *Evaluation of Alternative In-Flight Fire Suppressants for Full-Scale Testing in Simulated Aircraft Engine Nacelles and Dry Bays*, NIST Special Publication Number SP-861, 1994.

Hamins, A. and Seshadri, K., *Combust. Flame*, **64**, 43-54 (1986).

Jensen, J., Santrock, J., Strom, K.A., LeMieux, D., and Tewarson, A, *"Evaluation of Motor Vehicle Fire Initiation and Propagation, Part 1: Vehicle Crash and Fire Propagation Test Program,"* in preparation, 1999.

Jung, Ki-Chang, Kim, Hong, Kang, Young-Goo, "The Development of the FM-200 Gas Filled AFFF Fire Extinguisher for Automatic Fire Suppression Systems in the Engine Compartment of Automobiles," *International Symposium on Fire Science and Technology*, 1997, p. 598.

Klimenko, *Proceedings of the Halon Options Technical Working Conference*, Alberquerque, NM, pp. 368, May 1998.

Lataille, J. I., *"Environmental Issues in Fire Protection"*, in Fire Protection Handbook, 17th ed., pp. 8-77, 1995.

Levenson, M., personal communication, Statistical Engineering Division, NIST, January 2000.

Lim, Sung-Mook, Jung, Ki-Chang, Kang, Young-Goo, Kim, Hong, "A Study on the Assessment of the Performance of the Automatic Fire Suppression System Using the HCC-227ea Liquefied-Gas Filled AFFF Fire Extinguisher," *International Symposium on Fire Science and Technology*, 1997, p. 590.

Madrzyowski, D., NIST, *Personal Communication*, 1999.

Mangs, J., and Keski-Rahkonen, O., F, *Fire Safety Journal*, **23**,17-35 (1994).

McCullagh, P., and Nelder, J.A.,Generalized Linear Models (Second Edition) 1989, Chapman & Hall, Philidelphia.

McGrattan, K.B., Rehm, R.G., and Baum, H.,R., *J. Computational Physics*, **110**, 285-297 (1994).

McGrattan, K.B., Baum, H., and Deal, S., *Numerical Simulation of Rapid Combustion in an Underground Enclosure*, NISTIR 5809, 1996.

McGrattan, K.B., Baum, H.R., and Rehm, R.G., *Fire Safety Journal*, **30,**161-178 (1998a).

McGrattan, K.B., Hamins, A., and Stroup, D., *Sprinkler, Smoke & Heat Vent, Draft Curtain Interaction - Large Scale Experiments and Model Development*, NISTIR 6196-1, 1998b.

McKenna, L.A., Gottuck, D.T., DiNenno, P.J., "Extinguishment Tests of Continuously Energized Class C Fires," *Proceedings of the Halon Options Technical Working Conference*, pp. 80-90, Alberquerque, NM, May 1998.

Mitchell, M., "Hybrid Fire Extinguisher for Occupied and Unoccupied Spaces," *Proceedings of the Halon Options Technical Working Conference*, Alberquerque, NM, April 1999.

Montreal Protocol on Substances that Deplete the Ozone Layers, Final Act, United Nations Environmental Program and subsequent amendments (HMSO CM977), 1987.

National Highway Traffic Safety Administration, *B.01.17. Upgrade of Fuel System Integrity,* http://www-nrd.nhtsa.dot.gov/summaries/B0117.htm, 1998

Neidert, J., personal communication, 1999, Atlantic Research Corp., Gainesville, VA.

NFPA 10, "Standard for Portable Fire Extinguishers," *National Fire Codes*, National Fire Protection Administration, Quincy, MA, 1996.

Ohlemiller, T.J., and Cleary, T.G., *Aspects of the Motor Vehicle Fire Threat from Flammable Liquid Spills on a Road Surface*, NISTIR 6147, 1998.

Ohlemiller, T.J., and Shields, J.R., *Burning Behavior of Selected Automotive Parts from a Minivan*, NISTIR 6143, 1998.

Pitts, W.M., Nyden, M.R., Gann, R.G., Mallard, W.G. and Tsang, W., "Construction of an Exploratory List of Chemicals to Initiate the Search for Halon Alternatives," *NIST Technical Note 1279*, U.S. Government Printing Office, Washington, DC, 1990.

Pitts, W., Yang, J., Gmurczyk, G., Cooper, L.Y., Grosshandler, W., Clevelend, W.G., and Presser, C., "Fluid Fynamics of Agent Discharge," Chapter 3 in (Grosshandler, W., Gann, R.G., and Pitts, W.M., Eds.), "Evaluation of Alternative In-Flight Fire Suppressants for Full-Scale Testing in Simulated Aircraft Engine Nacelles and Dry Bays," NIST Special Publication Number SP-861, April 1994.

Santrock, J., *Report of Transducer Test Results for a Caravan Mini-Van (5-10-96 to 5-13-96)*, personal communication, 1996.

Santrock, J., *Post-Crash Fire Test Results for a Mini-Van*, in preparation, 1999a.

Santrock, J., *Comments on Evaluation of Active Suppression in Post-Collision Vehicle Fires*, personal communication, 1999b.

Scheffey, J.L., *Foam Extinguishing Agents and Systems*, Section 6, Chapter 22 in The Fire Protection Handbook (Ed.: A.E. Cote), 18th Edition, National Fire Protection Association, Quincy MA, 1997.

Sheinson, R.S., Penner-Hahn, J.E., and Indritz, D, *Fire Safety Journal*, **15**, 43 (1989).

Simiu, E., and Scanlan, R.H., *Wind Effects on Structures*, 3rd ed., John Wiley and Sons, NY, 1996.

Sivathanu, Y., personal communication, 1999, En'Urga Inc., West Lafayette, IN.

Smith, D.M., Rivers, P.E., Steckler, K., and Grosshandler, W., "Effectiveness of Clean Aagents on Burning Polymeric Materials Subjected to an External Energy Source," *Proceedings of the Halon Options Technical Working Conference*, Alberquerque, NM, April 1999.

Stewart, L.J., *U.S. Vehicle Fire Trends and Patterns Through 1993*, National Fire Protection Association, Quincy, MA, August 1996.

Takahashi, F., Schmoll, J., and Belovitch, V., "Effects of Obstruction on Flame Suppression Efficeiency," *Proceedings of the Halon Options Technical Working Conference*, Alberquerque, NM, April 1999.

Tapscott, R.E., "Commercialized Halon Options," *Proceedings of the Halon Options Technical Working Conference*, Alberquerque, NM, May 1998.

Taylor, B.N. and Kuyatt, C.E., Guidelines for Evaluating and Expressing the Uncertainty of NIST Measurement Results, NIST Technical Note 1297, 1993.

Tessmer, J., *An Analysis of Fires in Passenger Cars, Light Trucks and Vans*, National Highway Traffic Safety Administration, Technical Report No. DOT HS 808 208, December 1994.

Tieszen, S.R., and Lopez, A. R., "Issues in Numerical Simulation of Fire Suppression", *Proceedings of the Halon Options Technical Working Conference*, Alberquerque, NM, April 1999.

Tucker, D.M., Drysdale, D.D. and Rasbash, D.J., Combust. and Flame, **41**, 293 (1981).

U.S. Fire Administration, *Fire in the United Sates: 1985-1994*, 9th ed., July 1997.

Wierenga, P. H., personal communication, 1999, Primex Aerospace Co., Redmond, WA.

Windholz, M., Budavari, S., Blumetti, R.F., Otterbein, E.S., *The Merck Index*, Tenth Ed., Merck & Co., Rahway, N.J., 1983, p. 1230.

Williams, F.A., *Journal of Fire and Flammability*, **5**, 54 (1974).

Yang, J.C., Cleary, T., Vazquez, I., Boyer, C.I., King, M.D., Bureuel, Wolmeldorf, C., Grosshandler, W., Huber, M., Weber, L., and Gmurczyk, G., "Optimization of System Discharge," Section 8 in Volume II of (Gann, R.G., Ed.), "Fire Suppression System Performance of Alternative Suppressants in Aircraft Engine and Dry Bay Laboratory Simulations," NIST Special Publication Number SP-890, November 1995.

5. Acknowledgements

This work could not have been accomplished without industrial participation. The cooperation of Jamie Neidert, Robert Black, Donald MacElwee, Harry Stewart, Yudaya Sivathanu, Rony Joseph, Bernd Wendel, Detlef Goricke, Mark Grace, David Parkinson, William Moscrip, Paul Wierenga, and Gary Holland is gratefully acknowledged. Thanks are due to Tom Cleary, Mark Levenson, Daniel Madryzkowski, Kevin McGrattan, Roy McLane, Tom Ohlemiller, Eric Sutula, and Renaat VerEecke of NIST for helpful discussions and assistance. I am grateful to Robert Camplair and the staff at the Montgomery County Fire and Rescue Training Academy for providing a facility to perform the full-scale suppression experiments. This report was financed by General Motors pursuant to an agreement between General Motors and the United States Department of Transportation.